RAPHAEL PATCAS

Applicability of Cone-beam Computed Tomography in Craniofacial Imaging in Comparison to other Radiological Methods

ACADEMIC DISSERTATION
To be presented, with the permission of
the Board of the School of Medicine of the University of Tampere,
for public discussion in the Small Auditorium of Building M,
Pirkanmaa Hospital District, Teiskontie 35,
Tampere, on January 27th, 2014, at 12 o'clock.

UNIVERSITY OF TAMPERE

UNIVERSITY OF TAMPERE

ACADEMIC DISSERTATION
University of Tampere, School of Medicine
Finland

Supervised by
Docent Timo Peltomäki
University of Tampere
Finland

Reviewed by
Professor Demetrios Halazonetis
National and Kapodistrian University of Athens
Greece
Docent Jaakko Niinimäki
University of Oulu
Finland

Cover design by
Mikko Reinikka

Acta Universitatis Tamperensis 1890
ISBN 978-951-44-9314-0 (print)
ISSN-L 1455-1616
ISSN 1455-1616

Acta Electronica Universitatis Tamperensis 1372
ISBN 978-951-44-9315-7 (pdf)
ISSN 1456-954X
http://tampub.uta.fi

Suomen Yliopistopaino Oy – Juvenes Print
Tampere 2013

לְמַד לְשׁוֹנְךָ לוֹמַר אֵינִי יוֹדֵעַ

"Teach your tongue to say: I don't know"
Babylonian Talmud, Tractate Berakhot, Folio 4a

For my beloved parents

CONTENT

1. List of original publications

This investigation is mainly based on the following articles, referred to in the text by their Roman numerals.

(I) **Patcas R**, Müller L, Ullrich O and Peltomäki T (2012): *Accuracy of cone-beam computed tomography at different resolutions assessed on the bony covering of the mandibular anterior teeth.* Am J Orthod Dentofacial Orthop 141: 41-50.

(II) **Patcas R**, Markic G, Müller L, Ullrich O, Peltomäki T, Kellenberger CJ and Karlo CA (2012): *Accuracy of linear intraoral measurements using cone beam CT and multidetector CT: A tale of two CTs.* Dentomaxillofac Radiol 41: 637-44.

(III) Karlo CA, **Patcas R**, Kau T, Watzal H, Signorelli L, Müller L, Ullrich O, Luder HU and Kellenberger CJ (2012): *MRI of the temporo-mandibular joint: which sequence is best suited to assess the cortical bone of the mandibular condyle? A cadaveric study using micro-CT as the standard of reference.* Eur Radiol 22: 1579-85.

(IV) Markic G*, Müller L*, **Patcas R**, Roos M, Lochbühler N, Peltomäki T, Karlo C, Ullrich O and Kellenberger CJ (2013): *Assessing the length of the mandibular ramus and the condylar process: a comparison of OPG, CBCT, CT, MRI and lateral cephalometric measurements.* Submitted.

(V) **Patcas R**, Tausch D, Pandis N, Manestar M, Ullrich O, Karlo C, Peltomäki T and Kellenberger CJ (2013): *Illusions of fusions – Assessing cervical vertebral fusion on lateral cephalograms, multidetector computed tomographs, and cone-beam computed tomographs.* Am J Orthod Dentofacial Orthop 143: 213-20.

(VI) **Patcas R***, Signorelli L*, Peltomäki T and Schätzle M (2013): *Is the use of the cervical vertebrae maturation method justified to determine skeletal age? A comparison of radiation dose of two strategies for skeletal age estimation.* Eur J Orthod 35: 604-9.

** These authors contributed equally to the accomplishment of the manuscript.*

2. List of abreviations used

ABM	Alveolar bone margin
AI	Aluminium
ALARA	As low as reasonably achievable
AME	Absolute measurement error
AvIP	Average intensity projection
BMD	Bone mineral density
C2, C3, C4	second, third and fourth vertebrae
CBCT	Cone beam computed tomography
CI	Confidence interval
Co	Condyle
CP	Condylar process
CT	Computed tomography
CV	Coefficient of variation
CVA	Cervical vertebrae anomaly
CVM	Cervical vertebral maturation
DICOM	Digital imaging and communications in medicine
ENT	Ear, nose and throat
FOV	Field of view
Go	Gonial point
GP	Greulich and Pyle
Gy	Gray
H	Horizontal
HA	Hydroxylapatite
HU	Hounsfield unit
ICC	Intraclass correlation coefficient
ICP	Iterative closest points
ICRP	International commission on radiological protection
IE	Incisal edge
In	Incisura mandibulae
JIA	Juvenile idiopathic arthritis
kHz	Kilohertz
kV	Kilovoltage
LC	Lateral cephalogram
LOA	Limits of agreement

List of abreviations used - continued

mA/mAs	Milliampere/Milliamperes-second
MDCT	Multi-detector computed tomography
MGJ	Mucogingival junction
MIP	Maximum intensity projection
MinIP	Minimum intensity projection
MPR	Multiplanar reformatting
MRI	Magnetic resonance imaging
MSCT	Multi-slice computed tomography
NAS	Non-assessable site
OPG	Orthopantomogram
PACS	Picture archiving and communication system
Pb	Lead
RF	Radiofrequency
RH	Ramus height
SD	Standard deviation
SSD	Shaded surface display
STP	Standard temperature and pressure
Sv	Sievert
TLD	Thermoluminescent dosimeter
TMJ	Temporomandibular joint
TW	Tanner and Whitehouse
TWF	Tissue weighting factor
US	Ultrasonography
Voxel	Volumetric pixel, volumetric picture element
VR	Volume rendering

3. Abstract in English

Since its introduction to dental radiology in 1998, cone-beam computed tomography (CBCT) has been subject to a wealth of scientific reports. The two preeminent queries attempted to be answered are its degree of accuracy in the craniofacial region and the radiological burden of a CBCT examination.

The pertinent literature on accuracy can roughly be divided into three groups. Some studies evaluate the influence of device properties and settings, thereby altering voxel-size, varying beam properties (such as kilovoltage, milliampere, field of view, number of projections) or using different post-processing techniques and software. Other studies evaluate the impact different regions of interest have on CBCT accuracy. A third type of study assesses the accuracy by comparing CBCT measurements to other imaging methods of the craniofacial region.

Several studies were published reporting radiation doses of different CBCT devices or settings. However dose reduction implies also loss of information, and radiation doses should always be estimated in context of diagnostic efficacy to enable a risk-benefit assessment.

The aim of this thesis was to perform several investigations considered representative and clinically relevant to establish accuracy and diagnostic efficacy of CBCT, and to determine the radiobiological risk of CBCT examinations in different settings. More specifically, the first aim was to assess CBCT accuracy in the anterior alveolar buccal bone region and to establish the impact of different voxel sizes on accuracy. The second goal was to compare the accuracy of CBCT with multidetector computed tomography (MDCT), placing special emphasis on their sensitivity to metal artefacts. A further objective was the direct comparison of accuracy of linear measurements of mandibular ramus height and the condylar process based on data of 3D (CBCT, MDCT and magnetic resonance imaging (MRI)) and 2D imaging. For this, the best-suited MRI sequence for assessment of the condylar process had to be established, using micro-CT as reference. The purpose of the last investigation on

diagnostic efficacy was to validate the assessment of fusions and osteoarthritic changes in CBCT and MDCT. To evaluate the radiobiological burden of CBCT, dose analysis at different settings, with and without exposure of the cervical spine was performed with the aim to report a risk-benefit recommendation.

Unmitigated embalmed cadaver heads were used to obtain anatomical records which served as reference and corresponding radiological data of 2D imaging and 3D imaging (CBCT, MDCT, MRI, micro-CT) were generated.

The results indicate that voxel size affects precision of CBCT measurements and that alveolar bone of 1mm thickness might be missed completely, even with voxel size of 0.125mm. Compared to MDCT, CBCT appears to be less sensitive to metal artefacts and is slightly more reliable for linear intraoral measurements.

CBCT, MDCT and MRI are almost equal for measurements of mandibular ramus height and the condylar process and more reliable than 2D imaging. MRI is also well suited for cortical bone thickness measurement of the mandibular condyle and for evaluation of osteoarthritic changes in the condyle. Thus, although high reproducibility and precision of CBCT are shown for measurements of ramus height and the condylar process, MRI is recommended since it is not only an equal alternative to CBCT and MDCT, but also circumvents the issue of ionizing radiation.

CBCT data screened by oral radiologists are as reliable as MDCT data viewed by general radiologists to exclude fusions in the cervical spine, but general radiologists appraising MDCT perform better in the assessment of osteoarthritis.

The results of the radiation dose evaluation demonstrate that reducing the field of view or the application of a thyroid shield are both efficient methods to reduce the effective dose and must therefore be implemented.

In conclusion, the clinician's choice over which CBCT setting to use should depend on the intended diagnostic purpose of the scan and on the region of interest. Alternative imaging methods should always be considered and available methods must be implemented to reduce exposure of vulnerable craniofacial tissues.

4. Abstract in Finnish

Kartiokeilatietokonetomografiakuvaus (KKTT) on otettu käyttöön hammaslääketieteellisessä radiologiassa 1998. Tämän jälkeen kaksi pääasiallista tutkimuksen mielenkiinnon kohdetta ovat olleet KKTT:n tarkkuus ja sekä sädeannos kraniofakiaalisella alueella käytettynä.

Tarkkuutta käsittelevä kirjallisuus voidaan jakaa kolmeen ryhmään. Jotkut tutkimukset käsittelevät KKTT-laitteen ominaisuuksia ja asetuksia, kuvantamisvokselin koon vaihtelua, säteen ominaisuuksien vaihtelua (kV, mA, kuvantamiskenttä, projektioiden lukumäärä) tai kuvankäsittelyn tekniikoita ja ohjelmia. Toinen ryhmä tutkimuksia on tarkastellut kuinka kuvaustarkkuus vaihtelee eri anatomisten kohteiden välillä. Kolmanneksi on tutkittu KKTT:n kuvantamistarkkuutta verrattuna muihin menetelmiin.

Useat tutkimukset ovat raportoineet eri KKTT-laitteiden ja kuvausasetusten vaikutusta sädeannokseen. Tosiasia kuitenkin on, että sädeannoksen vähentäminen merkitsee kuvauksella saatavan informaation vähentymistä. Potilaan sädeannos tulisikin aina arvioida suhteessa diagnostiseen tarkkuuteen, jotta haitta-hyöty arvio voidaan tehdä.

Tämän tutkimuksen tarkoituksena oli tehdä useita kliinisesti edustavia tutkimuksia, joiden avulla voitaisiin määrittää KKTT:n diagnostinen tehokkuus ja säteilybiologinen riski käytettäessä erilaisia kuvausparametreja. Ensimmäisen tutkimuksen tarkoituksena oli tutkia KKTT:n tarkkuutta bukkaalisessa alveoliluussa ja määrittää eri vokselikoon vaikutus tarkkuuteen. Toisen tutkimuksen tarkoituksena oli verrata KKTT:n kuvantamistarkkuutta perinteisen monileiketietokonetomografian (monileike-TT) kanssa kiinnittäen erityistä huomiota metallin (hampaiden metallitäytteet, implantit) aiheuttamien artefaktojen haitalliseen vaikutukseen diagnostiikassa. Edelleen tarkoituksena oli tutkia alaleuan ramuksen ja nivelulokkeen pituusmittausten tarkkuutta käytettäessä kolmiulotteisia menetelmiä (KKTT, monileike-TT ja magneettikuvaus eli MRI) verrattuna kaksiulotteisiin

mittauksiin. Tätä varten parhaiten soveltuva MRI-kuvaussarja määritettiin käyttäen referenssinä mikroCT-kuvausta. Diagnostista tehokkuutta tarkastelevan viimeisen tutkimuksen tarkoituksena oli vertailla kaulanikamien mahdollisten fuusioiden ja artriitin havaitsemista KKTT:lla ja monileike-TT:lla. Säteilyn aiheuttaman haitta-hyöty suosituksen aikaansaamiseksi KKTT:n sädeannoksen määrää tutkittiin käyttämällä eri kuvausparametrejä sekä suojaamalla tai jättämättä kaularanka suojaamatta.

Tutkimuksessa käytettiin vahingoitumattomia kadaveripäitä, joista voitiin mitata suorat anatomiset mittaukset ja käyttää näitä referensseinä radiologisilla menetelmillä saaduille vastaaville mittauksille.

Tulokset osoittavat, että vokselikoko vaikuttaa KKTT:lla tehtyjen mittausten tarkkuuteen, ja että pienempi kuin 1mm alveoliluun paksuus saattaa jäädä havaitsematta, jopa käytettäessä 0.125mm vokselikokoa. Metalliartefaktat näyttävät vaikuttavan vähemmän KKTT:n kuin monileike-TT:n kuvanlaatuun. KKTT vaikuttaa myös olevan hieman luotettavampi lineaarisissa suun sisäisissä mittauksissa.

KKTT, monileike-TT ja MRI ovat lähes yhtä hyviä alaleuan pituusmittauksissa ja luotettavampia kuin kaksiulotteiseen kuvaukseen perustuvat mittaukset. MRI soveltuu myös hyvin leukanivelulokkeen kortikaaliluun paksuusmittauksiin ja artriittisten muutosten tarkasteluun. Huolimatta KKTT:n hyvästä toistettavuudesta ja tarkkuudesta alaleuan pituusmittauksissa magneettikuvausta voidaan suositella, koska näin vältetään säderasitus.

Oraaliradiologit tulkitsevat KKTT-dataa yhtä luotettavasti kuin yleisradiologit lukuunottamatta kaulanikamien fuusioita. Toisaalta yleisradiologit olivat hieman parempia havaitsemaan artriittisia muutoksia monileike-TT:llä kuin oraaliradiologit KKTT:llä.

Säteilyannostutkimukset osoittavat, että kuvauskohteen koon pienentäminen tai kilpirauhassuojan käyttäminen vähentävät sädeannosta ja tästä syystä näitä menetelmiä tulisi käyttää.

Yhteenvetona voidaan todeta, että KKTT:n asetuksia määritettäessä tulee ottaa huomioon kuvauksen diagnostinen tavoite sekä kuvauksen kohde. Vaihtoehtoisia kuvausmenetelmiä tulee aina harkita ja käytettävissä olevia menetelmiä soveltaa siten, että sädeannos jää mahdollisimman alhaiseksi.

5. Introduction

Cone-beam computed tomography (CBCT) was first developed in 1982 for angiography procedures (Robb et al. 1982). Since then, this imaging method has been in use in various settings. In 1998, CBCT was introduced to craniofacial imaging (Mozzo et al. 1998), and numerous scientific contributions in orthodontics have been published since 2003 (Baumrind et al. 2003).

Attempts to ascertain CBCT accuracy in the craniofacial region have been made as early as 2004 (Kobayashi et al. 2004, Lascala et al. 2004). Every approach to evaluate the accuracy of a radiological device encounters the problem of which model to use to render the anatomic truth reliably. The methods routinely applied to overcome this systematic problem are (1) the use of geometrical hardware phantoms; (2) the use of anthropomorphic phantoms; or (3) a comparison of the new imaging technology with an existing and established imaging technology (Loubele et al. 2008b).

All these methodologies, however, do not accurately reflect clinical application. Hence, several studies have used dry skulls or macerated mandibles immersed in water. This approach, too, has some serious limitations. Most importantly, the lack of soft tissue has been acknowledged to facilitate the detection of bone surface owing to the increased image contrast and reduced scatter radiation (Ganguly et al. 2011). And besides of failing to reproduce the clinical setting appropriately, the lack of soft tissue simply means to forfeit the possibility to measure it. To overcome all these shortcomings, the use of cadaver heads would be advantageous. Some studies have been performed on animal cadaver heads, especially miniature pigs, based on the fact that the physical properties of the examined tissues resemble those of humans (Wang et al. 2007). Yet, this approach also suffers from different inadequacies. A conscientious assessment must respect the fact that radiologic accuracy is not only determined by *inherent* qualities of the device and its properties and settings such as voxel size (Sun et al. 2011, Maret et al. 2012a),

voltage (Kwong et al. 2008) or current (Panmekiate et al. 2012), but is also constrained by *acquired* limitations. Metal artefacts (Draenert et al. 2007, Pauwels et al. 2011), positioning of the object within the field of view (Nackaerts et al. 2011) and even the mass outside the field of view (Katsumata et al. 2009) have an impact on image quality and accuracy.

Mindful of the abovementioned drawbacks, it would appear that only intact human cadaver heads will suffice to permit a more dependable evaluation. The obvious advantages in regard to accuracy assessment would entail the following:

- The object studied equals exactly the clinical situation in all aspects not necessitating any further approximate surrogate
- The availability of all craniofacial tissues allows to measure different region of interest separately
- The exact size and properties of soft and hard tissues permit to evaluate the accuracy of their measurements individually
- The proper dimensions permit a correct evaluation of the relationship between object and diverse fields of view
- The impact of metal artefacts in clinical setting can aptly be described

This present research will use intact human cadaver heads in order to benefit from all mentioned advantages and to specifically define the research aims according to the new opened possibilities.

Particularly, suggestions about the applicability of CBCT in different regions of interest will be explored. When establishing the benefits of exposing different craniofacial loci, an assessment of the radio-biologic risk will be carried out, in order to offer a clinical recommendation of the risk-benefit assessment involved.

6. Review of the literature on determining CBCT accuracy

6.1. Impact of different settings

6.1.1. Varying the voxel-size

Voxels (i.e. volumetric pixels) are volume elements frequently used in the visualization and analysis of medical data. In CBCT, voxels represent a density value on a regular grid in three-dimensional space. Altering the setting to smaller voxels will enhance the sharpness of the image, but will by the same token increase image noise (Al-Rawi et al. 2010) and, to overcome increased noise, radiation dose must be raised. As a sharper image is no guarantee for a superior diagnostic outcome, standardizing the selection of voxel size would be essential in respecting the "ALARA" (as low as reasonably achievable") principle (Ludlow et al. 2006).

Most CBCT devices offer the possibility to change the voxel size, and the readily availability to opt for different voxel sizes might have been the instigator to many research projects. A recently published systematic review of the literature on the impact of voxel size in CBCT identified 20 publications on this issue alone (Spin-Neto et al. 2013). Since the printing of this systematic review, at least four further articles have been published on the impact of different voxel size. Among these studies, most were based on categorical outcome, assessing:

- the detection of root fracture (Wenzel et al. 2009, Melo et al. 2010, Ozer 2011, da Silveira et al. 2013)
- the detection of internal or external root resorption (Liedke et al. 2009, Kamburoglu and Kursun 2010, Dalili et al. 2012, Neves et al. 2012)
- the detection of caries lesions (Haiter-Neto et al. 2008, Kamburoglu et al. 2010, Cheng et al. 2012)
- the detection of erosions in temporomandibular joints (Librizzi et al. 2011)
- the presence of root canals in molars (Bauman et al. 2011)
- the detection of peri-implant fenestration and dehiscences (de-Azevedo-Vaz et al. 2013)

The remaining studies were based on numerical data, assessing:

- linear bone measurements (Sun et al. 2011, Torres et al. 2012)
- linear tooth measurements (Sherrard et al. 2010)
- linear soft tissue measurements (Fourie et al. 2010)
- measurements of surface rendered reconstruction of teeth (Al-Rawi et al. 2010, Maret et al. 2012a, b, Ye et al. 2012) or bone (Damstra et al. 2010)

It is of interest to note that of all these studies, only one (Fourie et al. 2010) has been performed on intact human cadaver heads.

The results of the listed publications are often contradicting, both for categorical and numerical data. For example, some authors suggest that high resolution CBCT should be used when a root fracture must be diagnosed (Wenzel et al. 2009, Melo et al. 2010), whilst others do not find significant differences when altering the voxel size (Ozer 2011, da Silveira et al. 2013). Similarly, while some authors attest a greater accuracy of high-resolution scans detecting root resorption (Kamburoglu and Kursun 2010, Dalili et al. 2012, Neves et al. 2012), others produced similar results with different scan protocols (Liedke et al. 2009). When assessing accuracy in terms of numerical data, the same dichotomy can be observed. Bone measurement was found to be more exact with high-resolution scans by some authors (Sun et al. 2011), while, again, some differed (Damstra et al. 2010, Torres et al. 2012).

Spin-Neto and co-authors conclude in their systematic review that studies dealing with categorical data showed a tendency towards more accurate results with high-resolution protocols, while this was not the case for studies with numerical data (Spin-Neto et al. 2013). Hence, when assessing the impact of voxel size, it will be of importance to investigate the nature of the statistical approach as well (see 10.1.2. for an elaborate discussion on this subject).

6.1.2. Varying beam properties

Dose reduction implies loss of information. As mentioned above (6.1.1.), the amplitude of information loss due to voxel size increase has been subject of many investigations. To a much lesser extent, the impact of dose reduction on image quality due to alteration of beam properties has been explored. Kwong and co-authors (Kwong et al. 2008) noticed that the kilovolt setting did not affect overall image quality and images taken at lower milliampere settings showed good diagnostic quality. Their findings were partially echoed in other studies that demonstrated significant dose reduction achieved by reducing tube current without substantial loss of image quality in CBCT (Palomo et al. 2008, Sur et al. 2010). All three studies registered image quality according to subjective categorizing of independent observers. Only more recently, a further study was published establishing that lower peak kilovoltage and milliampere values might also be used for linear intraoral measurements, as no significant differences in the measured distances were found among the different combinations of radiographic parameters (Panmekiate et al. 2012).

Further contributions have been published intending to present optimized exposure parameters with specific values for electric potential and current in cone-beam CT for sialography (Jadu et al. 2011) and multi-detector CT for ENT-diagnostics (Lanfranchi 2012).

6.1.3. Other changes in image acquisition

Parsa and co-workers investigated the influence on image quality of scan settings, including field of view (FOV), spatial resolution, the number of projections and exposure time (Parsa et al. 2013). To determine image quality, the grey value variation at an implant site was chosen and compared to multislice CT (MSCT) values. They noticed that grey values significantly deviated from the Hounsfield unit values obtained with MSCT and were strongly influenced by FOV and spatial

resolution. Depending on the device, the number of projection, exposure time and dose selection also had a significant influence on grey values.

Reconstruction kernel also has an effect on resolution and noise. However, most if not all CBCT devices do not offer its alteration as a user selectable option.

The effect of slice thickness and interslice interval on reconstructed CBCT images was the subject of a study by Chadwick and Lam (Chadwick and Lam 2010). By measuring bone height, statistically significant differences could be observed when slice thickness varied by more than 1mm. This result underlines the importance to report the exact slice thickness used when reading the data, especially to enable proper comparative conclusions.

Numerous articles have highlighted the problems caused by the incorrect positioning of patients while obtaining panoramic radiographs, i.e. orthopantomograms (OPG) (Updegrave 1971, McDavid et al. 1981, Schulze et al. 2000), and similarly recent studies aimed to examine the influence of different positioning in CBCT on linear measurement accuracy (Dantas et al. 2005, Visconti et al. 2013). The authors of both studies independently discerned that only a deviation of more than 20° off the standard position presented problematic differences in the measurements of bone height. Interestingly, both studies also showed that image accuracy was affected differently at various locations. Congruently, the results of a further preliminary study on a dry skull suggest that the three-dimensional cephalometric analysis on CBCT data is influenced by patient scanning position (Frongia et al. 2012). Thus, the findings highlight the importance of proper positioning in CBCT.

6.1.4. Different post-processing techniques

Radiological 3D imaging data can be post-processed in various ways. The most common visualization modes include multiplanar reformatting (MPR), shaded surface display (SSD) and volume rendering (VR). Volume rendering is a set of visualization techniques used to display a 2D projection of a 3D discretely sampled

data set and includes several techniques, such as volume ray casting, maximum intensity projection (MIP), average intensity projection (AvIP) or minimum intensity projection (MinIP). In radiology, MIP and MinIP are probably the most commonly used methods. Maximum Intensity Projection (MIP) consists of projecting the voxel with the highest attenuation value on every view throughout the volume onto a 2D image, and it is therefore the method preferentially used to display bone and contrast material–filled structures. Conversely, Minimum intensity projection (MinIP) enables the detection of low-density structures and is optimal for hypodense structures.

No direct comparison of accuracy of different post-processing modalities has yet been performed in CBCT, but a recent review postulates that point-to-point measurements made in the MPR mode are highly accurate when compared with physical skull measurements, whereas the surface anatomy measured in VR and SSD modes have a greater measurement error when compared with direct physical measurements (Kapila et al. 2011).

Different post-processing protocols have, however, been compared directly to each other in multidetector computed tomography (MDCT). Zhang and co-workers assessed the detections of ossicular chain's damage in 70 patients with otitis media based on MPR, VR and SSD reconstructed data. They concluded that both MPR and VR were relative robust for representation of small ossicular osseous structures, but SSD is not effective for evaluation of such small structures, particularly the stapes (Zhang et al. 2013). Similarly, a study on CT-evaluation of glenoid bone defect in unilateral anterior gleno-humeral instability attested that the agreement between MPR- and VR-CT measurements to identify size and type of bone defect was so high that the two measurements could be considered interchangeable (Magarelli et al. 2012). For angiography purposes, there seems to be evidence that MIP is superior to MPR, but less reliable than VR (Sparacia et al. 2007). Assessing the role of different types of reconstruction of CT imaging, further research evinced similarly that depending of pathology and site, different post-processing protocols may be required to improve the diagnostic efficacy (Myga-Porosilo et al. 2011). If that is truly

the case, much ground might still have to be covered for CBCT, as only one study could be identified on this subject (Hassan et al. 2013). Hassan and co-authors assessed the precision of identifying cephalometric landmarks on CBCT on both VR and MPR images. Although not aiming to perform a direct comparison, their results indicate that adding MPR images does indeed seem to increase the precision of identifying cephalometric landmarks. The authors argued that thin pointed structures such as the anterior and posterior nasal spine can be extremely threshold sensitive and are therefore more reliably identified with MPR.

6.1.5. Influence of software

More recently, some publications have appeared on the influence of the software on image accuracy (Kim et al. 2012b, Spin-Neto et al. 2013, Wood et al. 2013). Although the evidence is based on this selected amount of studies, the results seem to indicate that the software choice does not alter image accuracy in a relevant way. The implication thereof is, that every practitioner or researcher reading CBCT data should use the software she or he feels most comfortable with, in order to enhance the confidence when evaluating the data.

6.2. Regions of interest to define CBCT accuracy

6.2.1. The lower front as region of interest

Lower incisors play an essential role in orthodontic treatment planning because of their very restricted anatomical leeway within the symphysis. Clinical experience indicates that important limitations to anterior-posterior incisor movement are operative and that alveolar bone does not accommodate unlimited tooth movement (Edwards 1976, Handelman 1996). Hence, the assessment of the bony covering is pivotal when planning any tooth movement of the mandibular incisors, as it has been demonstrated that excessive sagittal movements or tipping may result in significant recession of the gingival margin and in bony dehiscences (Batenhorst et al. 1974, Dorfman 1978, Hollender et al. 1980, Steiner et al. 1981, Wennstrom et al. 1987, Fuhrmann 1996, Handelman 1996, Sarikaya et al. 2002, Yared et al. 2006). Although some reports indicate that the very fact of merely having being treated orthodontically and retained with a fixed retainer may be a risk factor for recessions (Renkema et al. 2013b), it must be noted that many investigators failed to find any association between orthodontic tooth movement and gingival recessions (Artun and Krogstad 1987, Ruf et al. 1998, Djeu et al. 2002, Melsen and Allais 2005, Renkema et al. 2013a).

Clinical predictors of dehiscences and fenestrations have not been well defined, and apart from orthodontic tooth movement, several other etiologic factors have been examined and suggested, including developmental anomalies, frenulum attachments, as well as periodontal and endodontic pathologies (Rupprecht et al. 2001). Whilst alveolar dehiscences and fenestration in the lower front region are common findings described in various populations, it is agreed that an especially narrow symphysis is a common etiological factor in the development of fenestrations and dehiscences (Artun and Krogstad 1987, Wehrbein et al. 1996, Rupprecht et al. 2001). Thus, an exact image rendering of the bony covering in the lower front would be beneficial to examine this etiological factor. Due to its clinical importance, the

anterior alveolar bone is therefore a perfect site to base an evaluation on CBCT accuracy of delicate structures (Figure 1).

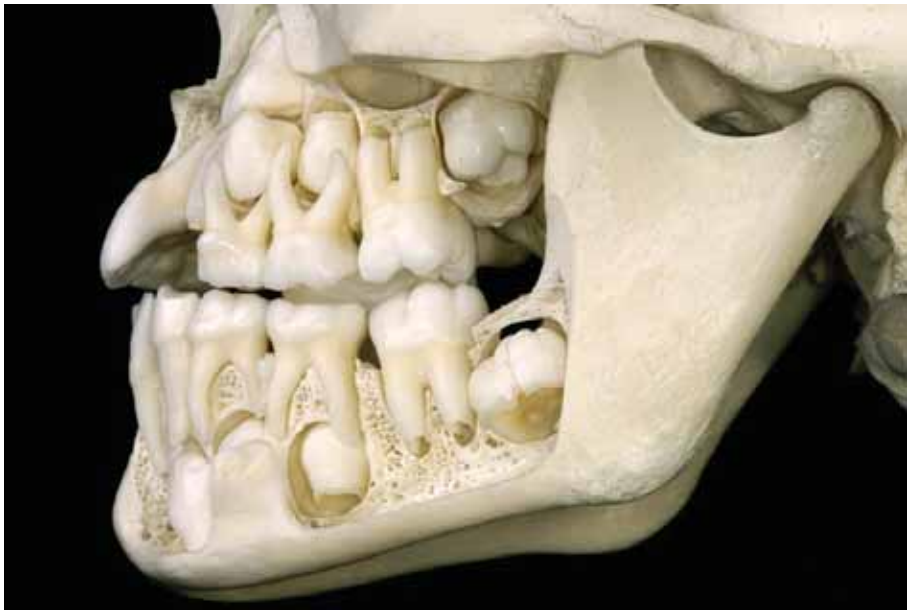

Figure 1. *Macerated and prepared human skull. Note the delicate bony structures. Specimen from the collection of the Department of Orthodontics and Pediatric Dentistry at the University of Zurich.*

6.2.2. The cervical spine as region of interest

In the last decade, orthodontists have expressed increasing interest to assess the cervical spine on a lateral cephalogram. In general, three clinical purposes are being stated:

(1) The depiction of the cervical vertebrae C2, C3 and C4 enables an assessment of skeletal maturity, based on the association between age-related morphological changes of these cervical vertebrae and the somatic growth curve (Hassel and Farman 1995, Baccetti et al. 2002).

(2) The delineation of the craniocervical angulation permits to characterize head posture. Head posture has been linked to nasorespiratory (Huggare and Laine-Alava 1997) and craniofacial morphology (Kylämarkula and Huggare 1985, Solow and Sandham 2002), and might therefore be of clinical relevance.

(3) The fact that the spine is clearly visible on cephalograms has perpetuated the recommendation of the study of congenital anomalies of the cervical

vertebrae, given that cervical vertebral anomalies (CVA), particularly fusions, could be related to certain craniofacial syndromes and other dentoskeletal malformations, and may likewise have an influence on the therapy.

These fusions are most common between the facet joints of the second and third vertebrae (C2-C3; see Figure 2).

Figure 2. *Congenital fusion of the right facet joint C2-C3. Note that this specimen is from the collection of the Anatomical Institute of the University of Zurich and is not part of the assessed specimens.*

Like all other CVAs, osseous fusions are usually asymptomatic (Klimo et al. 2007) and taxed as coincidental findings with no clinical relevance (McRae 1960). However, in a minority of patients, CVAs cause compression of neurological structures or biomechanical instability leading to chronic pain (Klimo et al. 2007). Associations between cervical vertebral anomalies, notably fusion of C2-C3, and congenital disorders or dentoskeletal malocclusions, have been studied extensively. These associations include syndromic and non-syndromic anomalies such as fetal alcohol syndrome (Tredwell et al. 1982) or cleft lip and palate (Ross and Lindsay 1965, Sandham 1986, Horswell 1991, Rajion et al. 2006). In recent studies using lateral cephalograms, high prevalence of CVAs, particularly fusions of C2-C3, was reported in orthodontic surgical patients with severe skeletal malocclusions. The described

associations between cephalometric measurements and fusions include skeletal Class III and mandibular overjet with 61.4% fusions (Sonnesen and Kjaer 2007a), skeletal deep bite with 41.5% fusions (Sonnesen and Kjaer 2007b), skeletal open bite with 42.1% fusions (Sonnesen and Kjaer 2008b), skeletal Class II and maxillary overjet with 28% and 52.9% fusions, respectively (Sonnesen and Kjaer 2008a, Arntsen and Sonnesen 2011). A similarly high prevalence of fusions has been documented in subjects with condylar hypoplasia with 72.7% fusions, of which 45% in C2-C3 (Sonnesen et al. 2007) and in patients with obstructive sleep apnea with 46% (Sonnesen et al. 2008b).

Awareness that the spine is of clinical interest has led to the recommendation to use cephalometric radiographs to routinely screen the cervical vertebrae for anomalies and even to develop a tracing technique of this region (Vastardis and Evans 1996).

CBCT assessments of the cervical spine are diverse, and few. The first reported investigation appeared in 2007 and aimed to present a novel segmentation algorithm for automatic 3-dimensional reconstruction of individual cervical vertebrae from CBCT volumetric data sets (Shi et al. 2007). Then, the evaluation of skeletal maturation has been the topic of two more recent investigations (Joshi et al. 2012, Shim et al. 2012), which contradicted each other on the reliability of the cervical maturation method based on CBCT images. Lastly, a recent study compared the detection of cervical fusion on CBCT and on lateral cephalograms in 21 patients (Bebnowski et al. 2012). Whilst nine cases yielded a potential fusion based on the tracing technique developed for lateral cephalograms, none of the suspected fusions could be confirmed by CBCT.

All other publications on CBCT assessments of the cervical spine focus on incidental findings in the cervical spine, and most of them are case reports. A single retrospective study on incidental findings in CBCT consultations concluded that CBCT scans frequently revealed pathologies in the spine region, and recommended a comprehensive review of the entire CBCT image (Pette et al. 2012). A further case

report portrayed a coincidentally detected osteomalacia in a 23-year-old female, represented with pseudo-fracture and porous vertebrae C2-C4 on CBCT image (Cakur et al. 2012).

Yet, most commonly, either fusions or clefts of vertebral bodies are being described. A recent paper reported the clinical case of Klippel-Feil syndrome, which is characterized by a clinical triad consisting of congenital fusion of at least 2 of 7 cervical vertebrae with a short neck, limited head motion, and a low posterior hairline. CBCT imaging revealed cervical vertebrae anomalies and a submucous cleft palate (Park et al. 2012). In another paper an incidental finding of an atlas cleft due to a defect in one of the ossification centres of the vertebrae is being discussed (Rogers et al. 2011), and an older publication likewise presents two patients for whom CBCT was carried out for orthodontic related purposes and incidental findings of cervical vertebrae clefts were diagnosed (Popat et al. 2008).

Many others have written that a comprehensive review of the entire CBCT image, preferably by radiologists, is necessary to reveal coincidental findings. However, as mentioned above, either fusions or clefts of vertebral bodies are usually being described. Although these pathologies may present themselves with various patterns ranging from transient pain to different degrees of cord compression, including myelopathy, most of the cases remain asymptomatic. One should consider that a significant number of those incidental findings may represent nothing else than normal anatomic variations, which do not require further intervention (Halazonetis 2012). Thus, in absence of any signs or symptoms, the clinical benefit of diagnosing such coincidental or occult finding appears very limited.

At present, the reliability of CBCT data in the cervical spine has not been adequately assessed. Yet, the increasing amount of publications of CBCT on the cervical spine and the fact that many cephalometric studies are being validated through CBCT data, render such an investigation a necessity. Thus, a clarification of the diagnostic use and reliability of CBCT data of the cervical spine would allow a more differentiated interpretation of the present literature.

6.2.3. The condyle and temporomandibular joint as region of interest

The temporomandibular joint (TMJ) and the condyle length are of utmost diagnostic importance (Figure 3). The lengthening of the mandibular ramus and the condylar process largely reflects the growth of the mandible, as was revealed by implant growth studies (Björk 1963, 1968). Length changes of mandibular ramus and condylar process not only reflect growth, but also destructive processes in the TMJ. In growing patients the TMJ has both articulation and growth function, and children diagnosed with destructive processes in the TMJ will experience impaired mandibular growth and compromised masticatory function (Bache 1964, Ronning et al. 1994, Kjellberg et al. 1995, Ronchezel et al. 1995).

Figure 3. *Detail of the temporomandibular joint. Especially condylar and ramus length are of high clinical significance.*

Juvenile idiopathic arthritis (JIA) is the most common rheumatic disease in childhood (Gare 1996), and can severely damage all involved joints and cause short- and long-term disabilities (Weiss and Ilowite 2005). All synovial joints can be affected including the TMJ (Pedersen et al. 2001, Twilt et al. 2004). Reported frequencies of TMJ involvement in JIA vary from approximately 17 to 87 per cent, depending on inclusion criteria and radiological approach used (Pirttiniemi et al. 2009). An

involvement of the TMJ will have an impact on craniofacial development and may involve a posterior rotated, retorgnathic and sometimes also micrognathic mandible with overall small dimensions, steep mandibular plane, short ramus, obtuse gonial angle with increased bone apposition and antegonial notching, decreased posterior facial height, increased anterior facial height, convexity with a bird face profile and usually a dental Angle Class II/1 with increased overjet and anterior open bite (Bache 1964, Barriga et al. 1974, Larheim and Haanaes 1981, Jämsä and Rönning 1985, Kreiborg et al. 1990). JIA cases with only unilaterally affected TMJ will develop skeletal and dental asymmetries of various degrees (Karhulahti et al. 1990, Twilt et al. 2004).

The therapeutic success in TMJ depends widely on an early diagnosis of JIA (Kjellberg et al. 1995, Kuseler et al. 2005, Twilt et al. 2007, Stoustrup et al. 2011), but clinical diagnosis is difficult because clinical signs and symptoms occur variably, occasionally with considerable time lag or are missing altogether (Twilt et al. 2004, Kuseler et al. 2005, Pedersen et al. 2008, Müller et al. 2009). It is generally thought that in JIA synovitis is the underlying cause of subsequent cartilage and then osseous changes. Activity of the disease, even before osseous changes appear, is therefore best appreciated with contrast enhanced MRI.

Measurements of condylar and ramus lengths are also considered of high diagnostic value for assessment of initial therapeutic success and an important indicator during follow-up (Stoustrup et al. 2008). Many studies have based their results on measurement of the condylar process and ramus height of JIA patients on different radiographic images, such as OPG, lateral and postero-anterior cephalograms, MDCT or more recently CBCT (Kjellberg et al. 1994, Kjellberg et al. 1995, Twilt et al. 2006, Stoustrup et al. 2008, Stoustrup et al. 2011).

Conversely, magnetic resonance imaging (MRI) of the TMJ is considered the imaging technique of choice for internal derangements in inflammatory conditions and degenerative changes (Magnusson et al. 2000, Moen et al. 2010). The main strengths of MRI are the detailed illustration of soft tissue abnormalities, including

the articular disc, as well as the reliable depiction of bone marrow oedema and detection of even small initial destructive lesions (Lee et al. 2008, Pirttiniemi et al. 2009). Although MRI has the ability to illustrate all common osseous signs of TMJ arthritis, i.e. condylar head flattening, osseous erosions, subchondral bone cysts and anterior osteophytes, their true extent remains uncertain (McGibbon et al. 2003).

Since MRI data contain pivotal information about the inflammatory process, it would be of great clinical interest to determine if MRI data could also be used for bone measurement of the condylar process and mandibular ramus. Therefore, an assessment of the reliability of the representation of cortical bone structure of the TMJ would yield an important clinical contribution.

As mentioned, measurements of condylar and ramus lengths are considered of high diagnostic value. The reliability of linear measurements of ramus and condyle in different imaging methods remains subject to clarification. Comparative research of measurements based on 3D data such as MRI, CBCT and MDCT imaging, as well as 2D data such as OPG and lateral cephalography, would therefore be a welcome addition to enrich the present state of knowledge.

6.3. Comparison of CBCT accuracy to other three-dimensional imaging methods

6.3.1. Comparison to MDCT

The independent findings of Hounsfield and Cormack revolutionized diagnostic imaging by introducing computed tomography (CT) (Angelopoulos et al. 2012). For the first time, practitioners had access to X-ray devices that could generate narrow cross-sectional images, usually perpendicular to the long axis of the human body. The original fan-beam technology has subsequently been refined to incorporate a helical or spiral synchronous motion, and multiple detector acquisition (MDCT), which enables fast scan times and provides images that can be combined into a volumetric dataset.

Multiple investigations have been conducted to compare CBCT and MDCT. Although very similar, both techniques comprise inherent differences, apparent in all four steps of the image acquisition, i.e. X-ray generation, X-ray detection, image reconstruction and display (Angelopoulos et al. 2012). An adequate understanding of the characteristic dissimilarities in the properties of both image data is necessary to draw an appropriate comparison.

One particular advantage of CBCT data volume is its composition of isotropic voxels providing the same spatial resolution when reconstructed in multiplanar image reformations (MPR) (Farman and Scarfe 2009). In contrast to this, conventional MDCT data are composed of anisotropic voxels, as the coronal dimension (i.e. along the z-axis) is determined by several factors like slice collimation and pitch (i.e. table travel per rotation divided by the collimation of the X-ray beam) (Silverman et al. 2001). The spatial resolution in the z-axis of current MDCT scanners is limited to 0.4 - 0.6mm, and therefore decreases when reconstructed from the original raw data. Most CBCT devices are capable of providing a minimal voxel resolution between 0.07 and 0.25 mm, exceeding most commercially available high resolution MDCT scanners (Farman and Scarfe 2009).

On the other hand, CBCT imaging presents a few drawbacks. The displayed grey scale values in CBCT are arbitrary, do not correspond to the Hounsfield unit (HU) scale used in MDCT, and reportedly differ from device to device (Mah et al. 2010). Yet the ability to derive HU from grey levels would open new opportunities for qualitative appraisals and comparative research. Mah and co-workers (Mah et al. 2010) attempted to convert grey scale in CBCT into a "rescaled HU" with a proposed coefficient. However, Bryant et al. argued that grey scale value of CBCT varies linearly with the total mass in the slice (Bryant et al. 2008, Bryant 2011). The grey scale value will therefore not only depend on the attenuation coefficient measurement as described by the Hounsfield equation, but also on the total mass of the object. A further limitation of CBCT imaging is that structures outside the limited field of view (FOV) may produce density variability in the scanned volume and cause a decrease of image contrast (van Daatselaar et al. 2004, Katsumata et al. 2007, 2009, Araki and Okano 2011). Last, as compared to MDCT, CBCT images are associated with increased noise and scatter radiation (Endo et al. 2001), which result in less soft tissue contrast resolution (Mozzo et al. 1998, Arai et al. 1999, Araki et al. 2004). Therefore, it has been argued that CBCT is solely suitable for evaluating calcified structures such as bone or teeth, since it provides images of highly contrasting structures well (Mozzo et al. 1998, Arai et al. 1999, Farman and Scarfe 2009).

Defining image quality and comparing differences between CT and CBCT systems is problematic. Objective assessment of image quality, at least in MDCT, is based on quantitative measurements of particular patterns in a test object (Angelopoulos et al. 2012). These measurements include MDCT contrast resolution, image homogeneity and uniformity, point spread or modulation transfer function, and metal artefacts; however, no such tool has been accepted for image quality assessment in CBCT (Angelopoulos et al. 2012). Because of these differences, only few investigators have compared directly the image quality of comparable objects using both CBCT and MDCT. Mostly, the evaluation was based on either a dry

mandible (Suomalainen et al. 2008, Liang et al. 2010a, Liang et al. 2010b), on a maxilla (Hashimoto et al. 2003, Hashimoto et al. 2006, Loubele et al. 2006, Hashimoto et al. 2007), on both (Mischkowski et al. 2007, Al-Ekrish and Ekram 2011), dry skulls (Kim et al. 2012a, Kim et al. 2012b, Zain and Alsadhan 2012) or on an anthropomorphic phantom (Hashimoto et al. 2003, Loubele et al. 2007, Mischkowski et al. 2007, Loubele et al. 2008a, Suomalainen et al. 2008, Carrafiello et al. 2010). To the best of our knowledge, only four studies have been published so far using intact human heads to compare the performance of CBCT and MDCT in the dentomaxillofacial area (Heiland et al. 2007, Carrafiello et al. 2010, Naitoh et al. 2010, Hofmann et al. 2013). However the focus has been laid predominantly on image quality, and not on accuracy of measurements. Furthermore, in all four studies the obtained measurements were not compared with anatomical measurements.

6.3.2. Comparison to MRI

In Magnetic Resonance Imaging (MRI), a strong static magnetic field is used to align the magnetization of ^{1}H, and radiofrequency (RF) pulse is applied, which causes the nuclear spins to resonate in the static magnetic field. This causes the protons to produce a rotating magnetic field and re-emit a RF signal detectable by the scanner. Based on this detectable water proton signal, MRI provides good contrast between the different soft tissues. Conventional MRI cannot, however, easily visualize calcified tissues such as bone or teeth because of their physical properties; the water signal is low, and has additionally a highly restricted molecular motion within the densely mineralized tissues, causing the signal to decay very quickly after RF excitation (Idiyatullin et al. 2011). In highly mineralized dental tissues with nearly no water, the signal decays before MRI signal digitization occurs, resulting in MRI images with little or no image intensity. Such areas are called “black zones”. The diagnosis of dental pulp diseases is further impaired because of its location within a relatively hard tissue, i.e. dentin (Idiyatullin et al. 2011).

Consequently, MRI of the dental and bony structures is very challenging, since teeth and bony structures give little to no MRI signal. Additionally, air content and metal artefacts within the oral cavity can seriously impair the quality of MRI data (Gaudino et al. 2011).

Most scientific contributions determining the clinical applicability of MRI in the maxillofacial area can basically be divided into two approaches:

- The study either focused on analysing the additional benefits of visualizing soft tissues with MRI,
- or evaluated if the information on hard tissues in MRI provided through contrast is sufficient to assess bony structures.

MRI assessment of soft tissues in dentistry has been applied to imaging pulp, periodontal ligament, the mandibular nerve and the temporomandibular joint disc (Gaudino et al. 2011, Idiyatullin et al. 2011, Chau 2012). Due to its excellent soft tissue contrast and its high sensitivity to detect oedema, MRI is recommended as a complementary imaging technique to visualize particular intraoral pathological processes such as pulp inflammation, periodontal pathologies or teeth vascularization after trauma or autotransplantation (Gaudino et al. 2011).

MRI proved to be superior to MDCT and to CBCT in visualizing periodontal structures and can be applied to differentiate a granuloma from a cyst (Kai et al. 2011). MRI images may also be helpful in identifying the mandibular nerve location. The high image contrast between the mandibular nerve and the bony structures provides lesser variability than CBCT images in determining the locations of the mandibular nerve, the mental and mandibular foramen (Chau 2012). Finally, a position paper stated that MRI is accepted as the most reliable modality on which to base TMJ diagnosis and therapeutic decisions (Brooks et al. 1997).

Several investigations have aimed to enhance the image quality of MRI in order to render this method more applicable to delicate structures which are of interest in dentistry. For example, MRI systems with higher magnetic field strength display an increased signal-to-noise ratio, producing clearer images. Analyses

comparing 1.5 Tesla to 3.0 Tesla MRI concluded that with comparable examination sequences and identical resolution, the 3.0 Tesla MRI of the temporomandibular joint increases the perceptibility of joint structures (Schmid-Schwap et al. 2009). Others developed a novel MRI technique called SWeep Imaging with Fourier Transformation (SWIFT). Magnetic resonance imaging based on SWIFT offers simultaneous three-dimensional hard and soft tissue imaging of teeth in clinically relevant scanning times (Idiyatullin et al. 2011). A third interesting approach consists in superimposing and registration of MRI data on CBCT data (Tai et al. 2011). CBCT and MRI images obtained within one week are registered by the iterative closest point (ICP) method. Measurement errors of composite MRI-CBCT have been studied and found to be not significant (Tai et al. 2011).

The second form of investigation on the general applicability of MRI in maxillofacial imaging is the evaluation of information gained on hard tissues through contrast. Although it is questionable whether measuring small structures of about 1 to 3 mm in MRI provides accurate data (Kai et al. 2011), reports seem to indicate that clinically valuable information can be deducted. Using CBCT as the reference, one study determined the diagnostic accuracy of MRI for assessing osseous abnormalities of TMJ (Alkhader et al. 2010). Although high specificity (84-98%) was obtained with MRI, it showed relatively low sensitivity (30-82%) for detecting osseous abnormalities of the TMJ. The authors concluded that the value of MRI remains limited for the detection of TMJ osseous pathologies. Another study evaluated the accuracy of linear measurements in MRI and CBCT (Kai et al. 2011). Measurements of the roof of the glenoid fossa were thicker on MRI than those on CBCT, but a moderately strong correlation existed between measurements by these 2 modalities.

Only one systematic evaluation has appeared so far comparing MDCT, CBCT and MRI imaging quality (Gaudino et al. 2011), and there is an evident lack of scientific data on this subject.

6.3.3. Comparison to micro-CT

The first publication on micro-computed tomography (μ-CT) appeared in 1982 (Elliott and Dover 1982). Due to the availability of commercial μ-CT systems, studies of microcomputed tomography have increased drastically over the last few years. μ-CT is ideal for imaging very small structures at submicron level, and is especially suited for biomedical and material specimens. Owing to the high resolution it offers, μ-CT measurements are regularly used as reference values. Although μ-CT has established itself as a technique of choice to evaluate CBCT accuracy, high radiation dose and long scanning time restrict its use to *in vitro* specimens.

Comparative research of CBCT and μ-CT is limited to linear alveolar bone measurements, volume measurements of osseous lesions, detection root resorption and root canal length assessments. Comparing CBCT measurements of alveolar bone to μ-CT data, Ferrare deduced that CBCT underestimated bone height and that thin bone may not be visualized on CBCT images (Ferrare et al. 2013). The accuracy of periapical lesion measurements has been investigated by two other studies (Ivekovic et al. 2012, Ahlowalia et al. 2013). Both described similar precision for volumetric measurements for CBCT and μ-CT of artificially created osseous cavities. In a further comparative evaluation of CBCT with μ-CT to visualize the root canal system, Szabo and co-workers demonstrated that only high resolution CBCT devices allow dentists detecting the full length of the root canal (Szabo et al. 2012). Two studies exist on the evaluation of CBCT accuracy of external root resorption with μ-CT as reference, but their results and conclusion are contradictory (Ponder et al. 2013, Wang et al. 2013).

A somewhat neglected feature of μ-CT in the maxillofacial area is the ability to perform diagnostics of bone microstructure, such as bone density, trabecular thickness or trabecular separation. In osteoporosis, bone mineral density (BMD) is reduced and bone microarchitecture deteriorated. The importance of monitoring bone microstructure and bone mass is becoming increasingly apparent, since in Western countries the majority of individuals aged 50 and above are affected by osteoporosis. New μ-CT devices for *in vivo* assessment of human radius and tibia

have therefore been introduced (Popp et al. 2012). Regrettably, there are no reports that these advances were ever implemented in the maxillofacial area, enabling *in-vivo* μ-CT assessments of alveolar bone and teeth.

6.3.4. Comparison to ultrasonography

Although the benefits of ultrasonography (US) as a non-invasive and painless method with no radiation burden would seem to make it a viable alternative, scientific reports on the use of ultrasound in the oral cavity are rare and often contradictory in their recommendations. Some studies conclude that the anatomy of the periodontal system is too complex for US examination (Palou et al. 1987, Aggarwal et al. 2008, Ghorayeb et al. 2008), while others suggest that the evaluation and monitoring of periodontal diseases could be performed with US (Chifor et al. 2010, Chifor et al. 2011, Salmon and Le Denmat 2012). Still others argued that ultrasound should be used as additional tool in sialography (Poul et al. 2008) or in differentiating periapical lesions, as it underestimates the extent of the disease, but could provide accurate information on the pathological nature of the lesion, i.e. cyst versus granuloma (Gundappa et al. 2006).

Two important technical barriers limit the oral application of ultrasonography. First, it is vital to know that increasing the frequency of ultrasonic transmission will improve the image resolution, but will at the same time decrease the depth of exploration. Thus, frequencies above 25 kHz are preferable, as a scant depth of exploration is often sufficient in maxillofacial imaging. Second, a miniaturized transducer is necessary for clinical ultrasound assessment in the oral cavity. Most scientific explorations in the oral region have, however, been performed from borrowed ophthalmological or dermatological clinical equipment with inferior frequencies and inadequate transducer size, and only recently custom-made devices have been tested to explore intraoral soft tissues (Salmon and Le Denmat 2012). Although feasibility and usability have been demonstrated satisfactorily, this

promising device still needs large-scale clinical studies to validate its diagnostic value to determine its accuracy of linear measurements and diagnostic efficacy.

Only two research reports assessing the accuracy of intraoral linear measurement of US are available (Palou et al. 1987, Chifor et al. 2011). Palou and co-authors evaluated its precision in comparison to direct anatomical measurements, Chifor and co-workers correlated ultrasound measurements to CBCT and direct microscopic measurements. Both studies, however, are of little value, as Palou's research reporting poor accuracy was performed over 25 years ago with devices no longer in use, and Chifor's statement of adequate accuracy is based on erroneous statistics and a sample consisting of 4 pig heads with a total of 20 performed measurements. It is therefore safe to voice concern that more comparative work with more dependable data is required to permit a valid statement on accuracy of intraoral ultrasonographic images.

In contrast to the irresolute use of ultrasonography for dental and periodontal measurements, US has successfully been applied to examine other surrounding facial tissues. Ultrasonography is an established method to measure the cross-section and thickness of muscles in vivo, thereby providing an indication of the maximal force a muscle can exert (Kiliaridis and Kalebo 1991). Thus, US has been proven to be a reliable diagnostic technique for the evaluation of several muscles of the head and neck (Raadsheer et al. 1994, Emshoff et al. 1999). More specifically, it has been in use to diagnose alterations of mastication muscles due to facial morphology (Kiliaridis and Kalebo 1991, Charalampidou et al. 2008) and to study muscles changes occurring during growth or orthodontic therapy (Kiliaridis et al. 2010). The consensus is that for the investigation of mastication muscles, it should be preferred in comparison to CT or MRI (Serra et al. 2008).

Moreover, US has been proposed as an alternative to MRI in the assessment of TMJ, allowing visualization of the joint in function (Jank et al. 2007). However, this has been disputed, as these authors only reported on diagnoses of *severe* destructive TMJ changes (Pirttiniemi et al. 2009).

Finally, US has been used as a tool to assess tongue posture (Volk et al. 2010) and swallowing pattern (Ovsenik et al. 2013). The latter study investigated the swallowing pattern and tongue function during swallowing in children with unilateral crossbite in deciduous dentition using B-mode (i.e. brightness mode) and M-mode (i.e. motion mode) ultrasonography. Yet, some claim that images performed with B-mode and M-mode are not suitable for differentiating between different swallowing patterns (Galen and Jost-Brinkmann 2010). Therefore, more dependable data are needed to declare US a suitable tool for the assessment of tongue posture and swallowing pattern.

Besides of imaging capabilities, ultrasonic sensors offer the possibility to evaluate the density of tissues. Recently, ultrasound transmission velocity (UTV) has been introduced, at least on a pre-clinical level including a comparative ex vivo study (Kammerer et al. 2012), as a non-invasive and non-ionizing method to analyse mechanical properties of bone (Al-Nawas et al. 2008, Klein et al. 2008, Kumar et al. 2012). Since bone porosity is the mechanical quality being considered of primary importance in dental implantology, it would seem that ultrasound, if not as imaging method, nevertheless could have its clinical intraoral use to obtain valuable information on bone quality.

6. 4. Investigating imaging efficacy

The efficacy of radiological imaging has routinely been portrayed in literature in a hierarchical model (Fineberg 1978, Fryback 1983, Fryback and Thornbury 1991). Most commonly, the following six-tiered model formulated by the Scientific Committee of the U.S. National Council on Radiation Protection and Measurements and described by Fryback and Thornbury (Fryback and Thornbury 1991) is used. Level 1 concerns the technical quality of the images; Level 2 addresses diagnostic accuracy, sensitivity, and specificity associated with interpretation of the images. Level 3 focuses on whether the information produces change in the referring physician's diagnostic thinking. Such a change is a logical prerequisite for Level 4 efficacy, which concerns effect on the patient management plan. Level 5 studies measure (or compute) the effects of the information on patient outcomes. At Level 6, analyses examine societal costs and benefits of a diagnostic imaging technology.

From the six theoretical levels discussed, the majority of the publications in the field reach only Level 1 or Level 2. Very rarely, Level 3 or, almost never, Level 4 will be reached (Schulze 2012). Regarding CBCT and its use in orthodontics, no studies have ever been conducted evaluating the top two Levels (Halazonetis 2012). There are, of course, ethical issues involved in carrying out studies on ionizing radiation that aim for higher efficacy levels. This general consideration cannot easily be ignored and will always be an obstacle in radiographic imaging (Schulze 2012).

7. Aim of the study

7.1. General aim of the study

This thesis aims at clarifying various aspects of CBCT efficacy. Demonstration of efficacy at each lower level (described in 6.4.) in the hierarchy is necessary to assure efficacy at higher levels. Hence, this thesis encompasses various aspects of all three lower levels of efficacy. As a comprehensive analysis of all components would prove impossible due to the immensity of the task, several investigations considered representative and clinically relevant will be performed to establish diagnostic efficacy.

All too often, the technical capabilities of a devise are confused with the benefits to the patients. In order to evaluate a risk-benefit assessment of a certain radiological image, an assessment of the radiobiological burden should be carried out. Thus, the radiological cost in form of ionizing radiation in CBCT will be addressed, and different imaging methods will be compared for their effective doses, focusing on the protection of the thyroid, in order to weigh potential benefits of radiation exposure against the radiation burden.

7.2. Specific aims of the study

- **STUDY I:** To determine the accuracy of CBCT imaging in assessing the anterior alveolar buccal bone and the impact of different voxel sizes on accuracy.
- **STUDY II:** To compare the accuracy of CBCT to MDCT in assessing the anterior buccal bone.
- **STUDY III:** To establish the best-suited MRI sequence for the assessment of cortical bone of the mandibular condyles using micro-CT as reference.
- **STUDY IV:** To compare the accuracy of CBCT to MRI, MDCT, OPG and lateral cephalogram for linear measurements of the mandibular ramus height and the condylar process.
- **STUDY V:** To evaluate the accuracy of CBCT and MDCT in diagnosing fusions in the cervical spine, and to validate the assessment of osteoarthritic changes in CBCT and MDCT against anatomical truth.
- **STUDY VI:** To assess the radiation burden of lateral cephalograms and CBCT at different settings, with and without radiological exposure of the cervical spine, to enable a risk-benefit assessment.

8. Materials and Methods

8.1. Materials and methods for cadaver studies (STUDIES I – V)

8.1.1. Subjects

The research was based on the analyses derived from radiologic and anatomic measurements and assessments of intact human cadaver heads obtained from the Anatomical Institute of the University of Zurich Switzerland. The sample consisted of eight unmitigated embalmed heads (5 women, 3 men, age range: 65-95 years, mean age 81). The inclusion criteria were a complete lower front dentition and no apparent orofacial pathologies. The fixation perfusion was carried out within 4 days after decease with a fixation liquid consisting of 2 parts alcohol (70%), 1 part glycerine and 2% Almudor (containing 8.1% formaldehyde, 10% Glyoxal and 3.7% glutaraldehyde).

8.1.2. Ethical considerations

The specimens were recruited from a voluntary body donation program of the Anatomical Institute at the University of Zurich, in accordance with State and Federal regulations (voluntary body donation program on the basis of informed consent), the Convention on Human Rights and Medicine (EU 2002) and the recommendation of the Swiss Academy of Medical Science (SAMW 2009).

8.1.3. Radiological imaging

- **A. Analogue lateral cephalogram**

The lateral cephalograms were taken with the head locked in position by ear rods and nasal support. The Frankfurt horizontal plane was set parallel to the floor and teeth were in centric occlusion. The radiographs were taken with a focus-coronal plane distance of 200cm and an enlargement of 7.5% with the following parameters:

tube voltage, 67 kV; tube current, 250 mA; exposure time, 0.04 sec; and tube current time product, 10 mAs.

Lateral cephalograms were screened and assessed for potential fusions of cervical vertebrae following the method prescribed in the literature: fusions were identified as an osseous continuity between C2 and C3 without complete separation (see Figure 4) at the articular facets or intervertebral disc space (Farman et al. 1979, Farman and Escobar 1982, Sandham 1986, Koletsi and Halazonetis 2010, Bebnowski et al. 2012). Four specimens (3 females, 1 male; aged 65, 75, 86 and 87, respectively; mean age, 78 years) had a suspected cervical spine fusion at the C2-C3 level and were subsequently used for the study of the cervical spine.

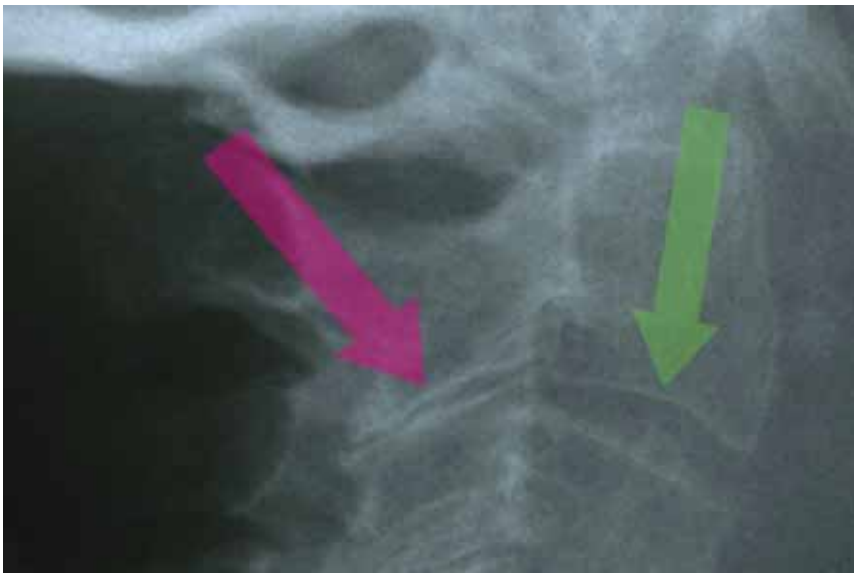

Figure 4. *Lateral cephalogram of a specimen with continuous radiolucent areas between the articular facets of C2 and C3 (purple arrow) and the intervertebral disc space (green arrow). This specimen was excluded from the study.*

- **B. Digital orthopantomogram**

The OPGs were produced using Cranex 3+ (SOREDEX, Tuusula, Finland) with the following settings: tube current, 6mA; tube voltage, 65 kV; exposition time, 20 sec. at 50 Hz, inherent filtration, 1.8mm AI; total filtration, 2.7mm AI. In order to minimize measurement errors as a consequence of distortion due to head positioning, the image acquisition was repeated until the result was satisfactory.

- **C. Cone-beam CT**

CBCT scans were performed on a CBCT scanner with an Amorphous Silicon Flat Panel (KaVo 3D exam; KaVo Dental GmbH, Bismarckring, Germany). The following scan parameters were kept identical during all CBCT exams: tube voltage, 120 kV; tube current time product, 37.07 mAs. CBCT scans were performed thrice, each time at a different isotropic voxel size: 0.125mm, 0.25mm and 0.4mm. Digital imaging and communication in medicine (DICOM) files were reformatted in multiplanar reconstructions (MPR) using two post-processing software (eXam Vision software, Imaging Sciences International LCC, Hatfield, Pa and ClearCanvas Workstation v.2.0 SP1, ClearCanvas Inc., Toronto ON, Canada).

- **D. Multidetector CT**

MDCT was performed on a 40-detector row CT system (Brilliance CT 40, Philips Healthcare, Eindhoven, the Netherlands) with the following scan parameters kept identical for all specimens: tube voltage, 120 kV; tube current time product, 70 mAs; slice collimation, 20 x 0.625 mm; pitch, 0.68; reconstruction slice thickness, 0.67 mm; reconstruction increment, 0.33 mm; window level setting, 200 / 2000 (Hounsfield Units, HU); voxel size, 0.39 mm [x], 0.39 mm [y] and 0.67 mm [z]. Sagittal and coronal reformatted images (slice thickness, 1mm; increment, 0.5mm) were viewed on a high resolution diagnostic workstation (dx IDS5, Sectra PACS, Linköping, Sweden).

- **E. Magnetic resonance imaging**

MRI examinations were carried out on a 1.5 Tesla MRI unit (Signa HDx, General Electric, Milwaukee, USA) using a 2-channel phased array surface coil dedicated for TMJ-imaging (i.e. DUALTMJ coil). All examinations were performed in closed mouth position. The sagittal sequences were planned to be acquired parallel to the mandibular rami, separately for each side. The MRI protocols (Table 1) included the following sagittal sequences: a T1-weighted 2D fast spoiled gradient recalled echo sequence (i.e. T1-2D-FSPGR), an intermediate-weighted proton density fast spin echo

sequence (i.e. PD-FSE), a T2-weighted fast spin echo sequence (i.e. T2-FSE), a T1-weighted 3D fast spoiled gradient recalled echo sequence (i.e. T1-3D-FSPGR) and a T1-weighted fast spin echo sequence (i.e. T1-FSE). The mean total examination time was 40 minutes per head. All DICOM files were viewed on a high resolution diagnostic workstation (dx IDS5, Sectra PACS, Linköping, Sweden).

Table 1. *The 8 different MRI protocols used.*

	Axial T2-FRFSE[1]	*Coronal T2-FRFSE[1]*	*Sagittal T1-2D-FSPGR[2]*	*Sagittal PD-FSE[3]*
Time to repetition (TR, ms)	3000	3000	370	3200
Time to echo (TE, ms)	102	102	4.2	24
Flip Angle (degrees)	90	90	80	90
Matrix (frequency x phase)	384 x 320	384 x 320	384 x 224	256 x 224
Slice Thickness (mm)	3	3	2	2
Spacing (mm)	11.6	4.1	2	2
Field of view (FOV, cm²)	22	22	12	12
Band Width (Hertz)	41.67	41.67	31.25	17.86
NEX (n. of excitations)	4	4	3	3
Echo train length	21	21	-	8

(Table 1 cont.)

	Sagittal T2-FSE[3]	*Sagittal T1-3D-FSPGR[2]*	*Sagittal T1-FSE[3]*	*Coronal T1-SE[4]*
Time to repetition (TR, ms)	6820	11.6	640	500
Time to echo (TE, ms)	85	4.1	10.7	11
Flip Angle (degrees)	90	20	90	90
Matrix (frequency x phase)	256 x 224	256 x 192	256 x 192	256 x 192
Slice Thickness (mm)	2	2	2	2
Spacing (mm)	2	1	2	2
Field of view (FOV, cm²)	12	10	12	16
Band Width (Hertz)	20.83	15.63	20.83	19.23
NEX (n. of excitations)	4	3	3	3
Echo train length	16	-	3	-

[1] = fast relaxation fast spin echo; [2] = fast spoiled gradient recalled echo; [3] = fast spin echo; [4] = spin echo

- **F. Micro-CT**

In preparation for the μCT exams, mandibular condyles were separated from the mandibles at the level of the mandibular neck (i.e. at the incisura semilunaris

mandibulae) with a hand piece electrical speed saw. μCT examinations of all condyles (n: 16) were performed using a commercially available μCT scanner (Specimen μCT 40, Scanco Medical, Brüttisellen, Switzerland) with all scan parameters kept identical during examinations: tube voltage, 70 kV; tube current, 114 μA; and isotropic resolution, 18 μm. The DICOM files were viewed on a high resolution diagnostic workstation (dx IDS5, Sectra PACS, Linköping, Sweden).

8.1.4. Anatomical Measurements

A digital calliper (accuracy: 0.01mm) was used for the direct measurements on the anatomical specimens. The clinical examination of the lower anterior front consisted of three measurements (see Figure 5-C in chapter 8.2.1.):

- **Soft tissue measurement (IE-MGJ):** The most basal point of the undulated mucogingival junction was used to evaluate the distance to the incisal edge (canine to canine, n: 48).
- **Vertical bony measurement (IE-ABM):** After the gingiva was removed, the distance from the buccal alveolar bone margin to the incisal edge was determined for every tooth (canine to canine, n: 48). Since the bone margin is not a horizontal line, but rather lunar-shaped, the most apical point was chosen.
- **Horizontal bony measurement (H):** A thin slat of the alveolar bone was removed with a scalpel. The thickness of the alveolar bone covering was measured at a distance of 15mm (n: 48) from the incisal edge (IE - H). Occasionally, a second site was chosen at 18mm distance (n: 13) from the incisal edge to increase the total amount of measures taken (total n: 61).

All measurements were repeated and the mean value was used for further analyses.

When necessary, parts of the cadaver were dislodged to guarantee an access to the organ to be measured.

8.1.5. Staining of the gingiva

With the aim to facilitate the study of the mucogingival junction's undulated devolution, the attached gingiva was stained with Schiller solution as described by Fasske and Morgenroth [iodide pure : potassium-iodide : distilled water = 10 : 20 : 300] (Fasske and Morgenroth 1958).

8.1.6. Maceration of the cervical spine

After image acquisition, the cervical spines were isolated *en bloc* from the cadaver heads. Lipids were dissolved in a Supralan UF solution (Bauer Handels GmbH, Fehraltorf, Switzerland), in the presence of sodium chloride. Enzymatic maceration was performed with Papain (Bauer Handels GmbH, Fehraltorf, Switzerland) at pH 6-7 in a Supralan UF and sodium chloride containing solution, for up to 14 days.

8.2. Measurements and methods applied to specific studies (STUDIES I-V)

8.2.1. The effect of different voxel sizes on buccal bone measurements (STUDY I)

The CBCT scans of 0.125mm and 0.4mm voxel size, described in 8.1.3. section C, were used. All images were reconstructed using MPR perpendicular to the curvature of the dentition, thereby enabling the depiction of every tooth in its buccolingual profile (Fig 5, A-B).

The radiological measurements were analogous to the anatomical examination of the vertical (IE -ABM) and horizontal (H) bony measures, as described in 8.1.4. and shown in Figure 5-C. All the measurements were taken twice by the same observer, at least one week apart, and the mean value was used for statistical testing.

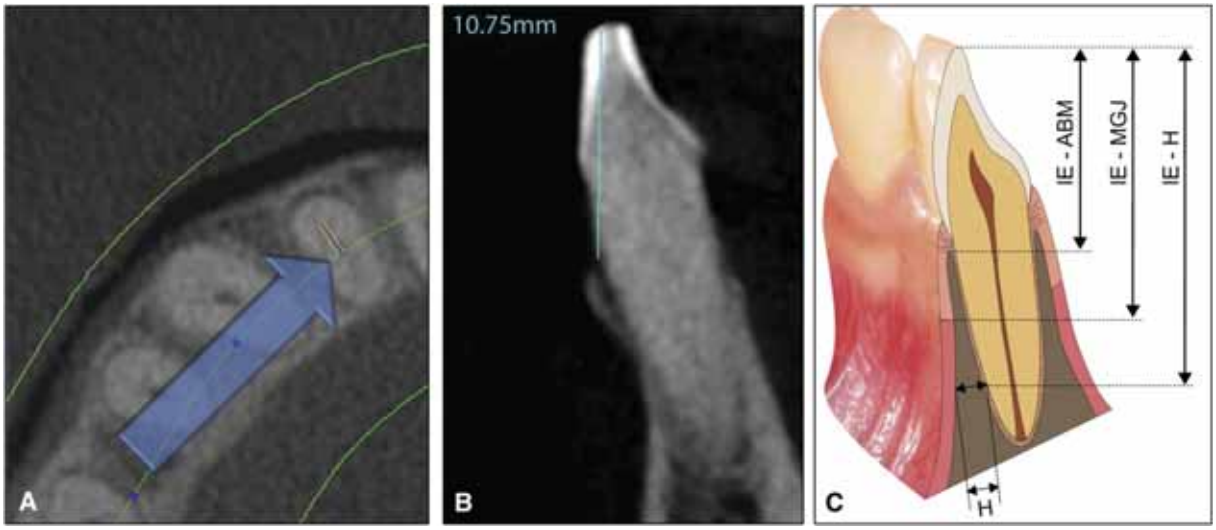

Figure 5. ***(A)*** *Axial rendering of the data showing the perpendicular curve of the reformatted slices along the thin green middle line (blue arrow: pointing to the slice depicted in B; bold green lines: outer boundaries of the curve, orange lines: slice thickness of slice depicted in B.* ***(B)*** *Representative reformatted image from which the radiological measurements were taken (light blue line: IE - ABM)* ***(C)*** *Graphic illustration of measurements taken. IE: Incisal edge, ABM: Alveolar bone margin, MGJ: Mucogingival junction. H: Horizontal measurement. The measurements IE-ABM and H were taken anatomically and radiologically, IE-MGJ only anatomically.*

- ***Statistical analysis***

To determine intraobserver reliability, the intraclass correlation coefficient (ICC) for absolute agreement based on a one-way random effects analysis of variance (ANOVA) was calculated for the repeated radiological measurements from the same observer for all four protocols (high resolution [0.125mm] and low resolution [0.4mm], vertical and horizontal measures respectively).

Descriptive statistics for anatomical measurements and for the differences between radiological and anatomical measures for each category were computed separately. In addition, the 95% confidence interval (95%CI) was calculated and the absolute measurement error (AME) was determined according to the following equation:

$$AME = | \text{radiological measurement} - \text{anatomical measurement} |$$

In order to disclose deterministic differences between both methods of measurement, one sample Student's t-test was applied to the differences. Moreover, the Bland-Altman method was applied and the limits of agreement were identified

(Bland and Altman 1986). In addition, the 95% CI of the limits of agreement was provided (Bland and Altman 1999).

The Levene-test was applied to detect an increase of variability of the differences with the increase of the magnitude of the measurements. The Pearson correlation coefficient was computed to evaluate the association of soft tissue measures to bony measures. In addition, the regression plot between soft tissue measures to bony measures together with the 95% prediction interval was provided. The assumption of normality for the differences of soft to bony tissue was investigated by the Kolmogorov-Smirnov test.

8.2.2. Accuracy of CBCT in comparison to MDCT for buccal bone measurements (STUDY II)

CBCT scans of 0.4mm, as described in 8.1.3. section C, and MDCT scans as described in 8.1.3. section D, were used and compared to each other. All images were reconstructed using MPR perpendicular to the curvature of the dentition (Figure 6-A), thereby enabling the depiction of every tooth in its buccolingual profile (Figure 6, B-C).

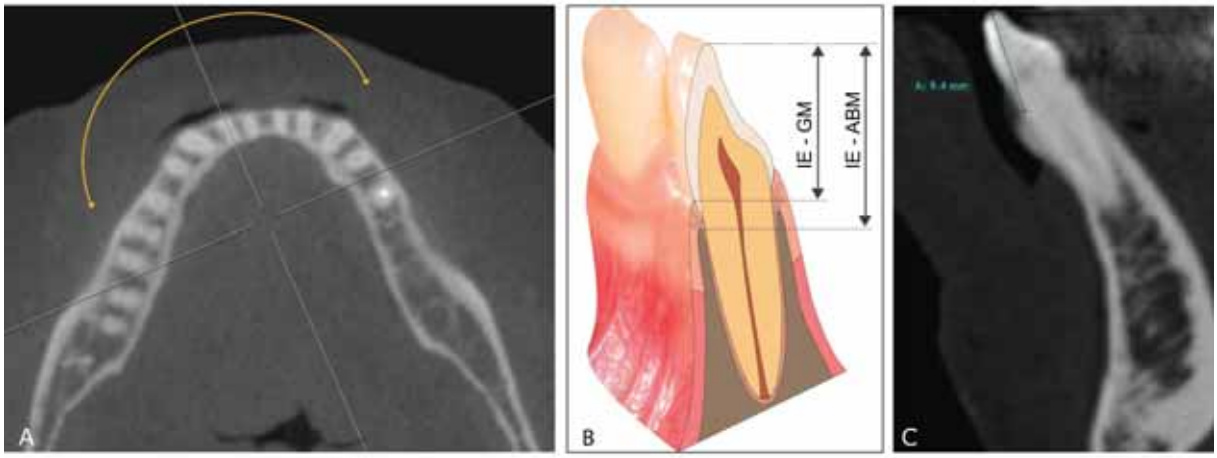

Figure 6. ***(A)*** *Orientation of the MPR images perpendicular to the dentition, enabling to view every tooth to be assessed in its buccolingual profile.* ***(B)*** *Measurements taken. IE: incisal edge, GM: gingival margin, ABM: alveolar bone margin;* ***(C)*** *Representative MDCT-scan, A: measurement of IE-ABM.*

MDCT image data were derived from axial-source raw data. All images were magnified on the monitor to the field of interest and an electronic calliper tool was used to measure the two distances corresponding to the anatomical measurements mentioned above in 8.1.4.

The bone measurements (IE - ABM) were evaluated on the CBCT and MDCT scans, the soft tissue measurements (IE-GM) only on the CBCT scans. All radiological measurements were taken twice, at least one week apart by the same observer. Due to metal induced beam hardening artefacts, a total of 7 sites were not assessable on MDCT and/or CBCT images. These sites were termed as non-assessable sites (NAS) and were excluded from further comparative data analyses. From the 41 remaining CBCT data sets, the gingiva could not be distinguished on 10 data sets due to very tight lip contact and these sites needed to be excluded from the soft tissue measurements (IE-GM), and thus only clearly depicted gingiva was assessed (n: 31).

- ***Statistical analysis***

To determine intraobserver reliability, the intraclass correlation coefficient (ICC) for absolute agreement based on a one-way random effects analysis of variance (ANOVA) was calculated for the radiological measurements. Descriptive statistics for the differences between radiological and anatomical measurements for each category (i.e. MDCT bone measurements, CBCT bone measurements, CBCT soft tissue measurements) were computed separately. In order to disclose deterministic differences between both methods, a one sample Student's t-test was applied to the differences. Furthermore, the Bland-Altman method was performed and the limits of agreement with their 95% CI were identified (Bland and Altman 1986, 1999).

8.2.3. Establishing the best-suited MRI sequence for the assessment of the condylar process using micro-CT as reference (STUDY III)

In order to evaluate the suitability of MRI to assess the cortical bone of the mandibular condyle, the most suitable sagittal MRI sequence for TMJ had to be

established. Eight different MRI scans were compared to micro-CT and the efficacy of all *five sagittal scans* was evaluated both through numerical data (i.e. cortical bone measurement) and categorical data (i.e. different signs of osteoarthritic changes). The image acquisition is described in 8.13. sections E and F, respectively.

One radiologist not involved in the data analysis prepared all μCT data by reconstructing MPR images in sagittal imaging planes aligned parallel to the mandibular ramus (i.e. corresponding to the alignment of the imaging planes of the sagittal MRI sequences) at a reconstruction slice thickness of 1 mm and a reconstruction increment of 0.6 mm. Subsequently all reconstructed DICOM data were archived into the picture archiving and communication system (PACS) for storage and image analysis. Two radiologists experienced in musculoskeletal radiology performed the following measurements:

- ***Cortical bone thickness measurements:*** The thickness of the cortical bone (CBT) of the anterior, superior and posterior portions of the mandibular condyles was measured on all sagittal MRI sequences at the level of the centre of the mandibular. All measurements were carried out using a calibrated measurement tool that was part of the hospital's PACS and allowed for sub-millimetre measurements.
- ***Subjective evaluation of the cortical bone:*** The two radiologists further assessed the anterior, superior and posterior portions of all mandibular condyles (n: 16) on the sagittal MRI sequences for the presence of
    - cortical bone thinning,
    - cortical bone erosions,
    - irregularities of the cortical bone surface,
    - subcortical bone cysts and
    - the presence of an anterior osteophyte.

The evaluations were carried out in a blinded fashion and a third radiologist not involved in MRI analysis assessed the μCT data sets for the same findings to

define the standard of reference for statistical analysis. See Figure 7, A-E for μCT imaging examples obtained from the present cadavers.

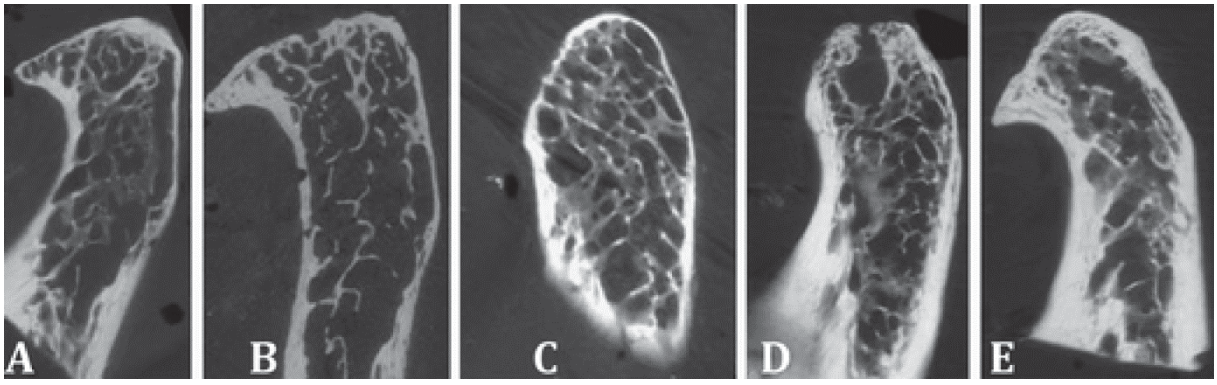

Figure 7. *Micro-CT imaging examples illustrating* ***(A)*** *cortical bone thinning of the superior portion of the mandibular condyle,* ***(B)*** *cortical erosion of the superior portion,* ***(C)*** *cortical surface irregularities of the anterior portion,* ***(D)*** *a large subcortical bone cyst and* ***(E)*** *an anterior osteophyte.*

- ***Statistical Analysis***

The data was descriptively reviewed and statistically analyzed using Kolmogorov-Smirnov's to test for normality. Interobserver agreements concerning all continuous variables (i.e. measurements of cortical bone thickness) were calculated using interclass correlation coefficients (ICC). The Wilcoxon signed ranks test was performed to test for statistically significant differences in cortical bone thickness measurements between the sagittal MRI sequence and the μCT based measurements, which served as the standard of reference.

Interobserver agreements regarding the subjective evaluation of presence of cortical bone thinning, cortical bone erosions, irregularities of the cortical bone surface, subcortical bone cysts and the presence of an anterior osteophyte were analyzed using Cohen's kappa statistics (Cohen 1960). Diagnostic accuracy, sensitivity, specificity, positive predictive value and negative predictive value regarding the subjective assessments were assessed separately for both observers from Chi-squared tests of contingency, and the 95% confidence intervals were calculated.

8.2.4. Accuracy of CBCT versus MDCT, MRI, OPG and lateral cephalogram for linear measurements of the mandibular ramus and condylar process (STUDY IV)

The data of CBCT scans with 0.4mm voxel size, MDCT, MRI, OPG and lateral cephalograms described in 8.1.4. sections A-E were used for image analysis of the mandibular ramus and the condylar process. From the 3D datasets (MDCT, CBCT and MRI), projection images of the mandibular ramus and condyle were reconstructed with commercially available image processing using maximum-intensity projection (MIP) for MDCT and CBCT, and minimum-intensity projection (MinIP) for MRI data. The orientation of the slices was standardized to intersect the center of the condylar process, the muscular process and the gonial angle. The slice thickness was defined as the smallest thickness, where the most cranial condylar point, the most caudal gonial point and the deepest point of the incisura mandibulae were included (Figure 8). The resulting 2D images as well as the unaltered 2D image of the OPG were exported and analyzed on a high resolution diagnostic workstation (dx IDS5, Sectra PACS, Linköping, Sweden).

The analogue lateral cephalograms were hand-traced using a 0.3 mm lead on a 0.10 mm matte acetate tracing paper.

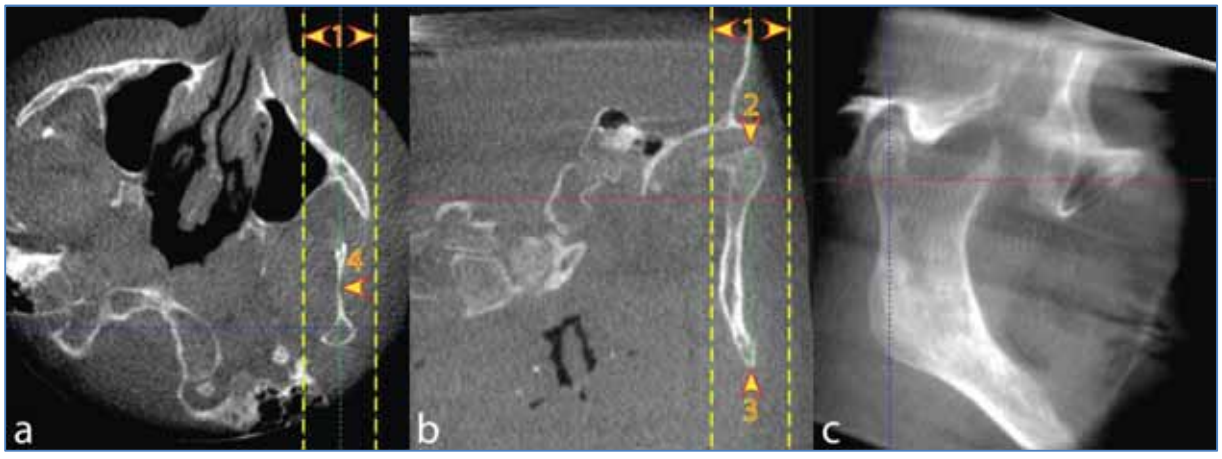

Figure 8. *Example of a 3D CT dataset visualized with MIP and MPR, with 3 orthogonal planes* ***(a-c)****. The orientation of slice* ***(c)****, used for linear measurements, was standardized to intersect the center of the coronoid process, the condylar process and gonial angle. The thickness (1) of slice* ***(c)*** *was defined as the smallest thickness, where the most cranial condylar point (2), the most caudal gonial point (3) and the deepest point of the incisura mandibulae (4) were included.*

- ***Measurements***

For every image and every side, three points (Co, Go and In) were constructed and two linear measurements were performed parallel to the tangent at the posterior border of the Ramus (Figure 9):

- ***Ramus Height (RH):*** Measured between the most cranial point of the condyle (Co) and the intersection point with the lower border of the ramus mandibulae, the gonial point (Go). Gonial point (Go) was defined as the intersection of a line obtained parallel to the tangent at the posterior border of the ramus and through the most cranial point of the condyle (Co).
- ***Height of the condylar process (CP):*** Measured parallel to the tangent between the most cranial point of the condyle (Co) and the most caudal point of incisura mandibulae (In).

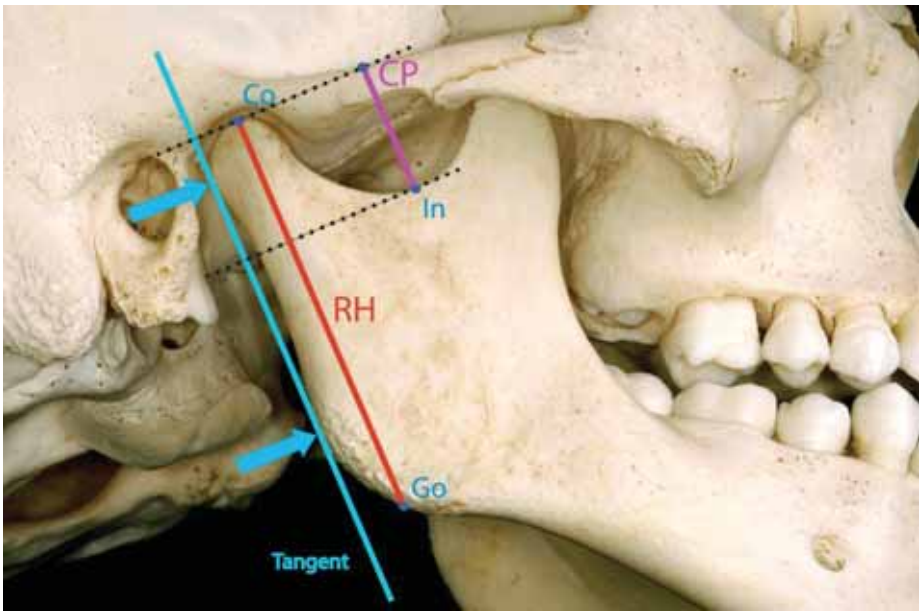

Figure 9. *Constructions for linear measurements (RH and CP) were performed parallel to the tangent at the posterior border of the ramus. RH: measured between most cranial point of the condyle (Co) and intersection point with the lower border of the ramus (Go). CP: measured between the most cranial point of the condyle (Co) and the most caudal point of incisura mandibulae (In).*

Calibration, construction of the reference lines, landmark definition and distance measurements of all 2D images related to CBCT, MDCT, MRI and OPG were performed digitally. The same construction lines and landmarks were defined on lateral cephalograms tracings. Landmarks on lateral cephalograms were digitized

using tablet digitizer Numonics AccuGrid (Numonics, Landsdale, PA, USA) with a resolution of 1 milli-Inch. The distances were computed and corrected for enlargement.

All measurements, constructions and tracings for all images were performed twice by two observers independently. The observers were blinded for all other first and second measurements, constructions and tracings.

- ***Statistical Analysis***

Intra- and interrater reliability were assessed using ICC to disclose differences between raters for each imaging method separately.

The values used in the assessment of agreement were computed as follows: for each linear measurement the mean of the four values (double measurements of two observers) was taken. This resulted in 16 values (left and right sides together) per linear measurement (RH and CP separately) with exception of the LC values. Because on a LC the left and right side could not be distinguished, the mean of left and right side values were taken resulting in only 8 values per measurement type. To assess the agreement between imaging methods for each measurement type Bland-Altman-Plots (Bland and Altman 1986, 1999) with limits of agreement extended by 95% confidence interval for mean difference (paired t-test) were computed.

To assess precision of the measurements, standard deviation (SD) and the coefficient of variation (CV) were computed for RH and CP separately. Computation of mean and standard deviation (SD) was based on the four values of a linear measurement (double measurements of the two observers). CV was defined according to formula ($CV = \frac{SD}{\text{mean length}}$). The measurements on the left and right side were considered to be independent.

Descriptive statistics for CV with respect to RH and CP were computed separately. Shapiro-Wilk and Kolmogorov-Smirnov tests were used to check normality assumptions. Differences in mean CV and SD between imaging methods was assessed using one-way ANOVA with Scheffé post-hoc after log-transformation

assuring normal distribution. Differences between RH and CP were evaluated by two-sample t-test for each imaging method separately.

8.2.5. Accuracy of CBCT, MDCT and lateral cephalogram in assessing the cervical spine (STUDY V)

The four lateral cephalograms screened and assessed for potential fusions, as described in 8.1.4. section A, were used for data analysis. Corresponding CBCT scans of 0.25mm voxel (8.1.4. section C) and MDCT scans (8.1.4. section D) were examined according to the following protocol: Five general radiologists evaluated the MDCT data, and five dentists with special postgraduate training in oral radiology evaluated the CBCT data.

Three areas were assessed for a potential congenital fusion: **Facet joint (C2-C3) of the left and right articular process** and the **intervertebral disc space** between the two bodies C2 and C3.

Additionally, the raters were requested to perform their radiological appraisal for the **left and right facet joints** in the following manner:

A. ***Normal joint***

B. ***Osteoarthritis*** *(joint space entirely preserved / partially preserved / or nonvisible)*

All radiologists assessed the images independently, in blinded fashion and without knowledge of the anatomical findings.

The four macerated vertebrae were subsequently analyzed for fusions and osteoarthritis by a board certified pathologist.

- ***Statistical analysis***

An unweighted Cohen's kappa test (Cohen 1960) was computed to evaluate the agreement between the CBCT and MDCT method. To determine inter-observer agreement between the 5 CBCT radiologists and the 5 MDCT radiologists respectively, a Fleiss' kappa test for multiple raters (Fleiss 1971) was calculated.

8.2.6. General notes on the statistical analyses

Three commercially available software packages (SPSS, version 17, Chicago Ill.; MedCalc, version 14.4.1.0, Mariakerke, Belgium and STATA version 10.1, Texas, USA) were used for data analysis. To perform the Fleiss' kappa test referred to in 8.2.5., StatTools was applied (Chang).

P-values smaller than 0.05 were considered statistically significant. Fleiss' and Cohen's kappa (κ) statistics were interpreted as follows: A κ-value greater than 0.81 corresponded to an excellent agreement, a κ-value of 0.61–0.80 to a very good interobserver agreement, a κ-value of 0.41–0.60 to a good interobserver agreement, and a κ-value of 0.21–0.40 to a moderate interobserver agreement (Landis and Koch 1977).

8.3. Materials and methods for radiation dose evaluation (STUDY VI)

Additional unpublished data on the effective dose of various CBCT scans were collected and used to supplement the data of the original publication.

8.3.1. Dosimeters

Thermoluminescent dosimeter (TLD) chips (3mm x 1mm x 1mm) were used on selected locations in the head and neck region of an adult male tissue-equivalent phantom (RANDO - radiation analog dosimetry system; The Phantom Laboratory, Salem, NY) to record the distribution of the absorbed radiation dose. The sites are listed in Table 2. These locations reflect critical organs known to be sensitive to radiation. For the assessment of the effective dose of hand-wrist radiographs, a TLD was placed directly on the magazine, corresponding to the location of the hand during the examination. The TLD chips were supplied by the Institute of Applied Radiophysics (I.A.R.) from the University of Lausanne, Switzerland, and the absorbed doses were computed by the I.A.R. in a blinded fashion. One unexposed dosimeter served as control for environmental radiation.

Table 2. *Locations of thermoluminescent dosimeter (TLD) chips on the RANDO phantom.*

Organ	*Location*	*TLD number*	*Phantom level*
Brain	Anterior/ posterior	18,19	1
	Right/left	16,17	2
	Hypophysis	13	3
Eyes	Right/left lens	14,15	3
Skull	Maxillary sinus right/left	9,10	5
Salivary glands	Right/left parotid	11, 12	5
	Right/left submandibular gland	7, 8	6
	Sublingual gland	5	
Thyroid	Right/left	1,2	9
Spine	C2	6	6
	Right/left	3,4	7

8.3.2. Radiological exposure

The radiological examinations were performed on a custom-made X-ray unit (COMET, 3175 Flamatt, Switzerland) with the following parameters for the lateral cephalogram: tube voltage, 67 kV; tube current, 250 mA; exposure time, 0.04 sec; tube current time product, 10 mAs. The parameters for the hand-wrist radiograph were chosen as follows: tube voltage, 40 kV; tube current, 250 mA; exposure time, 0.04 sec; tube current time product, 10 mAs. These parameters correspond to the clinical exposure factors commonly used. No intensifying screens were used.

The CBCT scans were made with the KaVo 3D eXam (KaVo 3D exam; KaVo Dental GmbH, Bismarckring, Germany) using three different scanning modes: *portrait mode* (scan height, 17cm; tube voltage, 120kV; tube current, 5mA; scan time, 8.9 sec; exposure time, 3.7 sec; tube current time product, 18.54mAs) and a *normal landscape mode* (reduced scan height of 13cm; other parameters left unaltered) and *fast scan landscape mode* (reduced scan height of 13cm; scan time, 5 sec; exposure time, 2 sec; other parameters left unaltered).

Radiological images were taken with a commercially available thyroid shield (3534-TS, WIROMA, 3145 Niederscherli, Switzerland) of 0.5mm Pb. In order to obtain the radiation dose without thyroid shield, TLDs in Phantom level 9 (corresponding to the topographical location of the thyroid shield, see Table 2) were replaced and new TLDs were independently exposed to radiation without shielding. In the subsequent analysis (see 8.3.3.) comparing the radiation burden with and without thyroid shielding, the results of the TLDs of Phantom level 1-8 were kept identical.

Because of the small amount of radiation required for a single examination, 10 exposures were performed to provide a reliable measure of radiation in the dosimeters. Mean value was used for calculations. In accordance to the recommendation of the International Commission on Radiological Protection (ICRP 2008), doses from TLDs at different positions within a tissue or organ were averaged to express the average tissue-absorbed dose in micrograys (μGy).

8.3.3. Calculation of the effective dose

The obtained values were used to calculate the equivalent dose H_T using the following equation:

$$H_T = \Sigma; W_R D_T$$

The equivalent dose H_T for a tissue or organ is defined as the product of the radiation weighting factor W_R (W_R equals 1 for X-radiation) and the measured absorbed dose D_T averaged over a particular tissue or organ (Valentin 2007).

Effective dose E has been recommended by the International Commission on Radiological Protection (ICRP 2008) as a means of comparing detriment of different exposures to ionizing radiation to an equivalent detriment produced by a full-body dose of radiation. Thus, the risk to the whole body is determined as the summation of the equivalent doses established for all tissues and organs (Valentin 2007). The effective dose (E_{ICRP60}), expressed in microsieverts (μSv), was calculated using the equation:

$$E = \Sigma w_T H_T$$

E is the product of the tissue weighting factor w_T, which represents the relative contribution of that organ or tissue to the overall risk, and the equivalent dose H_T. The weighting factors of the equivalent doses in accordance with the I.C.R.P. guidelines of 2008 for the hand-wrist radiogram and for the lateral cephalogram are given in Tables 3-A and 3-Bb, respectively.

Table 3-A. *Weighting of the Equivalent dose (H_T) for hand wrist radiation exposure.*

Tissue	*ICRP identified Organ*	*Fraction of total organ irradiated*	*Corresponding TLD numbers*	*Fraction irradiated*	*Weighting*	*Weighting in %*
Bone marrow	Bone	0.50%		0.50%	0.06	58.71%
Bone surface	Bone	0.50%		0.50%	0.02	22.70%
Skin	Skin	1.00%		1.00%	0.01	9.78%
Muscle	Muscle	1.00%		1.00%	0.01	8.81%
Remainder	-					

Table 3-B. *Weighting of the Equivalent dose (H_T) for lateral cephalometric radiation exposure.*

Tissue	*ICRP identified Organ*	*Fraction of total organ irradiated*	*Corresponding TLD numbers*	*Fraction irradiated*	*Weighting*	*Weighting in %*
Bone marrow				16.50%	1.98	17.86%
	Mandibula	1.30%	mean 7, 8			
	Calvarium	11.80%	mean 16 - 19			
	Spine	3.40%	mean 3, 4, 6			
Esophagus	Esophagus	10.00%	mean 1, 2	10.00%	4.00	36.08%
Thyroid	Thyroid	100.00%	mean 1, 2	100.00%	0.40	3.61%
Bone surface				16.50%	0.77	6.91%
	Mandible	1.30%	4.64 x mean 7, 8			
	Calvarium	11.80%	4.64 x mean 16, 17, 18, 19			
	Cervical spine	3.40%	4.64 x mean 3, 4, 6			
Brain	Brain	100.00%	mean 13, 16 - 19	100.00%	1.00	9.02%
Salivary glands				100.00%	0.05	0.45%
	Parotid	33.00%	mean 11, 12			
	Submandib.	33.00%	mean 7, 8			
	Sublingual	33.00%	5			
Skin	Skin	5.00%	mean 11, 12, 14, 15	5.00%	1.00	9.02%
Muscle	Muscle	5.00%	mean 1-8, 11-13	5.00%	0.05	0.41%
Remainder					1.85	16.64%
	Lymph. nodes	5.00%	mean 1-8, 11-12			
	Extrathoracic airway	100.00%	mean 1-8, 11-14			
	Oral mucosa	100.00%	mean 1-8, 11-15			

9. Results

9.1. Efficacy (STUDIES I-V)

9.1.1. The effect of different voxel sizes on buccal bone measurements (STUDY I)

The intraclass correlation coefficient (ICC) revealed a very good repeatability of the radiological measures. The ICC was for the high resolution protocols 0.95 (vertical measurements) and 0.99 (horizontal measurements), and for the low resolution protocols 0.96 (vertical measurements) and 0.90 (horizontal measurements), respectively.

The mean anatomical measurements were 12.13mm for the vertical measurements (SD: 1.58mm), 1.02mm for the horizontal measurements (SD: 0.77mm) and 1.67mm for the distance ABM-MGJ (SD: 1.08mm).

The accuracy of the measurements derived from the scans proved to be acceptable both for the high resolution and the low resolution protocol. The absolute measurement errors for all four protocols are given in Table 4.

Table 4. *Absolute measurement error for all four protocols.*

Absolute errors	*Mean (mm)*	*Median (mm)*	*SD (mm)*	*99% CI (mm)*
Vertical - Low resol. (n: 48)	0.70	0.53	0.84	(0.37 ; 1.02)
Vertical - High resol. (n: 48)	0.34	0.21	0.50	(0.14 ; 0.54)
Horizontal - Low resol. (n: 61)	0.54	0.42	0.46	(0.38 ; 0.69)
Horizontal - High resol. (n: 61)	0.37	0.25	0.43	(0.22 ; 0.52)

The descriptive statistics for the differences of the measurements and the one sample Student's t-test are shown in Table 5. The mean differences to the anatomical measures were for all measurements very close to 0 and ranged between -0.13mm and +0.13mm and 0 was within the 95% CI bounds confirming no systematic bias in

all four radiological readings. The one sample t-test revealed likewise no significant differences between the physical and the radiological measures.

To validate the different measurements, the differences between the measurements was plotted against the average as recommended by Bland and Altman (Fig 10, A-D) (Bland and Altman 1986). The limits of agreement were widest in the low resolution protocol for vertical measurements, and smallest in the high resolution protocol for horizontal measurements. All established limits of agreement were broader than ± 1mm, indicating that alveolar bone thickness of 1mm might be missed completely, even with high resolution images.

The Levene-test confirmed an increase of the variability of the differences as the magnitude of the measurements increases (p=0.001) for both graphs 10-C and 10-D. This indicates that for small horizontal measurements the differences were smaller than for large horizontal measurements.

Table 5. *Descriptive statistics, one sample t-test, 95%CI for differences and limits of agreement (LOA): positive numbers represent overestimation and negative numbers represent underestimation of the anatomical measurements with CBCT with respect to anatomical measurements (Anat).*

Differences CBCT-Anat	*P value*	*Mean diff. (mm)*	*SD (mm)*	*Range (mm)*	*95% CI (mm)*	*LOA (mm)*
Vertical - Low resol. (n: 48)	0.79	0.04	1.09	8.48	(-0.27 ; 0.35)	(-2.1 ; 2.2)
Vertical - High resol. (n: 48)	0.15	-0.13	0.59	3.91	(-0.30 ; 0.05)	(-1.3 ; 1.0)
Horizontal - Low resol. (n: 61)	0.63	0.04	0.71	4.18	(-0.14 ; 0.23)	(-1.4 ; 1.4)
Horizontal - High resol. (n: 61)	0.08	0.13	0.55	3.62	(-0.02 ; 0.28)	(-1.0 ; 1.2)

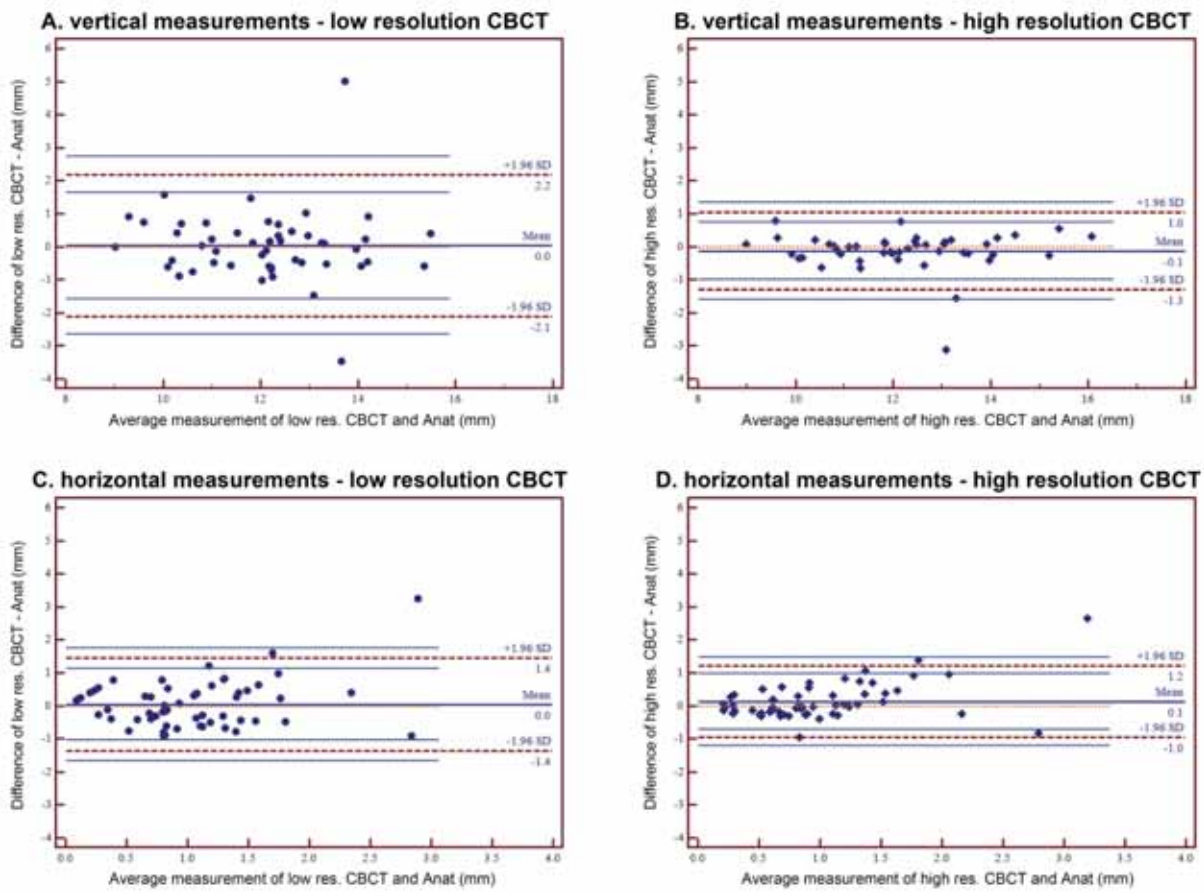

Figure 10. *Bland-Altman plots: Difference against the mean (solid middle blue line) of the anatomical and radiological measurements. The limits of agreement (broken brown lines) and the 95% CI of the limits of agreement (solid blue lines) are shown. Vertical measurements of* ***(A)*** *low resolution and* ***(B)*** *high resolution, horizontal measurements of* ***(C)*** *low resolution and* ***(D)*** *high resolution.*

The Pearson correlation coefficient (0.756, $p<0.001$) between two distances (IE-ABM and IE-MGJ; n: 48) proved to be moderate, but highly significant. The regression plot between both distances together with the 95% prediction interval is given in Figure 11-A. The distance from the alveolar bone margin to the mucogingival junction seems to follow a nearly ideal normal distribution ($p=0.194$) around the mean value of 1.67mm (SD: 1.08, 95% CI: (1.35 ; 1.98)) (Fig 11, B-C).

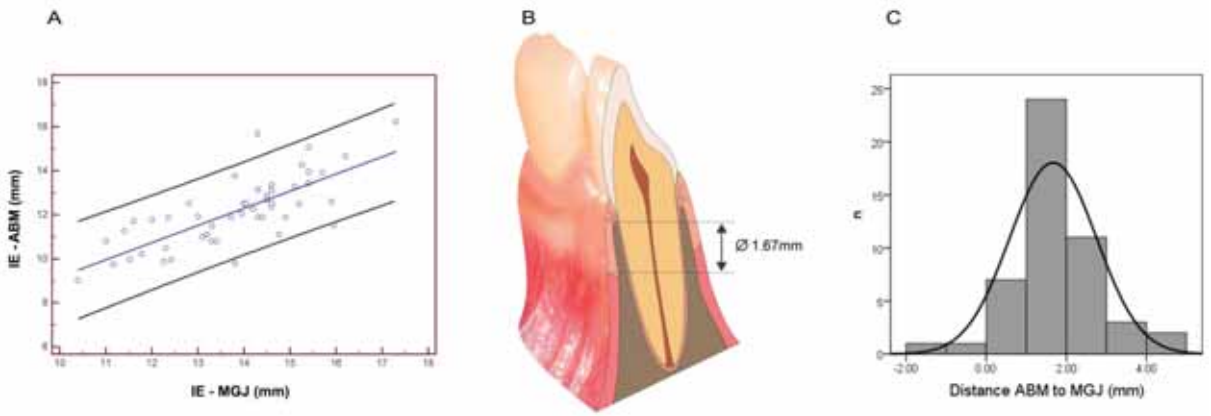

Figure 11. ***(A)*** *Regression plot for the two distances IE - MGJ and IE - ABM with the 95% prediction interval (blue line: regression line, bold black lines: 95% prediction interval).* ***(B)*** *Graphic illustration of the distance between the alveolar bone margin (ABM) and the mucogingival junction (MGJ).****(C)*** *Distribution of the distance between the alveolar bone margin (ABM) and the mucogingival junction (MGJ): mean value 1.67mm (black curve: normal distribution).*

9.1.2. Accuracy of CBCT in comparison to MDCT for buccal bone measurements (STUDY II)

The ICC revealed a very good repeatability of the radiological measurements [*r*: 0.92; 95% CI (0.86; 0.96)].

The accuracy of the measurements proved to be acceptable for all protocols (MDCT bone, CBCT bone and soft tissue). The results of the descriptive statistics and the one sample t-test are given in Table 6.

Table 6. *Descriptive statistics, one sample t-test, 95% CI for differences and limits of agreement: positive numbers represent overestimation and negative numbers underestimation of the radiological measurement (Rx) with respect to anatomical measurement (Anat). NAS: non-assessable sites.*

Differences Rx - Anat	*n*	*NAS (%)*	*P value*	*mean (mm)*	*SD (mm)*	*Range (mm)*	*95% CI (mm)*	*LOA (mm)*
MDCT bone	41	14.5	0.0667	0.23	0.81	4.42	(-0.02 ; 0.48)	(-1.35 ; 1.82)
CBCT bone	41	8.3	0.0956	0.14	0.55	2.07	(-0.02 ; 0.31)	(-0.93 ; 1.21)
CBCT soft tissue	31	-	0.0874	0.14	0.47	1.78	(-0.02 ; 0.32)	(-0.77 ; 1.07)

There were more NAS with MDCT (14.5%) than with CBCT (8.3%) (see Table 6). The mean difference for all readings was very close to 0 with 0.23mm for MDCT and 0.14mm for CBCT (bone and soft tissue, respectively). The one sample t-test revealed no significant differences between the radiological and anatomical measurements, and 0 was always within the 95% CI bound. The mean differences between the radiological and anatomical measurements are shown in Figure 12.

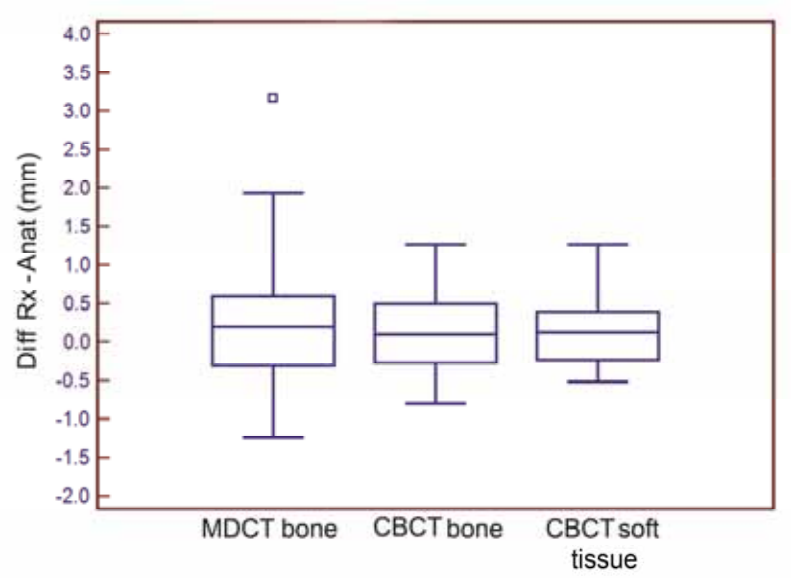

Figure 12. *Box and Whisker-Plot of the differences between the radiological and anatomical measurements.*

To validate the various measurements, the difference between the measurements was plotted against the mean (Fig. 13, A-D). The mean value, limits of agreement and the 95% CI for the limits of agreement are marked in the figures. These figures show that although the mean differences were all close to 0, the limits of agreement for bone measurements were broader in MDCT (-1.35mm ; 1.82mm) than in CBCT (-0.93mm ; 1.21mm). These results suggest that MDCT is to some extent less accurate. The limits of agreement for soft tissue measurements in CBCT, however, were smaller (-0.77mm ; 1.07mm), indicating a slightly higher accuracy for soft tissue measurements.

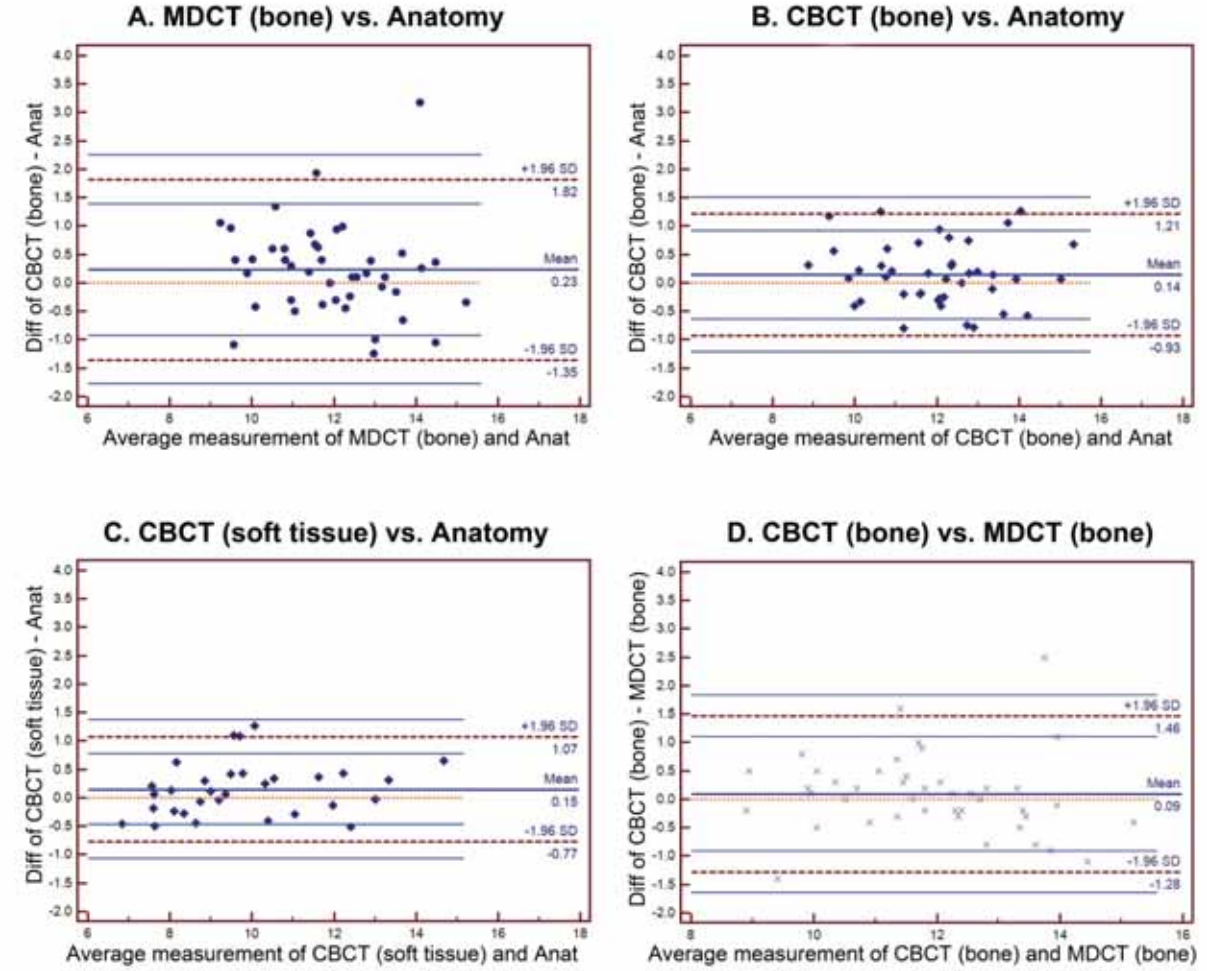

Figure 13. *Difference against the mean (solid middle blue line) of the anatomical and radiological measurements. The limits of agreement (broken brown lines) and the 95% CI of the limits of agreement (solid blue lines) are shown for* ***(A)*** *MDCT (bone),* ***(B)*** *CBCT (bone) and* ***(C)*** *CBCT (soft tissue) versus the anatomical measurements.* ***(D)*** *Difference against the mean of the bone measurements of CBCT versus MDCT.*

The precision of CBCT and MDCT was not only established through a comparison to the anatomical measurement, but also through direct comparison against each other (Figure 13-D): The agreement between bone measurements of CBCT and MDCT was investigated and the LOA (-1.28mm ; 1.46mm) as well as the range of agreement (2.74mm) were also established. The agreement between two radiological measurements is obsolete for this study, since the anatomical measurements could be used as comparative measurement. However, in a subsequent study (9.1.4.) no anatomical measurement could be obtained and the precision of the radiological measurements could only be assessed by comparing the agreement between various radiological measurements. It is for that forthcoming

study that the present results might deliver important information, as it allows to compare Bland-Altman plots of radiological measurements against each other to Bland-Altman plots of radiological measurements against anatomical measurements. Therefore, the interpretation of Figure 13-D will be given in 10.1.5., where the accuracy of CBCT versus various other radiological approaches is compared.

9.1.3. Establishing the best-suited MRI sequence for the assessment of the condylar process using micro-CT as reference (STUDY III)

Interobserver agreements for the detection of cortical bone thinning, cortical bone erosions, cortical bone surface irregularities and subcortical bone cysts ranged from very good to excellent for all locations (i.e. anterior, superior and posterior; κ = 0.67 - 0.85) and for all five sagittal MRI sequences (i.e. T1-2D-FSPGR, T2-FSE, T1-3D-FSPGR, PD-FS and T1-FSE: κ = 0.74 - 0.88).

Interobserver agreement for the detection of an anterior osteophyte was excellent for all MRI sequences (κ=1.0). Interobserver agreements for cortical bone thickness measurements were likewise excellent (r = 0.83 - 0.99, p<0.01). Thus, the mean of both observers' measurements was calculated and used for further statistical analyses.

- ***Objective analysis of cortical bone thickness measurements:***

All descriptive results for cortical bone thickness measurements are illustrated in Table 7. When compared to the μCT-based measurements, statistically significant differences were found for all cortical bone thickness measurements performed upon the T2-FSE, the PD-FSE and the T1-2D-FSPGR sequences (i.e. anterior, superior and posterior portions) as well as the anterior and posterior cortical bone thickness measurements performed upon the T1-FSE (each, p<0.05). No statistically significant differences were found for all T1-3D-FSPGR based measurements [i.e. anterior (p=0.14), superior (p=0.60) and posterior (p=0.22)] and for the superior T1-FSE based measurements (p=0.16) when compared to the μCT-based measurements.

Table 7. *Cortical bone thickness of the anterior, superior and posterior portions of the mandibular condyles as measured on all sagittal MRI sequences (mean of both readers, in mm).*

Specimen	T1-2D-FSPGR[1]			PD-FSE[2]			T2-FSE[2]		
	ANT	SUP	POST	ANT	SUP	POST	ANT	SUP	POST
1	0.74	0.52	0.33	0.94	0.66	0.35	0.66	0.66	0.66
2	0.74	0.52	0.34	0.94	0.47	0.67	0.66	0.68	0.66
3	0.75	0.33	0.48	0.66	0.66	0.48	0.94	0.94	0.48
4	0.66	0.33	0.33	0.94	0.66	0.66	0.94	0.64	0.66
5	0.70	0.58	0.52	0.95	0.57	0.66	0.66	0.70	0.66
6	0.70	0.52	0.33	0.94	0.49	0.47	0.68	0.66	0.66
7	0.66	0.52	0.33	0.68	0.56	0.50	0.68	0.66	0.66
8	0.54	0.35	0.33	0.66	0.60	0.47	0.66	0.60	0.66
9	0.66	0.99	0.34	0.94	1.05	0.66	0.94	0.93	0.66
10	0.86	0.85	0.52	1.06	0.94	0.94	0.94	1.05	0.66
11	0.97	0.52	0.47	0.94	0.66	0.66	1.05	0.66	0.67
12	0.70	0.52	0.47	0.94	0.66	0.67	0.94	0.65	0.66
13	0.74	0.50	0.33	0.66	0.47	0.42	0.66	0.66	0.66
14	0.97	0.52	0.50	1.06	0.66	0.47	1.06	0.66	0.66
15	0.66	0.52	0.52	0.94	0.94	1.06	0.66	1.05	1.05
16	0.52	0.52	0.52	0.66	0.94	0.66	0.66	0.94	0.66
Mean	**0.72**	**0.54**	**0.42**	**0.87**	**0.69**	**0.61**	**0.80**	**0.76**	**0.67**

(Table 7 cont.)

Specimen	T1-3D-FSPGR[1]			T1-FSE[2]		
	ANT	SUP	POST	ANT	SUP	POST
1	0.70	0.39	0.45	0.66	0.67	0.64
2	0.70	0.38	0.66	0.66	0.49	0.47
3	0.82	0.54	0.48	0.94	0.66	0.55
4	0.70	0.44	0.29	0.94	0.66	0.67
5	1.02	0.61	0.39	0.96	0.70	0.66
6	0.78	0.39	0.36	0.94	0.50	0.68
7	0.70	0.42	0.28	0.94	0.66	0.66
8	0.70	0.47	0.28	0.66	0.56	0.49
9	1.03	1.24	0.53	0.94	1.07	0.66
10	0.98	1.15	0.55	1.05	0.95	0.66
11	1.19	0.44	0.56	1.03	0.66	0.45
12	0.81	0.30	0.62	0.94	0.66	0.66
13	0.88	0.83	0.28	0.53	0.67	0.47
14	0.87	0.28	0.00	1.05	0.66	0.45
15	0.81	0.70	0.73	0.66	0.66	1.05
16	0.62	0.44	0.44	0.66	0.66	0.66
Mean	**0.83**	**0.56**	**0.43**	**0.85**	**0.68**	**0.62**

- ***Subjective evaluation of the cortical bone:***

The cortical bone of a total of 16 mandibular condyles divided into anterior, superior and posterior portions was investigated (total number of sites: 48). Imaging findings included cortical thinning (n: 16), cortical erosions (n: 6), cortical surface irregularities (n: 24), subcortical bone cysts (n: 3) and an anterior osteophyte (n: 4).

Accuracy, sensitivity, specificity, positive and negative predictive values for the depiction of cortical thinning, cortical erosions, cortical surface irregularities and subcortical bone cysts are illustrated in Table 8. When compared to the μCT-based evaluation, the T1-3D-FSPGR sequence was the most reliable in the assessment of cortical thinning, cortical erosions, cortical surface irregularities, subcortical bone cysts for both readers. The depiction of an anterior Osteophyte was perfect upon all sequences for both readers. For an imaging examples from **STUDY III**, see Figures 14 and 15.

Table 8. *Results from subjective analysis (mean of both readers). PPV: positive predictive value. NPV: Negative predictive value.*

	Cortical Bone Thinning						*Cortical Bone Surface Irregularities*				
	T1-2D-FSPGR[1]	**T2 FSE[2]**	**T1-3D-FSPGR[1]**	**PD FSE[2]**	**T1 FSE[2]**		**T1-2D-FSPGR[1]**	**T2 FSE[2]**	**T1-3D-FSPGR[1]**	**PD FSE[2]**	**T1 FSE[2]**
Accuracy	0.73	0.69	0.79	0.65	0.73		0.51	0.54	0.88	0.58	0.56
Sensitivity	0.28	0.21	0.78	0.50	0.50		0.17	0.08	0.83	0.25	0.38
Specificity	0.91	0.88	0.79	0.71	0.82		0.94	0.96	0.92	0.92	0.75
PPV	0.57	0.42	0.61	0.41	0.54		0.80	0.67	0.91	0.75	0.60
NPV	0.76	0.73	0.90	0.77	0.80		0.46	0.52	0.85	0.55	0.55
	Cortical Bone Erosions						*Subcortical Bone Cysts*				
	T1-2D-FSPGR[1]	**T2 FSE[2]**	**T1-3D-FSPGR[1]**	**PD FSE[2]**	**T1 FSE[2]**		**T1-2D-FSPGR[1]**	**T2 FSE[2]**	**T1-3D-FSPGR[1]**	**PD FSE[2]**	**T1 FSE[2]**
Accuracy	0.90	0.92	0.88	0.69	0.79		0.94	0.94	1.00	0.94	0.94
Sensitivity	0.33	0.33	0.83	0.50	0.33		0.33	0.33	1.00	0.33	0.33
Specificity	0.98	0.99	0.88	0.71	0.86		0.98	0.98	1.00	0.98	0.98
PPV	0.67	0.67	0.50	0.20	0.25		0.50	0.50	1.00	0.50	0.50
NPV	0.91	0.93	0.97	0.91	0.90		0.96	0.96	1.00	0.96	0.96

[1] = fast spoiled gradient recalled echo; [2] = fast spin echo;

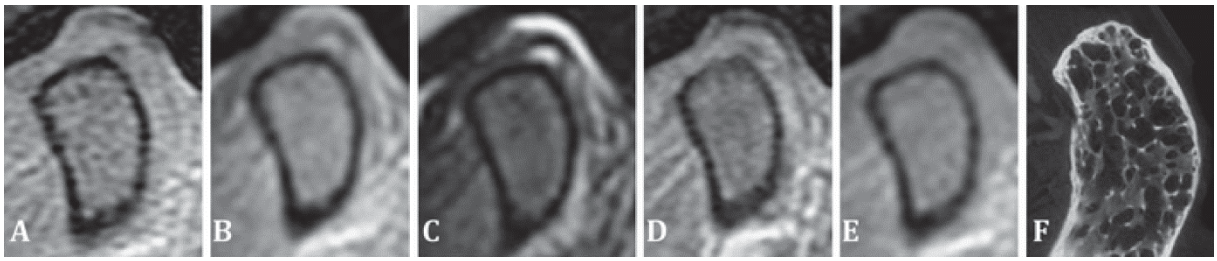

Figure 14. ***(A)*** *2D fast spoiled gradient recalled echo (2D FSPGR);* ***(B)*** *intermediate-weighted proton density fast spin echo (PD-FSE);* ***(C)*** *T2-weighted fast spin echo (T2-FSE);* ***(D)*** *T1-weighted 3D fast spoiled gradient recalled echo (T1-3D-FSPGR) and* ***(E)*** *T1-weighted fast spin echo sequences (T1-FSE). The cortical surface irregularities of the superior portion confirmed by* ***(F)*** *micro-CT are depicted by the T1-3D-FSPGR sequence only and seem to be absent on all other sequences.*

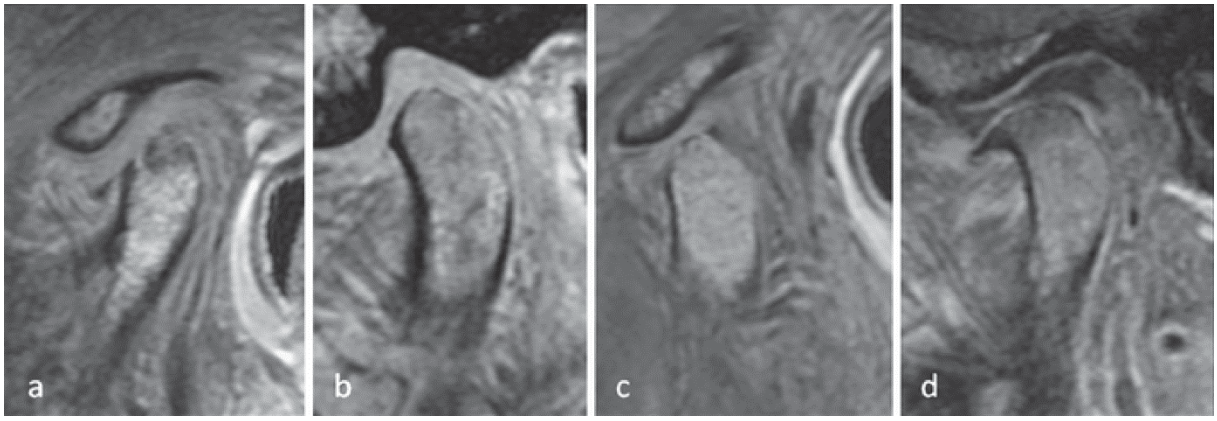

Figure 15. *Three imaging example illustrating the ability of the T1-3D-FSPGR sequence to depict* ***(a)*** *subcortical bone cysts;* ***(b)*** *osseous erosions,* ***(c)*** *cortical bone surface irregularities and* ***(d)*** *the presence of an anterior osteophyte and cortical bone thinning of the superior portion.*

9.1.4. Accuracy of CBCT versus MDCT, MRI, OPG and lateral cephalogram for linear measurements of the mandibular ramus and condylar process (STUDY IV)

Intra- and interobserver reliability showed excellent agreement (ICC >0.90) with exception of LC (Table 9). The highest ICC values were computed for OPG closely followed by CBCT, MDCT and MRI. ICC values for CP were generally smaller than values for RH with exception of OPG, MDCT and interobserver MRI. Interobserver ICC was generally smaller than intraobserver with exception of OPG and CBCT. LC values for CP (Intraobserver ICC: 0.79, Interobserver ICC: 0.59) and interobserver ICC for RH (0.82) were far below other measurements.

Table 9. *Intraclass Correlation Coefficient (ICC) demonstrating intra- and interobserver reliability per measurement type and imaging procedure.*

ICC	*Intraobserver*	*Interobserver*
Ramus height (RH)		
OPG	0.99	0.99
CBCT	0.99	0.99
MDCT	0.98	0.97
MRI	0.95	0.92
LC	0.93	0.82
Condylar process (CP)		
OPG	0.99	0.99
CBCT	0.98	0.98
MDCT	0.98	0.97
MRI	0.93	0.93
LC	0.79	0.59

The agreement was also judged with Bland and Altman-plots (Table 10 and Figure 16) and the range of agreement was defined as the range between the lower and the upper limit of agreement.

The narrowest range of agreement was identified between MRI and MDCT for both RH (4.4mm) and CP (1.9mm). For RH the range of agreement between MRI and CBCT (4.4mm) was even narrower than between CBCT and MDCT (5.1mm). For CP the limits of agreement between MRI and CBCT (5.5mm) were only little wider than between CBCT and MDCT (4.8mm).

MRI and OPG measurements for RH and CP were significantly smaller than the measurements of all other imaging methods (Table 10). OPG measurements were even significantly smaller than those obtained on MRI. The mean differences between MRI and MDCT measurements (MRI minus MDCT) were -0.4mm for RH and -1.2mm for CP. Mean differences between MRI and CBCT measurements (MRI minus CBCT) were -1.9mm for RH and -1.1mm for CP. OPG and LC showed least agreement with measurements based on 3D datasets and showed the widest limits of agreement.

Table 10. *Mean differences (upper value minus lower value). In brackets: range of LOA [mm] (bold) and LOA [mm] for CP (upper right) and RH (lower left).*

		Condylar Process (CP)				
		OPG	**CBCT**	**MDCT**	**MRI**	**LC**
Ramus height (RH)	**OPG**		3.1* (**8.4**: 7.3, -1.1)	3.2* (**5.7**: 6.1, 0.4)	2.1* (**6.0**: 5.1, -0.9)	4.1* (**6.2**: 7.2, -1.0)
	CBCT	-6.6* (**7.3**: -2.9, -10.2)		0.1 (**4.8**: 2.5, -2.3)	-1.1* (**5.5**: 1.7, -3.8)	1.0* (**4.4**: 3.2, -1.2)
	MDCT	-6.1* (**5.8**: -3.2, -9.0)	0.5 (**5.1**: 3.0, -2.1)		-1.2* (**1.9**: -0.2, -2.1)	0.9 (**4.1**: 2.9, -1.2)
	MRI	-4.3* (**4.3**: -2.1, -6.4)	1.9* (**4.4**: 4.1, -0.3)	1.4* (**4.4**: 3.6, -0.8)		2.0* (**5.2**: 4.6, -0.6)
	LC	-6.6* (**4.4**: -4.4, -8.8)	0.0 (**8.0**: 4.0, -4.0)	-0.5 (**8.2**: 3.6, -4.6)	-2.5* (**4.9**: -0.1, -5.0)	

** Significant mean differences between methods according to paired t-test.*

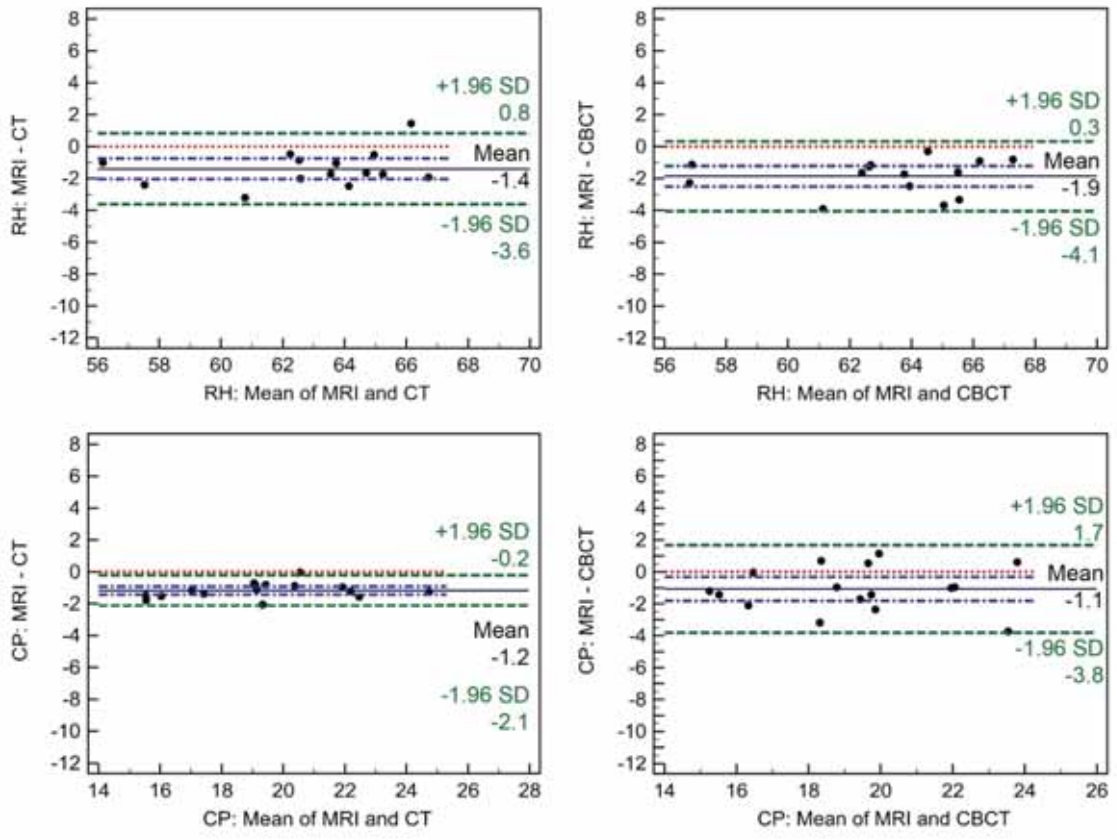

Figure 16. *Bland-Altman-Plots with mean difference (black line) extended by 95% CI (blue dash-dotted line) and limits of agreement (green dashed line) for RH and CP of MRI vs. MDCT and MRI vs. CBCT. In this figure, MDCT is abbreviated as CT.*

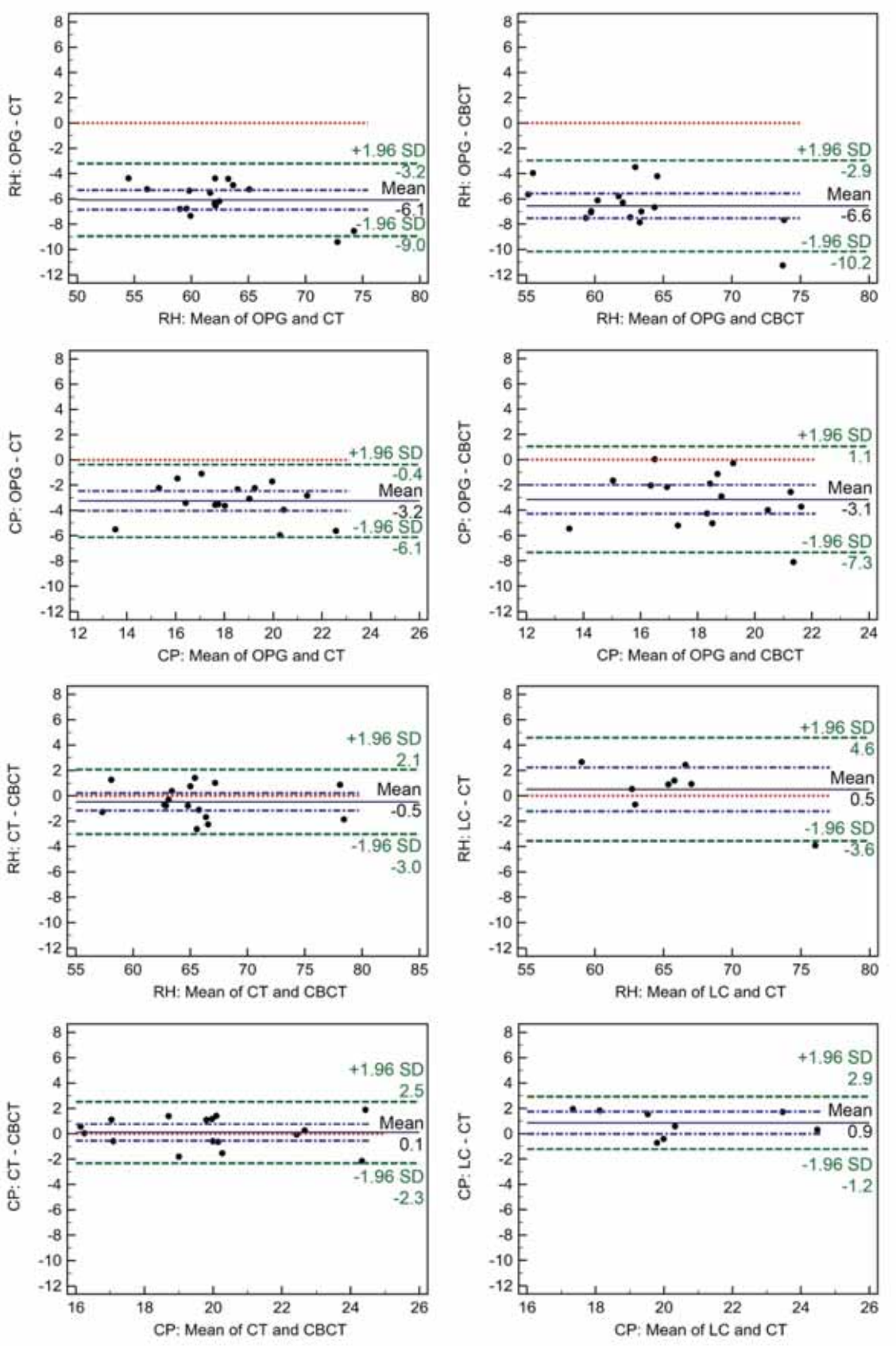

Figure 16 cont. *Bland-Altman-Plots with mean difference (black line) extended by 95% CI (blue dash-dotted line) and limits of agreement (green dashed line) for RH and CP of OPG vs. MDCT, OPG vs. CBCT, MDCT vs. CBCT and LC vs. MDCT. In this figure, MDCT is abbreviated as CT.*

Measurement precision judged in terms of coefficient of variation (CV) for both measurements (RH and CP) showed highest precision with OPG followed in descending order by CBCT, MDCT, MRI and LC (Tables 11-12 and Figure 17).

Table 11. *Descriptive statistics (mean, 95% CI) of Mean [mm] and SD [mm] of both linear measurements (RH and CP) used to calculate CV (Table 12) in all imaging methods.*

	Mean	*95% CI*		*Mean*	*95% CI*	
		lower	*upper*		*lower*	*upper*
	Mean of ramus height (RH)			**SD of ramus height (RH)**		
OPG	59.34	56.84	61.83	0.39	0.23	0.55
CBCT	65.89	62.84	68.94	0.57	0.44	0.71
MDCT	65.41	62.42	68.41	0.73	0.48	0.98
MRI	62.23	60.35	64.10	0.74	0.49	0.99
LC	65.93	63.71	68.14	1.35	0.89	1.81
	Mean of condylar process (CP)			**SD of condylar process (CP)**		
OPG	16.70	15.46	17.93	0.19	0.15	0.24
CBCT	19.83	18.39	21.28	0.33	0.22	0.43
MDCT	19.94	18.56	21.33	0.37	0.27	0.47
MRI	18.77	17.32	20.22	0.63	0.41	0.84
LC	20.80	19.54	22.06	1.35	0.93	1.78

Table 12. *Descriptive statistics of the Coefficient of Variation (CV) for linear measurements (RH and CP) and all imaging methods. ANOVA of CV with p-value computed per measurement type for all imaging procedures. Distinct letters (a, b, c) are significantly different according to Scheffé post-hoc test.*

	Mean	*95% CI*		*SD*	*Min*	*Max*	*ANOVA Scheffé post-hoc subgroups*
		lower	*upper*				
CV of ramus height (RH)							*(p<0.001)*
OPG	0.007	0.004	0.010	0.005	0.001	0.019	a
CBCT	0.009	0.007	0.011	0.004	0.003	0.017	a
MDCT	0.011	0.007	0.016	0.008	0.001	0.027	a, b
MRI	0.012	0.008	0.016	0.007	0.002	0.029	a, b
LC	0.021	0.014	0.028	0.014	0.004	0.049	b
CV of condylar process (CP)							*(p<0.001)*
OPG	0.012	0.009	0.014	0.005	0.003	0.020	a
CBCT	0.017	0.011	0.023	0.011	0.003	0.039	a
MDCT	0.019	0.014	0.024	0.010	0.008	0.046	a, b
MRI	0.033	0.023	0.043	0.019	0.005	0.090	b, c
LC	0.065	0.044	0.086	0.039	0.012	0.150	c

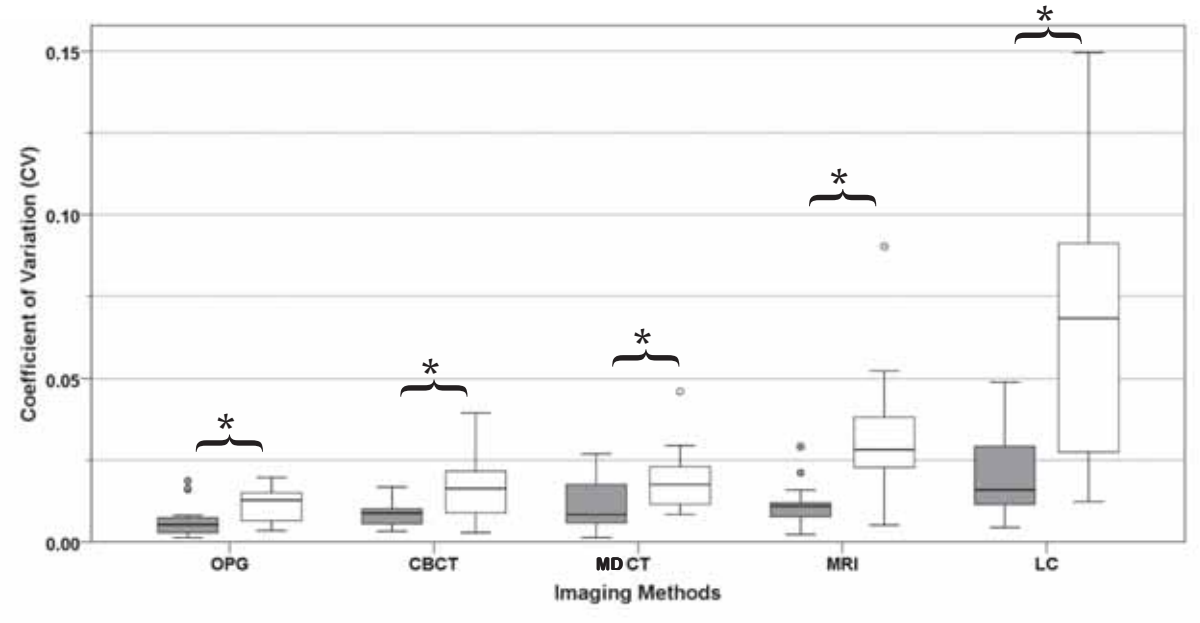

Figure 17. *Boxplots of CV for linear measurements of all imaging methods.*
** Significant differences according to two-sample t-test.*

For RH, only lateral cephalogram and for CP, both lateral cephalogram and MRI were significantly less precise than the other imaging methods (Table 12). Lateral cephalograms were significantly less precise than MRI for the CP measurements. Within the same imaging method, measurements of RH were significantly more precise than of CP when judged in terms of CV (Figure 17).

9.1.5. Accuracy of CBCT, MDCT and lateral cephalogram in assessing the cervical spine (STUDY V)

Following enzymatic maceration (see 8.1.6.), the vertebral bodies C2 and C3 of the four vertebrae assessed positively on lateral cephalogram (see 8.1.3.) could be completely mobilized, demonstrating the absence of a congenital bony fusion in these vertebral segments (see Figures 18-20).

All facet joints showed degenerative osteoarthritic changes including osteophytes, peripheral eburnisation, and gross irregularities of the subchondral joint surfaces of varying degree. The facets of specimens 3 and 4 were more severely affected, exhibiting extensive osteophytes and very ragged bony joint surfaces (see Figure 20).

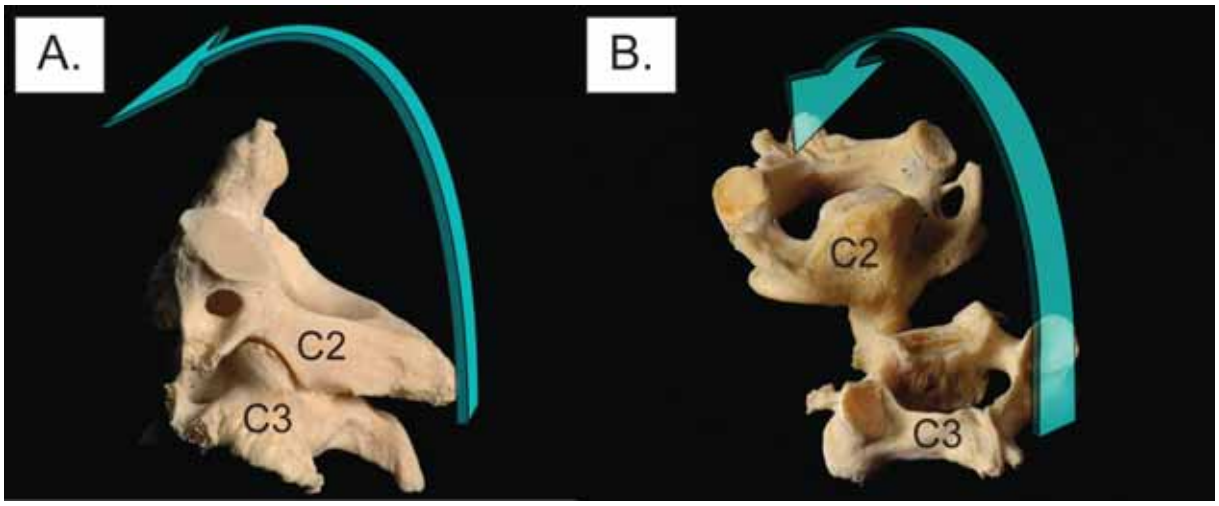

Figure 18. *Explanatory illustration of how the specimens are depicted in Figures 19 and 20. C2 is rotated 180° in order to enable a direct view of all facets of the joints of the left and right articular process and the intervertebral disc space.*

All raters agreed that no congenital fusion was found on MDCT or CBCT, but there was a disagreement concerning the prevalence of osteoarthritic deformities. General radiologists assessing MDCT recognized osteoarthritic changes in 100% (40/40) of the joints, oral radiologists evaluating CBCT found osteoarthritic changes in 93.3% (38/40) of the cases. Moreover, when evaluating the narrowing of the joint space in the affected osteoarthritic joints, the two rater groups differed substantially (Table 13). The concordance between the two rater groups was rather modest (70%) with a Kappa value of 0.452 (standard error: 0.132, 95% CI: 0.193 – 0.711), indicating a moderate agreement (Landis and Koch 1977).

Table 13. *Assessment of the osteoarthritic joints: Evaluation of the joint space narrowing.*

Osteoarthritic joint assessment	*General radiologists/MDCT*	*Oral Radiologists/CBCT*
Osteoarthritic joint, ***joint space entirely preserved***	80.0%	51.8%
Osteoarthritic joint, ***joint space partially preserved***	20.0%	48.2%
Osteoarthritic joint, ***joint space not visible***	0%	0%

In addition, there was a considerable difference regarding the agreement *within* a rater group when evaluating the narrowing of the joint space. General radiologists assessing MDCT data agreed more consistently with each other (κ = 0.612) than did the oral radiologists assessing CBCT data (κ= 0.240, see Table 14). The Kappa value of 0.240 for CBCT/oral radiologists corresponds to a fair agreement, and the Kappa value of 0.612 MDCT/general radiologists denotes a substantial agreement (Landis and Koch 1977).

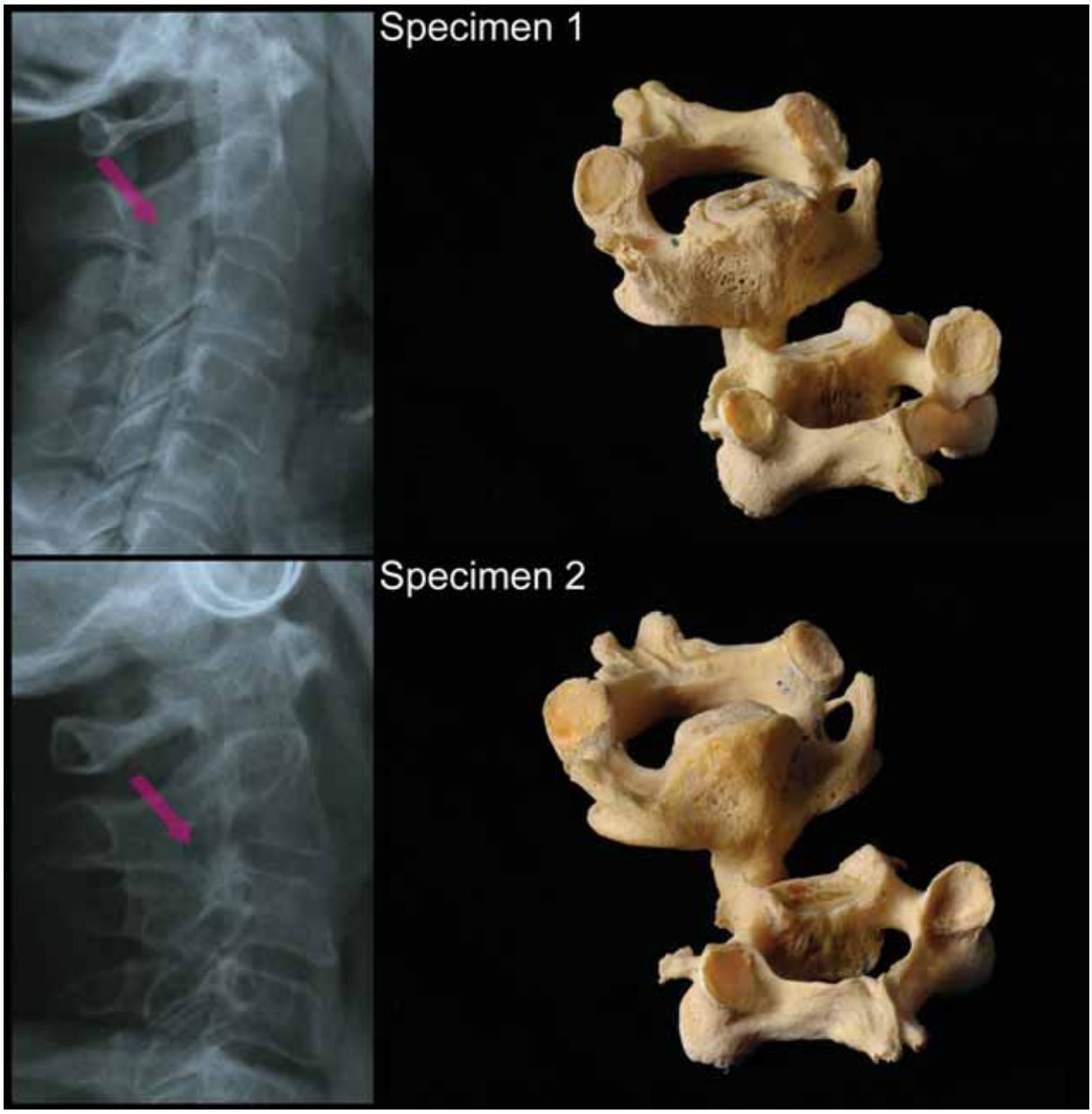

Figure 19. *Specimens 1 and 2: Left side shows the lateral cephalogram of the intact cadaver head, right side shows the macerated vertebral bodies of C2 and C3.The purple arrow points towards the suspected fusion.*

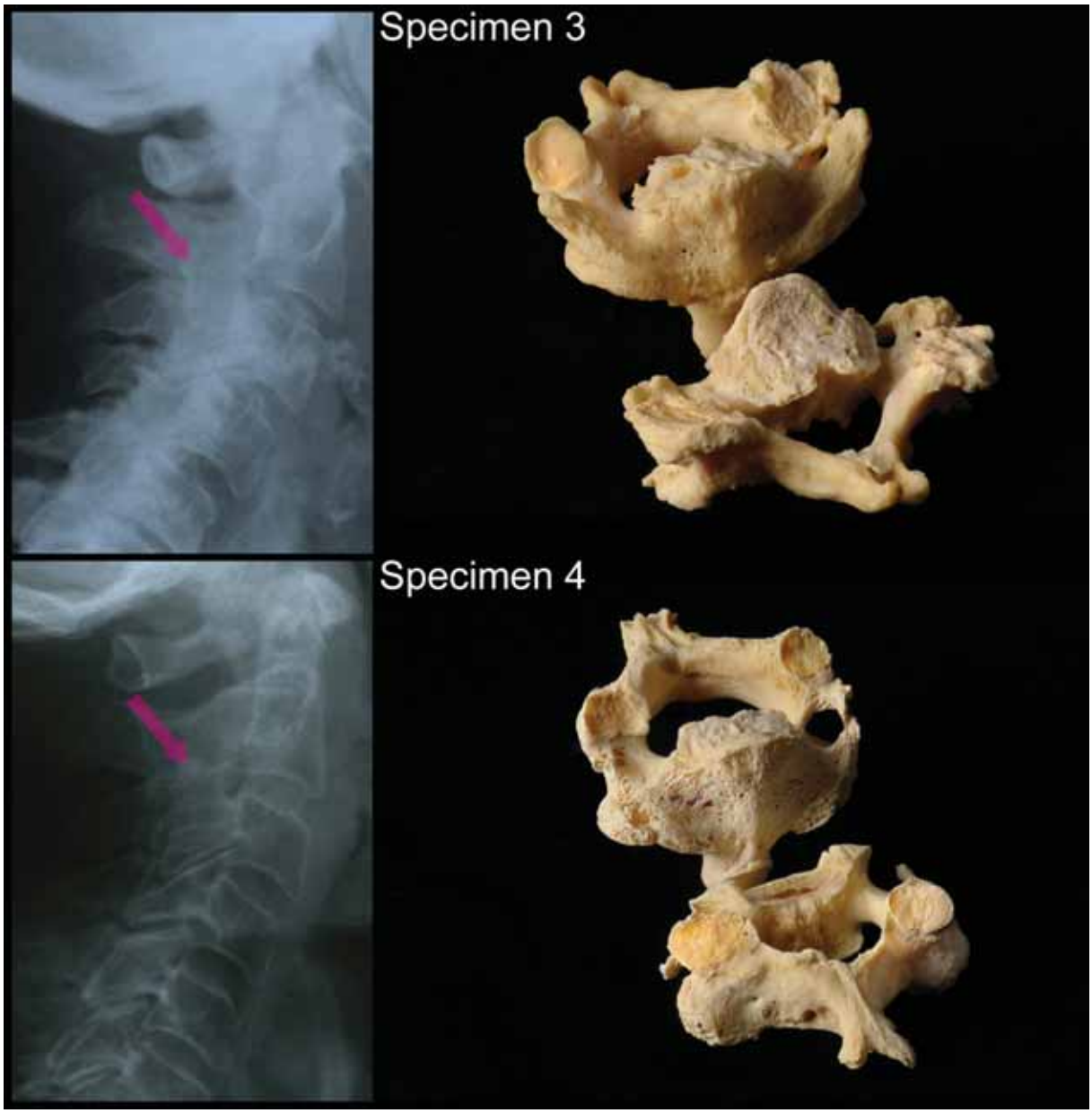

Figure 20. *Specimens 3 and 4: Left side shows the lateral cephalogram of the intact cadaver head, right side shows the macerated vertebral bodies of C2 and C3. The purple arrow points towards the suspected fusion.*

Table 14. *Fleiss' kappa for multiple raters: Agreement (within each group) of 5 general radiologists assessing MDCT and 5oral radiologists assessing CBCT, respectively.*

Method	*Kappa*	*Standard error*	*95% CI*
MDCT/general radiologists	0.612	0.068	0.479 – 0.745
CBCT/oral radiologists	0.240	0.078	0.088 – 0.392

9.2. Radiation dose evaluation (STUDY VI)

The effective dose according to the tissue weighting factor (TWF) of the ICRP 2007 was evaluated for the following radiological procedures:

- Hand-wrist radiograph (9.2.1.)
- Lateral cephalogram without thyroid shield (9.2.2.)
- Lateral cephalogram with a thyroid shield (9.2.3.)
- CBCT Portrait mode (17cm scan height) without a thyroid shield (9.2.4)
- CBCT Portrait mode (17cm scan height) with a thyroid shield (9.2.5.)
- CBCT Landscape mode (13cm scan height) without thyroid shield (9.2.6.)
- CBCT Landscape mode (13cm scan height), fast scan without thyroid shield (9.2.7.)

9.2.1. Radiological exposure: Hand-wrist radiograph

Table 15. *Calculation of the effective dose of a hand-and-wrist radiograph.*

Tissue	*Fraction of total organ irradiated*	*Absorbed dose mGy*	*Equivalent dose µSv*	*TWF ICRP 2007*	*Effective dose µSv*	*% of effective dose*
Bone marrow	0.50%	0.16	0.80	0.12	0.096	58.71%
Thyroid	0%	-	-	-	-	-
Esophagus	0%	-	-	-	-	-
Bone surface	0.50%	0.16	3.71	0.01	0.037	22.70%
Salivary glands	0%	-	-	-	-	-
Skin	1%	0.16	4.75	0.01	0.016	9.78%
Brain	0%	-	-	-	-	-
Muscle	1%	0.16	1.60	0.009	0.014	8.81%
Remainder	0%	-	-	-	-	-
Total					**0.164**	**100.00%**

9.2.2. Radiological exposure: Lateral cephalogram without thyroid shield

Table 16. *Calculation of the effective dose of a lateral cephalogram without a thyroid shield.*

Tissue	*Fraction of total organ irradiated*	*Absorbed dose mGy*	*Equivalent dose µSv*	*TWF ICRP 2007*	*Effective dose µSv*	*% of effective dose*
Bone marrow	16.50%	0.04	6.01	0.12	0.72	14.33%
Thyroid	100%	0.05	45.00	0.04	1.80	35.79%
Esophagus	10.00%	0.05	4.50	0.04	0.18	3.58%
Bone surface	16.50%	0.17	27.87	0.01	0.28	5.54%
Salivary glands	100.00%	0.06	59.99	0.01	0.60	11.93%
Skin	5%	0.06	2.88	0.01	0.03	0.57%
Brain	100%	0.03	30.00	0.01	0.30	5.97%
Muscle	5%	0.05	2.70	0.009	0.02	0.48%
Remainder	-	0.06	124.54	0.009	1.12	22.29%
Total					**5.03**	**100.00%**

9.2.3. Radiological exposure: Lateral cephalogram with a thyroid shield

Table 17. *Calculation of the effective dose of a lateral cephalogram with a thyroid shield.*

Tissue	*Fraction of total organ irradiated*	*Absorbed dose mGy*	*Equivalent dose µSv*	*TWF ICRP 2007*	*Effective dose µSv*	*% of effective dose*
Bone marrow	16.50%	0.04	6.01	0.12	0.72	21.85%
Thyroid	100%	0.01	8.00	0.04	0.32	9.70%
Esophagus	10.00%	0.01	0.80	0.04	0.03	0.97%
Bone surface	16.50%	0.17	27.87	0.01	0.28	8.45%
Salivary glands	100.00%	0.06	59.99	0.01	0.60	18.18%
Skin	5%	0.06	2.88	0.01	0.03	0.87%
Brain	100%	0.03	30.00	0.01	0.30	9.09%
Muscle	5%	0.05	2.70	0.009	0.02	0.48%
Remainder	-	0.05	113.23	0.009	1.02	30.89%
Total					**3.30**	**100.00%**

9.2.4. Radiological exposure: CBCT Portrait mode without a thyroid shield

Table 18. *Calculation of the effective dose of a CBCT scan (17cm FOV) without a thyroid shield.*

Tissue	*Fraction of total organ irradiated*	*Absorbed dose mGy*	*Equivalent dose µSv*	*TWF ICRP 2007*	*Effective dose µSv*	*% of effective dose*
Bone marrow	16.50%	1.15	189.08	0.12	22.69	17.23%
Thyroid	100%	1.09	1090.00	0.04	43.60	33.11%
Esophagus	10.00%	1.09	109.00	0.04	4.36	3.31%
Bone surface	16.50%	5.32	877.33	0.01	8.77	6.66%
Salivary glands	100.00%	1.47	1466.52	0.01	14.67	11.14%
Skin	5%	1.30	64.75	0.01	0.65	0.49%
Brain	100%	1.02	1020.00	0.01	10.20	7.75%
Remainder	210%	1.41	2971.20	0.009	26.74	20.31%
Total					**131.68**	**100.00%**

9.2.5. Radiological exposure: CBCT Portrait mode with a thyroid shield

Table 19. *Calculation of the effective dose of a CBCT scan (17cm FOV) with a thyroid shield.*

Tissue	*Fraction of total organ irradiated*	*Absorbed dose mGy*	*Equivalent dose µSv*	*TWF ICRP 2007*	*Effective dose µSv*	*% of effective dose*
Bone marrow	16.50%	1.15	189.08	0.12	22.69	23.58%
Thyroid	100%	0.33	332.00	0.04	13.28	13.80%
Esophagus	10.00%	0.33	33.20	0.04	1.33	1.38%
Bone surface	16.50%	5.32	877.33	0.01	8.77	9.12%
Salivary glands	100.00%	1.47	1466.52	0.01	14.67	15.24%
Skin	5%	1.30	64.75	0.01	0.65	0.67%
Brain	100%	1.02	1020.00	0.01	10.20	10.60%
Remainder	210%	1.30	2739.47	0.009	24.66	25.62%
Total					**96.24**	**100.00%**

9.2.6. Radiological exposure: CBCT Landscape mode without thyroid shield

Table 20. *Calculation of the effective dose of a CBCT scan (13cm FOV) without a thyroid shield.*

Tissue	*Fraction of total organ irradiated*	*Absorbed dose mGy*	*Equivalent dose µSv*	*TWF ICRP 2007*	*Effective dose µSv*	*% of effective dose*
Bone marrow	16.50%	0.75	123.32	0.12	14.80	16.26%
Thyroid	100%	0.31	306.00	0.04	12.24	13.45%
Esophagus	10.00%	0.31	30.60	0.04	1.22	1.35%
Bone surface	16.50%	3.47	572.19	0.01	5.72	6.29%
Salivary glands	100.00%	1.93	1926.47	0.01	19.26	21.17%
Skin	5%	1.85	92.50	0.01	0.93	1.02%
Brain	100%	0.50	502.40	0.01	5.02	5.52%
Remainder	210%	1.68	3532.46	0.009	31.79	34.94%
Total					**90.99**	**100.00%**

9.2.7. Radiological exposure: CBCT Landscape mode, fast-scan without thyroid shield

Table 21. *Calculation of the effective dose of a CBCT fast scan (13cm FOV) without a thyroid shield.*

Tissue	*Fraction of total organ irradiated*	*Absorbed dose mGy*	*Equivalent dose µSv*	*TWF ICRP 2007*	*Effective dose µSv*	*% of effective dose*
Bone marrow	16.50%	0.73	120.03	0.12	14.40	18.67%
Thyroid	100%	0.23	233.00	0.04	9.32	12.08%
Esophagus	10.00%	0.23	23.30	0.04	0.93	1.21%
Bone surface	16.50%	3.38	556.96	0.01	5.57	7.22%
Salivary glands	100.00%	1.52	1522.51	0.01	15.23	19.73%
Skin	5%	1.27	63.40	0.01	0.63	0.82%
Brain	100%	0.50	503.60	0.01	5.04	6.53%
Remainder	-	1.38	2894.42	0.009	26.05	33.76%
Total					**77.17**	**100.00%**

9.2.8. Impact of the thyroid shield

The use of a thyroid shield decreased the effective dose considerably in a conventional lateral cephalogram (from 5.03µSv to 3.30µSv) as well as in CBCT portrait mode (from 131.7µSv to 96.24µSv). This represents a dose reduction of 34% and 27%, respectively. Thus, a portrait mode scan (17cm FOV) *with* a thyroid shield has only little more radiation exposure (96.24µSv) than a landscape mode scan (13cm FOV) *without* a thyroid shield (90.99µSv).

The effective dose of a lateral cephalogram *without* thyroid shield was approximately 1.5-fold the cumulative effective dose of a hand-wrist radiogram and a lateral cephalogram with thyroid shield: Adding the effective dose of a hand-wrist radiogram to the effective dose of the lateral cephalogram with thyroid shield results in a cumulative effective dose of 3.46µSv. This equals a reduction of approximately 31% over the effective dose of a lateral cephalogram *without* thyroid shield.

It is further evident that applying a thyroid shield does not cause a relevant reduction in all imaging methods (Table 22).

Table 22. *Impact of shielding the thyroid on different readiological examinations. Effective dose (µSv) and dose reduction (%).*

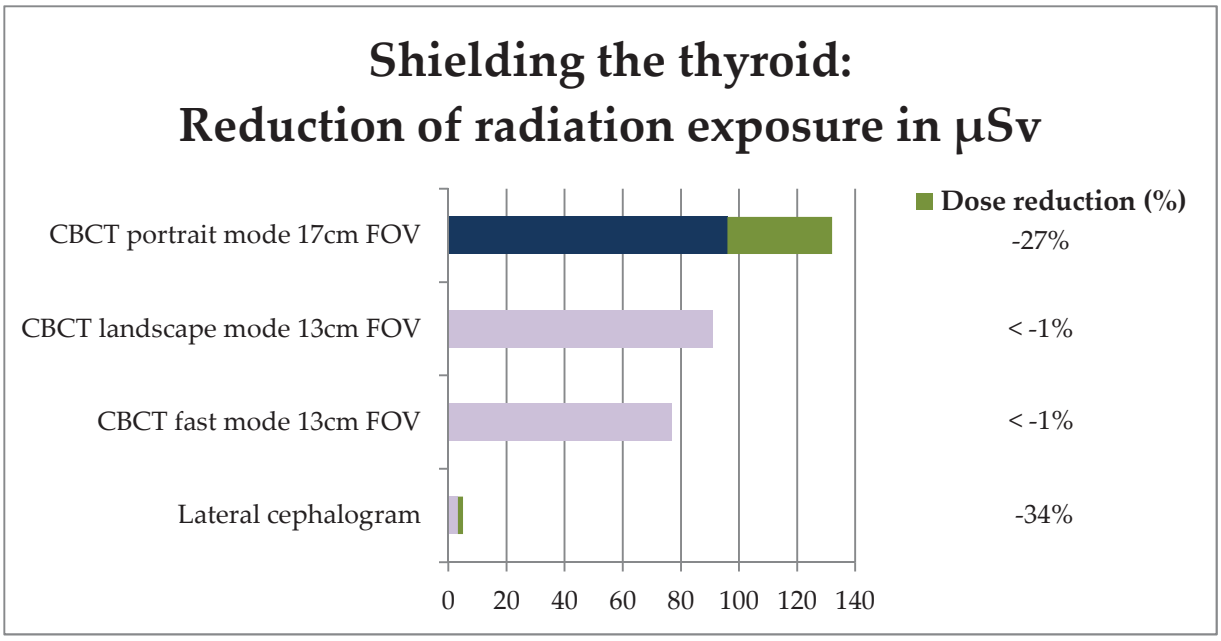

10. Discussion

10.1. Efficacy (STUDIES I – V)

10.1.1. Repeatability of radiological measurements

Repeatability is the ability of an experiment to be reproduced, either by the same examiner or by another examiner working independently. This attribute is regarded as a prerequisite for further comparisons of measurements. Thus, when evaluating the accuracy or reliability of radiological methods, the very first step is to demonstrate that the data are reproducible.

In **STUDIES I-IV**, intra- and/or interobserver agreement *for linear measurements* was calculated with the intraclass correlation coefficient (ICC) for absolute agreement based on a one-way random effects analysis of variance (ANOVA) was. ICC revealed mostly very good to excellent repeatability of all radiological linear measurements. The only exception is the reproducibility of linear measurements in lateral cephalograms, which is discussed more in detail in 10.1.5. A limitation in the method of **STUDIES I** and **II** is the fact that the measurements were only performed by one investigator, and the reliability tests had to be confined to intraobserver repeatability. Thus, the extent of interobserver error was not assessed, and potential systematic bias cannot be factored out. This issue of bias could be relevant and may even have been amplified inasmuch as only a small number of cadaver heads was examined.

In **STUDIES III** and **V**, interobserver agreement *for categorical* data was determined by means of Kappa statistics, were categorical data were produced for CBCT, MDCT and MRI. The results are presented above in 9.1.3. (MRI) and 9.1.5. (CBCT and MDCT), and discussed at length in 10.1.4 (MRI) and 10.1.6. (CBCT and MDCT).

Both ICC and Kappa have their shortcomings. Kappa is an uncomplicated way to calculate the level of chance-corrected agreement, yet the interpretation of the obtained values is subject of controversy. In the present dissertation, the interpretation of Kappa values followed the recommendation of Landis and Koch

(Landis and Koch 1977), as mentioned in 8.2.6. Landis and Koch's recommendation is by no means universally accepted. They supplied no evidence to support their grading system, and other formulae to calculate agreement were shown to be more reliable and less affected by prevalence and marginal probability (Wongpakaran et al. 2013).

The appropriateness of ICC for evaluating inter- and intra-observer error is debatable, too. Bland and Altman state that although the intraclass correlation would avoid the common pitfall of linear relationship being mistaken for agreement (as would be the case with simple correlations), it does not avoid other problems associated with correlation coefficients in this context, as it is still dependent on the range of the measurement and it is not related to the actual scale of measurement or to the size of error which might be clinically allowable (Bland and Altman 1990). Yet, according to Bland and Altman, a distinction between a correlation of repeated measures by the same method, and a correlation of measures by two different methods can be made, and for the former the ICC would be permissible (Bland and Altman 1990).

Based on these arguments, the ICC was calculated to determine intra- and interobserver reliability within an assessment method. However, in order to establish the agreement between two different methods (or more), Bland-Altman plots were performed and limits of agreement were identified (Bland and Altman 1986), with the 95%CI of the limits of agreement (Bland and Altman 1999).

10.1.2. The effect of different voxel sizes on buccal bone measurements (STUDY I)

The results on bone measurements (9.1.1.) revealed that voxel size has an impact on image accuracy and are in agreement with Sun et al. (Sun et al. 2011) who reported an improvement in accuracy when decreasing the voxel size. Yet, as mentioned in the introduction (6.1.1.), there are contradicting reports as to whether the voxel size affects the image accuracy. Moreover, a systematic review concluded that studies dealing with categorical data showed a tendency towards more accurate

results with high-resolution protocols, while this was not the case for studies with numerical data (Spin-Neto et al. 2013).

In order to interpret this within a proper context, a comprehensive understanding of the impact of voxel size on image accuracy is needed. Smaller voxels mean per definition a higher resolution of the acquired data. Higher spatial resolution will affect image accuracy in four ways, three of them will enhance accuracy, but the fourth will reduce it.

(1) Imaging an object that is smaller than the radiation beam or focal spot will cause the object to be recorded with a reduced value proportional to its size within the beam. As a result, any structure smaller than the beam will appear broadened or blurred (Maloul et al. 2011).

(2) The voxel size will also affect the partial volume averaging, which occurs when two objects (or more) with different density are within a voxel. In this case, since the voxel is only able to render a single value, the voxel will not be representative of the tissue of either object, but rather, it becomes a weighted average of the different density values (Scarfe and Farman 2008). This partial volume averaging effect occurs in all structures, but will have a higher impact on the representation of thin structures due to greater representation of edge elements (Maloul et al. 2011).

(3) Voxel size has an important influence on sampling. Sampling is the process of converting continuous analogue signals, such as anatomy, into discrete digital data by recording data points of analogue signals at regular intervals in space. The Nyquist-Shannon sampling theorem (Shannon 1998) defines how often each sample should be taken in space for an accurate reconstruction of the original analogue signals. For example, applying the Nyquist-Shannon sampling theorem in digital image processing to visualize and represent accurately anatomical structures that are at least 0.4 mm, a voxel size of 0.2 mm is required (Hatcher 2010).

(4) Original analogue signals can be corrupted by background noise (unwanted

signals). There are many sources of noise that can degrade a CBCT image. The most significant sources are related to patient motion and scatter artefact, particularly scatter artefacts associated with dense objects such as metallic restorations. Reducing the voxel size will increase the amount of analogue signals, and with it, the amount of unwanted signals (Hatcher 2010, Maloul et al. 2011).

Based on this, some rationale can be given on the fact that contradicting reports are available as to whether the voxel size affects the image accuracy. It is obvious that since many devices were used in all different studies, not all four developments described above will be represented equally. Furthermore, the size of the object in relation to the voxel size is of outmost importance. Since investigations on various objects of inequitable sizes (such as small structures like roots of teeth and thin bone covering, or large structures such as facial dimensions) were analysed, it should come as no surprise that dissimilar results were reported.

The second observation, i.e. the fact that studies dealing with categorical data showed a tendency towards more accurate results with high-resolution protocols, than studies with numerical data, is probably a ramification of the data analysis itself. Most of the previous studies suffer from unsuitable statistical evaluation. The authors either confined their results to mere descriptive statistics or the data were assessed by means of correlation analysis. But comparing two methods of measurement is "a common abuse of correlation" (Bland and Altman 1986, 1999, 2003), since the quest is not to analyze the agreement, but rather the difference of the two measurement methods and ultimately assess if the *disagreement* is small enough to deem the two methods interchangeable. Also the often assumed approach that considers the physical measures as the "ground truth", may be erroneous. Suomalainen et al. explained similarly that *"it is noteworthy that the values representing the gold standard also contain a source of error"*(Suomalainen et al. 2008). The Bland-Altman method is used to overcome these problems. By applying this method, it was possible to show the agreement both for vertical and horizontal measurements in the

low as well as high resolution protocol. In the low resolution protocol, the horizontal measures were somewhat more accurate. The obvious reason is that very small absolute measurements were taken when measuring alveolar bone thickness. Taking measurements very close to 0 causes the differences of the measurements to be smaller and creates a bias in the limits of agreement. Both the visual interpretation of the plots in Figures 10-C and 10-D (see 9.1.1.) and the Levene-test reveal that the distribution of the differences gets wider as the absolute measurements get larger. This crucial observation together with the fact that the limits of agreement are greater than the average thickness of the alveolar bone indicates that both resolution protocols are not accurate enough to enable measurements of such delicate structures as the width of the alveolar bone covering. Also, it is a partial proof of the suggestion given above that the variety of results reported on the impact of voxel size is probably due to the impact of the size of the examined object.

The decision regarding which voxel size to use should be based on the limits of agreement rather than on the mean value. The finding that a difference between the anatomical and radiological measurement can be as large as 2mm shows that the average alveolar bone thickness of 1mm may be missed completely. The limits of agreement presented in here give strong evidence to Sun and co-workers who reported that bone height loss can be overestimated by 1.5 - 2mm in a 0.4mm resolution protocol (Sun et al. 2011). Finally, present radiological measurements are less in accordance with physical findings shown by Damstra (Damstra et al. 2010) as well as most studies performed on dry specimens reporting submillimeter accuracy, suggesting that presence of soft tissues does indeed affect the accuracy of bony measures.

The alveolar bone covering can be very thin. In the studied specimens, the thinnest bone covering measured was 0.14mm, but despite that no relevant dehiscences or fenestrations were found. However on the radiological data, there were some sites where absolutely no covering was depictable (see Fig. 21, B1 - B3; Fig. 22).

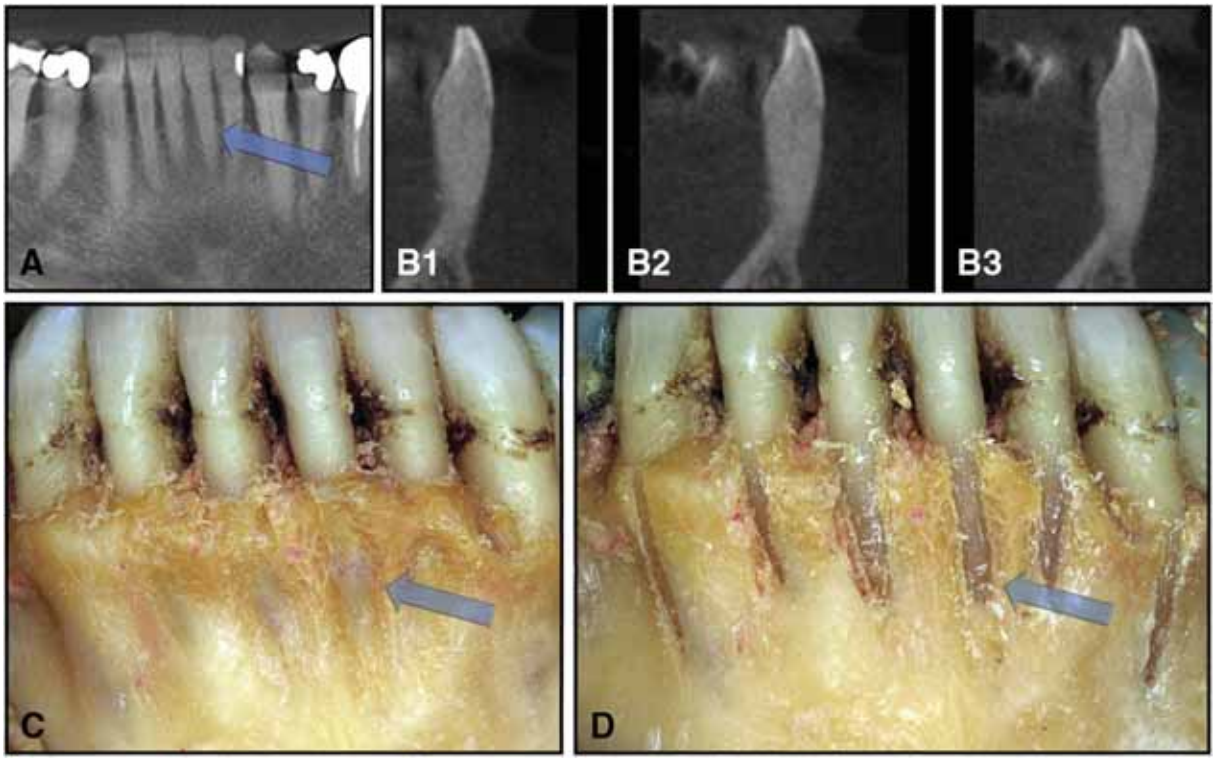

Figure 21. *Radiological data versus clinical findings: lower left first incisor as seen on the CBCT scan:* ***(A)*** *Reformatted OPG view and* ***(B)*** *3 slices in the sagittal view* ***(B1 - B3)****.* ***(C)*** *Clinical view after removing the gingiva and* ***(D)*** *after removing the alveolar bone covering. Note that no bone covering is being depicted on the sagittal scans* ***(B1 - B3)****.*

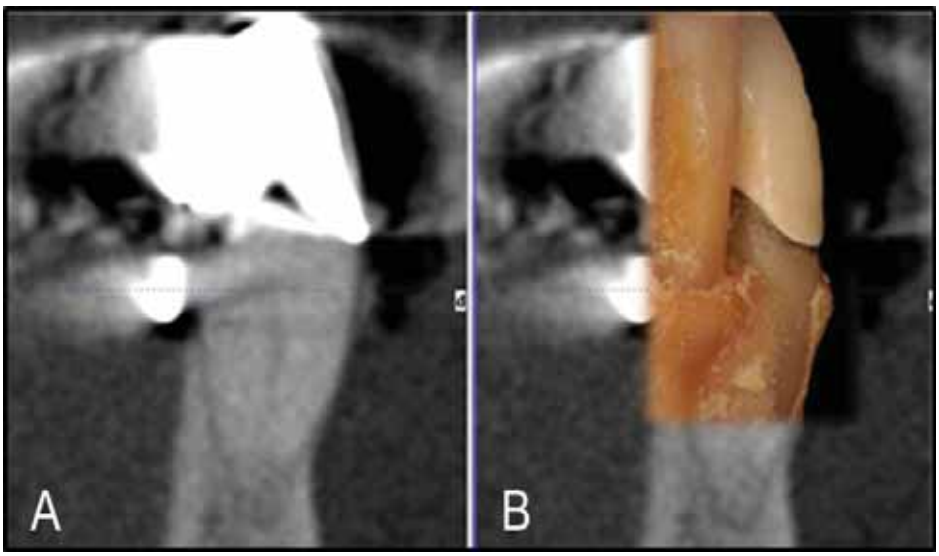

Figure 22. *Radiological data versus clinical findings:* ***(A)*** *lower right canine as seen on the CBCT scan: note that no continuous buccal bone covering is being depicted.* ***(B)*** *Superimposition of the clinical view of the same tooth with continuous buccal bone covering.*

Although a thickness difference of 0.14mm may not be statistically significant, clinically the absence or evidence of bony covering is highly relevant. This important

finding also has some ramifications on how to interpret CBCT scans. Previously, Sarikaya and co-authors (Sarikaya et al. 2002) examined the alveolar bone thickness on conventional CT scans. They postulated that dehiscences and fenestrations could be identified on CT scans that would remain otherwise undetected by cephalograms or clinical examination. The opinion to be capable to assess dehiscences and fenestrations correctly on MDCT data was already expressed in the 1990ies in few contributions (Fuhrmann et al. 1995, Fuhrmann 1996) and has reappeared more recently for CBCT (Ising et al. 2012, Vera et al. 2012a, Vera et al. 2012b). Based on this presumption, two articles from the same research group have been published evaluating the presence of dehiscenes in patients with different vertical growth patterns (Enhos et al. 2012) and different angle classification (Yagci et al. 2012) with CBCT. A third recent retrospective study assessed alveolar bone loss around lower incisors, and the amount and frequency of fenestrations was compared to upper incisors (Nahm et al. 2012).

The present study, however, indicates that there is a genuine risk of assuming fenestrations and dehiscences on CBCT radiographs which in fact do not exist clinically. This finding is in accordance with the observation by Leung et al. (Leung et al. 2010) who reported that fenestrations are seen 3 times more frequently on CBCT scans than compared to direct skull examination. Leung and co-authors, however, used dry skulls and measured on surface rendered volumetric 3D reconstructions. The present investigation shows that false positive detections of fenestrations also occur when soft tissue is present. In addition, it was demonstrated that a considerably more reliable image display to evaluate CBCT data, i.e. sagittal scans in multiplanar reformatted images (Hassan et al. 2013), does not improve the ability to assess fenestrations reliably.

In conclusion the following should be emphasized: A high precision and accuracy for CBCT measurements of the buccal bone has been attested through the results of this study and others (Sun et al. 2011, Timock et al. 2011, Torres et al. 2012). Yet, this does not permit a statement on fenestrations or dehiscences.

- ***The mucogingival junction***

The findings of the present study suggest that the undulated course of the mucogingival junction follows the alveolar bone margin in a parallel line. It is reasonable to assume that there is a topographic association between the mucogingival junction and the upper limit of the alveolar bone, since the attached gingiva is connected to the alveolar bone margin through periosteogingival fibre bundles (Feneis 1952). Yet this information has probably not been sufficiently appreciated. Most of the earlier studies that investigated the relationship between the attached gingiva and its bony support focused on the thickness of the keratinized soft tissue rather than on its height (Dorfman 1978, Wennstrom 1996, Yared et al. 2006). In fact, the height of the attached gingiva remains difficult to interpret. Dorfman (Dorfman 1978) noticed that the keratinized gingiva may vary in its apicocoronal length, and Ainamo and Talari (Ainamo and Talari 1976) observed an increase in length related to age. In addition, Wennström (Wennstrom 1996) wrote that a more lingual positioning of the tooth will result in an increase of the gingival height, but Wennström is in line with the finding of Ainamo and Talari that the mucogingival junction is a stable anatomical landmark. In summary, it has been recognized that the height of the attached gingiva is influenced by various parameters such as gingival inflammation, dental tipping or age, whereas the mucogingival junction would remain unaffected. It is concluded that the vertical position of the alveolar bone is therefore not connected to the height of the attached gingiva, but the results seem to imply that the mucogingival junction reflects somehow the location of the alveolar bone margin. This finding is probably limited to individuals with healthy periodontium. An inflammation or a severe recession will inevitably cause a derangement of the fibre bundles and affect the equilibrium between attached gingiva and alveolar bone. Yet it appears that in healthy individuals the mucogingival junction might be an additional aid to locate the alveolar bone margin appropriately.

This finding implies that some vital information on the bony covering of teeth might be clinically available and intensifies the question on the appropriateness of radiological examination in order to identify the extent of bone covering.

10.1.3. Accuracy of CBCT in comparison to MDCT for buccal bone measurements (STUDY II)

As mentioned in the introduction (6.3.1.), several studies exist that compare CBCT and MDCT (Hashimoto et al. 2003, Hashimoto et al. 2006, Loubele et al. 2006, Hashimoto et al. 2007, Loubele et al. 2007, Mischkowski et al. 2007, Loubele et al. 2008a, Loubele et al. 2008b, Suomalainen et al. 2008, Carrafiello et al. 2010, Liang et al. 2010a, Liang et al. 2010b, Naitoh et al. 2010, Al-Ekrish and Ekram 2011, Khedmat et al. 2012, Kim et al. 2012a, Zain and Alsadhan 2012, Hofmann et al. 2013). Focus has been laid, however, predominantly on image quality, and not on accuracy of measurements. Therefore, in most studies the obtained measurements were not compared with anatomical measurements. When studying the literature, a further drawback in many comparative studies becomes evident: The majority of previous studies compared high resolution CBCT protocols to standard MDCT protocols, sometimes comparing voxel sizes of 0.125mm x 0.125mm x 0.125mm (CBCT) to voxel sizes of 0.375mm x 0.375mm x 0.4mm (MDCT). It is obvious that using scan protocols with a substantial difference in voxel volume (1.95×10^{-3} mm^3 [CBCT] *vs.* 39.09×10^{-3} mm^3 [MDCT]) renders a comparison inappropriate.

Mindful of the limitations of the above studies and of the fact that only a selected amount of studies compared their radiological measurements to the anatomical findings (see 6.3.1.), a comparative study was performed, applying a *low-resolution* CBCT protocol – similar to the MDCT protocol - and comparing the obtained measurements to the anatomical truth. The broader limits of agreement in MDCT indicate that linear measurements are slightly more accurate when performed upon CBCT rather than MDCT data and confirm the results of previous studies (Kobayashi et al. 2004, Suomalainen et al. 2008, Al-Ekrish and Ekram 2011).

Moreover, present data are in accordance with studies reporting a generally better image quality of CBCT for hard tissue assessments (Hashimoto et al. 2003, Hashimoto et al. 2006, Honda et al. 2006, Liang et al. 2010b, Al-Ekrish and Ekram 2011, Hofmann et al. 2013) and higher sensitivity due to superior image quality (Khedmat et al. 2012).

- ***Metal artefacts***

Another method to compare image quality is the appraisal of image artefacts and their impact on the data reading. An image artefact may be defined as a visualized structure in the reconstructed data that is actually not present in the object under investigation (Schulze et al. 2011). Both CBCT and MDCT are susceptible to artefacts caused by image acquisition (e.g. beam hardening producing scatter streaks and dark bands), to patient-related artefacts (e.g. patient motion leading to lack of sharpness), to artefacts caused by the scanner itself (e.g. ring artefacts), or due to the beam projection geometry (e.g. distorted periphery) (Angelopoulos et al. 2012).

Reduced image quality due to metallic artefacts presents a major challenge and serious limitation in dentomaxillofacial imaging (Abrahams 2001). The presence of metal within the scan volume has the potential to cause several different effects that deteriorate regional image quality. Metal artefacts are particularly acute in metals with high atomic numbers (i.e. iron, steel, platinum), but less pronounced in metals with low atomic numbers (i.e. titanium). The two most important artefacts are:

(1) Beam-hardening artefacts: The lower energetic-rays of the polychromatic spectrum emitted by the X-ray source may suffer substantial absorption when passing through an object. This preferential absorption of lower-energy X-ray photons results in a gradual increase of the mean energy of the residual beam (i.e. beam-hardening). The changed characteristics of the X-ray beam may alter the attenuation characteristics of the tissue and consequently its appearance in the CT images (as dark streaks), which may impede the assessment of the neighbouring structures (Draenert et al. 2007, Schulze et al. 2011,

Angelopoulos et al. 2012).

(2) Streak artefacts: These are linear hyperdensities radiating from the metallic object and may extend to the width of the field, affecting even the visualization of areas on the opposite side (Angelopoulos et al. 2012).

Implants, dental reconstructions and orthodontic appliances may cause beam hardening and streaking artefacts (Naranjo et al. 2011). Despite the rather large amount of articles published on artefacts in the technical domain, Schulze and co-workers (Schulze et al. 2011), in their comprehensive review on artefacts in CBCT, were able to identify only three articles in oral and maxillofacial radiology journals that deal specifically with artefacts in CBCT. Two are purely descriptive (Draenert et al. 2007, Stuehmer et al. 2008), while the third focuses on an analysis of the causes of artefacts specifically induced by titanium implants (Schulze et al. 2010).

This current investigation was restricted to the evaluation of artefacts caused by *metallic* reconstruction with identical setting for CBCT and MDCT, and a set-up that excluded other patient-related artefacts.

In order to determine image quality, the number of non-assessable sites (NAS) due to metallic dental reconstructions was evaluated. The results show that, compared to the CBCT scans, MDCT scans produced more non-assessable sites in close proximity of the measured area to the metal reconstructions. Although it has been hypothesized that beam-hardening artefacts may be more pronounced in CBCT owing to the lower peak kilovolt presumably resulting in a lower mean energy of the X-ray beam (Scarfe and Farman 2008), this does not seem to be the case. The reason probably is that manufacturers of CT devices are constantly developing artefact-reducing algorithms, and the algorithms implemented in CBCT are probably better suited to counter-act specifically intraoral metallic alloys.

In regard to streak artefacts, the distinction between CBCT and MDCT becomes obvious. MDCT data were sometimes compromised in remote areas as well, owing to pronounced streaking or starburst artefacts (see Figure 23).

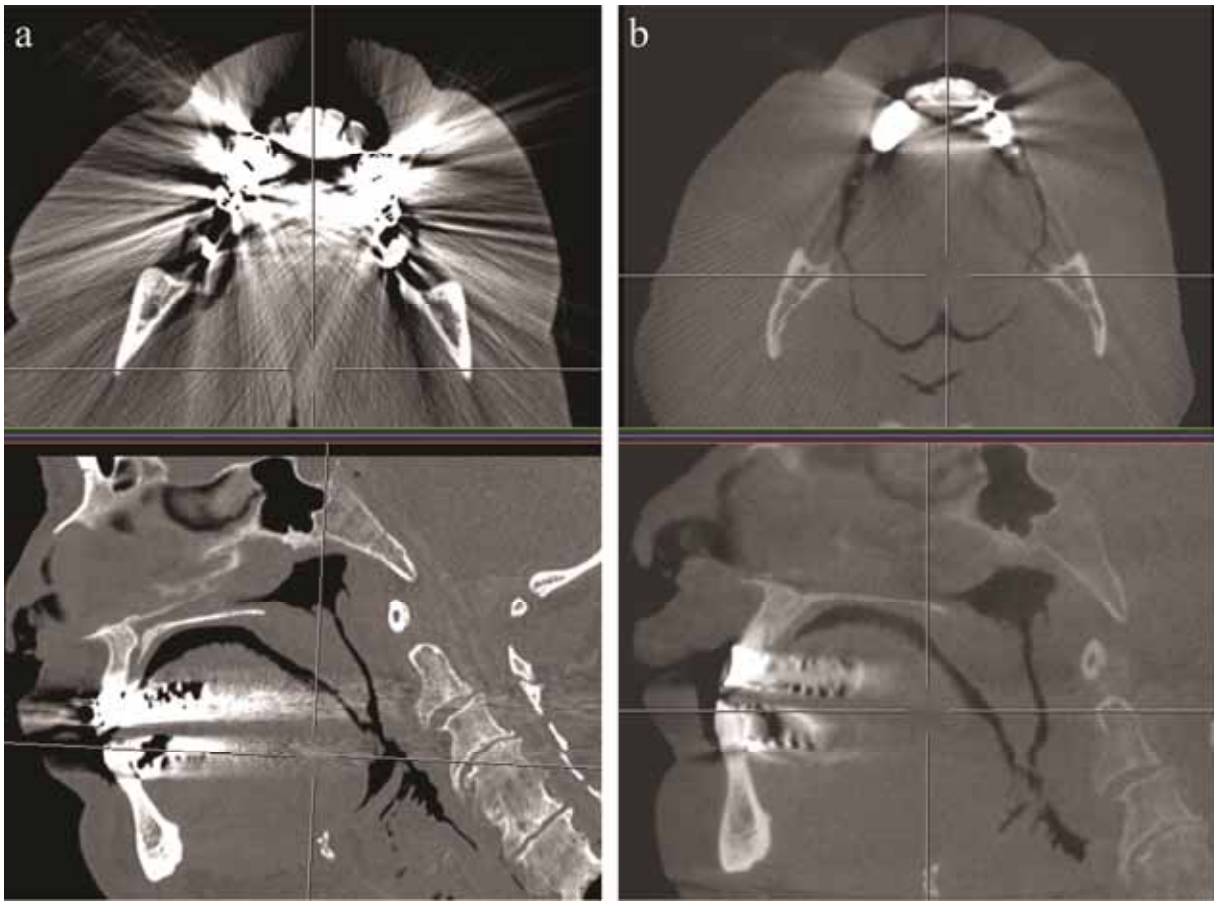

Figure 23. *Representative scan of the identical specimen (same region and same multiplanar reformatting) with typically constrained data from metal reconstruction.* ***(a)*** *MDCT,* ***(b)*** *CBCT.*

By quantifying the NAS (14.5% for MDCT *vs.* 8.3% for CBCT) the study shows a highly relevant clinical finding. Although the results are being supported by other investigators (Loubele et al. 2008a), they are not in accordance with Draenert and co-workers (Draenert et al. 2007) who found stronger beam hardening artefacts in CBCT compared to MDCT. A comparison of the two studies is difficult, since Draenert examined one dental implant (one metal alloy) in a dry skull. Present study, alternatively, aimed to approximate clinical practice with greater accuracy by use of intact cadaveric heads with most of the specimens containing a multitude of metallic reconstructions in various locations. This is important, since both variables, composition *and* orientation of metals, affect the data (Lee et al. 2007). In general, CBCT produced smoother images with reduced image contrast. Although this hinders the qualitative assessment of tissues, it proved beneficial for the quantitative appraisal of linear measurements.

- ***Soft tissue measurements***

To the best of our knowledge, the present study is the first to describe the accuracy of intraoral soft tissue measurements on CBCT in comparison to bone measurements. Interestingly, soft tissue measurements are slightly more accurate than bone measurements. The reason may simply be because no other tissue is in contact with the gingival surface, making gingiva surface easier to identify.

Comparative literature on the accuracy of CBCT-based soft tissue measurements is scarce. Januário and his research group measured gingival tissue by means of CBCT (Januario et al. 2008), and Barriviera and co-workers proposed that the palatal masticatory mucosa may be measured on CBCT data (Barriviera et al. 2009). Both failed to validate their measurements against anatomical reference measurements. Studies by Fourie and co-authors are apparently the only ones to have described so far the accuracy of facial (i.e. extraoral) soft tissue measurements in comparison to anatomical measurements (Fourie et al. 2010, 2011). However, their results may not be applied to intraoral measurements, because they deemed only mean absolute errors of more than 1.5 mm as clinically significant, which will not hold true for intraoral clinical queries. Furthermore, the CBCT-based measurements were taken from a generated 3D soft tissue surface model and not from multi-planar reconstructions. Finally, the evaluation of the scanned data on a laptop screen might have been a curtailing factor on the accuracy.

In clinical practice, ascertaining the thickness of the gingiva or mucosa would be highly advantageous. The success of surgical procedures in periodontology often depends on the thickness of the soft tissue present (Müller et al. 1999) as well as the thickness of the donor site when grafting connective tissues (Studer et al. 1997). Furthermore, the width of the free gingival-margin is directly related to more frequent and more severe recessions (Yared et al. 2006), and gingival problems occur generally more often in individuals with a thin gingival biotype.

Non-invasive methods to assess the thickness of the gingiva have long been sought. Müller and co-authors introduced an ultrasonic measuring method (Müller

et al. 1999), but concluded that it was not reliable enough. Although optimized ultrasonic devices with miniaturized transducer and higher frequencies were recently tested favourably, more dependable data are still required to permit a valid assertion (see 6.3.4.).

Januário and his research group published an innovative approach to expose the buccal gingiva during the scan by means of a lip retractor (Januario et al. 2008). However, their radiological measurements were not verified. **STUDY II** validated the accuracy of intraoral soft tissue measurements and legitimizes – within the expected accuracy reported in the Bland-Altman plots - radiological measurements of the gingiva and the masticatory mucosa.

10.1.4. Establishing the best-suited MRI sequence for the assessment of the condylar process using micro-CT as reference (STUDY III)

In order to evaluate the suitability of MRI to assess the cortical bone of the mandibular condyle, the most suitable sagittal MRI sequence for TMJ was established. The results strongly support the T1-weighted 3D fast spoiled gradient recalled echo sequence (i.e. T1-3D-FSPGR) to be the best-suited MRI sequence for this task. Numerical and categorical data derived from the readings indicate that this sequence performed superiorly to all other sequences in regard to both the objective analysis of cortical bone thickness measurements and the subjective evaluation of osteoarthritic changes of the mandibular condyle.

Previous studies demonstrated a limited use of MRI data for the evaluation of hard tissue through contrast (Alkhader et al. 2010, Kai et al. 2011). Although high specificity (84-98%) was obtained with MRI, it showed relatively low sensitivity (30-82%) for detecting osseous abnormalities of the TMJ. Present scores suggest that choosing the correct sequence can have a major effect on efficacy, and clarify the fact that no conclusions can be drawn on MRI performance based on previous studies, as the used sequences were not optimal.

Based on the clear results, it seems advisable to add the T1-3D-FSPGR sequence to any MRI protocol of the TMJ, as it increases the total examination time approximately by only 6 min.

Significant differences among the evaluated MRI sequences were discovered regarding objective and subjective cortical bone assessments. These differences could be attributed to previously described and well-known chemical shift and susceptibility artefacts occurring at the bordering regions between cortical bone and cartilage, fluid or soft-tissue structures of the TMJ (McGibbon et al. 1998, Peh and Chan 2001, McGibbon et al. 2003, Reichert et al. 2004, Phan et al. 2006). The resulting over- or underestimation, however, may lead to misinterpretation of the cortical bone surface and structure. Hence, a further comparative study assessing the linear measurements of MRI to other radiological data had to be implemented (see 8.2.4., 9.1.4. and 10.1.5).

Over the last few years, the demand for cortical bone imaging using MRI has increased. As opposed to MDCT, which has been considered the imaging technique of choice for the depiction of osseous pathological features so far, MRI operates without applying ionising radiation to the patients. Continuous advances in technology, such as higher magnetic field strengths (Schmid-Schwap et al. 2009) or more efficient software, and the on-going effort by the musculoskeletal research community have elevated MRI to become the new imaging method of choice for the assessment of cortical bone, especially for serial follow-up studies in young patients.

When performing MRI of the TMJ it is essential to evaluate the structure, thickness and shape of the cortical bone of the mandibular condyle. In patients with TMJ arthritis, especially in young patients and children suffering JIA, the assessment of these cortical bone structures becomes even more important because cortical bone thinning, flattening of the mandibular condyle, the development of subchondral cysts and the presence of anterior osteophytes are regarded as biomarkers for MRI monitoring of the activity and possible progression of JIA (Lee et al. 2008, Müller et al. 2009, Boyesen et al. 2011).

10.1.5. Accuracy of CBCT versus MDCT, MRI, OPG and lateral cephalogram for linear measurements of the mandibular ramus and condylar process (STUDY IV)

Regrettably, the ground truth values of the investigated measurements were not obtainable for this study. This makes the interpretation of the accuracy of each method difficult. Therefore, the agreement between the measurements rather than the accuracy of each measurement was assessed. To alleviate this weakness, the results of **STUDY II** are discussed (below), in which the anatomical ground truth was available and in which the agreement between the anatomical measurements and MDCT or CBCT were juxtaposed to the agreement of the measurements of MDCT against CBCT.

The agreement of the two measurements, i.e. ramus height (RH) and condylar process (CP) was evaluated between the different imaging modalities. The limits of agreement (LOA) were generally lower for CP than for RH for the 3D imaging modalities. The higher ranges of LOA for MDCT, CBCT and MRI for RH (from 4.4mm to 5.1mm) are clinically relevant. Assuming a mean condylar growth of 3mm per year in the juvenile period (Björk 1963), these ranges would correspond to a possible disagreement between almost 1½ to 2 years of mean condylar growth, which is not tolerable in follow-up of growing JIA patients, who are at any rate prone to reduced condylar growth. Due to higher ranges of agreement, and the fact that RH could increase due to appositional osseous growth in the gonial region, RH measurements can alone not be recommended for follow-up of JIA patients. As mentioned in the introduction (6.2.3.), JIA patients often show a growth pattern with posterior mandibular rotation, which is often associated with apposition at the gonial angle and antegonial notching (Jämsä and Rönning 1985, Kreiborg et al. 1990).

- ***Interpretation of the coefficient of variation for RH and CP***

When comparing the precision of measuring procedures with differing mean values, the use of a standardized precision measure such as the coefficient of variation (CV)

is desirable. CV describes the fraction of variance relative to the mean length and is mathematically described as: $CV = \frac{SD}{\text{mean length}}$.

In contrast to RH, CP data show significantly elevated CV estimates proving inferior accuracy of the CP measurements with respect to the mean CP length. Present data, however, show that significant differences in CV between CP and RH have to be interpreted with caution. First, with exception of LC, CV values are located for both RH and CP below 5%, demonstrating practically non-relevant deviations of the repeated measurements. Second, RH is on average more than 3 times longer than CP, but the impact of different lengths on SD is much lower (OPG, CBCT and MDCT) or even missing (MRI and LC). Therefore, it seems that the poor precision of CP judged in terms of CV is due to fact that RH and CP - which differ in length relevantly - are nevertheless measured on almost the same magnification.

In summary, with exception of LC, CV values are all below 5%, demonstrating very good precision with significant differences that are below clinical relevance. And since reference values for annual increments are published for RH (Savara and Tracy 1967), but not for CP, RH is recommended for follow-up of condylar growth.

- ***CBCT***

In interpreting the Bland-Altman-plots, the LOA of CBCT and MDCT for CP were twice as wide (range of agreement: 4.8mm) and between CBCT and MRI even more than twice as wide (range of agreement: 5.5mm) than between MDCT and MRI (range of agreement: 1.9mm). These data seem to indicate that CBCT measurements are neither directly comparable nor interchangeable with MDCT or MRI measurements. Yet, the low CV demonstrates that CBCT produces very dependable data in the temporomandibular region. The reported high reproducibility and precision render the use of CBCT data for linear measurement of RH and CP legitimate. As early as 2004, the radiologic examination of the temporomandibular joint using CBCT has been promulgated (Tsiklakis et al. 2004), and present results give evidence that CBCT can additionally be used to observe condylar growth.

- ***MDCT***

The range of LOA between MDCT and CBCT are 4.8mm for CP and 5.1mm for RH. Although not directly comparable, the LOA in **STUDY II** between the anatomical measurements and MDCT or CBCT were smaller (see 9.1.2.). Also the reported range of LOA between MDCT and CBCT was lower for the intraoral measurement (Range of LOA: 2.74mm). This observation is probably explicable. As mentioned, the Levene-test confirmed for some measurements an increase of the variability of the differences as the magnitude of the measurements increases, indicating that for small measurements the differences were smaller than for large measurements (see 9.1.1.). This could be true for CP and RH as well. A further explanation might be that a different image reconstruction was used (MIP) in this study (see "image reconstruction" below), precluding any comparison to the **STUDY II**.

- ***OPG***

Although OPG produced the best data in regard to precision and reliability, it demonstrated poor agreement with all 3D procedures (MDCT, CBCT and MRI). The reason for this discrepancy lies most likely in the study protocol and is a limitation of this study. All 2D images (LC and OPG) and 3D datasets were generated only once and all further processing was based on these data. For 3D imaging and lateral cephalometric images positioning of the specimen has very little effect. But OPG is, as reported (6.1.3.), highly sensitive to positioning issues leading to magnification errors and disproportional enlargement (Updegrave 1971, McDavid et al. 1981, Schulze et al. 2000). The OPG device used in this study produced images of excellent quality. Therefore constructions and landmark definitions were unambiguous, leading to very high precision and reliability of the measurements. But when assessing agreement between OPG and the 3D imaging methods, the positioning issue with distortion was evident. Agreement was poor, producing the widest limits of agreement (range of agreement: 5.7mm – 8.4mm). Moreover, the measurements were significantly smaller. This phenomenon seems to be a general drawback in OPG

devices, as it has been stated that magnification factors might differ from the ones reported by manufacturers (Van Elslande et al. 2008).

- ***Lateral cephalogram***

LC measurements showed the worst results in regard to precision, which were statistically and clinically significant. Intra- and interobserver reliability were far below all other imaging methods, especially for CP. Limits of agreement showed a very heterogeneous picture with partially very wide LOA to 3D imaging methods.

The limitation of analogue LC is based in the problems associated with landmark identification and hand-tracing. In contrast to 3D imaging techniques, lateral cephalography is a classic 2D radiography, where the 3D structures are flattened to a 2D image, rendering a distinction of either side almost impossible. Landmark detection is further impeded due to overprojecting structures. This is especially acute for the condylar point and the deepest point of the incisura mandibulae. The latter is determined by the edge of a narrowly tapered and thin bone formation, which is rendered as a density gradient. This makes a clear distinction between bone and soft tissue difficult. This observation is equally true for the condylar point. Conversely, the gonial point has a clear boundary between compact bone and soft tissue resulting in a clear step in density, but depends highly on the condylar point for its construction.

A further source of error might have been the hand-tracing and digitizing of LC, whereas all other images were measured on a computer screen using dedicated software. Recently, three studies were conducted where the landmark identification of LC using the same tablet digitizer (Numonics AccuGrid) was assessed and high intra- and interobserver agreement established (Beit et al. 2013, Gutermann et al. 2013, Mislik et al. 2013). These studies may serve as indirect proof that digitizing hand-traced measurements is not a major source of error. Yet, a more favored approach would indeed have been to scan the films and to measure the images with the same software.

- ***MRI***

The smallest range of all limits of agreement could be identified between MDCT and MRI (range of agreement: 1.9mm). This means that there is a 95% probability (±1.96 SD) of agreement between MDCT and MRI within 1.9mm, when MRI values are corrected for length differences. Assuming a mean condylar growth of 3mm per year in the juvenile period (Björk 1963), agreement between MDCT and MRI for CP is lower than the anticipated yearly increment of growth.

Measurements of the mandibular ramus and condylar process with MRI are comparable to MDCT and CBCT in terms of precision, intra- and interobserver reliability and agreement. Therefore, MRI can be used to quantitatively follow condylar growth by measuring ramus height and condylar process length, which are important indicators for long-term therapeutic success (Kuseler et al. 2005, Weiss et al. 2008). This can easily be implemented into a MRI study of the TMJs routinely performed for assessing soft tissue and bone marrow abnormalities as important parameters for disease activity, progression and treatment response in children with TMJ arthritis (Müller et al. 2009, Boyesen et al. 2011, Cannizzaro et al. 2011). Using only MRI would reduce costs and avoids the exposure to ionizing radiation with potential harm to growing children (Claus et al. 2012, Pearce et al. 2012). The present results are in concordance with a recently published study that found highly precise quantitative measurements on MRI, MDCT and CBCT (Gaudino et al. 2011).

Measurements conducted with MRI were smaller than with MDCT (RH: -1.4mm; CP: -1.2mm) and CBCT (RH: -1.9mm; CP: -1.1mm). This has to be taken into consideration when comparing MRI measurements to reference values based on other imaging procedures (Kjellberg et al. 1994, Kjellberg et al. 1995, Twilt et al. 2006, Stoustrup et al. 2008, Stoustrup et al. 2011). Therefore MDCT, CBCT and MRI may be deemed comparable, but not interchangeable without correction for length differences.

In summary, linear measurements with MRI are reliable, but must be corrected for length differences. Since MRI is recommended for soft tissue

assessment and has been shown in **STUDY III** to be reliable to assess bony pathologies and measurements (10.1.4.), MRI should be considered the imaging method of choice for TMJ imaging.

- ***Image reconstruction***

For the construction method of 2D images out of a 3D data set, it is crucial to use adequate methods for volume rendering. Using an averaged slice instead of a projection method (MIP or mIP) will probably result in worse agreement and reliability as well as lower precision. In MIP or mIP, only areas with highest density (MIP) or lowest intensity (mIP) are rendered within the slice and subsequently used for constructions and landmark definitions. Although this approach may exclude some voxels and lead to smaller measurements than the anatomical truth, differences in slice thickness and slice orientation will have only little or no effect on the measurement. In contrast, in the averaging method, which is the commonly used method in most DICOM viewers, these factors have a major effect. An averaged 2D image is based on the average of all voxels in a line orthogonal to the slice. For CBCT and MDCT, for example, thicker slices would include more soft tissue areas with lower density. As a consequence, bony areas would be rendered with lower density and edges would become blurred (Figure 24).

Figure 24. *Example of three sagittal slices with different thicknesses (a-c) of a 3D CBCT-dataset visualized using multiplanar reformatting. Slice thicknesses of* ***(a)*** *10mm,* ***(b)*** *20mm and* ***(c)*** *30mm.*

10.1.6. Accuracy of CBCT, MDCT and lateral cephalogram in assessing the cervical spine (STUDY V)

This study compared the different assessment outcomes between general radiologists evaluating MDCT and oral radiologists appraising CBCT of the cervical spine (see Figure 25). The results demonstrate two important findings: First, both rater groups performed equally well regarding the exclusion of possible fusions. Second, concerning the appraisal of osteoarthritic deformities, general radiologists assessing MDCT performed better. They diagnosed osteoarthritic changes correctly in 100% of the cases and did so with considerable consistency in regard to their assessment of the joint space. Conversely, oral radiologists evaluating CBCT diagnosed only 93.3% of the osteoarthritic cases correctly and did so with more disagreement among themselves in their assessment of the joint space.

Two possible assumptions may explain why oral radiologists evaluating CBCT data might not perform as well as general radiologists do with MDCT data. Oral radiologists may not be used to assessing joints since the only joint in the maxillofacial region is the temporomandibular joint, which differs remarkably from other joints. It can be argued that general radiologists probably perform better owing to their broader experience in assessment of articulo-osseous pathologies. On the other hand, there is an inherent problem in CBCT data. The image quality in the mid plane is superior to more peripheral regions because the data acquired in a circular cone-beam scan are only sufficient for accurate image reconstruction in the middle of the volume. It is a well-known fact that image reconstruction at the periphery of the volume will suffer from cone-beam artefacts (Yu et al. 2010). Thus, the location of the cervical spine, being very much off the center of the volume, could have been the cause behind the inferior results.

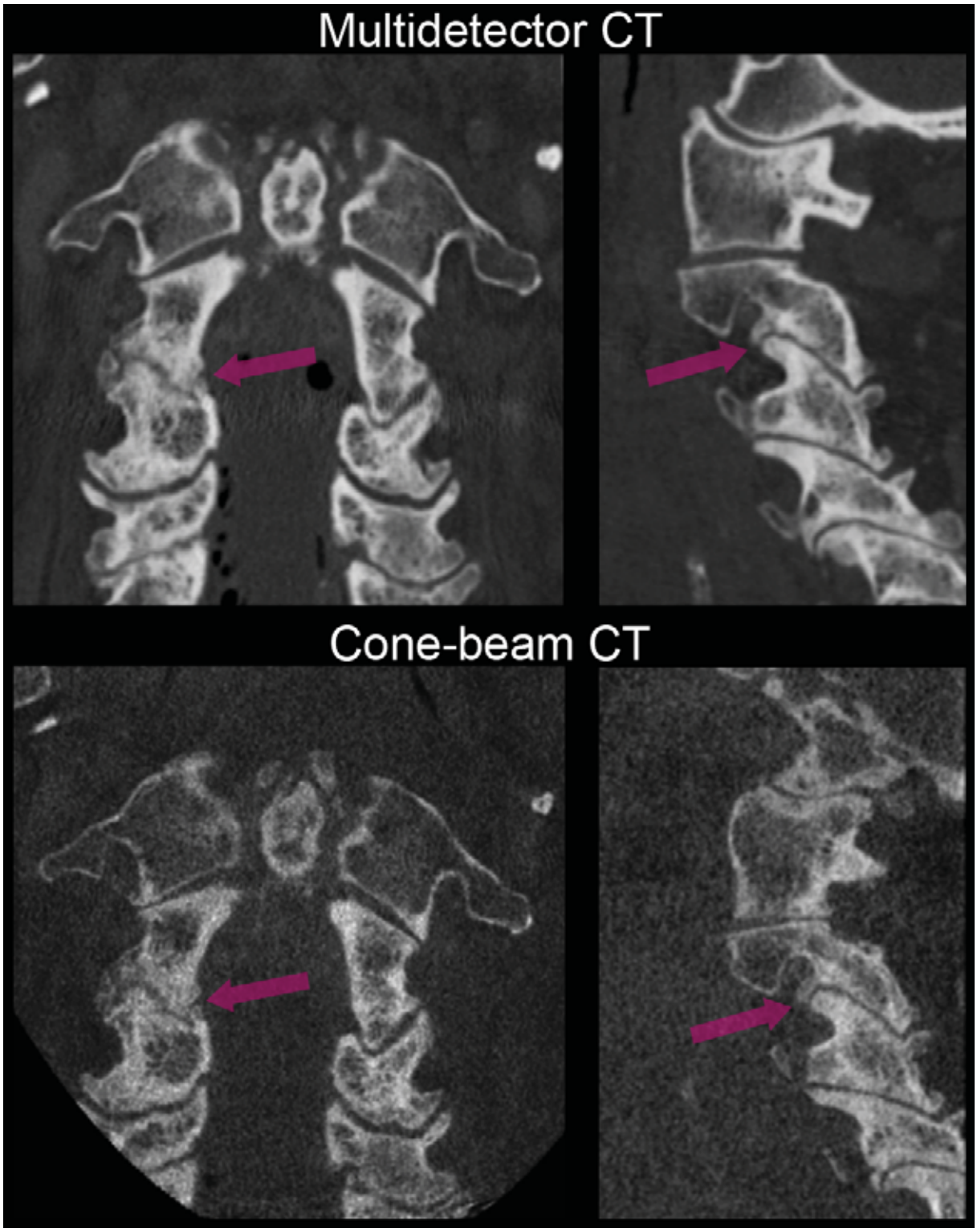

Figure 25. *Coronal (left) and sagittal (right) reformatted MDCT images (top) and CBCT images (bottom) of specimen 3. Purple arrows pointing at irregularly narrowed facet joints C2-C3 with subchondral sclerosis and spondylophytes, but no bony fusion (The images were rotated and cropped, to facilitate a direct comparison. Note the close proximity to the edge of the volume in CBCT, seen on the coronal slide).*

10.1.7. Limitations of cadaver studies

Every study designed on cadaver specimens faces several problems. The first constraint is that despite of unmitigated cadaver heads being considered the closest means to obtain clinical conditions, they still remain unquestionably an approximation. The lack of noise created on radiological data owing to the patient's movements probably improves the results, and the alcohol fixation of the cadaver may also have a slight impact on the generated data. Moreover, at certain times it is necessary to remove soft tissues in order to obtain a bony reference. A possible limitation is that the physical removal or maceration of soft tissue could impair the integrity of compact bone.

An alternative to cadaver study would be a comparison of radiological measurement to direct clinical measurement, either through transgingival probing (Greenberg et al. 1976), or during surgical exposure (Grimard et al. 2009, Herzog 2013). Both approaches suffer from the fact that only a limited amount of measurements is possible, from ethical considerations and from the settings of a clinical examination on a living patient, including most notably motion and bleeding.

Studies performed on cadavers face critical issues, too. Particularly the consequences of the fixation and maceration process on the specimens, as well as the statistical ramification of the small obtainable sample size need to be considered.

- ***Fixation***

The fixation solution used in the present studies contained low concentration of glutaraldehyde and formaldehyde, which are known to modify certain tissue properties, e.g. slight muscle expansion and fatty tissue shrinkage (Docquier et al. 2010) by extensive cross-linking (Comert et al. 2009, Hansen et al. 2009) and are known to alter periodontal fibre architecture (Burn-Murdoch and Tyler 1981). The alteration of tissue properties is especially problematic when accuracy of measurements on different types of tissues is evaluated. For example, a comparison of soft tissue and bone measurements must presuppose that fixation does not modify

the properties of these tissues differently. There is evidence supporting that glyoxal-based fixation (as used in **STUDIES I-V**, see 8.1.1.) is a suitable fixative for structural evaluation of soft tissue (Wang et al. 2011) and in addition, no significant differences have been reported in bone mineral density as well as the initial Young's modulus between alcohol fixation and fresh-frozen specimens (Unger et al. 2010).

- ***Maceration***

Maceration of specimens, especially after fixation, may also influence bone property and compromise the anatomic reference. Common maceration solutions contain aggressive detergents, which can also decalcify bone (Mairs et al. 2004). Enzymatic maceration (see 8.1.6.) is, however, an established method for removal of soft tissues while maintaining the structural integrity of compact bone (Sandstrom 1969, Yin et al. 2010). The ability to remove soft tissues from skeletons while maintaining the integrity of bony surfaces is crucial in many fields including zoology, anthropology, pathology and forensic medicine and in all these disciplines excellent results of enzymatic maceration have been published (Sandstrom 1969, Berland 1985, Horie and Murphy 1988, Belfie and Clark 1992, Steadman et al. 2006, Yin et al. 2010). The results of **STUDY V** corroborate the previous evidence that enzymatic maceration produces excellent results when applied to ethanol-fixed specimens (Bartels and Meyer 1991).

- ***Statistical ramifications of the small sample size of cadaver specimens***

The small amount of specimens usually available in a cadaver study may preclude the possibility of carrying out more comprehensive statistical testing. For a hypothesis-driven study, a large sample size is needed to account for statistical inferences. In theory, there are three possibilities to overcome the small sample size. These are:

a) *Generating more data by increasing the number of raters*
b) *Generating more data by defining the sample as the measurement site*
c) *To leave the data as is and restrict the statistical evaluation*

a) Generating more data by increasing the number of raters

Reports on statistical testing have proven that as the number of raters increases, the required amount of subjects or specimens decreases (Altaye et al. 2001a, Altaye et al. 2001b). This approach does indeed appear promising at first and would seem to allow statistical testing. But the savings in sample size obtained by increasing the numbers of raters rapidly diminishes after the accrual of five raters (Altaye et al. 2001a). A second problem that must be accounted for are clustering effects. Clusters are aggregates of individuals or a collection of multiple measurements belonging to the same person which are likely to be correlated (Koletsi et al. 2012). In studies using clusters, the outcome is most likely to be more similar within clusters compared to between clusters (Kerry and Bland 1998, Hayes and Bennett 1999). Although especially in orthodontics frequently not taken into account (Koletsi et al. 2012), clustering does matter and should be considered when the sample size for statistical testing is being evaluated (Harrison and Burnside 2012).

b) Generating more data by defining the sample as the measurement site

Many individual measurement sites can be defined on a single specimen as discrete entities. Defining the analytic unit as the amount of measurement sites is a common approach to produce a sample size sufficiently large for statistical testing (Imrey 1986). But this method also gives rise to certain statistical intricacies. Besides of the aforementioned clustering effects, concern may be raised as to whether multiple measurements on the same specimen can be interpreted as independent events as this probably violates the assumption of independence required for parametric statistical testing. This issue is discussed in full detail in periodontal research (Imrey 1986, Albandar and Goldstein 1992, Imrey and Chilton 1992) where each site is clearly dependent of the ubiquitous oral habitat and host factors. In radiology, this limitation is probably less acute than in periodontology, as the correlation between the measurements at different radiological sites will be weaker due to the impact of orientation and distance of the prevailing metal (implants,

dental reconstructions and orthodontic appliances) affecting the imaging (Abrahams 2001, Lee et al. 2007, Naranjo et al. 2011).

c) To leave the data as is and restrict the statistical evaluation

A large sample is needed in a hypothesis-driven study in order to account for statistical inference. Restricting the evaluation to descriptive statistics would alleviate the sample size issue. Inflating the amount of measurements in descriptive statistics will not generate any other results, but reduce the uncertainty; i.e. would reduce the magnitude of the standard error and of the confidence interval (Sadatsafavi et al. 2007). The same holds true for Kappa statistics (used in **STUDY III** and **STUDY V**) which was designed for descriptive purpose only. First described by Cohen (Cohen 1960), it is best defined as "the proportion of the total amount of agreement not explained by chance for which the observers accounted". Moreover, because Kappa is not used for null hypothesis, power calculations are not relevant (Tooth and Ottenbacher 2004). In order to determine if the sample size is large enough to be able to derive any conclusions from the descriptive statistics, a decision has to be made if the standard error and the confidence interval can be deemed as sufficiently small.

10.1.8. Implications of micro-CT as standard of reference

The use of μ-CT opens new dimensions in several aspects. First, it allows a non-destructive analysis of bony structure in micrometer resolution (Mizutani and Suzuki 2012) and may even be more accurate than direct anatomical measurements. In fact, it has been postulated that the diagnostic value of μ-CT for bone evaluations is superior than histology for surface structures, thickness, continuity of the cortex, and number, thickness and orientation of the trabeculae (Kuhn et al. 2007, Ruhli et al. 2007). Second, μ-CT generates data qualitatively superior than other CT devices, since its data are well calibrated and rendered in milligrams hydroxylapatite per cm^3 (HAg/cm^3), and μ-CT are not restricted to the Hounsfield equation.

- ***Clinical limitations of the Hounsfield unit scale and CBCT greyscale***

The Hounsfield unit (HU) scale is commonly used to represent the density of any given tissue. HU is defined by measuring the absorption or radiodensity of distilled water (at standard temperature and pressure: STP) and assigning it at 0 HU, while the radiodensity of air (at STP) is defined as -1000 HU. These defined points anchor a linear scale for converting any voxel (with average linear attenuation coefficient μ_x) into corresponding HU value. Therefore, the HU can be defined as:

$$HU = 1000 \times \frac{\mu_x - \mu_{water}}{\mu_{water}}$$

The implication of this approach is that the calibration will be very similar across different scanners for HU values between (or close enough) to the defined anchor points. All CT scanners will therefore deliver very similar HU for soft tissue readings. However, for tissues with different chemical composition and of higher attenuation coefficient, the linear scale will have to be extrapolated far beyond its defined points for higher absorbing materials like calcified tissue. In clinical terms, the HU may vary substantially for bone from one CT scanner to another. Moreover, the physical absorption and the scanner's readings depend not only on the material composition, but also on the applied X-ray spectrum, the detector, filter and the geometry of the scanner. Thus, especially dental cone-beam CT has been proven to be extremely difficult, if not impossible, to scale. (Yu et al. 2010, Bryant 2011, Hohlweg-Majert et al. 2011b, Nackaerts et al. 2011, Silva et al. 2012).

Mah et al. (Mah et al. 2010) attempted to calculate a conversion coefficient to deliver a calibrated grey scale from cone-beam units. However, Bryant et al. (Bryant 2011) as well as others challenged this approach and argued that the greyscale value of CBCT varies linearly with the total mass in the slice (Bryant et al. 2008), is being dependent on the location within the field of view (Yu et al. 2010, Nackaerts et al. 2011), on the volume outside the field of view (Bryant et al. 2008, Katsumata et al. 2009, Pauwels et al. 2013) and on several other parameters (Endo et al. 2001, Katsumata et al. 2007). The CBCT grey scale value will therefore not only depend on

the attenuation coefficient measurement as described by the Hounsfield equation, but on many factors, and will be unsuitable to provide a qualitative assessment of bone (Hohlweg-Majert et al. 2011a, Pauwels et al. 2013).

- ***Benefits of micro-CT***

Although μ-CT scanned data can be rendered in HU, they are usually given in mgHA/cm^3. In regard to bone density measurement, correlating the absorption with mgHA/cm^3 appears to be near to ideal, since HA-density is a measure of prime interest in bone, and thus a calibrated scale will not suffer from extrapolation. This characteristic serves to generate μ-CT data well attuned and uniform. Thus, μ-CT data will not only consist of a scanning of higher resolution, but the inherent property will enable to generate excellent results for qualitative appraisals. In contrast to the use of an anatomical reference, comparison to μ-CT data will therefore not be restricted to linear or volumetric measurements (Park et al. 2007), but enable also the assessments of 2D and 3D density measurements of bone (Kato and Ohno 2009), as well as histomorphometry. In fact, very few attempts have been made on comparative assessments of trabecular architecture and bone mineral density (Mulder et al. 2012), and no such data exist on the mandibular condyle. The present material, consisting of condyles with osteoarthritic changes of various degrees, would invite to investigate into the pattern of trabecular morphology and bone architecture corresponding to the surface pathology.

Lastly, the accuracy of processed images (such as surface rendering, finite element analysis or segmentation) of MDCT and CBCT data could be compared to corresponding processed images of μ-CT. This would allow determining the impact of the data acquisition method on the processing. Among the rare studies in this field, most compared the accuracy of 3D reconstructions of CBCT and μ-CT on teeth (Al-Rawi et al. 2010, Maret et al. 2012b, a) or developing germs of permanent teeth of historical macerated mandibles (Maret et al. 2010). To date, only one study was published on jawbone surface model accuracy of CBCT and MDCT with μ-CT as reference (Vandenberghe et al. 2012).

10.2. Radiation dose evaluation (STUDY VI)

In a well-received paper, Cohen calls attention to the fact that two radiation risks exist: The increased incidence of cancer secondary to radiation exposure, and the little-discussed risk of missing a diagnosis because of suboptimal image quality as a consequence of inappropriately low radiation settings (Cohen 2009). Cohen even argues that "for an individual patient, the consequences of missing an abnormality because radiation exposure is too low are significantly greater than the statistical long-term risk of cancer from radiation exposure that is too high." Cohen's message is a simple call to maintain a balanced perspective between two risks. But it is based on the understanding that more accurate imaging will reduce the risk of underestimation of an abnormality.

Although not explicitly mentioned by Cohen, the opposite is probably true as well: Owing to increased accuracy, higher radiation doses might cause overrepresentation of abnormalities. The issue of incidental findings has been portrayed in medical (Hall et al. 2009) and dental (Cha et al. 2007, Price et al. 2012) literature, both demonstrating a high prevalence of incidental findings. The authors all stress that their findings underscore the need to thoroughly examine all CBCT volumes for clinically significant findings. Nevertheless, incidental findings are no justification for additional radiation exposure, as a significant number of incidental findings may (a) represent anatomic variations of the norm that do not require any further intervention, (b) might already be known to the patient, (c) might have been detected with low-dose radiographic procedures as well, or (d) might be false-positive findings (Halazonetis 2012).

In summary, it is evident that every exposure to radiation in order to obtain diagnostic information involves balancing the risks of too low or too high radiation setting. It is in light of this thinking that the following discussion is based. Radiation dose reduction in itself is no goal to strive for, unless proven that the clinical queries can equally well be answered with a lower radiobiological risk. Thus, it will always be the clinical question at hand that will determine what device and which settings

are to be applied. Cohen's rhetorical question "how low can you go?" can only be answered by taking the diagnostic efficacy into the equation.

The following chapters will try to place the established radiation doses into context of diagnostic efficacy focusing on the cervical spine. Owing to its close topographic proximity to the thyroid glands and oesophagus, the exposure of the cervical spine to radiation will cause a significant increase to radiation. Hence, it is pivotal to know the diagnostic relevance of cervical spine imaging, and to determine which technique is to be implemented to obtain the highest diagnostic efficacy.

10.2.1. The diagnostic benefits of exposing the cervical spine to radiation

The chronological age is known not be a valid predictor of skeletal maturity (Bowden 1976, Kimura 1976, Hagg and Taranger 1982). Several approaches to assess skeletal maturation have been proposed, including biological indicators such as voice changes (Tofani 1972, Hagg and Taranger 1980b, a), dental development and eruption (Hellman 1923, Lewis and Garn 1960, Björk and Helm 1967) or body height changes (Björk 1963, Hunter 1966). More recently, the assessment of skeletal maturity has been performed on the cervical spine seen on a lateral cephalogram, based on the association between age-related morphological changes of the upper cervical vertebrae and the somatic growth curve (Lamparski 1975, Hassel and Farman 1995, Baccetti et al. 2002). Scientific contributions have further shown that diagnostic data can be obtained from cervical spine on a lateral cephalogram. In addition to skeletal age evaluation, it is possible to assess the craniocervical angulation in order to characterize head posture, which has been linked to nasorespiratory (Huggare and Laine-Alava 1997) and craniofacial morphology (Kylämarkula and Huggare 1985, Solow and Sandham 2002). Moreover, use of lateral cephalograms has also been recommended for the study of congenital anomalies of the cervical vertebrae, given that cervical vertebral anomalies, particularly fusions, could be related to certain craniofacial syndromes and other dentoskeletal malformations (Ross and Lindsay 1965, Tredwell et al. 1982, Sandham 1986, Horswell 1991, Rajion et al. 2006, Sonnesen

and Kjaer 2007b, a, Sonnesen et al. 2007, Sonnesen and Kjaer 2008a, b, Sonnesen et al. 2008a, Sonnesen et al. 2008b, Sonnesen et al. 2009, Sonnesen 2010, Arntsen and Sonnesen 2011).

However, some of these potential benefits have been seriously questioned. Natural head position can be assessed clinically without the help of a radiograph. In fact, many perform the lateral cephalogram with the head fixed parallel to the Frankfurt plane and not in natural head posture. The results of **STUDY VI** raise several questions on the benefits of exposing the cervical spine, and with it the thyroid glands, to radiation. The following sub-chapters contain a critical evaluation of the use of a thyroid shield, the suggested benefits of cervical age estimation and the assessment of cervical vertebral anomalies.

10.2.2. Ramifications of shielding the thyroid glands

Dosimetry assessment of CBCT devices on phantoms has been addressed in many studies, but the implication of the thyroid shield has yet not been evaluated in a comparative study. The thyroid is an organ highly sensitive to radiation exposure and avoiding ionizing radiation to hit the thyroid will reduce the radiation dose considerably, as demonstrated above (see chapter 9.2.). As demonstrated in **STUDY VI**, the use of a thyroid shield causes a reduction of the radiation dose in a cephalogram of 34% and in a CBCT portrait mode of 27%.

Hassel and Farman (Hassel and Farman 1995) have postulated that third and the fourth vertebrae, i.e. C3 and C4, can be visualized even when a thyroid shield is worn. Their claim, however, is not supported by scientific literature, but their assertion is rather based on the fact that in adulthood the topographical location of the thyroid usually corresponds to C5-C7. However, the location of the thyroid gland is evidently age dependent, as the thyroid experiences a caudal movement through puberty (Crelin 1973) and is closer to C3 and C4 in young individuals. Also, it should be appreciated that the thyroid position reportedly highly varies from person to person (Gray et al. 2005). All this implies that the thyroid shield should cover the

cervical spine above C5 as well, especially in pre-pubertal children and would hence, if applied correctly, forfeit the cervical vertebral maturation (CVM) method. In post-pubertal subjects the thyroid would most of the time be lower than C4 and, theoretically, the use of a neck shield would be commendable. In practical setting, it is very challenging to determine clinically by visual inspection and neck palpation the correct location of C5. Two retrospective surveys also demonstrated that thyroid shields are used inconsistently and if applied, C3 and C4 are entirely depicted in only 14% or 57% of all subjects, respectively (Hujoel et al. 2006, Beit et al. 2013).

10.2.3. Hand-wrist radiography in comparison to cervical age assessment

While the skeletal age can be assessed on a lateral cephalogram or CBCT with only a single method, i.e. the CVM method, a hand and wrist radiograph will allow various assessments (Serinelli et al. 2011). In fact, the strength of a hand and wrist radiograph is the cumulative results of different methods such as Greulich and Pyle (GP) (Greulich and Pyle 1959), Tanner and Whitehouse (TW) (Tanner et al. 1983), Bowden (Bowden 1971) or Fishman (Fishman 1979, 1982). For endocrinologists, the concordant result of GP together with TW still remains the gold standard with TW being the method of choice (Gilli 1996). Accuracy may be improved if further non-radiological indicators are used in addition to the hand-wrist radiograph (Sato et al. 2001). Although bone age assessment based on hand-wrist radiography proved to show good reproducibility (King et al. 1994) and high reliability (Flores-Mir et al. 2004), certain sources of error such as poor positioning of the hand (Cox 1996) as well as polymorphism in ossification sequencing (Garn et al. 1966) undeniably can affect the accuracy.

The validity of skeletal maturity assessment using the hand-wrist radiograph in relation to overall skeletal growth has been well established and has been validated for several ethnic groups (Bowden 1971, Helm et al. 1971, Kimura 1976, Grave and Brown 1979, Hagg and Taranger 1980b, 1982, King et al. 1994, Flores-Mir et al. 2004). Conversely, there is abundant literature that the reliability and

reproducibility of the CVM method is questionable (Gabriel et al. 2009, Fudalej and Bollen 2010, Nestman et al. 2011, Zhao et al. 2012). A recent systematic review revealed that studies on CVM method for radiographic assessment of skeletal maturation stages suffer from serious methodological failures (Santiago et al. 2012). Moreover, the CVM method does not allow to predict the final adult seize and it has been postulated that the poor reproducibility is not only based on the difficulty of staging, i.e. classifying the vertebral bodies as trapezoidal, rectangular horizontal, square or rectangular vertical (Nestman et al. 2011), but that the age-related morphological changes themselves do not contain enough information for accurate estimation (Chatzigianni and Halazonetis 2009, Beit et al. 2013).

10.2.4. Evaluation of cervical vertebral anomalies

The evaluation of congenital vertebral fusions on lateral cephalograms has been studied extensively in the orthodontic literature, associating fusions with diverse anomalies and malocclusions (see 6.2.2.). The use of lateral cephalograms, however, has been challenged by some who argued that it is difficult to reliably determine CVAs on a single lateral cephalogram (Massengill et al. 1997, Koletsi and Halazonetis 2010, Bebnowski et al. 2012), since two-dimensional radiographs may yield deceptive impressions of "pseudo-fusions" in C2–C3 facet joint due to their oblique orientation. In comparison to the studies that related CVA to dentoskeletal malformations (see 10.2.1.), considerably lower prevalence numbers (<0.9%) have been reported in other studies with normal populations (Brown et al. 1964, Ross and Lindsay 1965, Sandham 1986, Tetradis and Kantor 1999, Rajion et al. 2006, Koletsi and Halazonetis 2010). Although this could be due to the fact that patients with severe malocclusions would be significantly different than normal population, yet this dissonance in prevalence certainly raises the question as to whether lateral cephalograms can be considered a reliable tool to assess CVAs. In fact, Koletsi and Halazonetis stated that no study investigating the reliability of cephalometric radiography in the cervical region has been published to date (Koletsi and

Halazonetis 2010). In order to validate the assessment of the spine on lateral cephalograms, three-dimensional radiological data (McAfee et al. 1986, Hensinger 1991, Massengill et al. 1997, Guille and Sherk 2002, Rajion et al. 2006, Carreon et al. 2007, Shi et al. 2007, Bebnowski et al. 2012) and direct observation (on autopsy material) have been suggested (Brown et al. 1964, Templeton and Brown 1964).

True to both approaches suggested, this present dissertation investigated on the reliability of lateral cephalograms to assess CVAs. The results corroborate the concern on cephalogram-based diagnoses of the cervical spine by demonstrating that cephalograms do not provide reliable data. All four specimens assessed positively for fusions on lateral cephalograms proved to be false positives. None had a fusion. Hence, the absence of a continuous radiolucent area between the articular processes (on cephalograms) as the sole radiological criterion may not be a valid method to identify fusions on a single lateral cephalogram. All evaluated joints had osteoarthritic changes, some with gross irregularities and narrowed joint spaces. Based on the findings of the present study, a further reason for the erroneous assessment of fusions might be the misinterpretation of osteoarthritic changes as fusions. It is evident that a continuous radiolucent area may fade away because of irregularities, as shown in Figures 19 and 20 (see specimen 3).

10.2.5. Conclusive remarks on shielding the thyroid

The thyroid is an organ that is highly sensitive to radiation exposure. The present results reveal that a thyroid shield will reduce the effective dose remarkably. As presented in the results of **STUDY VI**, the use of the thyroid shield is not always necessary, and collimation of the field of view is also a possibility to reduce the radiation burden.

In light of the questionable benefits of radiological exposure of this sensitive area, the described findings give strong support to the use of a thyroid shield in a cephalogram or a CBCT with large FOV. Alternatively, the beam could be collimated to exclude the thyroid and hence reduce the effective dose. Whatever approach is

chosen to reduce the radiation of the thyroid, based on the present findings there does not seem to be a justification to expose the cervical spine for screening cervical vertebral anomalies. Should a clinical indication arise to assess skeletal age, an additional hand-wrist radiograph would be much more appropriate.

10.2.6. Comparative remarks on radiation dose reduction

The estimated effective doses and the evaluated reductions are, in absolute terms, very low. This fact becomes readily apparent when the doses are compared to the doses of natural (i.e. terrestrial and cosmic) radiation. Humans are permanently exposed to natural background radiation. The earth's crust contains several radionuclides, and the surface of the earth is constantly exposed to high-energy particles originating from outer space that generate "particle showers" in the lower atmosphere (UNSCEAR 2008).

-Terrestrial radiation

Naturally occurring radionuclides of terrestrial origin, also termed primordial radionuclides, are present in various degrees in all environmental materials, including the human body (e.g. ^{40}K). Of the approximately 2000 known nuclides, only around 250 are stable, whilst all the others are radioactive (BAG 2007). But it is mainly Radon that exists in sufficient quantity to contribute to population exposure, and γ-emitting radionuclides of the ^{40}K, ^{238}U and ^{232}Th families also have a fair share to terrestrial radiation (UNSCEAR 2008).

- Cosmic radiation

There are three types of cosmic radiation: galactic cosmic radiation, solar cosmic radiation and radiation from the earth's radiation belts (van Allen belts) (Spurny 2001). At the flight altitudes of civil aircraft the radiation field is highly modified and the exposure level on-board varies with the geomagnetic position. The comparison of medical radiation exposure to continental and intercontinental flights has been a

further approach to demonstrate the commensurability of the effective doses (Patcas et al. 2012).

It is evident that exposure to natural radiation sources (terrestrial and cosmic) is more significant for the world's population than most exposures to medical radiation sources (UNSCEAR 2000, 2008). The average worldwide exposure to environmental radiation sources of about 2400 μSv per year would seem to indicate that the described dose reduction achieved with the thyroid shield is negligible. Also compared to cosmic radiation experienced during flights, it would seem that iatrogenic radiation can be seen insignificant (Barish 2004b). Pregnant frequent flyers, pilots, and flight attendants experience exposures that exceed current recommended values (Barish 2004a, Kojo 2013) and the average occupational dose of flying personnel is 40 times higher than the average occupational dose of medical personnel in Germany (BMU 2010).

There are however, several caveats that must be brought into the equation, which might render the verdict not as simple as it might have seemed:

1. The average exposure probably does not pertain to any one individual, since there are wide distributions of exposures from each source and the exposures combine in various ways at each location, depending on the specific concentrations of radionuclides in the environment and in the body, the latitude and altitude of the location, and other factors (UNSCEAR 2008). In Switzerland, for example, the exposure to natural exposure ranges between 400μSv and 2000μSv (BAG 2007), which renders the average worldwide exposure of 2400μSv deceptive.
2. Some epidemiologic studies have found that radiation exposure during childhood carries a higher risk of cancer than at other ages (Yoshimoto et al. 1994, Miller 1995). Most patients in orthodontics are children or adolescents, and the radiation risk for them is not well-quantified, but probably much greater than for adults. Hence, established effective doses for adults are most likely to be of little use for younger subjects.

3. Safety values issued by legislative bodies do also not reveal the risks. For example, in Finland, the national radiation law (Radiation Act § 45) regulates that cosmic radiation must not exceed 6mSv per year for flying personnel, but there is convincing evidence for an elevated cancer risk among Nordic airline cabin crew (Kojo 2013).
4. All of the evidence available indicates that carcinogenesis induced by radiation is a stochastic late effect, implying that there is no threshold and that the risk and not the severity of the condition depends on the dose (Hall 1991). Thus, increasing the general dose on a population will not alter the severity of the biologic response in cancer cases, but will augment the amount of cancer patients. The probability of a stochastic effect can be evaluated mathematically: administering to each new orthodontic patient in the U.S. a CBCT (68 - 3687μSv) instead of an OPG and cephalogram (30μSv for both), will result in 10 to 80 additional cancer cases per year in the U.S. alone (Halazonetis 2012).
5. It is estimated that the radiation used in medical and dental diagnoses contributes to approximately 15% of the average annual effective dose to individuals in U.S. population from all sources (Fryback and Thornbury 1991). Scientific evidence has recently been provided that exposure to routine dental X-rays appears to be associated with an increased risk of intracranial meningioma (Claus et al. 2012) and vestibular schwannoma (Han et al. 2012), and CT scans in children might triple the risk of brain cancer and leukaemia (Pearce et al. 2012). In its most recent recommendation, the UNSCEAR concludes that there is emerging evidence from epidemiological studies indicating elevated risks of non-cancer diseases from low radiation exposure (UNSCEAR 2010).

Thus, unless proven differently, the task to reduce the ionizing risk of medical radiation will remain on dentists and the overriding principle of ALARA (As low as reasonably achievable) must be implemented accordingly.

11. Conclusions

11.1. Conclusions on efficacy (STUDIES I – V)

11.1.1. The effect of different voxel sizes on buccal bone measurements (STUDY I)

- Voxel size affects the precision of the measurements taken and the limits of agreement of the different resolution protocols should be considered prior to choosing the voxel size.
- The limits of agreement indicate that an alveolar bone thickness of 1mm might be missed completely, even with a high resolution protocol.
- There is a genuine risk of overestimating fenestrations and dehiscences on CBCT radiographs, both in high as well as low resolution protocols.
- The presence of soft tissue on CBCT data seems to have a curtailing effect on the accuracy when determining landmarks in the bony surface.
- The mucogingival junction may be helpful in localizing the alveolar bone margin.

11.1.2. Accuracy of CBCT in comparison to MDCT for buccal bone measurements (STUDY II)

- CBCT image data is inherently different from MDCT image data, generating smoother images with lower image contrast. CBCT's limitation in regard to qualitative appraisal of soft tissue and bone proved beneficial for the quantitative assessment of linear measurements.
- Compared to MDCT, CBCT appears to be less susceptible to metal artefacts and slightly more reliable for linear measurements.
- In practice, the clinician's choice over which CT device to use should depend on the intended diagnostic purpose of each scan to be performed.
- CBCT accuracy of linear soft tissue measurements is comparable to the accuracy of linear bone measurements.

11.1.3. Establishing the best-suited MRI sequence for the assessment of the condylar process using micro-CT as reference (STUDY III)

- T1-weighted 3D FSPGR sequence revealed to be the most suitable MRI sequence for the objective and subjective assessment of osseous structures of the mandibular condyle.
- The above mentioned MRI sequence can be recommended for cortical bone thickness measurement of the mandibular condyle.
- The above mentioned MRI sequence is suitable to evaluate the presence of cortical bone thinning, cortical bone erosions, irregularities of the cortical bone surface, subcortical bone cysts and the presence of an anterior osteophyte.

11.1.4. Accuracy of CBCT versus MDCT, MRI, OPG and lateral cephalogram for linear measurements of the mandibular ramus and condylar process (STUDY IV)

- All 3D imaging procedures were almost equal for measuring CP and RH. Thus, MRI is recommended since it is not only an equal alternative for CBCT and MDCT, but also circumvents the issue of ionizing radiation.
- The limits of agreement were higher for RH than for CP, but still clinically acceptable. Since reference values for RH are available, RH is recommended for follow-up studies.
- The reported high reproducibility and precision of CBCT data for linear measurement of RH and CP make it a legitimate tool to observe condylar growth.
- MRI measurements were generally smaller than those obtained by MDCT and CBCT, and must be corrected for length differences.
- The susceptibility of OPG to head positioning leads to a poor agreement with the 3D imaging procedures, and make the use of OPG in TMJ assessment obsolete
- The overall poor results of LC render its measurements of either RH or CP useless.

11.1.5. Accuracy of CBCT, MDCT and lateral cephalogram in assessing the cervical spine (STUDY V)

- Lateral cephalograms cause false positive detections of fusions and are therefore a questionable means to assess cervical spine anomalies.
- Previous studies evaluating fusions in the cervical spines, based on a single lateral cephalogram, seem to be highly problematic.
- MDCT data viewed by general radiologists and CBCT data screened by oral radiologists are both reliable methods to exclude fusions.
- General radiologists appraising MDCT data performed better in the assessment of osteoarthritic changes of the joints than did oral radiologists with CBCT data, but further studies with larger number of specimens would be welcomed to confirm this finding.

11.2. Conclusions on radiation dose evaluation (STUDY VI)

- The assessment of skeletal maturation of cervical vertebrae on a lateral cephalogram is to be questioned and the use of a thyroid shield is strongly to be advocated.
- If an evaluation of skeletal age is deemed necessary, an additional hand-wrist radiogram seems much more justifiable than removing the thyroid shield which would cause highly vulnerable tissue to be exposed to direct radiation.
- In CBCT, reducing the height of the field of view is an advisable method to reduce the effective dose and must be implemented.
- There is no need to shield the thyroid in OPG and in CBCT with reduced field of view.

12. Acknowledgements

I wish to express my sincerest thanks and profound gratitude to my supervisor, Docent Timo Peltomäki, DDS, PhD who gave me the opportunity to write this thesis. It was a privilege to experience his invaluable guidance and unstinted support throughout the whole project.

I am indebted to Prof. Theodore Eliades, DDS, MS, PhD for his continuous support in helping me to pursue all my academic aspirations.

Debts of gratitude are due to all co-authors of the original publications that formed the basis of this dissertation. It was a great privilege to perform research with such knowledgeable and motivating people as these.

I would like to express my great appreciation to the referees, Prof. Demetrios Halazonetis, DDS, MS and Docent Jaakko Niinimäki, MD, PhD for consenting to review the dissertation and for providing critical comments and valuable inputs to improve the manuscript.

I am particularly grateful to Prof. Pertti Pirttiniemi, DDS, PhD for agreeing to act as the opponent at the public defence.

I owe special thanks to Mrs. Goldie Maxwell, MA for her assistance in editing most of the original publications.

Words are inadequate to describe the unwavering support of my wife Debby, my parents and my children. They were a constant source of encouragement and inspiration and were eternally patient during all those months of researching and writing.

Zürich, November 2013

Raphael Patcas

13. References

Abrahams JJ (2001): *Dental CT imaging: a look at the jaw*. Radiology 219: 334-345.

Aggarwal V, Logani A and Shah N (2008): *The evaluation of computed tomography scans and ultrasounds in the differential diagnosis of periapical lesions*. J Endod 34: 1312-1315.

Ahlowalia MS, Patel S, Anwar HM, Cama G, Austin RS, Wilson R and Mannocci F (2013): *Accuracy of CBCT for volumetric measurement of simulated periapical lesions*. Int Endod J 46: 538-546.

Ainamo J and Talari A (1976): *The increase with age of the width of attached gingiva*. J Periodontal Res 11: 182-188.

Al-Ekrish AA and Ekram M (2011): *A comparative study of the accuracy and reliability of multidetector computed tomography and cone beam computed tomography in the assessment of dental implant site dimensions*. Dentomaxillofac Radiol 40: 67-75.

Al-Nawas B, Klein MO, Gotz H, Vaterod J, Duschner H, Grotz KA and Kann PH (2008): *Dental implantation: ultrasound transmission velocity to evaluate critical bone quality--an animal model*. Ultraschall Med 29: 302-307.

Al-Rawi B, Hassan B, Vandenberge B and Jacobs R (2010): *Accuracy assessment of three-dimensional surface reconstructions of teeth from cone beam computed tomography scans*. J Oral Rehabil 37: 352-358.

Albandar JM and Goldstein H (1992): *Multi-level statistical models in studies of periodontal diseases*. J Periodontol 63: 690-695.

Alkhader M, Ohbayashi N, Tetsumura A, Nakamura S, Okochi K, Momin MA and Kurabayashi T (2010): *Diagnostic performance of magnetic resonance imaging for detecting osseous abnormalities of the temporomandibular joint and its correlation with cone beam computed tomography*. Dentomaxillofac Radiol 39: 270-276.

Altaye M, Donner A and Eliasziw M (2001a): *A general goodness-of-fit approach for inference procedures concerning the kappa statistic*. Stat Med 20: 2479-2488.

Altaye M, Donner A and Klar N (2001b): *Inference procedures for assessing interobserver agreement among multiple raters*. Biometrics 57: 584-588.

Angelopoulos C, Scarfe WC and Farman AG (2012): *A comparison of maxillofacial CBCT and medical CT*. Atlas Oral Maxillofacial Surg Clin N Am 20: 1-17.

Arai Y, Tammisalo E, Iwai K, Hashimoto K and Shinoda K (1999): *Development of a compact computed tomographic apparatus for dental use*. Dentomaxillofac Radiol 28: 245-248.

Araki K, Maki K, Seki K, Sakamaki K, Harata Y, Sakaino R, Okano T and Seo K (2004): *Characteristics of a newly developed dentomaxillofacial X-ray cone beam CT scanner (CB MercuRay): system configuration and physical properties*. Dentomaxillofac Radiol 33: 51-59.

Araki K and Okano T (2011): *The effect of surrounding conditions on pixel value of cone beam computed tomography*. Clin Oral Implants Res 24: 862-865.

Arntsen T and Sonnesen L (2011): *Cervical vertebral column morphology related to craniofacial morphology and head posture in preorthodontic children with Class II malocclusion and horizontal maxillary overjet*. Am J Orthod Dentofacial Orthop 140: e1-7.

Artun J and Krogstad O (1987): *Periodontal status of mandibular incisors following excessive proclination. A study in adults with surgically treated mandibular prognathism*. Am J Orthod Dentofacial Orthop 91: 225-232.

Baccetti T, Franchi L and McNamara JA, Jr. (2002): *An improved version of the cervical vertebral maturation (CVM) method for the assessment of mandibular growth*. Angle Orthod 72: 316-323.

Bache C (1964): *Mandibular Growth and Dental Occlusion in Juvenile Rheumatoid Arthritis*. Acta Rheumatol Scand 10: 142-153.

BAG (2007): *Radioaktivität und Strahlenschutz*. Bundesamt für Gesundheit, Bern.

Barish RJ (2004a): *In-flight radiation exposure during pregnancy*. Obstet Gynecol 103: 1326-1330.

Barish RJ (2004b): *Radiation risk from airline travel*. J Am Coll Radiol 1: 784-785.

Barriga B, Lewis TM and Law DB (1974): *An investigation of the dental occlusion in children with juvenile rheumatoid arthritis*. Angle Orthod 44: 329-335.

Barriviera M, Duarte WR, Januario AL, Faber J and Bezerra AC (2009): *A new method to assess and measure palatal masticatory mucosa by cone-beam computerized tomography*. J Clin Periodontol 36: 564-568.

Bartels T and Meyer W (1991): *[A quick and effective method for the maceration of vertebrates]*. Dtsch Tierarztl Wochenschr 98: 407-409.

Batenhorst KF, Bowers GM and Williams JE, Jr. (1974): *Tissue changes resulting from facial tipping and extrusion of incisors in monkeys*. J Periodontology 45: 660-668.

Bauman R, Scarfe W, Clark S, Morelli J, Scheetz J and Farman A (2011): *Ex vivo detection of mesiobuccal canals in maxillary molars using CBCT at four different isotropic voxel dimensions*. Int Endod J 44: 752-758.

Baumrind S, Carlson S, Beers A, Curry S, Norris K and Boyd RL (2003): *Using three-dimensional imaging to assess treatment outcomes in orthodontics: a progress report from the University of the Pacific*. Orthod Craniofac Res 6 Suppl 1: 132-142.

Bebnowski D, Hanggi MP, Markic G, Roos M and Peltomaki T (2012): *Cervical vertebrae anomalies in subjects with Class II malocclusion assessed by lateral cephalogram and cone beam computed tomography*. Eur J Orthod 34: 226-231.

Beit P, Peltomaki T, Schätzle M, Signorelli L and Patcas R (2013): *Evaluating the agreement of skeletal age assessment based on hand-wrist and cervical vertebrae radiography*. Am J Orthod Dentofacial Orthop 144: 838-847.

Belfie DJ and Clark JM (1992): *Enzymatic preparation of allograft bone*. Clin Res 40: A134-A134.

Berland B (1985): *Chemical maceration and other practical methods*. Fauna 38: 146-151.

Björk A (1963): *Variations in the growth pattern of the human mandible: longitudinal radiographic study by the implant method*. J Dent Res 42: 400-411.

Björk A (1968): *The use of metallic implants in the study of facial growth in children: method and application*. Am J Phys Anthropol 29: 243-254.

Björk A and Helm S (1967): *Prediction of the age of maximum puberal growth in body height*. Angle Orthod 37: 134-143.

Bland JM and Altman DG (1986): *Statistical methods for assessing agreement between two methods of clinical measurement*. Lancet 8476: 307-310.

Bland JM and Altman DG (1990): *A note on the use of the intraclass correlation-coefficient in the evaluation of agreement between 2 methods of measurement*. Comput Biol Med 20: 337-340.

Bland JM and Altman DG (1999): *Measuring agreement in method comparison studies*. Stat Methods Med Res 8: 135-160.

Bland JM and Altman DG (2003): *Applying the right statistics: analyses of measurement studies*. Ultrasound Obstet Gynecol 22: 85-93.

BMU (2010): *Umweltradioaktivität und Strahlenbelastung: Jahresbericht 2009: 236-240*. Bundesministerium für Umwelt, Naturschutz und Reaktorsiherheit, Bonn.

Bowden BD (1971): *Sesamoid bone appearance as an indicator of adolescence*. Aust Orthod J 2: 242-248.

Bowden BD (1976): *Epiphysial changes in the hand/wrist area as indicators of adolescent stage*. Aust Orthod J 4: 87-104.

Boyesen P, Haavardsholm EA, van der Heijde D, Ostergaard M, Hammer HB, Sesseng S and Kvien TK (2011): *Prediction of MRI erosive progression: a comparison of modern imaging modalities in early rheumatoid arthritis patients*. Ann Rheum Dis 70: 176-179.

Brooks SL, Brand JW, Gibbs SJ, Hollender L, Lurie AG, Omnell KA, Westesson PL and White SC (1997): *Imaging of the temporomandibular joint: a position paper of the American Academy of Oral and Maxillofacial Radiology*. Oral Surg Oral Med Oral Pathol Oral Radiol Endod 83: 609-618.

Brown MW, Templeton AW and Hodges FJ, 3rd (1964): *The incidence of acquired and congenital fusions in the cervical spine*. Am J Roentgenol Radium Ther Nucl Med 92: 1255-1259.

Bryant J (2011): *Deriving Hounsfield units from the grey scale of a CBCT?* Dentomaxillofac Radiol 40: 65; author reply 66.

Bryant JA, Drage NA and Richmond S (2008): *Study of the scan uniformity from an i-CAT cone beam computed tomography dental imaging system*. Dentomaxillofac Radiol 37: 365-374.

Burn-Murdoch RA and Tyler DW (1981): *Physiological evidence that periodontal collagen in the rat exists as fibres prior to histological fixation*. Arch Oral Biol 26: 995-999.

Cakur B, Sumbullu MA, Dagistan S and Durna D (2012): *The importance of cone beam CT in the radiological detection of osteomalacia*. Dentomaxillofac Radiol 41: 84-88.

Cannizzaro E, Schroeder S, Muller LM, Kellenberger CJ and Saurenmann RK (2011): *Temporomandibular joint involvement in children with juvenile idiopathic arthritis*. J Rheumat 38: 510-515.

Carrafiello G, Dizonno M, Colli V, Strocchi S, Pozzi Taubert S, Leonardi A, Giorgianni A, Barresi M, Macchi A, Bracchi E, Conte L and Fugazzola C (2010): *Comparative study of jaws with multislice computed tomography and cone-beam computed tomography*. Radiol Med 115: 600-611.

Carreon LY, Djurasovic M, Glassman SD and Sailer P (2007): *Diagnostic accuracy and reliability of fine-cut CT scans with reconstructions to determine the status of an instrumented posterolateral fusion with surgical exploration as reference standard*. Spine (Phila Pa 1976) 32: 892-895.

Cha JY, Mah J and Sinclair P (2007): *Incidental findings in the maxillofacial area with 3-dimensional cone-beam imaging*. Am J Orthod Dentofacial Orthop 132: 7-14.

Chadwick JW and Lam EW (2010): *The effects of slice thickness and interslice interval on reconstructed cone beam computed tomographic images*. Oral Surg Oral Med Oral Pathol Oral Radiol Endod 110: e37-42.

Chang A *StatTools; available at: http://www.stattools.net/CohenKappa_Pgm.php. Accessed on 03th July 2012.*

Charalampidou M, Kjellberg H, Georgiakaki I and Kiliaridis S (2008): *Masseter muscle thickness and mechanical advantage in relation to vertical craniofacial morphology in children*. Acta Odontol Scand 66: 23-30.

Chatzigianni A and Halazonetis DJ (2009): *Geometric morphometric evaluation of cervical vertebrae shape and its relationship to skeletal maturation*. Am J Orthod Dentofacial Orthop 136: 481 e481-489; discussion 481-483.

Chau A (2012): *Comparison between the use of magnetic resonance imaging and conebeam computed tomography for mandibular nerve identification*. Clin Oral Implants Res 23: 253-256.

Cheng JG, Zhang ZL, Wang XY, Zhang ZY, Ma XC and Li G (2012): *Detection accuracy of proximal caries by phosphor plate and cone-beam computerized tomography images scanned with different resolutions*. Clin Oral Investig 16: 1015-1021.

Chifor R, Badea ME, Hedesiu M, Serbanescu A and Badea AF (2010): *Experimental model for measuring and characterisation of the dento-alveolar system using high frequencies ultrasound techniques*. Med Ultrason 12: 127-132.

Chifor R, Hedesiu M, Bolfa P, Catoi C, Crisan M, Serbanescu A, Badea AF, Moga I and Badea ME (2011): *The evaluation of 20 MHz ultrasonography, computed tomography scans as compared to direct microscopy for periodontal system assessment*. Med Ultrason 13: 120-126.

Claus EB, Calvocoressi L, Bondy ML, Schildkraut JM, Wiemels JL and Wrensch M (2012): *Dental x-rays and risk of meningioma*. Cancer 118: 4530-4537.

Cohen J (1960): *A Coefficient of Agreement for Nominal Scales*. Educ Psychol Meas 20: 37-46.

Cohen MD (2009): *Pediatric CT radiation dose: how low can you go?* AJR Am J Roentgenol 192: 1292-1303.

Comert A, Kokat AM, Akkocaoglu M, Tekdemir I, Akca K and Cehreli MC (2009): *Fresh-frozen vs. embalmed bone: is it possible to use formalin-fixed human bone for biomechanical experiments on implants?* Clin Oral Implants Res 20: 521-525.

Cox LA (1996): *Tanner-Whitehouse method of assessing skeletal maturity: problems and common errors*. Horm Res 45 Suppl 2: 53-55.

Crelin ES (1973): *Functional anatomy of the newborn*. Yale University Press, New Haven.

da Silveira PF, Vizzotto MB, Liedke GS, da Silveira HLD, Montagner F and da Silveira HED (2013): *Detection of vertical root fractures by conventional radiographic examination and cone beam computed tomography - an in vitro analysis*. Dent Traumatol 29: 41-46.

Dalili Z, Taramsari M, Mousavi Mehr SZ and Salamat F (2012): *Diagnostic value of two modes of cone-beam computed tomography in evaluation of simulated external root resorption: an in vitro study*. Imaging Sci Dent 42: 19-24.

Damstra J, Fourie Z, Huddleston Slater JJ and Ren Y (2010): *Accuracy of linear measurements from cone-beam computed tomography-derived surface models of different voxel sizes*. Am J Orthod Dentofacial Orthop 137: 16 e11-16; discussion 16-17.

Dantas JA, Montebello Filho A and Campos PS (2005): *Computed tomography for dental implants: the influence of the gantry angle and mandibular positioning on the bone height and width*. Dentomaxillofac Radiol 34: 9-15.

de-Azevedo-Vaz SL, Vasconcelos Kde F, Neves FS, Melo SL, Campos PS and Haiter-Neto F (2013): *Detection of periimplant fenestration and dehiscence with the use of two scan modes and the smallest voxel sizes of a cone-beam computed tomography device*. Oral Surg Oral Med Oral Pathol Oral Radiol Endod 115: 121-127.

Djeu G, Hayes C and Zawaideh S (2002): *Correlation between mandibular central incisor proclination and gingival recession during fixed appliance therapy*. Angle Orthod 72: 238-245.

Docquier P-L, Paul L, Cartiaux O, Lecouvet F, Dufrane D, Delloye C and Galant C (2010): *Formalin fixation could interfere with the clinical assessment of the tumor-free margin in tumor surgery: magnetic resonance imaging-based study*. Oncology 78: 115-124.

Dorfman HS (1978): *Mucogingival changes resulting from mandibular incisor tooth movement*. Am J Orthod 74: 286-297.

Draenert FG, Coppenrath E, Herzog P, Muller S and Mueller-Lisse UG (2007): *Beam hardening artefacts occur in dental implant scans with the NewTom cone beam CT but not with the dental 4-row multidetector CT*. Dentomaxillofac Radiol 36: 198-203.

Edwards JG (1976): *A study of the anterior portion of the palate as it relates to orthodontic therapy*. Am J Orthod 69: 249-273.

Elliott JC and Dover SD (1982): *X-ray microtomography*. J Microsc 126: 211-213.

Emshoff R, Bertram S and Strobl H (1999): *Ultrasonographic cross-sectional characteristics of muscles of the head and neck*. Oral Surg Oral Med Oral Pathol Oral Radiol Endod 87: 93-106.

Endo M, Tsunoo T, Nakamori N and Yoshida K (2001): *Effect of scattered radiation on image noise in cone beam CT*. Med Phys 28: 469-474.

Enhos S, Uysal T, Yagci A, Veli I, Ucar FI and Ozer T (2012): *Dehiscence and fenestration in patients with different vertical growth patterns assessed with cone-beam computed tomography*. Angle Orthod 82: 868-874.

EU (2002): *Additional protocol to the convention on human rights and biomedicine, on transplantation of organs and tissues of human origin. ETS 186, Art 16–18*. European Union, Strasbourg.

Farman AG and Escobar V (1982): *Radiographic appearance of the cervical vertebrae in normal and abnormal development*. Br J Oral Surg 20: 264-274.

Farman AG, Nortje CJ and Joubert JJ (1979): *Radiographic profile of the first cervical vertebra*. J Anat 128: 595-600.

Farman AG and Scarfe WC (2009): *The basics of maxillofacial cone beam computed tomography*. Semin Orthod 15: 2-13.

Fasske E and Morgenroth K (1958): *Vergleichende stomatoskopische und histochemische Untersuchungen am Zahnfleischrand des Menschen*. Dtsch Zahnarztl Z 13: 562-567.

Feneis H (1952): *[Anatomy and physiology of the normal gingiva]*. Dtsch Zahnarztl Z 7: 467-476.

Ferrare N, Leite AF, Caracas HC, de Azevedo RB, de Melo NS and de Souza Figueiredo PT (2013): *Cone-beam computed tomography and microtomography for alveolar bone measurements*. Surg Radiol Anat 35: 495-502.

Fineberg HV (1978): *Evaluation of computed tomography: achievement and challenge*. AJR Am J Roentgenol 131: 1-4.

Fishman LS (1979): *Chronological versus skeletal age, an evaluation of craniofacial growth*. Angle Orthod 49: 181-189.

Fishman LS (1982): *Radiographic evaluation of skeletal maturation. A clinically oriented method based on hand-wrist films*. Angle Orthod 52: 88-112.

Fleiss JL (1971): *Measuring nominal scale agreement among many raters*. Psychol Bull 76: 378-382.

Flores-Mir C, Nebbe B and Major PW (2004): *Use of skeletal maturation based on hand-wrist radiographic analysis as a predictor of facial growth: a systematic review*. Angle Orthod 74: 118-124.

Fourie Z, Damstra J, Gerrits PO and Ren Y (2010): *Accuracy and reliability of facial soft tissue depth measurements using cone beam computer tomography*. Forensic Sci Int 199: 9-14.

Fourie Z, Damstra J, Gerrits PO and Ren Y (2011): *Accuracy and repeatability of anthropometric facial measurements using cone beam computed tomography*. Cleft Palate Craniofac J 48: 623-630.

Frongia G, Piancino MG and Bracco P (2012): *Cone-beam computed tomography: accuracy of three-dimensional cephalometry analysis and influence of patient scanning position*. J Craniofac Surg 23: 1038-1043.

Fryback DG (1983): *A conceptual model for output measures in cost-effectiveness evaluation of diagnostic imaging*. J Neuroradiol 10: 94-96.

Fryback DG and Thornbury JR (1991): *The efficacy of diagnostic imaging*. Med Decis Making 11: 88-94.

Fudalej P and Bollen AM (2010): *Effectiveness of the cervical vertebral maturation method to predict postpeak circumpubertal growth of craniofacial structures*. Am J Orthod Dentofacial Orthop 137: 59-65.

Fuhrmann R (1996): *Three-dimensional interpretation of periodontal lesions and remodeling during orthodontic treatment. Part III*. J Orofac Orthop 57: 224-237.

Fuhrmann RA, Wehrbein H, Langen HJ and Diedrich PR (1995): *Assessment of the dentate alveolar process with high resolution computed tomography*. Dentomaxillofac Radiol 24: 50-54.

Gabriel DB, Southard KA, Qian F, Marshall SD, Franciscus RG and Southard TE (2009): *Cervical vertebrae maturation method: poor reproducibility*. Am J Orthod Dentofacial Orthop 136: 478 e471-477; discussion 478-480.

Galen S and Jost-Brinkmann PG (2010): *B-mode and M-mode Ultrasonography of Tongue Movements during Swallowing*. J Orofac Orthop 71: 125-135.

Ganguly R, Ruprecht A, Vincent S, Hellstein J, Timmons S and Qian F (2011): *Accuracy of linear measurement in the Galileos cone beam computed tomography under simulated clinical conditions*. Dentomaxillofac Radiol 40: 299-305.

Gare BA (1996): *Epidemiology of rheumatic disease in children*. Curr Opin Rheumatol 8: 449-454.

Garn SM, Rohmann CG and Blumenthal T (1966): *Ossification sequence polymorphism and sexual dimorphism in skeletal development*. Am J Phys Anthropol 24: 101-115.

Gaudino C, Cosgarea R, Heiland S, Csernus R, Beomonte Zobel B, Pham M, Kim TS, Bendszus M and Rohde S (2011): *MR-Imaging of teeth and periodontal apparatus: an experimental study comparing high-resolution MRI with MDCT and CBCT*. Eur Radiol 21: 2575-2583.

Ghorayeb SR, Bertoncini CA and Hinders MK (2008): *Ultrasonography in dentistry*. IEEE Trans Ultrason Ferroelectr Freq Control 55: 1256-1266.

Gilli G (1996): *The assessment of skeletal maturation*. Horm Res 45 Suppl 2: 49-52.

Grave KC and Brown T (1979): *Carpal radiographs in orthodontic treatment*. Am J Orthod 75: 27-45.

Gray H, Standring S, Ellis H, Collins P, Wigley C and Berkovitz BKB (2005): *Gray's anatomy: the anatomical basis of clinical practice*. Elsevier Churchill Livingstone, New York.

Greenberg J, Laster L and Listgarten MA (1976): *Transgingival probing as a potential estimator of alveolar bone level*. J Periodontol 47: 514-517.

Greulich WW and Pyle SI (1959): *Radiographic Atlas of Skeletal Development of the Hand and Wrist. Stanford. Stanford University Press*. Stanford University Press, Stanford.

Grimard BA, Hoidal MJ, Mills MP, Mellonig JT, Nummikoski PV and Mealey BL (2009): *Comparison of clinical, periapical radiograph, and cone-beam volume tomography measurement techniques for assessing bone level changes following regenerative periodontal therapy*. J Periodontol 80: 48-55.

Guille JT and Sherk HH (2002): *Congenital osseous anomalies of the upper and lower cervical spine in children*. J Bone Joint Surg Am 84-A: 277-288.

Gundappa M, Ng SY and Whaites EJ (2006): *Comparison of ultrasound, digital and conventional radiography in differentiating periapical lesions*. Dentomaxillofac Radiol 35: 326-333.

Gutermann C, Peltomaki T, Markic G, Hanggi M, Schatzle M, Signorelli L and Patcas R (2013): *The inclination of mandibular incisors revisited*. Angle Orthod [Epub ahead of print] DOI: 10.2319/040413-262.1.

Hagg U and Taranger J (1980a): *Menarche and voice change as indicators of the pubertal growth spurt*. Acta Odontol Scand 38: 179-186.

Hagg U and Taranger J (1980b): *Skeletal stages of the hand and wrist as indicators of the pubertal growth spurt*. Acta Odontol Scand 38: 187-200.

Hagg U and Taranger J (1982): *Maturation indicators and the pubertal growth spurt*. Am J Orthod 82: 299-309.

Haiter-Neto F, Wenzel A and Gotfredsen E (2008): *Diagnostic accuracy of cone beam computed tomography scans compared with intraoral image modalities for detection of caries lesions*. Dentomaxillofac Radiol 37: 18-22.

Halazonetis DJ (2012): *Cone-beam computed tomography is not the imaging technique of choice for comprehensive orthodontic assessment*. Am J Orthod Dentofacial Orthop 141: 403, 405, 407 passim.

Hall EJ (1991): *Scientific view of low-level radiation risks*. Radiographics 11: 509-518.

Hall WB, Truitt SG, Scheunemann LP, Shah SA, Rivera MP, Parker LA and Carson SS (2009): *The prevalence of clinically relevant incidental findings on chest computed tomographic angiograms ordered to diagnose pulmonary embolism*. Arch Intern Med 169: 1961-1965.

Han YY, Berkowitz O, Talbott E, Kondziolka D, Donovan M and Lunsford LD (2012): *Are frequent dental x-ray examinations associated with increased risk of vestibular schwannoma?* J Neurosurg 117 Suppl: 78-83.

Handelman CS (1996): *The anterior alveolus: its importance in limiting orthodontic treatment and its influence on the occurrence of iatrogenic sequelae*. Angle Orthod 66: 95-109; discussion 109-110.

Hansen P, Hassenkam T, Svensson RB, Aagaard P, Trappe T, Haraldsson BT, Kjaer M and Magnusson P (2009): *Glutaraldehyde cross-linking of tendon--mechanical effects at the level of the tendon fascicle and fibril*. Connect Tissue Res 50: 211-222.

Harrison JE and Burnside G (2012): *Why does clustering matter in orthodontic trials?* Eur J Orthod 34: 293-295.

Hashimoto K, Arai Y, Iwai K, Araki M, Kawashima S and Terakado M (2003): *A comparison of a new limited cone beam computed tomography machine for dental use with a multidetector row helical CT machine*. Oral Surg Oral Med Oral Pathol Oral Radiol Endod 95: 371-377.

Hashimoto K, Kawashima S, Araki M, Iwai K, Sawada K and Akiyama Y (2006): *Comparison of image performance between cone-beam computed tomography for dental use and four-row multidetector helical CT*. J Oral Sci 48: 27-34.

Hashimoto K, Kawashima S, Kameoka S, Akiyama Y, Honjoya T, Ejima K and Sawada K (2007): *Comparison of image validity between cone beam computed tomography for dental use and multidetector row helical computed tomography*. Dentomaxillofac Radiol 36: 465-471.

Hassan B, Nijkamp P, Verheij H, Tairie J, Vink C, van der Stelt P and van Beek H (2013): *Precision of identifying cephalometric landmarks with cone beam computed tomography in vivo*. Eur J Orthod 35: 38-44.

Hassel B and Farman AG (1995): *Skeletal maturation evaluation using cervical vertebrae*. Am J Orthod Dentofacial Orthop 107: 58-66.

Hatcher DC (2010): *Operational principles for cone-beam computed tomography*. J Am Dent Assoc 141 Suppl 3: 3-6.

Hayes RJ and Bennett S (1999): *Simple sample size calculation for cluster-randomized trials*. Int J Epidemiol 28: 319-326.

Heiland M, Pohlenz P, Blessmann M, Habermann CR, Oesterhelweg L, Begemann PC, Schmidgunst C, Blake FA, Puschel K, Schmelzle R and Schulze D (2007): *Cervical soft tissue imaging using a mobile CBCT scanner with a flat panel detector in comparison with corresponding CT and MRI data sets*. Oral Surg Oral Med Oral Pathol Oral Radiol Endod 104: 814-820.

Hellman M (1923): *The process of dentition and its effects on occlusion*. Dental Cosmos 65: 1329-1344.

Helm S, Siersbaek-Nielsen S, Skieller V and Bjork A (1971): *Skeletal maturation of the hand in relation to maximum puberal growth in body height*. Tandlaegebladet 75: 1223-1234.

Hensinger RN (1991): *Congenital anomalies of the cervical spine*. Clin Orthop Relat Res: 16-38.

Herzog C (2013): *Die Genauigkeit der digitalen Volumentomographie zur Bestimmung des labialen Knochenniveaus in der Unterkieferfront.* Inaugural-Dissertation. University of Zurich, Zurich.

Hofmann E, Schmid M, Sedlmair M, Banckwitz R, Hirschfelder U and Lell M (2013): *Comparative study of image quality and radiation dose of cone beam and low-dose multislice computed tomography - an in-vitro investigation*. Clin Oral Investig [Epub ahead of print] DOI: 10.1007/s00784-013-0948-9.

Hohlweg-Majert B, Metzger MC, Kummer T and Schulze D (2011a): *Morphometric analysis - Cone beam computed tomography to predict bone quality and quantity*. J Craniomaxillofac Surg 39: 330-334.

Hohlweg-Majert B, Pautke C, Deppe H, Metzger MC, Wagner K and Schulze D (2011b): *Qualitative and quantitative evaluation of bony structures based on DICOM dataset*. J Oral Maxillofac Surg 69: 2763-2770.

Hollender L, Ronnerman A and Thilander B (1980): *Root resorption, marginal bone support and clinical crown length in orthodontically treated patients*. Eur J Orthod 2: 197-205.

Honda K, Larheim TA, Maruhashi K, Matsumoto K and Iwai K (2006): *Osseous abnormalities of the mandibular condyle: diagnostic reliability of cone beam computed tomography compared with helical computed tomography based on an autopsy material*. Dentomaxillofac Radiol 35: 152-157.

Horie CV and Murphy RG (1988): *Conservation of Natural History Specimens: Vertebrates. In: Proceedings of the Short Course at Manchester University*. Department of Environmental Biology and The Manchester Museum, Manchester.

Horswell BB (1991): *The incidence and relationship of cervical spine anomalies in patients with cleft lip and/or palate*. J Oral Maxillofac Surg 49: 693-697.

Huggare JA and Laine-Alava MT (1997): *Nasorespiratory function and head posture*. Am J Orthod Dentofacial Orthop 112: 507-511.

Hujoel P, Hollender L, Bollen AM, Young JD, Cunha-Cruz J, McGee M and Grosso A (2006): *Thyroid shields and neck exposures in cephalometric radiography*. BMC Med Imaging 6: 1-7.

Hunter CJ (1966): *The correlation of facial growth with body height and skeletal maturation at adolescence*. Angle Orthod 36: 44-54.

ICRP (2008): *Radiation dose to patients from radiopharmaceuticals. Addendum 3 to ICRP Publication 53. ICRP Publication 106. Approved by the Commission in October 2007*. Ann ICRP 38: 1-197.

Idiyatullin D, Corum C, Moeller S, Prasad HS, Garwood M and Nixdorf DR (2011): *Dental magnetic resonance imaging: making the invisible visible*. J Endod 37: 745-752.

Imrey PB (1986): *Considerations in the statistical analysis of clinical trials in periodontitis*. J Clin Periodontol 13: 517-532.

Imrey PB and Chilton NW (1992): *Design and analytic concepts for periodontal clinical trials*. J Periodontol 63: 1124-1140.

Ising N, Kim KB, Araujo E and Buschang P (2012): *Evaluation of dehiscences using cone beam computed tomography*. Angle Orthod 82: 122-130.

Ivekovic S, McIntyre GT, Gillgrass T, Thomson DA, Menhinick A and Mossey PA (2012): *Validation of the volumetric measurement of a simulated maxillary alveolarbone defect using cone-beam computed tomography*. Cleft Palate Craniofac J [Epub ahead of print] DOI: 10.1597/12-161.

Jadu FM, Hill ML, Yaffe MJ and Lam EW (2011): *Optimization of exposure parameters for cone beam computed tomography sialography*. Dentomaxillofac Radiol 40: 362-368.

Jämsä T and Rönning O (1985): *The facial skeleton in children affected by rheumatoid arthritis--a roentgen-cephalometric study*. Eur J Orthod 7: 48-56.

Jank S, Haase S, Strobl H, Michels H, Hafner R, Missmann M, Bodner G, Mur E and Schroeder D (2007): *Sonographic investigation of the temporomandibular joint in patients with juvenile idiopathic arthritis: a pilot study*. Arthritis Rheum 57: 213-218.

Januario AL, Barriviera M and Duarte WR (2008): *Soft tissue cone-beam computed tomography: a novel method for the measurement of gingival tissue and the dimensions of the dentogingival unit*. J Esthet Restor Dent 20: 366-373; discussion 374.

Joshi V, Yamaguchi T, Matsuda Y, Kaneko N, Maki K and Okano T (2012): *Skeletal maturity assessment with the use of cone-beam computerized tomography*. Oral Surg Oral Med Oral Pathol Oral Radiol Endod 113: 841-849.

Kai Y, Matsumoto K, Ejima K, Araki M, Yonehara Y and Honda K (2011): *Evaluation of the usefulness of magnetic resonance imaging in the assessment of the thickness of the roof of the glenoid fossa of the temporomandibular joint*. Oral Surg Oral Med Oral Pathol Oral Radiol Endod 112: 508-514.

Kamburoglu K and Kursun S (2010): *A comparison of the diagnostic accuracy of CBCT images of different voxel resolutions used to detect simulated small internal resorption cavities*. Int Endod J 43: 798-807.

Kamburoglu K, Murat S, Yuksel SP, Cebeci AR and Paksoy CS (2010): *Occlusal caries detection by using a cone-beam CT with different voxel resolutions and a digital intraoral sensor*. Oral Surg Oral Med Oral Pathol Oral Radiol Endod 109: e63-69.

Kammerer PW, Kumar VV, Brullmann D, Gotz H, Kann PH, Al-Nawas B and Klein MO (2012): *Evaluation of ultrasound transmission velocity and 3-dimensional radiology in different bone types for dental implantology: a comparative ex vivo study*. Oral Surg Oral Med Oral Pathol Oral Radiol Endod 116: 77-84.

Kapila S, Conley RS and Harrell WE, Jr. (2011): *The current status of cone beam computed tomography imaging in orthodontics*. Dentomaxillofac Radiol 40: 24-34.

Karhulahti T, Ronning O and Jamsa T (1990): *Mandibular condyle lesions, jaw movements, and occlusal status in 15-year-old children with juvenile rheumatoid arthritis*. Scand J Dent Res 98: 17-26.

Kato A and Ohno N (2009): *Construction of three-dimensional tooth model by micro-computed tomography and application for data sharing*. Clin Oral Investig 13: 43-46.

Katsumata A, Hirukawa A, Okumura S, Naitoh M, Fujishita M, Ariji E and Langlais RP (2007): *Effects of image artifacts on gray-value density in limited-volume cone-beam computerized tomography*. Oral Surg Oral Med Oral Pathol Oral Radiol Endod 104: 829-836.

Katsumata A, Hirukawa A, Okumura S, Naitoh M, Fujishita M, Ariji E and Langlais RP (2009): *Relationship between density variability and imaging volume size in cone-beam computerized tomographic scanning of the maxillofacial region: an in vitro study*. Oral Surg Oral Med Oral Pathol Oral Radiol Endod 107: 420-425.

Kerry SM and Bland JM (1998): *Analysis of a trial randomised in clusters*. Brit Med J 316: 54.

Khedmat S, Rouhi N, Drage N, Shokouhinejad N and Nekoofar MH (2012): *Evaluation of three imaging techniques for the detection of vertical root fractures in the absence and presence of gutta-percha root fillings*. Int Endod J 45: 1004-1009.

Kiliaridis S and Kalebo P (1991): *Masseter muscle thickness measured by ultrasonography and its relation to facial morphology*. J Dent Res 70: 1262-1265.

Kiliaridis S, Mills CM and Antonarakis GS (2010): *Masseter muscle thickness as a predictive variable in treatment outcome of the twin-block appliance and masseteric thickness changes during treatment*. Orthod Craniofac Res 13: 203-213.

Kim M, Huh KH, Yi WJ, Heo MS, Lee SS and Choi SC (2012a): *Evaluation of accuracy of 3D reconstruction images using multi-detector CT and cone-beam CT*. Imaging Sci Dent 42: 25-33.

Kim MK, Kang SH, Lee EH, Lee SH and Park W (2012b): *Accuracy and validity of stitching sectional cone beam computed tomographic images*. J Craniofac Surg 23: 1071-1076.

Kimura K (1976): *Growth of the second metacarpal according to chronological age and skeletal maturation*. Anat Rec 184: 147-157.

King DG, Steventon DM, O'Sullivan MP, Cook AM, Hornsby VP, Jefferson IG and King PR (1994): *Reproducibility of bone ages when performed by radiology registrars: an audit of Tanner and Whitehouse II versus Greulich and Pyle methods*. Br J Radiol 67: 848-851.

Kjellberg H, Ekestubbe A, Kiliaridis S and Thilander B (1994): *Condylar height on panoramic radiographs. A methodologic study with a clinical application*. Acta Odontol Scand 52: 43-50.

Kjellberg H, Fasth A, Kiliaridis S, Wenneberg B and Thilander B (1995): *Craniofacial structure in children with juvenile chronic arthritis (JCA) compared with healthy-children with ideal or postnormal occlusion*. Am J Orthod Dentofacial Orthop 107: 67-78.

Klein MO, Grotz KA, Manefeld B, Kann PH and Al-Nawas B (2008): *Ultrasound transmission velocity for noninvasive evaluation of jaw bone quality in vivo before dental implantation*. Ultrasound Med Biol 34: 1966-1971.

Klimo P, Jr., Rao G and Brockmeyer D (2007): *Congenital anomalies of the cervical spine*. Neurosurg Clin N Am 18: 463-478.

Kobayashi K, Shimoda S, Nakagawa Y and Yamamoto A (2004): *Accuracy in measurement of distance using limited cone-beam computerized tomography*. Int J Oral Maxillofac Implants 19: 228-231.

Kojo K (2013): *Occupational cosmic radiation exposure and cancer in airline cabin crew.* Academic dissertation. University of Tampere, Tampere.

Koletsi DD and Halazonetis DJ (2010): *Cervical vertebrae anomalies in orthodontic patients: a growth-based superimpositional approach*. Eur J Orthod 32: 36-42.

Koletsi DD, Pandis N, Polychronopoulou A and Eliades T (2012): *Does published orthodontic research account for clustering effects during statistical data analysis?* Eur J Orthod 34: 287-292.

Kreiborg S, Bakke M, Kirkeby S, Michler L, Vedtofte P, Seidler B and Moller E (1990): *Facial growth and oral function in a case of juvenile rheumatoid arthritis during an 8-year period*. Eur J Orthod 12: 119-134.

Kuhn G, Schultz M, Muller R and Ruhli FJ (2007): *Diagnostic value of micro-CT in comparison with histology in the qualitative assessment of historical human postcranial bone pathologies*. Homo 58: 97-115.

Kumar VV, Sagheb K, Klein MO, Al-Nawas B, Kann PH and Kammerer PW (2012): *Relation between bone quality values from ultrasound transmission velocity and implant stability parameters--an ex vivo study*. Clin Oral Implants Res 23: 975-980.

Kuseler A, Pedersen TK, Gelineck J and Herlin T (2005): *A 2 year followup study of enhanced magnetic resonance imaging and clinical examination of the temporomandibular joint in children with juvenile idiopathic arthritis*. J Rheumat 32: 162-169.

Kwong JC, Palomo JM, Landers MA, Figueroa A and Hans MG (2008): *Image quality produced by different cone-beam computed tomography settings*. Am J Orthod Dentofacial Orthop 133: 317-327.

Kylämarkula S and Huggare J (1985): *Head posture and the morphology of the first cervical vertebra*. Eur J Orthod 7: 151-156.

Lamparski D (1975): *Skeletal age assessment utilizing cervical vertebrae*. Am J Orthod 67: 458-459.

Landis JR and Koch GG (1977): *The measurement of observer agreement for categorical data*. Biometrics 33: 159-174.

Lanfranchi M (2012): *Strahlenschutz und Strahlenrisiko in der Computertomographie: Strahlendosis und Bildqualität der Computertomographie des Gesichtsschädels mit einem „low-dose" Protokoll für Patienten des Hals-Nase-Ohren Fachbereiches.* Master Thesis. University of Zurich, Zurich

Larheim TA and Haanaes HR (1981): *Micrognathia, temporomandibular joint changes and dental occlusion in juvenile rheumatoid arthritis of adolescents and adults*. Scand J Dent Res 89: 329-338.

Lascala CA, Panella J and Marques MM (2004): *Analysis of the accuracy of linear measurements obtained by cone beam computed tomography (CBCT-NewTom)*. Dentomaxillofac Radiol 33: 291-294.

Lee EY, Sundel RP, Kim S, Zurakowski D and Kleinman PK (2008): *MRI findings of juvenile psoriatic arthritis*. Skel Radiol 37: 987-996.

Lee M-J, Kim S, Lee S-A, Song H-T, Huh Y-M, Kim D-H, Han SH and Suh J-S (2007): *Overcoming artifacts from metallic orthopedic implants at high-field-strength MR imaging and multi-detector CT*. Radiographics 27: 791-803.

Leung CC, Palomo L, Griffith R and Hans MG (2010): *Accuracy and reliability of cone-beam computed tomography for measuring alveolar bone height and detecting bony dehiscences and fenestrations*. Am J Orthod Dentofacial Orthop 137: S109-119.

Lewis AB and Garn SM (1960): *The relationship between tooth formation and other maturational factors*. Angle Orthod 30: 70-77.

Liang X, Jacobs R, Hassan B, Li L, Pauwels R, Corpas L, Souza PC, Martens W, Shahbazian M, Alonso A and Lambrichts I (2010a): *A comparative evaluation of Cone Beam Computed Tomography (CBCT) and Multi-Slice CT (MSCT) Part I. On subjective image quality*. Eur J Radiol 75: 265-269.

Liang X, Lambrichts I, Sun Y, Denis K, Hassan B, Li L, Pauwels R and Jacobs R (2010b): *A comparative evaluation of Cone Beam Computed Tomography (CBCT) and Multi-Slice CT (MSCT). Part II: On 3D model accuracy*. Eur J Radiol 75: 270-274.

Librizzi ZT, Tadinada AS, Valiyaparambil JV, Lurie AG and Mallya SM (2011): *Cone-beam computed tomography to detect erosions of the temporomandibular joint: Effect of field of view and voxel size on diagnostic efficacy and effective dose*. Am J Orthod Dentofacial Orthop 140: e25-30.

Liedke GS, da Silveira HE, da Silveira HL, Dutra V and de Figueiredo JA (2009): *Influence of voxel size in the diagnostic ability of cone beam tomography to evaluate simulated external root resorption*. J Endod 35: 233-235.

Loubele M, Guerrero ME, Jacobs R, Suetens P and van Steenberghe D (2007): *A comparison of jaw dimensional and quality assessments of bone characteristics with cone-beam CT, spiral tomography, and multi-slice spiral CT*. Int J Oral Maxillofac Implants 22: 446-454.

Loubele M, Maes F, Jacobs R, van Steenberghe D, White SC and Suetens P (2008a): *Comparative study of image quality for MSCT and CBCT scanners for dentomaxillofacial radiology applications*. Radiat Prot Dosim 129: 222-226.

Loubele M, Maes F, Schutyser F, Marchal G, Jacobs R and Suetens P (2006): *Assessment of bone segmentation quality of cone-beam CT versus multislice spiral CT: a pilot study*. Oral Surg Oral Med Oral Pathol Oral Radiol Endod 102: 225-234.

Loubele M, Van Assche N, Carpentier K, Maes F, Jacobs R, van Steenberghe D and Suetens P (2008b): *Comparative localized linear accuracy of small-field cone-beam CT and multislice CT for alveolar bone measurements*. Oral Surg Oral Med Oral Pathol Oral Radiol Endod 105: 512-518.

Ludlow JB, Davies-Ludlow LE, Brooks SL and Howerton WB (2006): *Dosimetry of 3 CBCT devices for oral and maxillofacial radiology: CB Mercuray, NewTom 3G and i-CAT*. Dentomaxillofac Radiol 35: 219-226.

Magarelli N, Milano G, Baudi P, Santagada DA, Righi P, Spina V, Leone A, Amelia R, Fabbriciani C and Bonomo L (2012): *Comparison between 2D and 3D computed tomography evaluation of glenoid bone defect in unilateral anterior gleno-humeral instability*. Radiol Med 117: 102-111.

Magnusson T, Egermark I and Carlsson GE (2000): *A longitudinal epidemiologic study of signs and symptoms of temporomandibular disorders from 15 to 35 years of age*. J Orofac Pain 14: 310-319.

Mah P, Reeves TE and McDavid WD (2010): *Deriving Hounsfield units using grey levels in cone beam computed tomography*. Dentomaxillofac Radiol 39: 323-335.

Mairs S, Swift B and Rutty GN (2004): *Detergent: an alternative approach to traditional bone cleaning methods for forensic practice*. Am J Forensic Med Pathol 25: 276-284.

Maloul A, Fialkov J and Whyne C (2011): *The impact of voxel size-based inaccuracies on the mechanical behavior of thin bone structures*. Ann Biomed Eng 39: 1092-1100.

Maret D, Molinier F, Braga J, Peters OA, Telmon N, Treil J, Inglese JM, Cossie A, Kahn JL and Sixou M (2010): *Accuracy of 3D Reconstructions Based on Cone Beam Computed Tomography*. J Dent Res 89: 1465-1469.

Maret D, Telmon N, Peters OA, Lepage B, Treil J, Inglese JM, Peyre A, Kahn JL and Sixou M (2012a): *Effect of voxel size on accuracy of 3D reconstructions with cone beam CT*. Dentomaxillofac Radiol [Epub ahead of print] DOI: 10.1259/dmfr/81804525.

Maret D, Telmon N, Peters OA, Lepage B, Treil J, Inglese JM, Peyre A, Kahn JL and Sixou M (2012b): *Effect of voxel size on the accuracy of 3D reconstructions with cone beam CT*. Dentomaxillofac Radiol 41: 649-655.

Massengill AD, Huynh SL and Harris JH, Jr. (1997): *C2-3 facet joint "pseudo-fusion": anatomic basis of a normal variant*. Skeletal Radiol 26: 27-30.

McAfee PC, Bohlman HH, Han JS and Salvagno RT (1986): *Comparison of nuclear magnetic resonance imaging and computed tomography in the diagnosis of upper cervical spinal cord compression*. Spine (Phila Pa 1976) 11: 295-304.

McDavid WD, Tronje G, Welander U and Morris CR (1981): *Effects of errors in film speed and beam alignment on the image layer in rotational panoramic radiography*. Oral Surg Oral Med Oral Pathol Oral Radiol Endod 52: 561-564.

McGibbon CA, Bencardino J, Yeh ED and Palmer WE (2003): *Accuracy of cartilage and subchondral bone spatial thickness distribution from MRI*. J Magn Reson Imaging 17: 703-715.

McGibbon CA, Dupuy DE, Palmer WE and Krebs DE (1998): *Cartilage and subchondral bone thickness distribution with MR imaging*. Acad Radiol 5: 20-25.

McRae DL (1960): *The Significance of Abnormalities of the Cervical Spine - Caldwell Lecture, 1959*. Amer J Roentgenol Ra 84: 3.

Melo SL, Bortoluzzi EA, Abreu M, Jr., Correa LR and Correa M (2010): *Diagnostic ability of a cone-beam computed tomography scan to assess longitudinal root fractures in prosthetically treated teeth*. J Endod 36: 1879-1882.

Melsen B and Allais D (2005): *Factors of importance for the development of dehiscences during labial movement of mandibular incisors: a retrospective study of adult orthodontic patients*. Am J Orthod Dentofacial Orthop 127: 552-561.

Miller RW (1995): *Special susceptibility of the child to certain radiation-induced cancers*. Environ Health Perspect 103 Suppl 6: 41-44.

Mischkowski RA, Pulsfort R, Ritter L, Neugebauer J, Brochhagen HG, Keeve E and Zoller JE (2007): *Geometric accuracy of a newly developed cone-beam device for maxillofacial imaging*. Oral Surg Oral Med Oral Pathol Oral Radiol Endod 104: 551-559.

Mislik B, Hanggi MP, Signorelli L, Peltomaki TA and Patcas R (2013): *Pharyngeal airway dimensions: a cephalometric, growth-study-based analysis of physiological variations in children aged 6-17*. Eur J Orthod [Epub ahead of print] DOI: 10.1093/ejo/cjt068.

Mizutani R and Suzuki Y (2012): *X-ray microtomography in biology*. Micron 43: 104-115.

Moen K, Hellem S, Geitung JT and Skartveit L (2010): *A practical approach to interpretation of MRI of the temporomandibular joint*. Acta Radiol 51: 1021-1027.

Mozzo P, Procacci C, Tacconi A, Martini PT and Andreis IA (1998): *A new volumetric CT machine for dental imaging based on the cone-beam technique: preliminary results*. Eur Radiol 8: 1558-1564.

Mulder L, van Rietbergen B, Noordhoek NJ and Ito K (2012): *Determination of vertebral and femoral trabecular morphology and stiffness using a flat-panel C-arm-based CT approach*. Bone 50: 200-208.

Müller HP, Schaller N and Eger T (1999): *Ultrasonic determination of thickness of masticatory mucosa: a methodologic study*. Oral Surg Oral Med Oral Pathol Oral Radiol Endod 88: 248-253.

Müller L, Kellenberger CJ, Cannizzaro E, Ettlin D, Schraner T, Bolt IB, Peltomäki T and Saurenmann RK (2009): *Early diagnosis of temporomandibular joint involvement in juvenile idiopathic arthritis: a pilot study comparing clinical examination and ultrasound to magnetic resonance imaging*. Rheumatology 48: 680-685.

Myga-Porosilo J, Skrzelewski S, Sraga W, Borowiak H, Jackowska Z and Kluczewska E (2011): *CT Imaging of facial trauma. Role of different types of reconstruction. Part I - bones*. Pol J Radiol 76: 41-51.

Nackaerts O, Maes F, Yan H, Couto Souza P, Pauwels R and Jacobs R (2011): *Analysis of intensity variability in multislice and cone beam computed tomography*. Clin Oral Implants Res 22: 873-879.

Nahm KY, Kang JH, Moon SC, Choi YS, Kook YA, Kim SH and Huang J (2012): *Alveolar bone loss around incisors in Class I bidentoalveolar protrusion patients: a retrospective three-dimensional cone beam CT study*. Dentomaxillofac Radiol 41: 481-488.

Naitoh M, Nakahara K, Suenaga Y, Gotoh K, Kondo S and Ariji E (2010): *Comparison between cone-beam and multislice computed tomography depicting mandibular neurovascular canal structures*. Oral Surg Oral Med Oral Pathol Oral Radiol Endod 109: e25-31.

Naranjo V, Llorens R, Alcaniz M and Lopez-Mir F (2011): *Metal artifact reduction in dental CT images using polar mathematical morphology*. Comput Methods Programs Biomed 102: 64-74.

Nestman TS, Marshall SD, Qian F, Holton N, Franciscus RG and Southard TE (2011): *Cervical vertebrae maturation method morphologic criteria: poor reproducibility*. Am J Orthod Dentofacial Orthop 140: 182-188.

Neves FS, de Freitas DQ, Campos PS, de Almeida SM and Haiter-Neto F (2012): *In vitro comparison of cone beam computed tomography with different voxel sizes for detection of simulated external root resorption*. J Oral Sci 54: 219-225.

Ovsenik M, Volk J and Marolt MM (2013): *A 2D ultrasound evaluation of swallowing in children with unilateral posterior crossbite*. Eur J Orthod [Epub ahead of print] DOI: 10.1093/ejo/cjt028.

Ozer SY (2011): *Detection of vertical root fractures by using cone beam computed tomography with variable voxel sizes in an in vitro model*. J Endod 37: 75-79.

Palomo JM, Rao PS and Hans MG (2008): *Influence of CBCT exposure conditions on radiation dose*. Oral Surg Oral Med Oral Pathol Oral Radiol Endod 105: 773-782.

Palou ME, McQuade MJ and Rossmann JA (1987): *The use of ultrasound for the determination of periodontal bone morphology*. J Periodontol 58: 262-265.

Panmekiate S, Apinhasmit W and Petersson A (2012): *Effect of electric potential and current on mandibular linear measurements in cone beam CT*. Dentomaxillofac Radiol [Epub ahead of print] DOI: 10.1259/dmfr/51664704.

Park CH, Abramson ZR, Taba M, Jr., Jin Q, Chang J, Kreider JM, Goldstein SA and Giannobile WV (2007): *Three-dimensional micro-computed tomographic imaging of alveolar bone in experimental bone loss or repair*. J Periodontol 78: 273-281.

Park JH, Tai K, Sato Y, Nishiyama A and Shin JW (2012): *A case of Klippel-Feil and Turner syndromes*. Pediatr Dent 34: e35-39.

Parsa A, Ibrahim N, Hassan B, Motroni A, van der Stelt P and Wismeijer D (2013): *Influence of cone beam CT scanning parameters on grey value measurements at an implant site*. Dentomaxillofac Radiol [Epub ahead of print] DOI: 10.1259/dmfr/79884780.

Patcas R, Schmidlin PR, Zimmermann R and Gnoinski W (2012): *[Dental care in pregnancy. Ten questions and answers]*. Schweiz Monatsschr Zahnmed 122: 729-739.

Pauwels R, Nackaerts O, Bellaiche N, Stamatakis H, Tsiklakis K, Walker A, Bosmans H, Bogaerts R, Jacobs R and Horner K (2013): *Variability of dental cone beam CT grey values for density estimations*. Br J Radiol [Epub ahead of print] DOI: 10.1259/bjr.20120135.

Pauwels R, Stamatakis H, Bosmans H, Bogaerts R, Jacobs R, Horner K and Tsiklakis K (2011): *Quantification of metal artifacts on cone beam computed tomography images*. Clin Oral Implants Res [Epub ahead of print] DOI: 10.1111/j.1600-0501.2011.02382.x.

Pearce MS, Salotti JA, Little MP, McHugh K, Lee C, Kim KP, Howe NL, Ronckers CM, Rajaraman P, Sir Craft AW, Parker L and Berrington de Gonzalez A (2012): *Radiation exposure from CT scans in childhood and subsequent risk of leukaemia and brain tumours: a retrospective cohort study*. Lancet 380: 499-505.

Pedersen TK, Jensen JJ, Melsen B and Herlin T (2001): *Resorption of the temporomandibular condylar bone according to subtypes of juvenile chronic arthritis*. J Rheumat 28: 2109-2115.

Pedersen TK, Kuseler A, Gelineck J and Herlin T (2008): *A prospective study of magnetic resonance and radiographic imaging in relation to symptoms and clinical findings of the temporomandibular joint in children with juvenile idiopathic arthritis*. J Rheumat 35: 1668-1675.

Peh WC and Chan JH (2001): *Artifacts in musculoskeletal magnetic resonance imaging: identification and correction*. Skel Radiol 30: 179-191.

Pette GA, Norkin FJ, Ganeles J, Hardigan P, Lask E, Zfaz S and Parker W (2012): *Incidental findings from a retrospective study of 318 cone beam computed tomography consultation reports*. Int J Oral Maxillofac Implants 27: 595-603.

Phan CM, Matsuura M, Bauer JS, Dunn TC, Newitt D, Lochmueller EM, Eckstein F, Majumdar S and Link TM (2006): *Trabecular bone structure of the calcaneus: comparison of MR imaging at 3.0 and 1.5 T with micro-CT as the standard of reference*. Radiology 239: 488-496.

Pirttiniemi P, Peltomäki T, Müller L and Luder HU (2009): *Abnormal mandibular growth and the condylar cartilage*. Eur J Orthod 31: 1-11.

Ponder SN, Benavides E, Kapila S and Hatch NE (2013): *Quantification of external root resorption by low- vs high-resolution cone-beam computed tomography and periapical radiography: A volumetric and linear analysis*. Am J Orthod Dentofacial Orthop 143: 77-91.

Popat H, Drage N and Durning P (2008): *Mid-line clefts of the cervical vertebrae - an incidental finding arising from cone beam computed tomography of the dental patient*. Br Dent J 204: 303-306.

Popp AW, Windolf M, Senn C, Tami A, Richards RG, Brianza S and Schiuma D (2012): *Prediction of bone strength at the distal tibia by HR-pQCT and DXA*. Bone 50: 296-300.

Poul JH, Brown JE and Davies J (2008): *Retrospective study of the effectiveness of high-resolution ultrasound compared with sialography in the diagnosis of Sjogren's syndrome*. Dentomaxillofac Radiol 37: 392-397.

Price JB, Thaw KL, Tyndall DA, Ludlow JB and Padilla RJ (2012): *Incidental findings from cone beam computed tomography of the maxillofacial region: a descriptive retrospective study*. Clin Oral Implants Res 23: 1261-1268.

Raadsheer MC, Van Eijden TM, Van Spronsen PH, Van Ginkel FC, Kiliaridis S and Prahl-Andersen B (1994): *A comparison of human masseter muscle thickness measured by ultrasonography and magnetic resonance imaging*. Arch Oral Biol 39: 1079-1084.

Rajion ZA, Townsend GC, Netherway DJ, Anderson PJ, Yusof A, Hughes T, Shuaib IL, Halim AS, Samsudin AR and David DJ (2006): *A three-dimensional computed tomographic analysis of the cervical spine in unoperated infants with cleft lip and palate*. Cleft Palate Craniofac J 43: 513-518.

Reichert IL, Benjamin M, Gatehouse PD, Chappell KE, Holmes J, He T and Bydder GM (2004): *Magnetic resonance imaging of periosteum with ultrashort TE pulse sequences*. J Magn Reson Imaging 19: 99-107.

Renkema AM, Fudalej PS, Renkema A, Bronkhorst E and Katsaros C (2013a): *Gingival recessions and the change of inclination of mandibular incisors during orthodontic treatment*. Eur J Orthod 35: 249-255.

Renkema AM, Fudalej PS, Renkema AA, Abbas F, Bronkhorst E and Katsaros C (2013b): *Gingival labial recessions in orthodontically treated and untreated individuals: a case - control study*. J Clin Periodontol 40: 631-637.

Robb RA, Sinak LJ, Hoffman EA, Kinsey JH, Harris LD and Ritman EL (1982): *Dynamic volume imaging of moving organs*. J Med Syst 6: 539-554.

Rogers SA, Drage N and Durning P (2011): *Incidental findings arising with cone beam computed tomography imaging of the orthodontic patient*. Angle Orthod 81: 350-355.

Ronchezel MV, Hilario MOE, Goldenberg J, Lederman HM, Faltin K, Deazevedo MF and Naspitz CK (1995): *Temporomandibular-Joint and Mandibular Growth Alterations in Patients with Juvenile Rheumatoid-Arthritis*. J Rheumatol 22: 1956-1961.

Ronning O, Barnes SAR, Pearson MH and Pledger DM (1994): *Juvenile Chronic Arthritis - a Cephalometric Analysis of the Facial Skeleton*. Eur J Orthod 16: 53-62.

Ross RB and Lindsay WK (1965): *The cervical vertebrae as a factor in etiology of cleft palate*. Cleft Palate J 36: 273-281.

Ruf S, Hansen K and Pancherz H (1998): *Does orthodontic proclination of lower incisors in children and adolescents cause gingival recession?* Am J Orthod Dentofacial Orthop 114: 100-106.

Ruhli FJ, Kuhn G, Evison R, Muller R and Schultz M (2007): *Diagnostic value of micro-CT in comparison with histology in the qualitative assessment of historical human skull bone pathologies*. Am J Phys Anthropol 133: 1099-1111.

Rupprecht RD, Horning GM, Nicoll BK and Cohen ME (2001): *Prevalence of dehiscences and fenestrations in modern American skulls*. J Periodontol 72: 722-729.

Sadatsafavi M, Moayyeri A, Bahrami H and Soltani A (2007): *The value of Bayes theorem in the interpretation of subjective diagnostic findings: what can we learn from agreement studies?* Med Decis Making 27: 735-743.

Salmon B and Le Denmat D (2012): *Intraoral ultrasonography: development of a specific high-frequency probe and clinical pilot study*. Clin Oral Investig 16: 643-649.

SAMW (2009): *Verwendung von Leichen und Leichenteilen in der medizinischen Forschung sowie Aus-, Weiter- und Fortbildung. Schweizerische Akademie der medizinischen Wissenschaften*. Schweiz Ärzteztg 90: 102-107.

Sandham A (1986): *Cervical Vertebral Anomalies in Cleft-Lip and Palate*. Cleft Palate J 23: 206-214.

Sandstrom B (1969): *Enzymatic maceration of delicate bone and small skeletons*. Acta Anat (Basel) 74: 487-488.

Santiago RC, de Miranda Costa LF, Vitral RW, Fraga MR, Bolognese AM and Maia LC (2012): *Cervical vertebral maturation as a biologic indicator of skeletal maturity*. Angle Orthod 82: 1123-1131.

Sarikaya S, Haydar B, Ciger S and Ariyurek M (2002): *Changes in alveolar bone thickness due to retraction of anterior teeth*. Am J Orthod Dentofacial Orthop 122: 15-26.

Sato K, Mito T and Mitani H (2001): *An accurate method of predicting mandibular growth potential based on bone maturity*. Am J Orthod Dentofacial Orthop 120: 286-293.

Savara BS and Tracy WE (1967): *Norms of size and annual increments for five anatomical measures of the mandible in boys from three to sixteen years of age*. Arch Oral Biol 12: 469-486.

Scarfe WC and Farman AG (2008): *What is cone-beam CT and how does it work?* Dent Clin North Am 52: 707-730.

Schmid-Schwap M, Drahanowsky W, Bristela M, Kundi M, Piehslinger E and Robinson S (2009): *Diagnosis of temporomandibular dysfunction syndrome--image quality at 1.5 and 3.0 Tesla magnetic resonance imaging*. Eur Radiol 19: 1239-1245.

Schulze R (2012): *Editorial*. Dentomaxillofac Radiol 41: 443.

Schulze R, Heil U, Gross D, Bruellmann DD, Dranischnikow E, Schwanecke U and Schoemer E (2011): *Artefacts in CBCT: a review*. Dentomaxillofac Radiol 40: 265-273.

Schulze R, Krummenauer F, Schalldach F and d'Hoedt B (2000): *Precision and accuracy of measurements in digital panoramic radiography*. Dentomaxillofac Radiol 29: 52-56.

Schulze RK, Berndt D and d'Hoedt B (2010): *On cone-beam computed tomography artifacts induced by titanium implants*. Clin Oral Implants Res 21: 100-107.

Serinelli S, Panetta V, Pasqualetti P and Marchetti D (2011): *Accuracy of three age determination X-ray methods on the left hand-wrist: a systematic review and meta-analysis*. Leg Med (Tokyo) 13: 120-133.

Serra MD, Duarte Gaviao MB and dos Santos Uchoa MN (2008): *The use of ultrasound in the investigation of the muscles of mastication*. Ultrasound Med Biol 34: 1875-1884.

Shannon CE (1998): *Communication in the presence of noise*. Proc IEEE 86: 447-457.

Sherrard JF, Rossouw PE, Benson BW, Carrillo R and Buschang PH (2010): *Accuracy and reliability of tooth and root lengths measured on cone-beam computed tomographs*. Am J Orthod Dentofacial Orthop 137: 100-108.

Shi H, Scarfe WC and Farman AG (2007): *Three-dimensional reconstruction of individual cervical vertebrae from cone-beam computed-tomography images*. Am J Orthod Dentofacial Orthop 131: 426-432.

Shim JJ, Heo G and Lagravere MO (2012): *Assessment of skeletal maturation based on cervical vertebrae in CBCT*. Int Orthod 10: 351-362.

Silva IM, Freitas DQ, Ambrosano GM, Boscolo FN and Almeida SM (2012): *Bone density: comparative evaluation of Hounsfield units in multislice and cone-beam computed tomography*. Braz Oral Res 26: 550-556.

Silverman PM, Kalender WA and Hazle JD (2001): *Common terminology for single and multislice helical CT*. AJR Am J Roentgenol 176: 1135-1136.

Solow B and Sandham A (2002): *Cranio-cervical posture: a factor in the development and function of the dentofacial structures*. Eur J Orthod 24: 447-456.

Sonnesen L (2010): *Associations between the Cervical Vertebral Column and Craniofacial Morphology*. Int J Dent [Epub ahead of print] DOI: 10.1155/2010/295728.

Sonnesen L and Kjaer I (2007a): *Cervical column morphology in patients with skeletal Class III malocclusion and mandibular overjet*. Am J Orthod Dentofacial Orthop 132: e7-12.

Sonnesen L and Kjaer I (2007b): *Cervical vertebral body fusions in patients with skeletal deep bite*. Eur J Orthod 29: 464-470.

Sonnesen L and Kjaer I (2008a): *Anomalies of the cervical vertebrae in patients with skeletal Class II malocclusion and horizontal maxillary overjet*. Am J Orthod Dentofacial Orthop 133: e15-20.

Sonnesen L and Kjaer I (2008b): *Cervical column morphology in patients with skeletal open bite*. Orthod Craniofac Res 11: 17-23.

Sonnesen L, Nolting D, Engel U and Kjaer I (2009): *Cervical vertebrae, cranial base, and mandibular retrognathia in human triploid fetuses*. Am J Med Genet 149A: 177-187.

Sonnesen L, Pallisgaard C and Kjaer I (2008a): *Cervical column morphology and craniofacial profiles in monozygotic twins*. Twin Res Hum Genet 11: 84-92.

Sonnesen L, Pedersen CE and Kjaer I (2007): *Cervical column morphology related to head posture, cranial base angle, and condylar malformation*. Eur J Orthod 29: 398-403.

Sonnesen L, Petri N, Kjaer I and Svanholt P (2008b): *Cervical column morphology in adult patients with obstructive sleep apnoea*. Eur J Orthod 30: 521-526.

Sparacia G, Bencivinni F, Banco A, Sarno C, Bartolotta TV and Lagalla R (2007): *Imaging processing for CT angiography of the cervicocranial arteries: evaluation of reformatting technique*. Radiol Med 112: 224-238.

Spin-Neto R, Gotfredsen E and Wenzel A (2013): *Impact of Voxel Size Variation on CBCT-Based Diagnostic Outcome in Dentistry: a Systematic Review*. J Digit Imaging 26: 813-820.

Spurny F (2001): *Radiation doses at high altitudes and during space flights*. Radiat Phys Chem 61: 301-307.

Steadman DW, DiAntonio LL, Wilson JJ, Sheridan KE and Tammariello SP (2006): *The effects of chemical and heat maceration techniques on the recovery of nuclear and mitochondrial DNA from bone*. J Forensic Sci 51: 11-17.

Steiner GG, Pearson JK and Ainamo J (1981): *Changes of the marginal periodontium as a result of labial tooth movement in monkeys*. J Period 52: 314-320.

Stoustrup P, Kristensen KD, Kuseler A, Gelineck J, Cattaneo PM, Pedersen TK and Herlin T (2008): *Reduced mandibular growth in experimental arthritis in the temporomandibular joint treated with intra-articular corticosteroid*. Eur J Orthod 30: 111-119.

Stoustrup P, Kuseler A, Kristensen KD, Herlin T and Pedersen TK (2011): *Orthopaedic splint treatment can reduce mandibular asymmetry caused by unilateral temporomandibular involvement in juvenile idiopathic arthritis*. Eur J Orthod 35: 191-198.

Studer SP, Allen EP, Rees TC and Kouba A (1997): *The thickness of masticatory mucosa in the human hard palate and tuberosity as potential donor sites for ridge augmentation procedures*. J Periodontol 68: 145-151.

Stuehmer C, Essig H, Bormann KH, Majdani O, Gellrich NC and Rucker M (2008): *Cone beam CT imaging of airgun injuries to the craniomaxillofacial region*. Int J Oral Maxillofac Surg 37: 903-906.

Sun Z, Smith T, Kortam S, Kim DG, Tee BC and Fields H (2011): *Effect of bone thickness on alveolar bone-height measurements from cone-beam computed tomography images*. Am J Orthod Dentofacial Orthop 139: e117-127.

Suomalainen A, Vehmas T, Kortesniemi M, Robinson S and Peltola J (2008): *Accuracy of linear measurements using dental cone beam and conventional multislice computed tomography*. Dentomaxillofac Radiol 37: 10-17.

Sur J, Seki K, Koizumi H, Nakajima K and Okano T (2010): *Effects of tube current on cone-beam computerized tomography image quality for presurgical implant planning in vitro*. Oral Surg Oral Med Oral Pathol Oral Radiol Endod 110: e29-33.

Szabo BT, Pataky L, Mikusi R, Fejerdy P and Dobo-Nagy C (2012): *Comparative evaluation of cone-beam CT equipment with micro-CT in the visualization of root canal system*. Ann Ist Super Sanita 48: 49-52.

Tai K, Park JH, Hayashi K, Yanagi Y, Asaumi JI, Iida S and Shin JW (2011): *Preliminary study evaluating the accuracy of MRI images on CBCT images in the field of orthodontics*. J Clin Pediatr Dent 36: 211-218.

Tanner JM, Whitehouse RH, Cameron N, Marshall WA, Healy MJR and Goldstein H (1983): *Assessment of Skeletal Maturity and Prediction of Adult Height (TW2 Method). Academic Press. London.*

Templeton AW and Brown MW (1964): *The transverse processes of the cervical vertebral ssegment. A correlation of oblique roentgenograms with skeletonized material*. Radiology 82: 912-915.

Tetradis S and Kantor ML (1999): *Prevalence of skeletal and dental anomalies and normal variants seen in cephalometric and other radiographs of orthodontic patients.* Am J Orthod Dentofacial Orthop 116: 572-577.

Timock AM, Cook V, McDonald T, Leo MC, Crowe J, Benninger BL and Covell DA, Jr. (2011): *Accuracy and reliability of buccal bone height and thickness measurements from cone-beam computed tomography imaging*. Am J Orthod Dentofacial Orthop 140: 734-744.

Tofani MI (1972): *Mandibular growth at puberty*. Am J Orthod 62: 176-195.

Tooth LR and Ottenbacher KJ (2004): *The kappa statistic in rehabilitation research: an examination*. Arch Phys Med Rehabil 85: 1371-1376.

Torres MG, Campos PS, Segundo NP, Navarro M and Crusoe-Rebello I (2012): *Accuracy of linear measurements in cone beam computed tomography with different voxel sizes*. Implant Dent 21: 150-155.

Tredwell SJ, Smith DF, Macleod PJ and Wood BJ (1982): *Cervical spine anomalies in fetal alcohol syndrome*. Spine (Phila Pa 1976) 7: 331-334.

Tsiklakis K, Syriopoulos K and Stamatakis HC (2004): *Radiographic examination of the temporomandibular joint using cone beam computed tomography*. Dentomaxillofac Radiol 33: 196-201.

Twilt M, Arends LR, Cate RT and van Suijlekom-Smit LW (2007): *Incidence of temporomandibular involvement in juvenile idiopathic arthritis*. Scand J Rheumatol 36: 184-188.

Twilt M, Mobers SM, Arends LR, ten Cate R and van Suijlekom-Smit L (2004): *Temporomandibular involvement in juvenile idiopathic arthritis*. J Rheumatol 31: 1418-1422.

Twilt M, Schulten AJ, Nicolaas P, Dulger A and van Suijlekom-Smit LW (2006): *Facioskeletal changes in children with juvenile idiopathic arthritis*. Ann Rheum Dis 65: 823-825.

Unger S, Blauth M and Schmoelz W (2010): *Effects of three different preservation methods on the mechanical properties of human and bovine cortical bone*. Bone 47: 1048-1053.

UNSCEAR (2000): *United Nations Scientific Committee on the Effects of Atomic Radiation Report to the General Assembly,with scientific annexes. Annex B: Exposures from natural radiation sources*. United Nations, Vienna.

UNSCEAR (2008): *United Nations Scientific Committee on the Effects of Atomic Radiation Report to the General Assembly,with scientific annexes. Annex B: Exposures of the public and workers from various sources of radiation*. United Nations, Vienna.

UNSCEAR (2010): *United Nations Scientific Committee on the Effects of Atomic Radiation, 2010 Report: "Summary of low-dose radiation effects on health"*. United Nations, Vienna.

Updegrave WJ (1971): *Visualizing the mandibular ramus in panoramic radiography*. Oral Surg Oral Med Oral Pathol 31: 422-429.

Valentin J (2007): *Managing patient dose in multi-detector computed tomography (MDCT). ICRP Publication 102*. Ann ICRP 37: 1-79.

van Daatselaar AN, van der Stelt PF and Weenen J (2004): *Effect of number of projections on image quality of local CT*. Dentomaxillofac Radiol 33: 361-369.

Van Elslande DC, Russett SJ, Major PW and Flores-Mir C (2008): *Mandibular asymmetry diagnosis with panoramic imaging*. Am J Orthod Dentofacial Orthop 134: 183-192.

Vandenberghe B, Luchsinger S, Hostens J, Dhoore E and Jacobs R (2012): *The influence of exposure parameters on jawbone model accuracy using cone beam CT and multislice CT*. Dentomaxillofac Radiol 41: 466-474.

Vastardis H and Evans CA (1996): *Evaluation of cervical spine abnormalities on cephalometric radiographs*. Am J Orthod Dentofacial Orthop 109: 581-588.

Vera C, De Kok IJ, Chen W, Reside G, Tyndall D and Cooper LF (2012a): *Evaluation of post-implant buccal bone resorption using cone beam computed tomography: a clinical pilot study*. Int J Oral Maxillofac Implants 27: 1249-1257.

Vera C, De Kok IJ, Reinhold D, Limpiphipatanakorn P, Yap AK, Tyndall D and Cooper LF (2012b): *Evaluation of buccal alveolar bone dimension of maxillary anterior and premolar teeth: a cone beam computed tomography investigation*. Int J Oral Maxillofac Implants 27: 1514-1519.

Visconti MA, Verner FS, Assis NM and Devito KL (2013): *Influence of maxillomandibular positioning in cone beam computed tomography for implant planning*. Int J Oral Maxillofac Surg 42: 880-886.

Volk J, Kadivec M, Music MM and Ovsenik M (2010): *Three-dimensional ultrasound diagnostics of tongue posture in children with unilateral posterior crossbite*. Am J Orthod Dentofacial Orthop 138: 608-612.

Wang S, Liu Y, Fang D and Shi S (2007): *The miniature pig: a useful large animal model for dental and orofacial research*. Oral Dis 13: 530-537.

Wang Y, He S, Guo Y, Wang S and Chen S (2013): *Accuracy of volumetric measurement of simulated root resorption lacunas based on cone beam computed tomography*. Orthod Craniofac Res 6: 169-176.

Wang YN, Lee K, Pai S and Ledoux WR (2011): *Histomorphometric comparison after fixation with formaldehyde or glyoxal*. Biotech Histochem 86: 359-365.

Wehrbein H, Bauer W and Diedrich P (1996): *Mandibular incisors, alveolar bone, and symphysis after orthodontic treatment. A retrospective study*. Am J Orthod Dentofacial Orthop 110: 239-246.

Weiss JE and Ilowite NT (2005): *Juvenile idiopathic arthritis*. Pediatr Clin North Am 52: 413-442.

Weiss PF, Arabshahi B, Johnson A, Bilaniuk LT, Zarnow D, Cahill AM, Feudtner C and Cron RQ (2008): *High prevalence of temporomandibular joint arthritis at disease onset in children with juvenile idiopathic arthritis, as detected by magnetic resonance imaging but not by ultrasound*. Arthritis Rheum 58: 1189-1196.

Wennstrom JL (1996): *Mucogingival considerations in orthodontic treatment*. Semin Orthod 2: 46-54.

Wennstrom JL, Lindhe J, Sinclair F and Thilander B (1987): *Some periodontal tissue reactions to orthodontic tooth movement in monkeys*. J Clin Period 14: 121-129.

Wenzel A, Haiter-Neto F, Frydenberg M and Kirkevang L-L (2009): *Variable-resolution cone-beam computerized tomography with enhancement filtration compared with intraoral photostimulable phosphor radiography in detection of transverse root fractures in an in vitro model*. Oral Surg Oral Med Oral Pathol Oral Radiol Endod 108: 939-945.

Wongpakaran N, Wongpakaran T, Wedding D and Gwet KL (2013): *A comparison of Cohen's Kappa and Gwet's AC1 when calculating inter-rater reliability coefficients: a study conducted with personality disorder samples*. BMC Med Res Methodol 13: 61.

Wood R, Sun Z, Chaudhry J, Tee BC, Kim D-G, Leblebicioglu B and England G (2013): *Factors affecting the accuracy of buccal alveolar bone height measurements from cone-beam computed tomography images*. Am J Orthod Dentofacial Orthop 143: 353-363.

Yagci A, Veli I, Uysal T, Ucar FI, Ozer T and Enhos S (2012): *Dehiscence and fenestration in skeletal Class I, II, and III malocclusions assessed with cone-beam computed tomography*. Angle Orthod 82: 67-74.

Yared KF, Zenobio EG and Pacheco W (2006): *Periodontal status of mandibular central incisors after orthodontic proclination in adults*. Am J Orthod Dentofacial Orthop 130: 6 e1-8.

Ye N, Jian F, Xue J, Wang S, Liao L, Huang W, Yang X, Zhou Y, Lai W, Li J and Wang J (2012): *Accuracy of in-vitro tooth volumetric measurements from cone-beam computed tomography*. Am J Orthod Dentofacial Orthop 142: 879-887.

Yin L, Venkatesan S, Kalyanasundaram S and Qin QH (2010): *Influence of enzymatic maceration on the microstructure and microhardness of compact bone*. Biomed Mater 5: 15006.

Yoshimoto Y, Delongchamp R and Mabuchi K (1994): *In-utero exposed atomic bomb survivors: cancer risk update*. Lancet 344: 345-346.

Yu L, Vrieze TJ, Bruesewitz MR, Kofler JM, DeLone DR, Pallanch JF, Lindell EP and McCollough CH (2010): *Dose and image quality evaluation of a dedicated cone-beam CT system for high-contrast neurologic applications*. AJR Am J Roentgenol 194: 193-201.

Zain EH and Alsadhan RI (2012): *A comparative study of accuracy of detection of surface osseous changes in the temporomandibular joint using multidetector CT and cone beam CT*. Dentomaxillofac Radiol 41: 185-191.

Zhang LC, Tong B, Wang ZM, Sha Y, Zhang F, Lao Z and Zhang TY (2013): *A comparison of three MDCT post-processing protocols: preoperative assessment of the ossicular chain in otitis media*. Eur Arch Otorhinolaryngol [Epub ahead of print] DOI: 10.1007/s00405-013-2415-2.

Zhao XG, Lin J, Jiang JH, Wang Q and Ng SH (2012): *Validity and reliability of a method for assessment of cervical vertebral maturation*. Angle Orthod 82: 229-234.

14. Original publications

ORIGINAL ARTICLE CE AJO-DO

Accuracy of cone-beam computed tomography at different resolutions assessed on the bony covering of the mandibular anterior teeth

Raphael Patcas,[a] Lukas Müller,[a] Oliver Ullrich,[b] and Timo Peltomäki[c]
Zurich, Switzerland, and Tampere, Finland

Introduction: The aim of this study was to determine the accuracy of cone-beam computed tomography (CBCT) with different voxel resolutions. Measurements were made of the bony covering of the mandibular anterior teeth because this region is crucial in orthodontic treatment planning. **Methods:** CBCT data at 2 resolutions (0.125-mm and 0.4-mm voxels) were collected from 8 intact cadaver heads. The vertical position of the mucogingival junction was clinically assessed. After removal of the gingiva, vertical and horizontal bony measurements were taken, and the buccal alveolar bone margin was determined. Anatomic bony measures were compared with the CBCT measures, and the correlation of the mucogingival junction measures to the buccal alveolar bone margin measures was evaluated. **Results:** Bony measures obtained with CBCT were accurate and differed only slightly from the physical findings. The mean differences, ranging from −0.13 to +0.13 mm, were statistically not significant, but the limits of agreement showed discrepancies in the measurements as large as 2.10 mm, depending on measurement and resolution. Buccal alveolar bone margin measurements correlated with the mucogingival junction measurements ($P < 0.001$). On average, the mucogingival junction was 1.67 mm more apical than the buccal alveolar bone margin (CI 95%, 1.35-1.98 mm). **Conclusions:** CBCT renders anatomic measures reliably and is an appropriate tool for linear measurements. Presence of soft tissue as well as different voxel size affect the precision of the data. A customized resolution protocol must be chosen according to the accuracy needed. However, even the 0.125-mm voxel protocol does not depict the thin buccal alveolar bone covering reliably, and there is a risk of overestimating fenestrations and dehiscences. The mucogingival junction appears to follow the buccal alveolar bone margin in a parallel line. (Am J Orthod Dentofacial Orthop 2012;141:41-50)

Cone-beam computed tomography (CBCT) has been used in the craniofacial region since 1998,[1] and scientific contributions in orthodontics have been published since 2003.[2] This new technology is attractive because of its high performance, low cost, and reduced radiation dose compared with conventional computed tomography. These advantages have led to a clearer definition of clinical applications of CBCT in implantology, oral and maxillofacial surgery, and orthodontics. However, as with every new development, CBCT data should be validated for their accuracy. Although the need to ascertain CBCT accuracy is not controversial, its accuracy has not been satisfactorily verified.

The first studies of CBCT accuracy in the oral and maxillofacial region appeared in 2004,[3,4] and since then various attempts have been made to analyze the accuracy of these data based on the comparative measurements of physical objects.[5-22] Every study made to ascertain the accuracy encounters the problem of what model to use to depict the anatomic truth reliably. Physical models, dry skulls, and mandibles immersed in solutions are common approaches to overcome this problem. These methodologies, however, do not accurately reflect clinical applications. The lack of soft tissues has been acknowledged to be a serious limitation in these studies,[13,23] particularly since absence of soft tissues would likely facilitate the detection of bone surfaces.[15] Use of cadaver heads would partly overcome this methodologic shortcoming.[13]

[a]Senior lecturer, Clinic for Orthodontics and Pediatric Dentistry, Center of Dental Medicine, University of Zurich, Zurich, Switzerland.
[b]Director and professor, Institute of Anatomy, Faculty of Medicine, University of Zurich, Zurich, Switzerland.
[c]Head orthodontist, Dental and Oral Diseases Outpatient Clinic, Department of Ear and Oral Diseases, Tampere University Hospital, and Department of Otolaryngology, University of Tampere, Tampere, Finland.
The authors report no commercial, proprietary, or financial interest in the products or companies described in this article.
Reprint requests to: Raphael Patcas, Clinic for Orthodontics and Pediatric Dentistry, Center of Dental Medicine, University of Zurich, Plattenstrasse 11, 8032 Zurich, Switzerland; e-mail, raphael.patcas@zzm.uzh.ch.
Submitted, February 2011; revised and accepted, June 2011.
0889-5406/$36.00

doi:10.1016/j.ajodo.2011.06.034

An additional factor that could influence accuracy is the resolution of the obtained data volume. CBCT image data are acquired in digital format from a single 360° rotational scan. Image reconstruction from these projections is made by using an algorithm for volumetric tomography that renders the information into 3-dimensional images consisting of voxel elements.[24] The size of each voxel is determined by its height, width, and thickness. Therefore, a study evaluating the accuracy should preferably also contain a comparison of different voxel settings, since the results depend not only on the examined object, but also on the inherent qualities of the acquired data. This way, the influence of both aspects can be juxtaposed.

The mandibular anterior incisors play an essential role in orthodontic treatment planning because of their restricted anatomic leeway in the symphysis. Hence, the assessment of the bony covering is pivotal when planning any tooth movement of the mandibular incisors, since it has been demonstrated that excessive sagittal movements or tipping can result in significant recession of the gingival margin and in bony dehiscences.[25–31] Although some investigators found no association between orthodontic tooth movement and gingival recessions,[32–35] it is commonly agreed that an especially narrow symphysis is an etiologic factor in the development of fenestrations and dehiscences.[35,36] It is therefore important to investigate the possible limitations of CBCT data beyond the actual voxel sizes and to evaluate the clinical relevance of the obtained information about the bony covering.

The aims of this study were threefold: (1) to validate the accuracy of linear measurements of CBCT on intact cadaver heads, (2) to compare different voxel size settings and their impacts on the achieved accuracy, and (3) to examine the clinical relevance of the acquired data.

To validate the accuracy of the radiologic measures, the following statistical hypothesis was tested: there is no difference between the clinical and radiologic measurements.

MATERIAL AND METHODS

Eight intact human cadaver heads (5 women, 3 men; age range, 65-95 years) with complete canine-to-canine dentitions in the mandibular front were supplied by the Anatomical Institute of the University of Zurich in accordance with state and federal regulations (voluntary body donation program on the basis of informed consent), the Convention on Human Rights and Medicine,[37] and the recommendation of the Swiss Academy of Medical Science.[38] Perfusion was carried out within 4 days after death with a fixation liquid consisting of the following formula: 2 parts alcohol (70%), 1 part glycerine, and 2% almudor (containing 8.10% formaldehyde, 10% glyoxal, and 3.70% glutaraldehyde). No specimen had an inflammation or recessions in the mandibular front.

Two CBCT scans (KaVo 3D eXam, KaVo Dental AG, Brugg, Switzerland) with different settings were performed on each head: high resolution (0.125-mm voxel) and low resolution (0.4-mm voxel) at 120 kV and 5mA. The radiologic measurements were made with a postprocessing software tool for DICOM data (eXam Vision software, Imaging Sciences International, Hatfield, Pa). All images were reconstructed by using multiplanar reformatting perpendicular to the curvature of the dentition, thereby enabling the depiction of every tooth in its buccolingual profile (Fig 1, *A* and *B*).

The radiologic measures were analogous to the clinical examination of the vertical (incisal edge-buccal alveolar bone margin) and horizontal bony measures, as shown in Figure 1, *C*. All measurements were taken twice by the same observer (R.P.), at least a week apart.

The clinical examination consisted of 3 measurements (Fig 1, *C*).

1. Soft-tissue measurement (incisal edge-mucogingival junction; IE-MGJ): the width of the attached gingiva was determined for all mandibular front teeth. The most basal point of the undulated mucogingival junction was used to evaluate the distance to the incisal edge (canine to canine, n = 48). The attached gingiva was stained with Schiller solution as described by Fasske and Morgenroth[39] (iodide pure: potassium-iodide: distilled water = 10:20:300) to facilitate locating the junction.
2. Vertical bony measurement (incisal edge-buccal alveolar bone margin; IE-ABM): after the gingiva was removed, the distance from the buccal alveolar bone margin to the incisal edge was determined for every tooth (canine to canine, n = 48). Since the bone margin is not a horizontal line but lunar shaped, the most apical point was chosen.
3. Horizontal bony measurement (H): a thin slat of the alveolar bone was removed with a scalpel. The thickness of the alveolar bone covering was measured at a distance of 15 mm (n = 48) from the incisal edge (incisal edge-horizontal). Occasionally, a second site was chosen at 18 mm (n = 13) from the incisal edge to increase the total measurements taken (n = 61).

Two electronic digital calipers were used for the clinical measures (accuracy of 0.01 mm): a customary caliper for measuring the length and the other especially designed for depth measurement. All clinical measures were repeated on different occasions and the mean value was used.

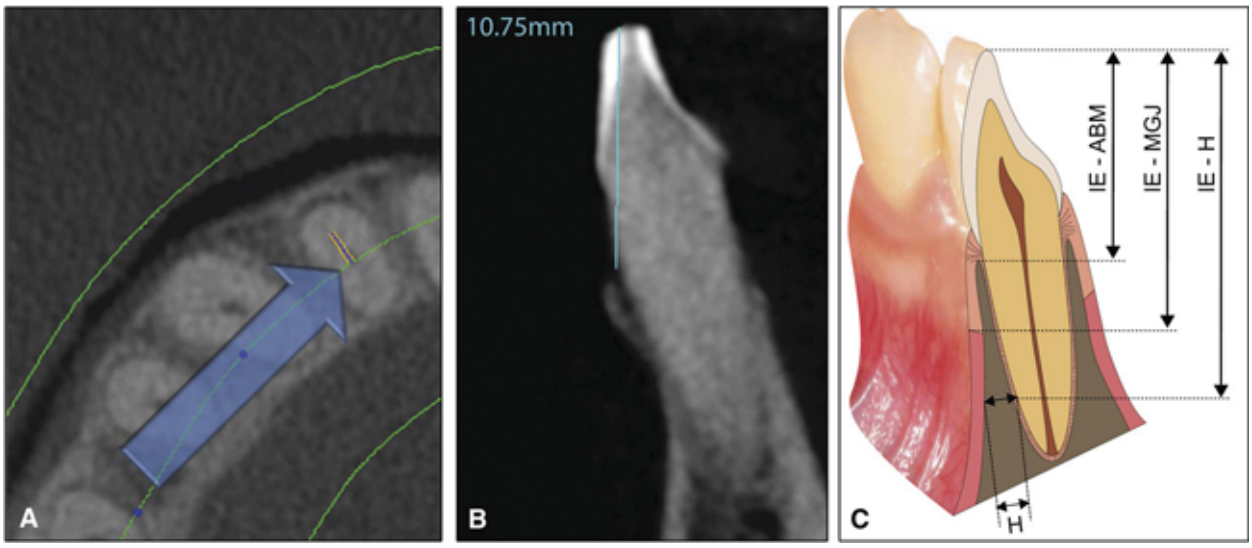

Fig 1. **A**, Axial rendering of the data showing the perpendicular curve of the reformatted slices along the *thin green middle line* (*blue arrow* points to the slice depicted in *B*; *bold green lines*, outer boundaries of the curve; *orange lines*, thickness of slice depicted in *B*. **B**, Representative reformatted image from which the radiologic measurements were taken (*light blue line*, incisal edge-buccal alveolar bone margin; IE-ABM). **C**, Graphic illustration of measurements taken: *IE*, Incisal edge; *ABM*, alveolar bone margin; *MGJ*, mucogingival junction; *H*, horizontal measurement. The measurements *IE-ABM* and *H* were taken clinically and radiologically, and the *IE-MGJ* measurement was taken only clinically.

Table I. Intraclass correlation coefficients (ICC) for all 4 protocols for intraobserver repeatability

ICC	*Low resolution*	*High resolution*
Vertical measurements	0.96	0.99
Horizontal measurements	0.90	0.95

Statistical analysis

Two standard statistical software packages (version 17; SPSS, Chicago, Ill; and version 11.4.1.0; MedCalc, Mariakerke, Belgium) were used for data analysis. To determine intraobserver reliability, the intraclass correlation coefficient for absolute agreement based on a 1-way random-effects analysis of variance (ANOVA) was calculated for the repeated radiologic measurements from the same observer for all 4 protocols (low and high resolutions, vertical and horizontal measures).

Descriptive statistics for the clinical measurements and for the differences between the radiologic and clinical measures for each category were computed separately. In addition, the 95% CI was calculated, and the absolute measurement error (AME) was determined according to the following equation:

$$AME = | \text{radiological measurement} - \text{clinical measurement} |$$

To disclose deterministic differences between both methods of measurement, a 1-sample Student t test was applied to the differences. Moreover, the Bland-Altman method[40–43] was applied, and the limits of agreement were identified. The Levene test was used to detect an increase of variability of the differences with the increase of the magnitude of the measurements. The Pearson correlation coefficient was computed to evaluate the association of soft-tissue measures to bony measures. In addition, the regression plot between soft-tissue measures to bony measures together with the 95% prediction interval was provided. The assumption of normality for the differences of soft to bony tissues was investigated by the Kolmogorov-Smirnov test. The results of the statistical analysis with P values smaller than 5% were considered to be statistically significant.

RESULTS

The intraclass correlation coefficient showed good repeatability of the radiologic measures. The values for all 4 protocols ranged between 0.90 and 0.99 as illustrated in Table I. The results of the descriptive statistics for the clinical measurements are provided in Table II.

The accuracy of the scans proved to be acceptable for both the high-resolution and low-resolution protocols. The absolute measurement errors for all 4 protocols are given in Table III. The descriptive statistics for the differences of the measurements and the 1-sample Student t test are shown in Table IV. The mean difference between

Table II. Descriptive statistics of clinical measurements

Clinical measurements	*Mean (mm)*	*Median (mm)*	*SD (mm)*	*95% CI (mm)*
Vertical (n = 48)	12.13	11.93	1.58	(11.67-12.58)
Horizontal (n = 61)	1.02	0.82	0.77	(0.82-1.22)
Distance ABM-MGJ (n = 48)	1.67	1.78	1.08	(1.36-1.98)

ABM-MGJ, Alveolar bone margin to mucogingival junction.

Table III. Absolute measurement error for all 4 protocols

Absolute errors	*Mean (mm)*	*Median (mm)*	*SD (mm)*	*99% CI (mm)*
Vertical, low resolution (n = 48)	0.70	0.53	0.84	(0.37-1.02)
Vertical, high resolution (n = 48)	0.34	0.21	0.50	(0.14-0.54)
Horizontal, low resolution (n = 61)	0.54	0.42	0.46	(0.38-0.69)
Horizontal, high resolution (n = 61)	0.37	0.25	0.43	(0.22-0.52)

Table IV. Descriptive statistics, 1-sample *t* test, and 95% CI values for differences and limits of agreement (positive numbers represent overestimations, and negative numbers represent underestimations of measurements with CBCT with respect to clinical measurements [Clin])

Differences CBCT-Clin	P *value*	*Mean difference (mm)*	*SD (mm)*	*Range (mm)*	*95% CI (mm)*	*Limits of agreement (mm)*
Vertical, low resolution (n = 48)	0.79	0.04	1.09	8.48	(−0.27-0.35)	(−2.1-2.2)
Vertical, high resolution (n = 48)	0.15	−0.13	0.59	3.91	(−0.30-0.05)	(−1.3-1.0)
Horizontal, low resolution (n = 61)	0.63	0.04	0.71	4.18	(−0.14-0.23)	(−1.4-1.4)
Horizontal, high resolution (n = 61)	0.08	0.13	0.55	3.62	(−0.02-0.28)	(−1.0-1.2)

the clinical and radiologic measures were for all protocols close to 0 and ranged between −0.13 and +0.13 mm; 0 was within the 95% CI bounds, confirming no systematic bias in all 4 radiologic readings. The 1-sample *t* test showed no significant differences between the physical and the radiologic measures; consequently, the statistical hypothesis could not be rejected.

To validate the different measurements, the differences between the radiologic and clinical measurements were plotted against the average as recommended by Bland and Altman[40] (Fig 2). The limits of agreement were defined as ±1.96*SD, and the 95% CI values for the limits of agreement were identified and are marked in the figures. The Levene test confirmed for the horizontal measurements an increase of the variability of the differences as the magnitude of the measurements increased ($P = 0.001$) (Fig 2, *C* and *D*). This indicates that for small horizontal measurements the differences were smaller than for large horizontal measurements.

The Pearson correlation coefficient (0.756, $P < 0.001$) between 2 distances (incisal edge-buccal alveolar bone margin and incisal edge-mucogingival junction; n = 48) proved to be moderate, but highly significant. The regression plot between both distances together with the 95% prediction interval is given in Figure 3. The distance from the alveolar bone margin to the mucogingival junction seemed to follow a nearly ideal normal distribution ($P = 0.194$) around the mean value of 1.67 mm (SD, 1.08; 95% CI, 1.35-1.98) (Fig 4).

DISCUSSION

The rationales behind this investigation were to overcome the deficiencies in the designs of previous studies and to revisit the poorly understood point of anatomic interest of the bony covering in the mandibular front. Yet when comparing our data with those of earlier studies, we were faced with another problem: most previous studies suffer from unsuitable statistical evaluations. Either the authors confined their results to mere descriptive statistics, or the data were assessed by means of correlation analysis. But comparing 2 methods of measurement is "a common abuse of correlation,"[40,44] since the quest is not to analyze the agreement but, rather, the dissimilarity of the 2 measurement methods, and ultimately assess whether the disagreement is small enough to deem the 2 methods interchangeable. Also, the often-assumed approach that considers the physical measures as the "gold standard" might be erroneous.[13] The Bland-Altman method was used to overcome these problems. By applying this method, we were able to

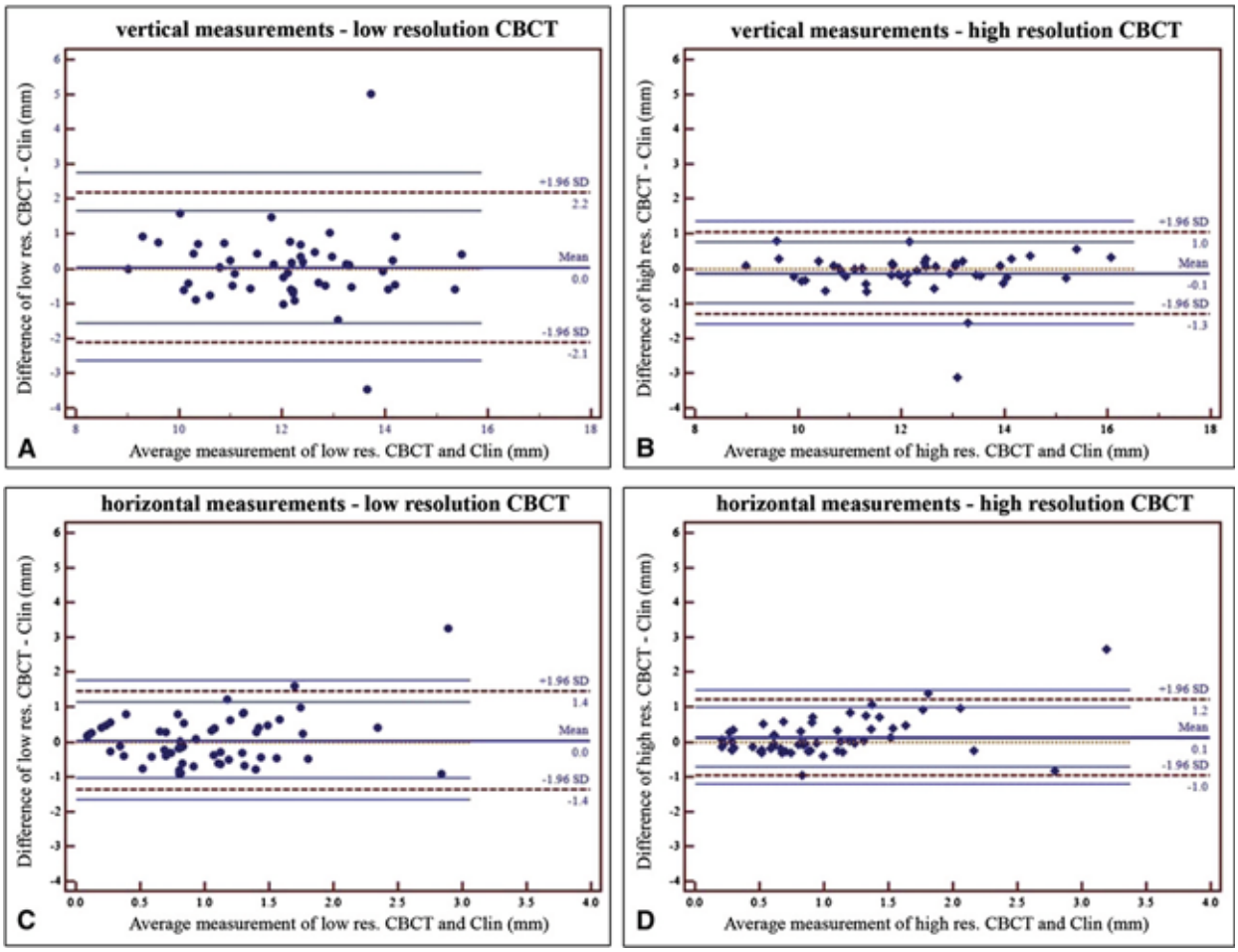

Fig 2. Bland-Altman plots: difference against the mean (*thick solid middle blue line*) of the clinical and radiologic measurements. The limits of agreement (*dashed brown lines*) and the 95% CI of the limits of agreement (*thin solid blue lines*) are shown. Vertical measurements of **A,** low resolution and **B**, high resolution; horizontal measurements of **C**, low resolution and **D**, high resolution. *Circles*, Measurement of the low-resolution protocol; *diamonds*, measurement of the high-resolution protocol; *dotted brown line*, 0.

show the obtained agreement for both vertical and horizontal measurements in the low-resolution and the high-resolution protocols. In the low-resolution protocol, the horizontal measures were somewhat more accurate. The obvious reason is that small absolute measurements were taken when measuring alveolar bone thickness. Taking measurements close to 0 causes the differences of the measurements to be smaller and creates a bias in the limits of agreement. Both the visual interpretation of the plots in Figure 2, *C* and *D*, and the Levene test show that the distribution of the differences is wider as the absolute measurements become larger. This crucial observation and the fact that the limits of agreement are greater than the average thickness of the alveolar bone indicate that both resolution protocols are not accurate enough to measure such delicate structures as the width of the alveolar bone covering.

Our results show that linear measurements of several millimeters made with CBCT of 0.4-mm and 0.125-mm voxel resolutions are accurate. Moreover, our results agree with those of Sun et al,[23] who reported improved accuracy when decreasing the voxel size. Yet, Damstra et al[15] evaluated the accuracy of CBCT on an identical KaVo 3D eXam apparatus at 2 resolutions (0.25-mm and 0.4-mm voxels). Their results showed mean absolute measurement errors of 0.05 mm (±0.04 mm) for the 0.25-mm voxel group and 0.07 mm (±0.05 mm) for the 0.4-mm voxel group. Since there was no tangible difference in accuracy, the authors concluded that the 0.4-mm voxel resolution was adequate for measurements of

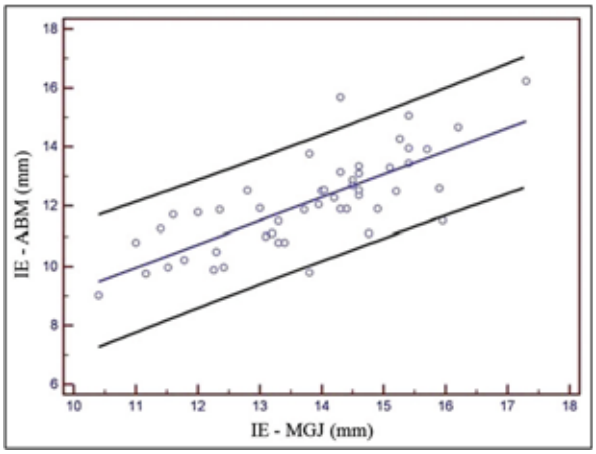

Fig 3. Regression plot for the 2 distances—incisal edge-mucogingival junction and incisal edge-buccal alveolar bone margin—with the 95% prediction interval (*blue line*, Regression line; *bold black lines*, 95% prediction interval; *circles*, clincal measurements).

craniofacial structures. Although there was a difference in methodology in our study (Damstra et al evaluated surface-rendered 3-dimensional models), ours seems to indicate similarly a resemblance in accuracy level for both resolutions in regard to the mean difference. Yet, in light of our findings, the mean difference is not the only aspect that must be evaluated. In the low-resolution protocol, the broader limits of agreement, the greater absolute measurement error, and the wider span of the measurement differences indicate that, although both resolutions are similarly accurate, the low-resolution protocol is less reliably so. In clinical practice, the question should therefore be reformulated; ie, the issue is not primarily how accurate the data should be, but how much inaccuracy is still tolerable in the worst case. Hence, in practice, the decision regarding which voxel size to use should be based on the limits of agreement rather than on the mean value. The finding that a difference between the clinical and radiologic measurements can be as large as 2 mm shows that the average alveolar bone thickness of 1 mm might be missed completely. The limits of agreement in our study give strong evidence to the results of Sun et al,[23] who reported that bone height loss can be overestimated by 1.5 to 2 mm in a 0.4-mm resolution protocol. The established limits of agreement also indicate that, with the voxel resolutions currently available, CBCT cannot be used to determine the bony limits of tooth movement accurately.

Finally, our radiologic measurements are less in accordance with the physical findings than those of Damstra et al,[15] as well as most studies on dry specimens reporting submillimeter accuracy, suggesting that soft tissues do affect the accuracy of bony measures.

Our study also has some noticeable limitations concerning the assessment of accuracy. First, even though intact cadaver heads are probably the closest means to obtain clinical truth, it is still unquestionably an approximation. The lack of noise created normally on radiologic data by the patient's movements probably improved the results, and the alcohol fixation of the specimens might also have had a slight impact on the data. The fixation solution contained low concentrations of glutaraldehyde and formaldehyde, which are known to modify certain tissue properties—eg, a slight muscle expansion and fatty tissue shrinkage[45] by extensive cross-linking[46,47]—and are known to alter periodontal fiber architecture.[48] The second constraint is obvious: using 1 CBCT apparatus does not necessarily reflect the accuracy of other devices. Yet, in 2 patients who had a gingiva flap Herzog et al[49] investigated the accuracy of CBCT measurements of alveolar bone covering with another CBCT device (3D Accuitomo, 0.125-mm voxel size). The similar results (mean difference, 0.092 mm; SD, 0.307 mm) obtained in their study corroborates the assumption that the aforementioned limitation of the use of cadaver heads is clinically negligible. Also, when using identical voxel sizes, the accuracy level of different CBCT devices appears hardly distinguishable.

Another limitation was that only 1 observer measured the data. The bias of only 1 investigator could probably give greater consistency in radiologic landmark identification than the varied interpretations of landmarks by several investigators. According to a meta-analysis on identification and reproducibility of radiologic (cephalometric) landmarks, however, the number of observers does not play a significant role in landmark identification and does not influence the magnitude of the measurement error.[50] On the other hand, one might argue that landmark identification in volumetric data could probably not be compared, since it is unquestionably a more demanding task with a greater likelihood of bias. But in a recent study, de Oliveira et al[51] demonstrated excellent interobserver reliability in CBCT landmark reproducibility in all 3 planes of space.

The alveolar bone covering can be thin. In our specimens, the thinnest bone covering measured was 0.14 mm, but neither did we find relevant dehiscences nor any fenestrations. However, in the radiologic data, there were some sites with absolutely no covering detectable (Fig 5, *B*). Although a thickness difference of 0.14 mm might not be statistically relevant, clinically, the absence or the evidence of bony covering is highly relevant. This important finding also has some ramifications on how to interpret CBCT scans. Previously, Sarikaya

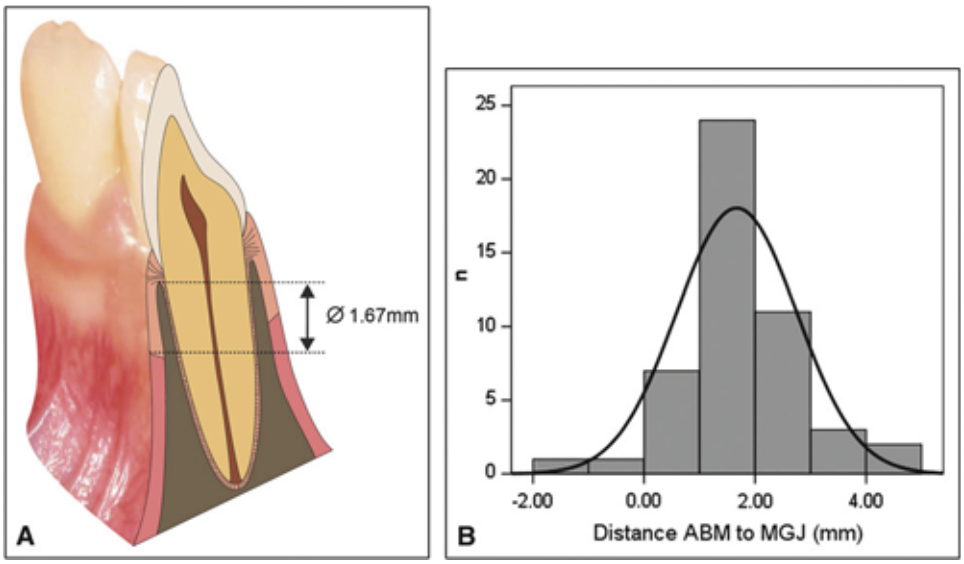

Fig 4. **A**, Graphic illustration of the distance between the alveolar bone margin and the mucogingival junction; **B**, distribution of the distance between the alveolar bone margin and the mucogingival junction. Mean value, 1.67 mm (*black curve*, Normal distribution).

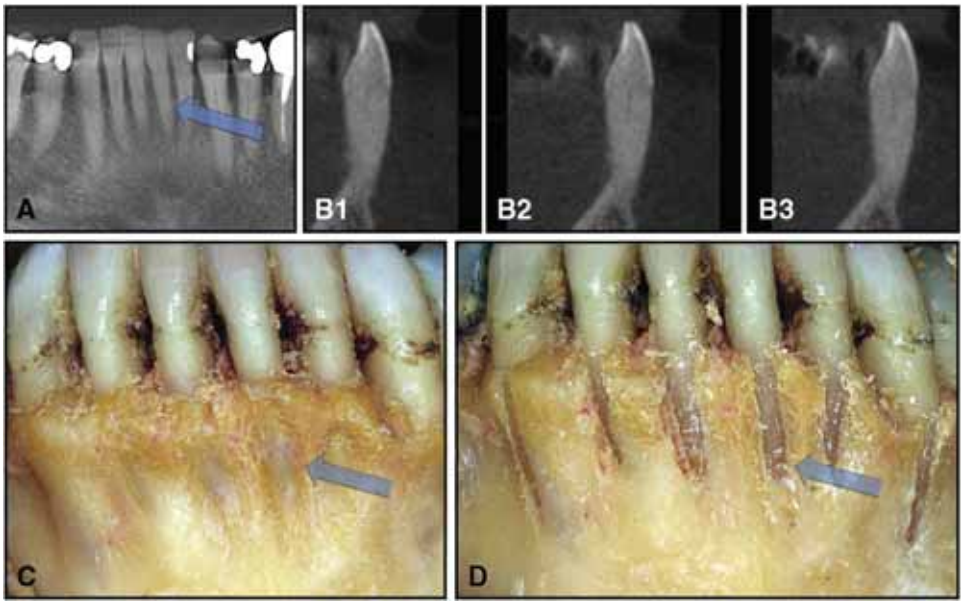

Fig 5. Radiologic data vs clinical findings: mandibular left first incisor as seen on the CBCT scan: **A**, reformatted orthopantomogram view; **B1-B3**, 3 slices in the sagittal view; **C**, clinical views after removing the gingiva; and **D**, after removing the alveolar bone covering. The *blue arrows* in *A*, *C*, and *D* point to the tooth depicted in B1-B3. Note that no bone covering is shown in the sagittal scans (*B1-B3*).

et al[27] examined the alveolar bone thickness on computed tomography scans. Based on their results, they postulated that dehiscences and fenestrations could be identified on computed tomography scans that would be otherwise undetected by cephalograms or clinical examinations. Our study, however, indicates that there is a genuine risk of assuming fenestrations and dehiscences on CBCT radiographs that do not exist clinically. This finding agrees with the observation of Leung et al,[20] who similarly reported that fenestrations are seen 3 times as often on

CBCT scans compared with direct skull examinations. However, they used dry skulls and measured on surface-rendered volumetric 3-dimensional reconstructions. Our study shows that false-positive detections of fenestrations also occur when soft tissue is present. In addition, we demonstrated that a considerably more reliable image display to evaluate CBCT data—sagittal views in multiplanar reformatted images—does not improve the ability to assess fenestrations reliably.

The findings of our study suggest that the undulated course of the mucogingival junction follows the alveolar bone margin in a parallel line. It is reasonable to assume that there is a topographic association between the mucogingival junction and the upper limit of the alveolar bone, since the attached gingiva is connected to the alveolar bone margin through periosteogingival fiber bundles.[52] Yet, this information has probably not been sufficiently appreciated. Most earlier studies that investigated the relationship between the attached gingiva and its bony support focused on the thickness of the keratinized soft tissue rather than on its height.[28,32,53] The height of the attached gingiva is difficult to interpret. Dorfman[29] noticed that the keratinized gingiva can vary in its apicocoronal length, and Ainamo and Talari[54] observed an increase in length related to age. In addition, Wennström[53] wrote that a more lingual position of the tooth results in increased gingival height, but he agreed with the finding of Ainamo and Talari that the mucogingival line is a stable anatomic landmark. It has been recognized that the height of the attached gingiva is influenced by various parameters such as gingival inflammation, dental tipping, and age, whereas the mucogingival junction remains unaffected. We concluded that the vertical position of the alveolar bone is therefore not connected to the height of the attached gingiva, but our results seem to imply that the mucogingival junction reflects somehow the location of the alveolar bone margin. This finding is probably limited to subjects with a healthy periodontium. An inflammation or a severe recession inevitably causes derangement of the fiber bundles and affects the described equilibrium between the attached gingiva and the alveolar bone. Yet, it appears that in healthy patients the mucogingival junction might be an additional aid to locate the alveolar bone margin appropriately.

CONCLUSIONS

1. Both CBCT resolutions provided accurate data and depicted the anatomic truth reliably. CBCT is therefore an appropriate tool for linear intraoral measurements.
2. Voxel size affects the precision of the measurements. The limits of agreement of the different resolution protocols should be considered when choosing the voxel size.
3. There is a genuine risk of overestimating fenestrations and dehiscences on CBCT radiographs, in both the high-resolution and low-resolution protocols. The limits of agreement indicate that an alveolar bone thickness of 1 mm might be missed completely, even with a high-resolution protocol.
4. The presence of soft tissue seems to have a curtailing effect on the accuracy of the CBCT data when determining bony landmarks.
5. The mucogingival junction might be helpful in localizing the alveolar bone margin.

We thank Dr Gordian Rutz for his assistance in designing Figures 1 and 3.

REFERENCES

1. Mozzo P, Procacci C, Tacconi A, Martini PT, Andreis IA. A new volumetric CT machine for dental imaging based on the cone-beam technique: preliminary results. Eur Radiol 1998;8:1558-64.
2. Baumrind S, Carlson S, Beers A, Curry S, Norris K, Boyd RL. Using three-dimensional imaging to assess treatment outcomes in orthodontics: a progress report from the University of the Pacific. Orthod Craniofac Res 2003;6(Suppl 1):132-42.
3. Kobayashi K, Shimoda S, Nakagawa Y, Yamamoto A. Accuracy in measurement of distance using limited cone-beam computerized tomography. Int J Oral Maxillofac Implants 2004;19:228-31.
4. Lascala CA, Panella J, Marques MM. Analysis of the accuracy of linear measurements obtained by cone beam computed tomography (CBCT-NewTom). Dentomaxillofac Radiol 2004;33:291-4.
5. Marmulla R, Wortche R, Muhling J, Hassfeld S. Geometric accuracy of the NewTom 9000 cone beam CT. Dentomaxillofac Radiol 2005;34:28-31.
6. Pinsky HM, Dyda S, Pinsky RW, Misch KA, Sarment DP. Accuracy of three-dimensional measurements using cone-beam CT. Dentomaxillofac Radiol 2006;35:410-6.
7. Kumar V, Ludlow JB, Mol A, Cevidanes L. Comparison of conventional and cone beam CT synthesized cephalograms. Dentomaxillofac Radiol 2007;36:263-9.
8. Loubele M, Guerrero ME, Jacobs R, Suetens P, van Steenberghe D. A comparison of jaw dimensional and quality assessments of bone characteristics with cone-beam CT, spiral tomography, and multi-slice spiral CT. Int J Oral Maxillofac Implants 2007;22:446-54.
9. Loubele M, Van Assche N, Carpentier K, Maes F, Jacobs R, van Steenberghe D, et al. Comparative localized linear accuracy of small-field cone-beam CT and multislice CT for alveolar bone measurements. Oral Surg Oral Med Oral Pathol Oral Radiol Endod 2008;105:512-8.
10. Ludlow JB, Laster WS, See M, Bailey LJ, Hershey HG. Accuracy of measurements of mandibular anatomy in cone beam computed tomography images. Oral Surg Oral Med Oral Pathol Oral Radiol Endod 2007;103:534-42.
11. Periago DR, Scarfe WC, Moshiri M, Scheetz JP, Silveira AM, Farman AG. Linear accuracy and reliability of cone beam CT

derived 3-dimensional images constructed using an orthodontic volumetric rendering program. Angle Orthod 2008;78:387-95.
12. Stratemann SA, Huang JC, Maki K, Miller AJ, Hatcher DC. Comparison of cone beam computed tomography imaging with physical measures. Dentomaxillofac Radiol 2008;37:80-93.
13. Suomalainen A, Vehmas T, Kortesniemi M, Robinson S, Peltola J. Accuracy of linear measurements using dental cone beam and conventional multislice computed tomography. Dentomaxillofac Radiol 2008;37:10-7.
14. Brown AA, Scarfe WC, Scheetz JP, Silveira AM, Farman AG. Linear accuracy of cone beam CT derived 3D images. Angle Orthod 2009; 79:150-7.
15. Damstra J, Fourie Z, Huddleston Slater JJ, Ren Y. Accuracy of linear measurements from cone-beam computed tomography-derived surface models of different voxel sizes. Am J Orthod Dentofacial Orthop 2010;137:16.e1-6; discussion 16-7.
16. Fourie Z, Damstra J, Gerrits PO, Ren Y. Evaluation of anthropometric accuracy and reliability using different three-dimensional scanning systems. Forensic Sci Int 2011;207:127-34.
17. Fourie Z, Damstra J, Gerrits PO, Ren Y. Accuracy and repeatability of anthropometric facial measurements using cone beam computed tomography. Cleft Palate Craniofac J 2011;48:623-30.
18. Fourie Z, Damstra J, Gerrits PO, Ren Y. Accuracy and reliability of facial soft tissue depth measurements using cone beam computer tomography. Forensic Sci Int 2010;199:9-14.
19. Howe RB. First molar radicular bone near the maxillary sinus: a comparison of CBCT analysis and gross anatomic dissection for small bony measurement. Oral Surg Oral Med Oral Pathol Oral Radiol Endod 2009;108:264-9.
20. Leung CC, Palomo L, Griffith R, Hans MG. Accuracy and reliability of cone-beam computed tomography for measuring alveolar bone height and detecting bony dehiscences and fenestrations. Am J Orthod Dentofacial Orthop 2010;137(Suppl):S109-19.
21. Mol A, Balasundaram A. In vitro cone beam computed tomography imaging of periodontal bone. Dentomaxillofac Radiol 2008;37: 319-24.
22. Vandenberghe B, Jacobs R, Yang J. Detection of periodontal bone loss using digital intraoral and cone beam computed tomography images: an in vitro assessment of bony and/or infrabony defects. Dentomaxillofac Radiol 2008;37:252-60.
23. Sun Z, Smith T, Kortam S, Kim DG, Tee BC, Fields H. Effect of bone thickness on alveolar bone-height measurements from cone-beam computed tomography images. Am J Orthod Dentofacial Orthop 2011;139:e117-27.
24. Cho PS, Johnson RH, Griffin TW. Cone-beam CT for radiotherapy applications. Phys Med Biol 1995;40:1863-83.
25. Steiner GG, Pearson JK, Ainamo J. Changes of the marginal periodontium as a result of labial tooth movement in monkeys. J Periodontol 1981;52:314-20.
26. Batenhorst KF, Bowers GM, Williams JE Jr. Tissue changes resulting from facial tipping and extrusion of incisors in monkeys. J Periodontol 1974;45:660-8.
27. Sarikaya S, Haydar B, Cier S, Ariyürek M. Changes in alveolar bone thickness due to retraction of anterior teeth. Am J Orthod Dentofacial Orthop 2002;122:15-26.
28. Yared KF, Zenobio EG, Pacheco W. Periodontal status of mandibular central incisors after orthodontic proclination in adults. Am J Orthod Dentofacial Orthop 2006;130:6.e1-8.
29. Dorfman HS. Mucogingival changes resulting from mandibular incisor tooth movement. Am J Orthod 1978;74:286-97.
30. Hollender L, Ronnerman A, Thilander B. Root resorption, marginal bone support and clinical crown length in orthodontically treated patients. Eur J Orthod 1980;2:197-205.
31. Wennstrom JL, Lindhe J, Sinclair F, Thilander B. Some periodontal tissue reactions to orthodontic tooth movement in monkeys. J Clin Periodontol 1987;14:121-9.
32. Melsen B, Allais D. Factors of importance for the development of dehiscences during labial movement of mandibular incisors: a retrospective study of adult orthodontic patients. Am J Orthod Dentofacial Orthop 2005;127:552-61.
33. Ruf S, Hansen K, Pancherz H. Does orthodontic proclination of lower incisors in children and adolescents cause gingival recession? Am J Orthod Dentofacial Orthop 1998;114:100-6.
34. Djeu G, Hayes C, Zawaideh S. Correlation between mandibular central incisor proclination and gingival recession during fixed appliance therapy. Angle Orthod 2002;72:238-45.
35. Årtun J, Krogstad O. Periodontal status of mandibular incisors following excessive proclination. A study in adults with surgically treated mandibular prognathism. Am J Orthod Dentofacial Orthop 1987;91:225-32.
36. Wehrbein H, Bauer W, Diedrich P. Mandibular incisors, alveolar bone, and symphysis after orthodontic treatment. A retrospective study. Am J Orthod Dentofacial Orthop 1996;110:239-46.
37. European Union. Additional protocol to the convention on human rights and biomedicine, on transplantation of organs and tissues of human origin ETS 186, Art. 16-18; 2002. Strasburg, France; 2002 Jan 24. Available at: http://conventions.coe.int/Treaty/en/Treaties/Html/186.htm.
38. Swiss Academy of Medical Science. Verwendung von Leichen und Leichenteilen in der medizinischen Forschung sowie Aus-, Weiter- und Fortbildung. Medical-ethical guidelines and recommendations; 2008; Basel, Switzerland. p1-11. Available at: http://www.samw.ch/de/Publikationen/Empfehlungen.html.
39. Fasske E, Morgenroth K. Vergleichende stomatoskopische und histochemische Untersuchungen am Zahnfleischrand des Menschen. Dtsch Zahnarztl Z 1958;13:562-7.
40. Bland JM, Altman DG. Statistical methods for assessing agreement between two methods of clinical measurement. Lancet 1986;1: 307-10.
41. Bland JM, Altman DG. Comparing methods of measurement: why plotting difference against standard method is misleading. Lancet 1995;346:1085-7.
42. Bland JM, Altman DG. Applying the right statistics: analyses of measurement studies. Ultrasound Obstet Gynecol 2003;22:85-93.
43. Bland JM, Altman DG. Measuring agreement in method comparison studies. Stat Methods Med Res 1999;8:135-60.
44. Ludbrook J. Statistics in biomedical laboratory and clinical science: applications, issues and pitfalls. Med Princ Pract 2008;17:1-13.
45. Docquier PL, Paul L, Cartiaux O, Lecouvet F, Dufrane D, Delloye C, et al. Formalin fixation could interfere with the clinical assessment of the tumor-free margin in tumor surgery: magnetic resonance imaging-based study. Oncology 2010;78:115-24.
46. Comert A, Kokat AM, Akkocaoglu M, Tekdemir I, Akca K, Cehreli MC. Fresh-frozen vs. embalmed bone: is it possible to use formalin-fixed human bone for biomechanical experiments on implants? Clin Oral Implants Res 2009;20:521-5.
47. Hansen P, Hassenkam T, Svensson RB, Aagaard P, Trappe T, Haraldsson BT, et al. Glutaraldehyde cross-linking of tendon—mechanical effects at the level of the tendon fascicle and fibril. Connect Tissue Res 2009;50:211-22.
48. Burn-Murdoch RA, Tyler DW. Physiological evidence that periodontal collagen in the rat exists as fibres prior to histological fixation. Arch Oral Biol 1981;26:995-9.
49. Herzog C, Herzog G, Peltomäki T. Accuracy of CBCT in determining labial alveolar bone level in the lower front area. Poster presented at: Proceedings of the 85th Congress of the European Orthodontic

Society; 2009 Jun 10-14; Helsinki, Finland. European Orthodontic Society; 2009. p. 77.
50. Trpkova B, Major P, Prasad N, Nebbe B. Cephalometric landmarks identification and reproducibility: a meta analysis. Am J Orthod Dentofacial Orthop 1997;112:165-70.
51. de Oliveira AEF, Cevidanes LHS, Phillips C, Motta A, Burke B, Tyndall D. Observer reliability of three-dimensional cephalometric landmark identification on cone-beam computerized tomography. Oral Surg Oral Med Oral Pathol Oral Radiol Endod 2009;107: 256-65.
52. Feneis H. Anatomy and physiology of the normal gingiva. Dtsch Zahnarztl Z 1952;7:467-76.
53. Wennström JL. Mucogingival considerations in orthodontic treatment. Semin Orthod 1996;2:46-54.
54. Ainamo J, Talari A. The increase with age of the width of attached gingiva. J Periodontal Res 1976;11:182-8.

Dentomaxillofacial Radiology (2012) 41, 637–644

http://dmfr.birjournals.org

RESEARCH

Accuracy of linear intraoral measurements using cone beam CT and multidetector CT: a tale of two CTs

R Patcas*[,1], G Markic[1], L Müller[1], O Ullrich[2], T Peltomäki[3], CJ Kellenberger[4] and CA Karlo[5]

[1]Clinic for Orthodontics and Pediatric Dentistry, University of Zurich, Zurich, Switzerland; [2]Institute of Anatomy, Faculty of Medicine, University of Zurich, Zurich, Switzerland; [3]Dental and Oral Diseases Outpatient Clinic, Tampere University Hospital, Tampere, Finland; [4]Department of Diagnostic Imaging, University Children's Hospital Zurich, Zurich, Switzerland; [5]Institute of Diagnostic and Interventional Radiology, University Hospital Zurich, Zurich, Switzerland

Objectives: The aim was to compare the accuracy of linear bone measurements of cone beam CT (CBCT) with multidetector CT (MDCT) and validate intraoral soft-tissue measurements in CBCT.
Methods: Comparable views of CBCT and MDCT were obtained from eight intact cadaveric heads. The anatomical positions of the gingival margin and the buccal alveolar bone ridge were determined. Image measurements (CBCT/MDCT) were performed upon multiplanar reformatted data sets and compared with the anatomical measurements; the number of non-assessable sites (NASs) was evaluated.
Results: Radiological measurements were accurate with a mean difference from anatomical measurements of 0.14 mm (CBCT) and 0.23 mm (MDCT). These differences were statistically not significant, but the limits of agreement for bone measurements were broader in MDCT (−1.35 mm; 1.82 mm) than in CBCT (−0.93 mm; 1.21 mm). The limits of agreement for soft-tissue measurements in CBCT were smaller (−0.77 mm; 1.07 mm), indicating a slightly higher accuracy. More NASs occurred in MDCT (14.5%) than in CBCT (8.3%).
Conclusions: CBCT is slightly more reliable for linear measurements than MDCT and less affected by metal artefacts. CBCT accuracy of linear intraoral soft-tissue measurements is similar to the accuracy of bone measurements.
Dentomaxillofacial Radiology (2012) **41,** 637–644. doi: 10.1259/dmfr/21152480

Keywords: computed tomography; CBCT; image quality; accuracy; soft tissue

Introduction

Cone beam CT (CBCT) was originally developed at the Mayo Clinic in 1982 for angiography procedures.[1] Since its introduction into craniofacial imaging, CBCT has proved to be a valuable diagnostic tool, primarily because of its lower radiation exposure than multidetector CT (MDCT),[2–6] but also for the short acquisition time, small physical size and moderate costs.[7–9] Today clinicians frequently request linear measurements performed upon cross-sectional image data. The question has therefore been raised whether CBCT may be capable of replacing MDCT for these needs in dentomaxillofacial imaging. So far, various efforts have been made to compare accuracy and image quality of CBCT and MDCT. However, an adequate understanding of the inherent differences in the properties of both types of image data is necessary to draw an appropriate comparison.

One particular advantage of CBCT data volume is its composition of isotropic voxels providing the same spatial resolution when reconstructed in multiplanar image reformations (MPRs).[9] In contrast to this, conventional MDCT data are composed of anisotropic voxels, as the coronal dimension (*i.e.* along the *z*-axis) is determined by several factors such as slice collimation and pitch (*i.e.* table travel per rotation divided by the collimation of the X-ray beam).[10] The spatial resolution in the *z*-axis of current MDCT scanners is limited to 0.4–0.6 mm, and therefore decreases when reconstructed from the original raw data. A further advantage is the comparably shorter acquisition time, which may help reduce motion artefacts due to patient movement. Most CBCT devices are capable of providing a minimal voxel

*Correspondence to: Dr Raphael Patcas, Clinic for Orthodontics and Pediatric Dentistry, Center of Dental Medicine, University of Zurich, Plattenstrasse 11, 8032 Zurich, Switzerland. E-mail: raphael.patcas@zzm.uzh.ch
Received 17 June 2011; revised 6 October 2011; accepted 13 December 2011

resolution between 0.07 mm and 0.25 mm, exceeding most commercially available high-resolution MDCT scanners.[9]

On the other hand, CBCT imaging presents a few drawbacks. The displayed greyscale values in CBCT are arbitrary, do not correspond to the Hounsfield unit (HU) scale used in MDCT, and reportedly differ from device to device.[11] Yet the ability to derive HUs from grey levels would open new opportunities for qualitative appraisals and comparative research. Mah et al[11] attempted to convert greyscale in CBCT into a ''rescaled HU'' with a proposed coefficient. However, Bryant and colleagues[12,13] argued that the greyscale value of CBCT varies linearly with the total mass in the slice. The greyscale value will therefore not only depend on the attenuation coefficient measurement, as described by the Hounsfield equation, but also on the total mass of the object. A further limitation of CBCT imaging is that structures outside the limited field of view (FOV) may produce density variability in the scanned volume and cause a decrease of image contrast.[14–16] Lastly, compared with MDCT, CBCT images are associated with increased noise and scatter radiation,[17] which result in less soft-tissue contrast resolution.[2,7,18] Therefore, it has been argued that CBCT is solely suitable for evaluating calcified structures such as bone or teeth, as CBCT provides images of highly contrasting structures well.[2,7,9]

Since 2004,[19,20] numerous attempts have been made to ascertain CBCT accuracy. The methods routinely applied are (1) the use of geometrical hardware phantoms; (2) the use of anthropomorphic phantoms; or (3) a comparison of a new imaging modality with an extant established imaging modality.[21] But validating a new method through comparison lacks a standardized reference, and phantom studies do not render clinical application. Furthermore, the lack of soft tissue in previous studies presents another limitation. Besides failing to reproduce clinical truth appropriately, absence of soft tissue means simply forfeiting the opportunity to measure it. Thus, our study aims to offer a fourth approach: the use of intact cadaveric heads, which may facilitate the depiction of the clinical truth authentically and may enable us to establish a reference value by performing direct soft-tissue measurements.

The aim of this study was (a) to compare the image quality and accuracy of CBCT and MDCT compared with anatomical reference standard measurements, and (b) to compare intraoral soft-tissue measurements with bone measurements upon CBCT data. To overcome the limitations of previous comparative studies, we sought to evaluate similar scan protocols for CBCT and MDCT and optimally approximate a clinical situation using intact cadaveric heads.

Materials and methods

Specimen

The sample consisted of eight unmitigated cadaveric heads (five females, three males; age range 65–95 years; mean age 81 years). Each specimen had a complete canine-to-canine dentition in the mandible. The specimens were obtained from a voluntary body donation programme and were supplied by the Anatomical Institute of the local university in accordance with State and Federal regulations (voluntary body donation programme on the basis of informed consent), the Convention on Human Rights and Medicine[22] and the recommendation of the National Academy of Medical Science.[23] The perfusion was carried out within 4 days after death with a fixation liquid consisting of 2 parts alcohol (70%), 1 part glycerine and 2% Almudor® (Isspest Control, Dietikon, Switzerland; containing 8.1% formaldehyde, 10% glyoxal and 3.7% glutaraldehyde).

Image acquisition

All MDCT and CBCT examinations were carried out prior to the removal of the gingiva. The MDCT scans were performed on a commercially available 40-detector row CT system (Brilliance CT 40, Philips Healthcare, Eindhoven, Netherlands) with the following scan parameters kept identical for all specimens: tube voltage, 120 kV; tube current–time product, 70 mAs; slice collimation, 20×0.625 mm; pitch, 0.68; reconstruction slice thickness, 0.67 mm; reconstruction increment, 0.33 mm; window level setting, 2000/500 HU; voxel size, 0.39 mm (x), 0.39 mm (y) and 0.67 mm (z).

All CBCT scans were performed on a commercially available CBCT scanner with an Amorphous Silicon Flat Panel (KaVo 3D eXam®; KaVo Dental GmbH, Bismarckring, Germany). The following scan parameters were kept identical during all CBCT examinations: tube voltage, 120 kV; tube current–time product, 37.07 mAs; reconstruction thickness, 0.4 mm; reconstruction increment, 0.4 mm; voxel size, 0.4 mm (x), 0.4 mm (y) and 0.4 mm (z).

Anatomical measurements (Figure 1a)

An electronic digital calliper was used for all anatomical measurements (accuracy 0.01 mm, DIN 862). All clinical measurements were repeated after 2 weeks and the mean values were used for further statistical analysis.

Soft tissue measurement: The distance between the incisal edge (IE) and the gingival margin (GM) of all lower front teeth (canine to canine, $n = 48$).

Bone measurement: The distance between the incisal edge and the alveolar bone ridge (ABR) of all lower front teeth (after gentle removal of the gingiva; canine to canine, $n = 48$).

The most apical point of the lunar-shaped devolution of the bone ridge was selected.

Image analysis/radiological measurements

The radiological measurements were performed using a dedicated, commercially available post-processing software tool for digital imaging and communications in medicine (DICOM) data review (Synedra View Personal,

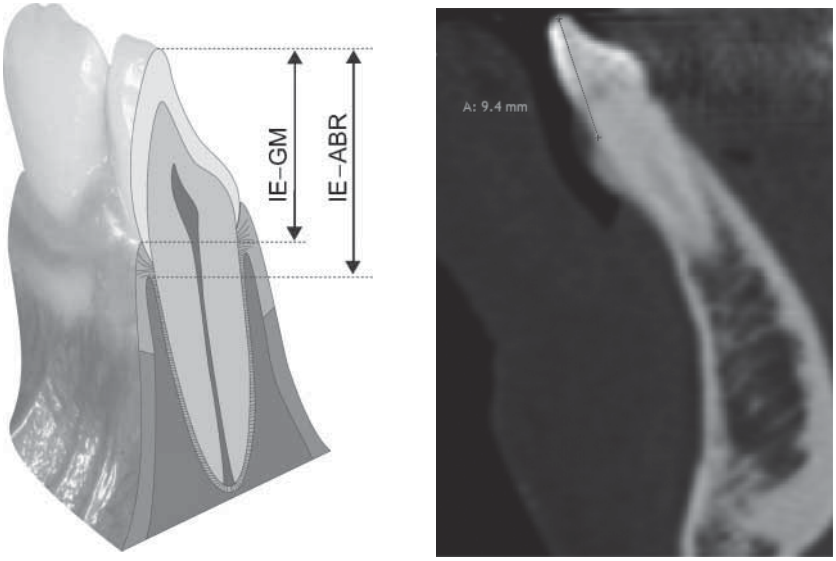

a b

Figure 1 (a) Measurements taken. IE, incisal edge; GM, gingival margin; ABR, alveolar bone ridge. (b) Representative multidetector CT scan, specimen 949

v. 1.0.12.1). All images were reconstructed using multiplanar reformatting perpendicular to the curvature of the dentition, making it possible to depict every tooth in its buccolingual profile (Figure 2). MDCT image data were derived from axial-source raw data. All images were magnified on the monitor to the field of interest, and an electronic calliper tool was used to measure the two distances corresponding to the anatomical measurements mentioned above (Figure 1b). The bone measurements (IE–ABR) were evaluated on the CBCT and MDCT scans, and the soft-tissue measurements (IE–GM) only on the CBCT scans. All radiological measurements were taken twice, at least 1 week apart, by the same observer. The monitor used to view the images and measure the distances was set at the highest resolution setting (1680×1050, pixel pitch 0.258 mm).

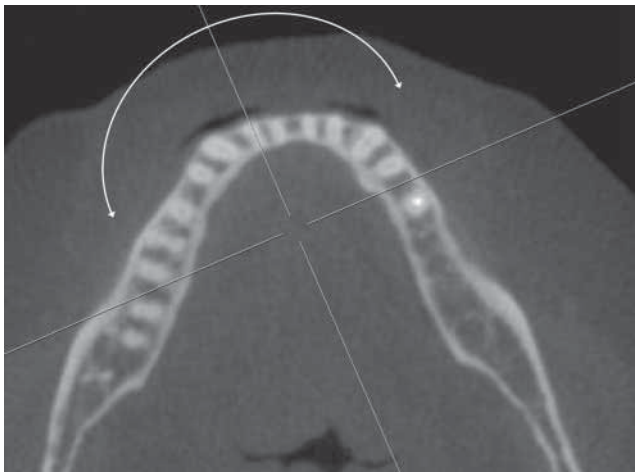

Figure 2 Orientation of the multiplanar image reformations perpendicular to the dentition, enabling one to view every assessed tooth in its buccolingual profile

Owing to metal-induced beam hardening artefacts, a total of seven sites were not assessable on MDCT and/or CBCT images. These sites were excluded from further data analyses. From the 41 remaining CBCT data sets, the gingiva could not be distinguished on 10 data sets owing to very tight lip contact, and these sites needed to be excluded from the soft-tissue measurements (IE–GM), and thus only clearly depicted gingiva were assessed ($n = 31$).

Statistical analysis

Two commercially available software packages (SPSS® v. 17; SPSS Inc., Chicago, IL, and MedCalc v. 11.4.1.0; MedCalc Software, Mariakerke, Belgium) were used for all statistical analyses. To determine intraobserver reliability, the intraclass correlation coefficient (ICC) for absolute agreement based on a one-way random effects analysis of variance was calculated for the radiological measurements. Descriptive statistics for the differences between radiological and anatomical measurements for each category (*i.e.* MDCT bone measurements, CBCT bone measurements, CBCT soft-tissue measurements) were computed separately. In order to disclose deterministic differences between both methods of measurement, a one-sample Student's *t*-test was applied to the differences. Furthermore, the Bland–Altman method[24,25] was performed and the limits of agreement were identified. *p*-values less than 0.05 were considered as statistically significant.

Results

The ICC revealed a very good repeatability of the radiological measurements [$r = 0.92$; 95% confidence

Table 1 Descriptive statistics, one sample *t*-test, 95% confidence interval (CI) for differences and limits of agreement: positive numbers represent overestimation and negative numbers underestimation of the radiological measurement (Rx) with respect to anatomical measurement (Anat)

Differences Rx–Anat	n	*NASs (%)*	p-*value*	*Mean (mm)*	*SD (mm)*	*Range (mm)*	*95% CI (mm)*	*Limits of agreement (mm)*
MDCT bone	41	14.5	0.0667	0.23	0.81	4.42	−0.02; 0.48	−1.35; 1.82
CBCT bone	41	8.3	0.0956	0.14	0.55	2.07	−0.02; 0.31	−0.93; 1.21
CBCT soft tissue	31	–	0.0874	0.14	0.47	1.78	−0.02; 0.32	−0.77; 1.07

CBCT, cone beam CT; MDCT, multidetector CT; NASs, non-assessable sites; SD, standard deviation.

intervals (CI) 0.86 mm; 0.96 mm)]. This high intraobserver reliability is considered a prerequisite for further comparisons of measurements.

The accuracy of the measurements proved to be acceptable for all protocols (MDCT bone, CBCT bone and soft tissue). The results of the descriptive statistics and the one-sample *t*-test are given in Table 1. There were more non-assessable sites (NASs) with MDCT (14.5%) than with CBCT (8.3%). The mean difference for all readings was very close to 0 mm, with 0.23 mm for MDCT and 0.14 mm for CBCT (bone and soft tissue, respectively). The one-sample *t*-test revealed no significant differences between the radiological and clinical measurements, and 0 mm was always within the 95% CI bound. The mean differences between the radiological and anatomical measurements are plotted in Figure 3.

To validate the various measurements, the difference between the measurements was plotted against the mean as recommended by Bland and Altman (Figure 4a–c). The mean value, limits of agreement and the 95% CI for the limits of agreement are marked in the figures. These figures show that, although the mean differences were all close to 0 mm, the limits of agreement for bone measurements were broader in MDCT (−1.35 mm; 1.82 mm) than in CBCT (−0.93 mm; 1.21 mm). These results suggests that MDCT is to some extent less accurate. The limits of agreement for soft-tissue measurements in CBCT, however, were smaller (–0.77 mm; 1.07 mm), indicating a slightly higher accuracy for soft-tissue measurements.

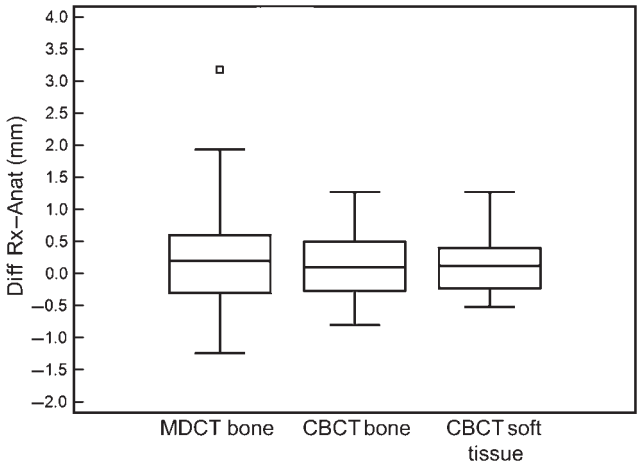

Figure 3 Box and whisker plot of the differences (Diff) between the radiological (Rx) and anatomical (Anat) measurements. CBCT, cone beam CT; MDCT, multidetector CT

Discussion

Over the last decade, CBCT has gained increased influence in the field of diagnostic maxillofacial imaging, being referred to as the "modality of choice".[26] However, the absolute value of CBCT and its role as a standard of reference remains questionable until it has been carefully and adequately compared with the existing standard of reference, which is MDCT.

Multiple investigations have been conducted to compare CBCT and MDCT using either a dry mandible,[27–29] a maxilla,[3,30,31] both,[32,33] or an anthropomorphic phantom.[3,33–36] To the best of our knowledge, only three studies[26,36,37] have been published so far using intact human heads to compare the performance of CBCT and MDCT in the dentomaxillofacial area. However, the focus has been laid predominantly on image quality, and not on accuracy of measurements. Hence, in all three studies the obtained measurements were not compared with anatomical measurements. Moreover, it is obvious that measurements taken from images obtained from lower-resolution protocols are prone to giving inferior results.[38] However, many previous studies compared high-resolution CBCT protocols with standard MDCT protocols,[27–32,35] *i.e.* comparing voxel sizes of $0.125 \times 0.125 \times 0.125$ mm (CBCT) with voxel sizes of $0.375 \times 0.375 \times 0.4$ mm (MDCT).[21] We believe that using scan protocols with a substantial difference in voxel volume [1.95×10^{-3} mm^3 (CBCT) *vs.* 39.09×10^{-3} mm^3 (MDCT)] renders a comparison inappropriate.

Mindful of the limitations of the above studies, we attempted to perform a comparative study applying a *low-resolution* CBCT protocol and comparing the obtained measurements with the anatomical truth.

Reduced image quality due to metallic artefacts presents a challenge and serious limitation in dentomaxillofacial imaging.[39] Implants, dental reconstructions and orthodontic appliances may cause beam hardening and streaking artefacts, thus decreasing image quality.[40] To determine image quality in our study, we have evaluated the number of NASs due to metallic dental reconstructions. The results show that, compared with the CBCT scans, MDCT scans showed more NASs because of the close proximity of the measured area to the metal reconstructions. Moreover, the MDCT data were sometimes compromised in remote areas as well, owing to pronounced streaking or starburst artefacts (Figure 5). By quantifying the NASs (14.5% for MDCT *vs* 8.3% for CBCT) our study

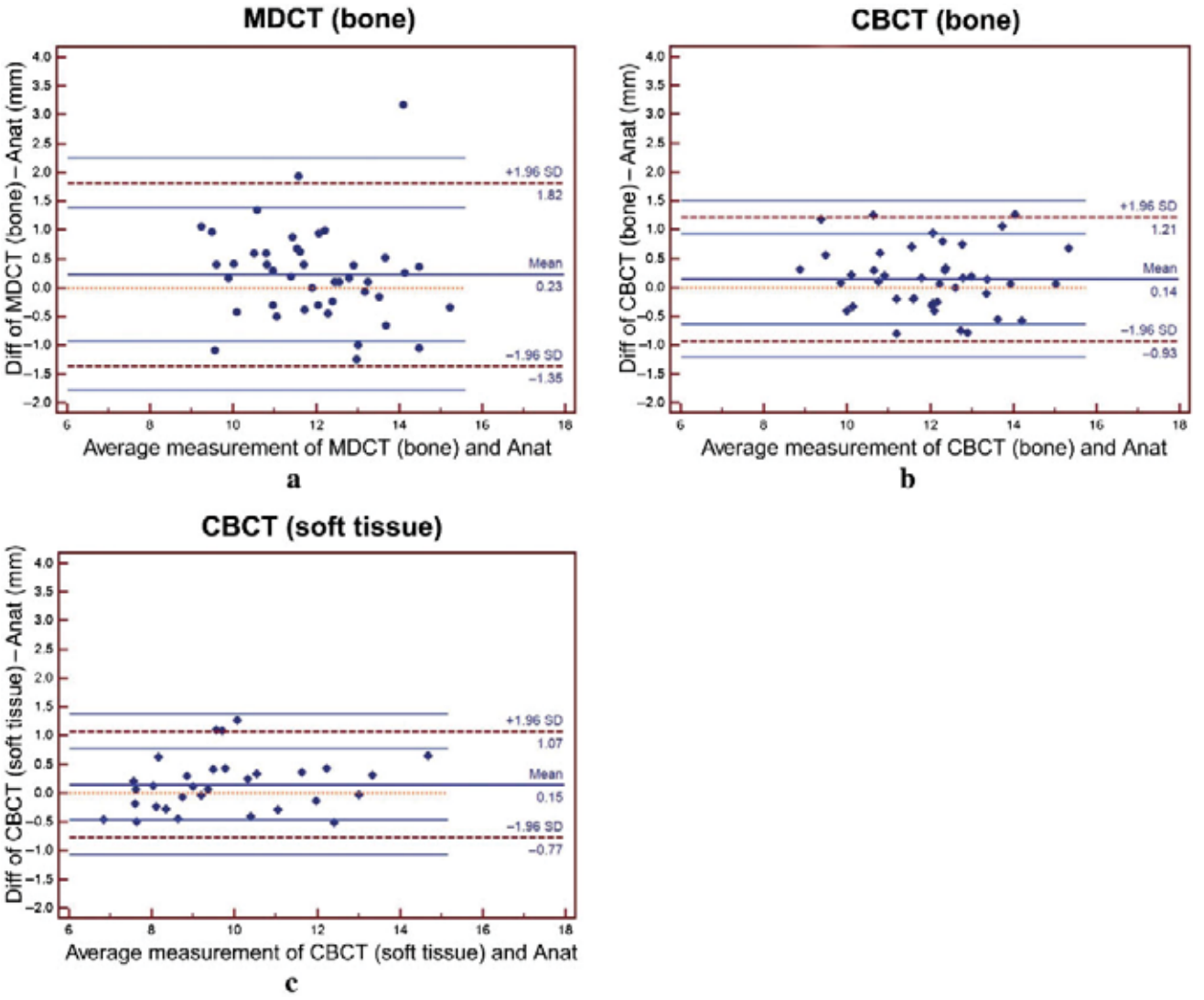

Figure 4 Bland–Altman plots for (a) multidetector CT (bone), (b) cone beam CT (CBCT) (bone) and (c) CBCT (soft tissue). Mean value (solid thick middle line), limits of agreement (broken lines) and 95% confidence intervals of the limits of agreement (solid thin lines) are shown. Anat, anatomical; Diff, difference; SD, standard deviation

shows a highly relevant finding for clinical practice. However, this is not in accordance with Draenert et al,[41] who found stronger beam hardening artefacts in CBCT than in MDCT. A comparison of the two studies is difficult, however, because Draenert et al examined one dental implant (one metal alloy) in a dry skull. The present study, alternatively, aims to approximate clinical practice with greater accuracy using intact cadaveric heads: most of the specimens contained a multitude of metallic reconstructions in various locations. This is important because both variables, composition *and* orientation of metals, affect the data.[38] In general, CBCT produced smoother images with reduced image contrast. Although this hinders the qualitative assessment of tissues, it proved beneficial for the quantitative appraisal of linear measurements.

The broader limits of agreement in MDCT indicate that linear measurements are slightly more accurate when performed upon CBCT rather than MDCT data and confirm the results of previously published studies.[19,27,32] Moreover, our data are in accordance with studies reporting a generally better image quality of CBCT for hard-tissue assessments.[3,28,31,42]

Literature on the accuracy of CBCT-based soft-tissue measurements is scarce. Januário et al[43] measured gingival tissue by means of CBCT, and Barriviera et al[44] proposed that the palatal masticatory mucosa may be measured on CBCT data. However, both failed to validate their obtained measurements against anatomical reference measurements. In two further studies, Fourie et al[45,46] described the accuracy of facial (*i.e.* extraoral) soft-tissue measurements. However, these results may not be applied to intraoral measurements, because Fourie deemed only mean absolute errors of more than 1.5 mm as clinically significant, which will not hold true for intraoral clinical queries. Furthermore, the

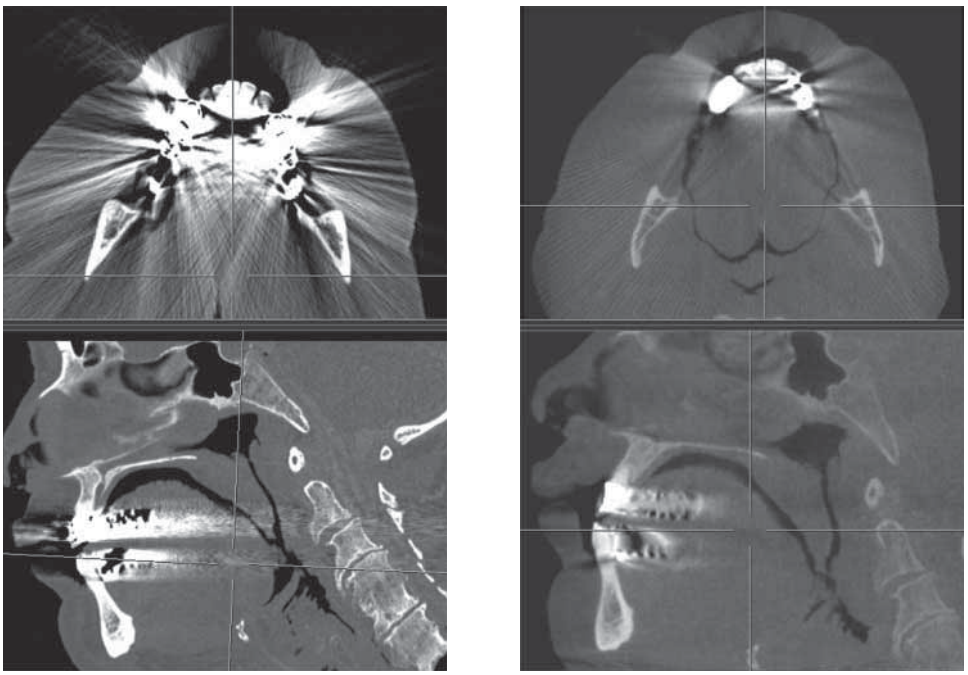

a b

Figure 5 Representative scan of the identical specimen (same region and same multiplanar reformatting) with typically constrained data from metal reconstruction. (a) Multidetector CT, (b) cone beam CT. Note the obvious difference in image quality

CBCT-based measurements were taken from a generated three-dimensional soft-tissue surface model and not from multiplanar reconstructions. Finally, the evaluation of the scanned data on a laptop screen might have been a curtailing factor on the accuracy.

To the best of our knowledge, the present study is the first to describe the accuracy of intraoral soft-tissue measurements on CBCT compared with bone measurements. Interestingly, soft-tissue measurements are slightly more accurate than bone measurements. The reason might simply be because no other tissue is in contact with the gingival surface, making the gingival surface easier to identify.

In clinical practice, ascertaining the thickness of the gingiva or mucosa would be highly advantageous. The success of surgical procedures in periodontology often depends on the thickness of the soft tissue present,[47] as well as the thickness of the donor site when grafting connective tissues.[48] Furthermore, the width of the free gingival margin is directly related to more frequent and more severe recessions,[49] and gingival problems occur generally more often in individuals with a thin gingival biotype.[50] Additionally, considerable intra- as well as interindividual variations in thickness of the masticatory mucosa exist.[51] As a result, a non-invasive method to assess the thickness of the gingiva has long been sought. Müller et al[47] introduced an ultrasonic measuring method, but were forced to admit that it was not reliable enough. More recently, Januário et al[43] published an innovative approach to expose the buccal gingiva during the scan by means of a lip retractor (Figure 6). However, their radiological measurements were not verified. The findings of our study validated the accuracy of intraoral soft-tissue measurements and legitimate radiological measures of the gingiva and the masticatory mucosa. Hence, the use of a lip retractor seems highly commendable to expose the buccal gingiva.

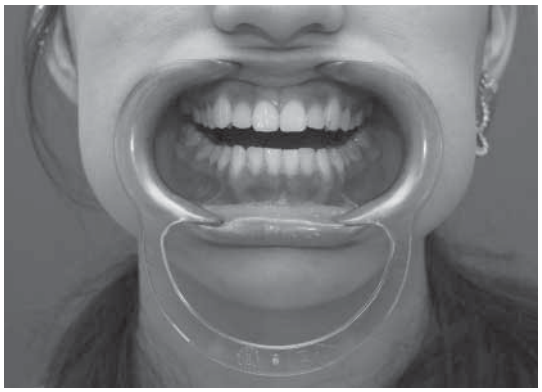

Figure 6 Lip retractor commonly used in orthodontics. This tool might be useful in cone beam CT image acquisition for gingival measurements

Limitations

One limitation is the possible bias of a single observer, probably yielding greater consistency in radiological landmark identification than the varied interpretations of a landmark by several observers. A meta-analysis on identification and reproducibility of radiological (cephalometric) landmarks, however, indicates that the number of observers does not play a significant role in landmark identification,[52] and in a more recent study

de Oliveira et al[53] demonstrated a likewise excellent interobserver reliability in CBCT landmark reproducibility in all three planes of space.

A second constraint may be that unmitigated cadaveric heads render only an approximation of clinical truth. Specifically, the alcohol fixation of the specimens contained low concentrations of glutaraldehyde and formaldehyde, which are known to modify certain tissue properties, *e.g.* slight muscle expansion and fatty tissue shrinkage,[54] and are known to alter periodontal fibre architecture.[55] Yet a comparison of soft-tissue and bone measurements must presuppose that fixation does not modify tissue properties. There is evidence supporting glyoxal-based fixation as a suitable fixative for structural evaluation of soft tissue.[56] In addition, no significant differences have been reported in bone mineral density and the initial Young's modulus between alcohol fixation and fresh-frozen specimens.[57]

Lastly, some concern may be raised as to whether multiple measurements on the same head could be interpreted as independent samples, as this probably violates the assumption of independence required for parametric statistical testing. This problem is discussed in periodontal research[58] and is common for all cadaveric studies. In radiology this limitation is possibly less acute than in periodontology (where each site is clearly dependent of the ubiquitous oral habitat and host factors), as the correlation between measurements at different radiological sites is weaker owing to the impact of orientation and distance to metal affecting the imaging.

In conclusion, CBCT image data is inherently different from MDCT image data, generating smoother images with lower image contrast. This serious limitation in regard to qualitative appraisal of soft tissue and bone proved beneficial for the quantitative assessment of linear measurements. Compared with MDCT, CBCT appears to be less susceptible to metal artefacts and slightly more reliable for linear measurements. Therefore, in practice, the clinician's choice over which CT device to use should depend on the intended diagnostic purpose of each scan to be performed. A further finding is that CBCT accuracy of linear soft-tissue measurements is similar to the accuracy of linear bone measurements. The use of a lip retractor is recommended to enable the exposure of the buccal gingiva.

References

1. Robb RA, Sinak LJ, Hoffman EA, Kinsey JH, Harris LD, Ritman EL. Dynamic volume imaging of moving organs. *J Med Syst* 1982; **6**: 539–554.
2. Arai Y, Tammisalo E, Iwai K, Hashimoto K, Shinoda K. Development of a compact computed tomographic apparatus for dental use. *Dentomaxillofac Radiol* 1999; **28**: 245–248.
3. Hashimoto K, Arai Y, Iwai K, Araki M, Kawashima S, Terakado M. A comparison of a new limited cone beam computed tomography machine for dental use with a multidetector row helical CT machine. *Oral Surg Oral Med Oral Pathol Oral Radiol Endod* 2003; **95**: 371–377.
4. Ludlow J, Davies-Ludlow L, Brooks S. Dosimetry of two extraoral direct digital imaging devices: NewTom cone beam CT and Orthophos Plus DS panoramic unit. *Dentomaxillofac Radiol* 2003; **32**: 229–234.
5. Schulze D, Heiland M, Thurmann H, Adam G. Radiation exposure during midfacial imaging using 4- and 16-slice computed tomography, cone beam computed tomography systems and conventional radiography. *Dentomaxillofac Radiol* 2004; **33**: 83–86.
6. Ludlow JB, Davies-Ludlow LE, Brooks SL, Howerton WB. Dosimetry of 3 CBCT devices for oral and maxillofacial radiology: CB Mercuray, NewTom 3G and i-CAT. *Dentomaxillofac Radiol* 2006; **35**: 219–226.
7. Mozzo P, Procacci C, Tacconi A, Martini PT, Andreis IA. A new volumetric CT machine for dental imaging based on the cone-beam technique: preliminary results. *Eur Radiol* 1998; **8**: 1558–1564.
8. Sukovic P. Cone beam computed tomography in craniofacial imaging. *Orthod Craniofac Res* 2003; **6**: 31–36.
9. Farman AG, Scarfe WC. The basics of maxillofacial cone beam computed tomography. *Semin Orthod* 2009; **15**: 2–13.
10. Silverman PM, Kalender WA, Hazle JD. Common terminology for single and multislice helical CT. *AJR Am J Roentgenol* 2001; **176**: 1135–1136.
11. Mah P, Reeves TE, McDavid WD. Deriving Hounsfield units using grey levels in cone beam computed tomography. *Dentomaxillofac Radiol* 2010; **39**: 323–335.
12. Bryant J. Deriving Hounsfield units from the grey scale of a CBCT? *Dentomaxillofac Radiol* 2011; **40**: 65.
13. Bryant JA, Drage NA, Richmond S. Study of the scan uniformity from an i-CAT cone beam computed tomography dental imaging system. *Dentomaxillofac Radiol* 2008; **37**: 365–374.
14. Katsumata A, Hirukawa A, Okumura S, Naitoh M, Fujishita M, Ariji E, et al. Relationship between density variability and imaging volume size in cone-beam computerized tomographic scanning of the maxillofacial region: an in vitro study. *Oral Surg Oral Med Oral Pathol Oral Radiol Endod* 2009; **107**: 420–425.
15. Katsumata A, Hirukawa A, Okumura S, Naitoh M, Fujishita M, Ariji E, et al. Effects of image artifacts on gray-value density in limited-volume cone-beam computerized tomography. *Oral Surg Oral Med Oral Pathol Oral Radiol Endod* 2007; **104**: 829–836.
16. van Daatselaar AN, van der Stelt PF, Weenen J. Effect of number of projections on image quality of local CT. *Dentomaxillofac Radiol* 2004; **33**: 361–369.
17. Endo M, Tsunoo T, Nakamori N, Yoshida K. Effect of scattered radiation on image noise in cone beam CT. *Med Phys* 2001; **28**: 469–474.
18. Araki K, Maki K, Seki K, Sakamaki K, Harata Y, Sakaino R, et al. Characteristics of a newly developed dentomaxillofacial X-ray cone beam CT scanner (CB MercuRayTM): system configuration and physical properties. *Dentomaxillofac Radiol* 2004; **33**: 51–59.
19. Kobayashi K, Shimoda S, Nakagawa Y, Yamamoto A. Accuracy in measurement of distance using limited cone-beam computerized tomography. *Int J Oral Maxillofac Implants* 2004; **19**: 228–231.
20. Lascala CA, Panella J, Marques MM. Analysis of the accuracy of linear measurements obtained by cone beam computed tomography (CBCT-NewTom). *Dentomaxillofac Radiol* 2004; **33**: 291–294.
21. Loubele M, Van Assche N, Carpentier K, Maes F, Jacobs R, van Steenberghe D, et al. Comparative localized linear accuracy of small-field cone-beam CT and multislice CT for alveolar bone measurements. *Oral Surg Oral Med Oral Pathol Oral Radiol Endod* 2008; **105**: 512–518.
22. European Union. Additional protocol to the convention on human rights and biomedicine, on transplantation of organs and tissues of human origin. ETS 186, Art 16–18; 2002.
23. Swiss Academy of Medical Science. Verwendung von Leichen und Leichenteilen in der medizinischen Forschung sowie Aus-, Weiter- und Fortbildung. *Schweiz. Ärzteztg* 2009; **90**: 102–107.

24. Bland JM, Altman DG. Statistical methods for assessing agreement between two methods of clinical measurement. *Lancet* 1986; **1**: 307–310.
25. Bland JM, Altman DG. Comparing methods of measurement: why plotting difference against standard method is misleading. *Lancet* 1995; **346**: 1085–1087.
26. Heiland M, Pohlenz P, Blessmann M, Habermann CR, Oesterhelweg L, Begemann PC, et al. Cervical soft tissue imaging using a mobile CBCT scanner with a flat panel detector in comparison with corresponding CT and MRI data sets. *Oral Surg Oral Med Oral Pathol Oral Radiol Endod* 2007; **104**: 814–820.
27. Suomalainen A, Vehmas T, Kortesniemi M, Robinson S, Peltola J. Accuracy of linear measurements using dental cone beam and conventional multislice computed tomography. *Dentomaxillofac Radiol* 2008; **37**: 10–107.
28. Liang X, Jacobs R, Hassan B, Li L, Pauwels R, Corpas L, et al. A comparative evaluation of cone beam computed tomography (CBCT) and multi-slice CT (MSCT): Part I. On subjective image quality. *Eur Radiol* 2010; **75**: 265–269.
29. Liang X, Lambrichts I, Sun Y, Denis K, Hassan B, Li L, et al. A comparative evaluation of cone beam computed tomography (CBCT) and multi-slice CT (MSCT). Part II: On 3D model accuracy. *Eur Radiol* 2010; **75**: 270–274.
30. Loubele M, Maes F, Schutyser F, Marchal G, Jacobs R, Suetens P. Assessment of bone segmentation quality of cone-beam CT versus multislice spiral CT: a pilot study. *Oral Surg Oral Med Oral Pathol Oral Radiol Endod* 2006; **102**: 225–234.
31. Hashimoto K, Kawashima S, Araki M, Iwai K, Sawada K, Akiyama Y. Comparison of image performance between cone-beam computed tomography for dental use and four-row multidetector helical CT. *J Oral Sci* 2006; **48**: 27–34.
32. Al-Ekrish AA, Ekram M. A comparative study of the accuracy and reliability of multidetector computed tomography and cone beam computed tomography in the assessment of dental implant site dimensions. *Dentomaxillofac Radiol* 2011; **40**: 67–75.
33. Mischkowski RA, Pulsfort R, Ritter L, Neugebauer J, Brochhagen HG, Keeve E, et al. Geometric accuracy of a newly developed cone-beam device for maxillofacial imaging. *Oral Surg Oral Med Oral Pathol Oral Radiol Endod* 2007; **104**: 551–559.
34. Loubele M, Guerrero ME, Jacobs R, Suetens P, van Steenberghe D. A comparison of jaw dimensional and quality assessments of bone characteristics with cone-beam CT, spiral tomography, and multi-slice spiral CT. *Int J Oral Maxillofac Implants* 2007; **22**: 446–454.
35. Suomalainen A, Kiljunen T, Kaser Y, Peltola J, Kortesniemi M. Dosimetry and image quality of four dental cone beam computed tomography scanners compared with multislice computed tomography scanners. *Dentomaxillofac Radiol* 2009; **38**: 367–378.
36. Carrafiello G, Dizonno M, Colli V, Strocchi S, Pozzi Taubert S, Leonardi A, et al. Comparative study of jaws with multislice computed tomography and cone-beam computed tomography. *Radiol Med* 2010; **115**: 600–611.
37. Naitoh M, Nakahara K, Suenaga Y, Gotoh K, Kondo S, Ariji E. Comparison between cone-beam and multislice computed tomography depicting mandibular neurovascular canal structures. *Oral Surg Oral Med Oral Pathol Oral Radiol Endod* 2010; **109**: e25–31.
38. Lee M-J, Kim S, Lee S-A, Song H-T, Huh Y-M, Kim D-H, et al. Overcoming artifacts from metallic orthopedic implants at high-field-strength MR imaging and multi-detector CT1. *Radiographics* 2007; **27**: 791–803.
39. Abrahams JJ. Dental CT imaging: a look at the jaw. *Radiology* 2001; **219**: 334–345.
40. Naranjo V, Llorens R, Alcaniz M, Lopez-Mir F. Metal artifact reduction in dental CT images using polar mathematical morphology. *Comput Methods Programs Biomed* 2011; **102**: 64–74.
41. Draenert FG, Coppenrath E, Herzog P, Muller S, Mueller-Lisse UG. Beam hardening artefacts occur in dental implant scans with the NewTom cone beam CT but not with the dental 4-row multidetector CT. *Dentomaxillofac Radiol* 2007; **36**: 198–203.
42. Honda K, Larheim TA, Maruhashi K, Matsumoto K, Iwai K. Osseous abnormalities of the mandibular condyle: diagnostic reliability of cone beam computed tomography compared with helical computed tomography based on an autopsy material. *Dentomaxillofac Radiol* 2006; **35**: 152–157.
43. Januário AL, Barriviera M, Duarte WR. Soft tissue cone-beam computed tomography: a novel method for the measurement of gingival tissue and the dimensions of the dentogingival unit. *J Esthet Restor Dent* 2008; **20**: 366–373; discussion 74.
44. Barriviera M, Duarte WR, Januario AL, Faber J, Bezerra AC. A new method to assess and measure palatal masticatory mucosa by cone-beam computerized tomography. *J Clin Periodontol* 2009; **36**: 564–568.
45. Fourie Z, Damstra J, Gerrits PO, Ren Y. Accuracy and repeatability of anthropometric facial measurements using cone beam computed tomography. *Cleft Palate Craniofac J* 2011; **48**: 623–630.
46. Fourie Z, Damstra J, Gerrits PO, Ren Y. Accuracy and reliability of facial soft tissue depth measurements using cone beam computer tomography. *Forensic Sci Int* 2010; **199**: 9–14.
47. Müller H-P, Schaller N, Eger T. Ultrasonic determination of thickness of masticatory mucosa: A methodologic study. *Oral Surg Oral Med Oral Pathol Oral Radiol Endod* 1999; **88**: 248–253.
48. Studer SP, Allen EP, Rees TC, Kouba A. The thickness of masticatory mucosa in the human hard palate and tuberosity as potential donor sites for ridge augmentation procedures. *J Periodontol* 1997; **68**: 145–151.
49. Yared KFG, Zenobio EG, Pacheco W. Periodontal status of mandibular central incisors after orthodontic proclination in adults. *Am J Orthod Dentofacial Orthop* 2006; **130**: 6.e1–6.e8.
50. Seibert J, Lindhe J. *Esthetics in periodontal therapy*. 3rd edn. Copenhagen: Munksgaard; 1997. pp. 647–681.
51. Muller HP, Schaller N, Eger T, Heinecke A. Thickness of masticatory mucosa. *J Clin Periodontol* 2000; **27**: 431–436.
52. Trpkova B, Major P, Prasad N, Nebbe B. Cephalometric landmarks identification and reproducibility: a meta analysis. *Am J Orthod Dentofacial Orthop* 1997; **112**: 165–170.
53. de Oliveira AEF, Cevidanes LHS, Phillips C, Motta A, Burke B, Tyndall D. Observer reliability of three-dimensional cephalometric landmark identification on cone-beam computerized tomography. *Oral Surg Oral Med Oral Pathol Oral Radiol Endod* 2009; **107**: 256–265.
54. Docquier PL, Paul L, Cartiaux O, Lecouvet F, Dufrane D, Delloye C, et al. Formalin fixation could interfere with the clinical assessment of the tumor-free margin in tumor surgery: magnetic resonance imaging-based study. *Oncology* 2010; **78**: 115–124.
55. Burn-Murdoch RA, Tyler DW. Physiological evidence that periodontal collagen in the rat exists as fibres prior to histological fixation. *Arch Oral Biol* 1981; **26**: 995–999.
56. Wang Y, Lee K, Pai S, Ledoux W. Histomorphometric comparison after fixation with formaldehyde or glyoxal. *Biotech Histochem* 2011; **86**: 359–365.
57. Stefan U, Michael B, Werner S. Effects of three different preservation methods on the mechanical properties of human and bovine cortical bone. *Bone* 2010; **47**: 1048–1053.
58. Imrey PB. Considerations in the statistical analysis of clinical trials in periodontitis. *J Clin Periodontol* 1986; **13**: 517–532.

Eur Radiol (2012) 22:1579–1585
DOI 10.1007/s00330-012-2391-8

MUSCULOSKELETAL

MRI of the temporo-mandibular joint: which sequence is best suited to assess the cortical bone of the mandibular condyle? A cadaveric study using micro-CT as the standard of reference

Christoph A. Karlo · Raphael Patcas · Thomas Kau · Helmut Watzal · Luca Signorelli · Lukas Müller · Oliver Ullrich · Hans-Ulrich Luder · Christian J. Kellenberger

Received: 20 October 2011 / Revised: 5 December 2011 / Accepted: 21 December 2011 / Published online: 10 February 2012

Abstract
Objective To determine the best suited sagittal MRI sequence out of a standard temporo-mandibular joint (TMJ) imaging protocol for the assessment of the cortical bone of the mandibular condyles of cadaveric specimens using micro-CT as the standard of reference.
Methods Sixteen TMJs in 8 human cadaveric heads (mean age, 81 years) were examined by MRI. Upon all sagittal sequences, two observers measured the cortical bone thickness (CBT) of the anterior, superior and posterior portions of the mandibular condyles (i.e. objective analysis), and assessed for the presence of cortical bone thinning, erosions or surface irregularities as well as subcortical bone cysts and anterior osteophytes (i.e. subjective analysis). Micro-CT of the condyles was performed to serve as the standard of reference for statistical analysis.
Results Inter-observer agreements for objective ($r=0.83$-0.99, $P<0.01$) and subjective ($\kappa=0.67$-0.88) analyses were very good. Mean CBT measurements were most accurate, and cortical bone thinning, erosions, surface irregularities and subcortical bone cysts were best depicted on the 3D fast spoiled gradient echo recalled sequence (3D FSPGR).
Conclusion The most reliable MRI sequence to assess the cortical bone of the mandibular condyles on sagittal imaging planes is the 3D FSPGR sequence.
Key Points
- *MRI may be used to assess the cortical bone of the TMJ.*
- *Depiction of cortical bone is best on 3D FSPGR sequences.*
- *MRI can assess treatment response in patients with TMJ abnormalities.*

Keywords Mandibular condyle · MRI · Micro-CT · TMJ · JIA

C. A. Karlo (✉)
Department of Diagnostic and Interventional Radiology,
University Hospital Zurich,
Rämistrasse 100,
8091, Zurich, Switzerland
e-mail: christoph.karlo@gmail.com

C. A. Karlo · T. Kau · H. Watzal · C. J. Kellenberger
Department of Diagnostic Imaging,
University Children's Hospital Zurich,
Zurich, Switzerland

R. Patcas · L. Signorelli · L. Müller
Clinic for Orthodontics and Pediatric Dentistry, Center of Dental Medicine, University of Zurich,
Zurich, Switzerland

O. Ullrich
Institute of Anatomy, Faculty of Medicine, University of Zurich,
Zurich, Switzerland

H.-U. Luder
Section of Orofacial Structures and Development,
Center of Dental Medicine, University of Zurich,
Zurich, Switzerland

Introduction

Magnetic resonance imaging (MRI) of the temporo-mandibular joint (TMJ) is considered the diagnostic imaging technique of choice for the initial workup and follow-up of patients with TMJ abnormalities. These include internal derangements (i.e. deformation or displacement of the

articular disc), inflammatory conditions (i.e. TMJ arthritis) and degenerative changes (i.e. TMJ arthrosis) [1, 2].

The main strengths of MRI are the detailed illustration of soft tissue abnormalities as well as the reliable depiction of bone marrow oedema, undoubtedly an important biomarker for disease progression and treatment response especially in patients suffering from TMJ arthritis [3–8]. As opposed to bone marrow oedema representing an indicator for early bone involvement, flattening of the condylar head, osseous erosions, subchondral bone cysts and anterior osteophytes represent frequent findings in patients with advanced TMJ disease [2].

Although MRI has the ability to illustrate these findings, their true (i.e. in vivo) extent may be uncertain [9]. Based on the close observation of the cortical bone structures of paediatric TMJs in more than 100 MRI examinations performed at our institution per year, the hypothesis arose that the cortical bone structure of the mandibular condyle may present itself differently when different sagittal MRI sequences are used. The reasons for these different appearances are probably chemical shift and susceptibility artefacts occurring at the bordering regions between cortical bone and the adjacent soft tissue. These artefacts usually manifest as a loss of signal at bone–tissue interfaces owing to a dephasing of signals. They usually produce an expanding low signal just beyond the periphery of cortical bone [10–12].

Therefore the purpose of this study was to determine the most suitable sagittal MRI sequence out of our standard TMJ protocol for the evaluation of the cortical bone of the mandibular condyles.

Materials and methods

Subjects

Eight intact human cadaveric heads (5 female, 3 male; mean age, 81 years; age range, 65–95 years) were supplied by the Anatomical Institute of the local university in accordance with state and federal regulations (voluntary body donation programme on the basis of informed consent), the Convention on Human Rights and Medicine [13] and the recommendation of the National Academy of Medical Science [14]. Perfusion was carried out within 4 days of decease with a fixation solution consisting of two parts alcohol (70%), one part glycerine and 2% almudor (i.e. containing: 8.1% formaldehyde, 10% glyoxal and 3.7% glutaraldehyde).

Image data acquisition

All MRI examinations of all heads (n=8) were carried out on a commercially available 1.5-T MRI unit (Signa HDx, General Electric, Milwaukee, WI, USA) using a commercially available, two-channel phased array surface coil dedicated to TMJ imaging (DUALTMJ coil). All examinations were performed in closed mouth position. All sagittal sequences were planned to be acquired parallel to the mandibular rami, separately for each side (i.e. left and right). The MRI protocol included the following sagittal sequences: a T1-weighted 2D fast spoiled gradient recalled echo sequence (T1-2D-FSPGR), an intermediate-weighted proton density fast spin echo sequence (PD-FSE), a T2-weighted fast spin echo sequence (T2-FSE), a T1-weighted 3D fast spoiled gradient recalled echo sequence (T1-3D-FSPGR) and a T1-weighted fast spin echo sequence (T1-FSE). For the complete MRI protocol, please refer to Table 1. The mean total examination time was 40 min per head.

In preparation for the micro-CT (μCT) examinations, a member of the Anatomical Institute resected and cleaned all mandibles. Subsequently the mandibular condyles and articular discs were separated from the rami at the level of the mandibular notch (i.e. at the incisura mandibulae). Care was taken not to injure the mandibular condyle during resection.

All μCT examinations of the condyles (n=16) were performed using a commercially available μCT unit (Specimen microCT μCT 40, Scanco Medical, Brüttisellen, Switzerland) with all imaging parameters kept identical during all examinations (tube voltage, 70 kV, tube current 114 μA; isotropic resolution, 18 μm).

One radiologist not involved in further data analysis prepared all μCT data by reconstructing multi-planar reformatted (MPR) images in sagittal imaging planes aligned parallel to the mandibular ramus (i.e. corresponding to the alignment of the imaging planes of the sagittal MRI sequences) at a reconstruction slice thickness of 1 mm and a reconstruction increment of 0.6 mm. Subsequently all reconstructed DICOM data were archived into the hospital's PACS (picture archive and communication system) for storage and further image analysis.

Cortical bone thickness measurements

The thickness of the cortical bone (CBT) of the anterior, superior and posterior portions of the mandibular condyles was measured on all sagittal MRI sequences at the level of the centre of the mandibular condyle in a blinded fashion by two radiologists experienced in musculoskeletal radiology. All measurements were carried out using a calibrated measurement tool that was part of the hospital's PACS and allowed for sub-millimetre measurements. A third radiologist who was not involved in MRI measurements performed the corresponding CBT measurements on the sagittal MPR images of the μCT data, which served as the standard of reference for statistical analysis.

Table 1 MRI protocol used for imaging of the temporo-mandibular joints

	Axial T2-FRFSE	Coronal T2-FRFSE	Sagittal T1-2D-FSPGR	Sagittal PD-FSE	Sagittal T2-FSE	Sagittal T1-3D-FSPGR	Sagittal T1-FSE	Coronal T1-SE
Time to repetition (TR, ms)	3,000	3,000	370	3,200	6,820	11.6	640	500
Time to echo (TE, ms)	102	102	4.2	24	85	4.1	10.7	11
Flip angle (°)	90	90	80	90	90	20	90	90
Matrix (frequency × phase, pixels)	384×320	384×320	384×224	256×224	256×224	256×192	256×192	256×192
Slice thickness (mm)	3	3	2	2	2	2	2	2
Spacing (mm)	11.6	4.1	2	2	2	1	2	2
Field of view (FOV, cm^2)	22	22	12	12	12	10	12	16
Band width (Hertz)	41.67	41.67	31.25	17.86	20.83	15.63	20.83	19.23
NEX (number of excitations)	4	4	3	3	4	3	3	3
Echo train length	21	21	–	8	16	–	3	–

FRFSE fast relaxation fast spin echo, *FSPGR* fast spoiled gradient recalled echo, *FSE* fast spin echo, *SE* spin echo

Subjective evaluation of the cortical bone

In a separate analysis session, the same radiologists also assessed the anterior, superior and posterior portions of the mandibular condyles (n=16) on the sagittal MRI sequences for cortical bone thinning, cortical bone erosions, irregularities of the cortical bone surface, subcortical bone cysts and the presence of an anterior osteophyte in a blinded fashion. The third radiologist not involved in MRI analysis assessed the μCT data sets for the same findings to define the standard of reference for statistical analysis. See Fig. 1 for micro-CT imaging examples.

Statistical analysis

All quantitative variables are described as mean ± standard deviation. The data were descriptively reviewed and statistically analysed using Kolmogorov-Smirnov's test for normality. P values <0.05 were considered statistically significant. All statistical analyses were performed using commercially available software (SPSS, release 17.0, Chicago, IL, USA).

Interobserver agreements regarding the presence of cortical bone thinning, cortical bone erosions, irregularities of the cortical bone surface, subcortical bone cysts and the presence of an anterior osteophyte were analysed using Cohen's kappa (κ) statistics and interpreted as follows: A κ-value greater than 0.81 corresponded to excellent agreement, 0.61–0.80 to very good interobserver agreement, 0.41–0.60 to good interobserver agreement and 0.21–0.40 to moderate interobserver agreement. Interobserver agreements concerning all continuous variables (i.e. measurements of cortical bone thickness) were calculated using interclass correlation coefficients (ICC).

Diagnostic accuracy, sensitivity, specificity, positive predictive value and negative predictive value regarding the assessment of cortical bone thinning, cortical bone erosions, cortical bone surface irregularities and subcortical bone cysts were assessed separately by both observers from chi-squared tests of contingency, and the 95% confidence intervals were calculated. The Wilcoxon signed ranks test was performed to test for statistically significant differences in cortical bone thickness measurements between the sagittal MRI sequence and the μCT-based measurements, which served as the standard of reference.

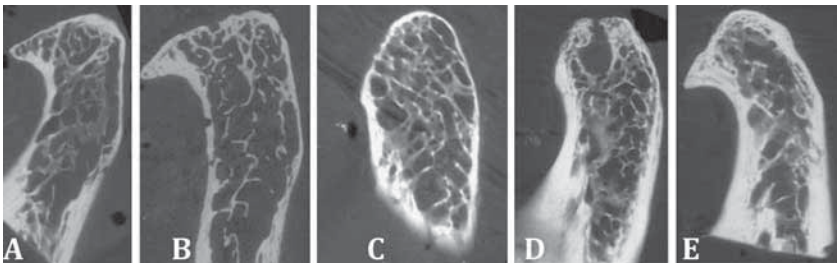

Fig. 1 Micro-CT imaging examples illustrating **a** cortical bone thinning of the superior portion of the mandibular condyle, **b** cortical erosion of the superior portion, **c** cortical surface irregularities of the anterior portion, **d** a large subcortical bone cyst and **e** an anterior osteophyte

Table 2 Cortical bone thickness of the anterior, superior and posterior portions of the mandibular condyles as measured on all sagittal MRI sequences (mean of both readers, in mm) and on the micro-CT images

Specimen	T1-2D-FSPGR			PD-FSE			T2-FSE			T1-3D-FSPGR			T1-FSE			Micro CT		
	ANT	SUP	POST	ANT	SUP	POST	ANT	SUP	POST	ANT	SUP	POST	ANT	SUP	POST	ANT	SUP	POST
1	0.74	0.52	0.33	0.94	0.66	0.35	0.66	0.66	0.66	0.70	0.39	0.45	0.66	0.67	0.64	0.78	0.51	0.50
2	0.74	0.52	0.34	0.94	0.47	0.67	0.66	0.68	0.66	0.70	0.38	0.66	0.66	0.49	0.47	0.68	0.32	0.56
3	0.75	0.33	0.48	0.66	0.66	0.48	0.94	0.94	0.48	0.82	0.54	0.48	0.94	0.66	0.55	0.89	0.44	0.42
4	0.66	0.33	0.33	0.94	0.66	0.66	0.94	0.64	0.66	0.70	0.44	0.29	0.94	0.66	0.67	0.70	0.35	0.40
5	0.70	0.58	0.52	0.95	0.57	0.66	0.66	0.70	0.66	1.02	0.61	0.39	0.96	0.70	0.66	0.92	0.59	0.37
6	0.70	0.52	0.33	0.94	0.49	0.47	0.68	0.66	0.66	0.78	0.39	0.36	0.94	0.50	0.68	0.71	0.31	0.24
7	0.66	0.52	0.33	0.68	0.56	0.50	0.68	0.66	0.66	0.70	0.42	0.28	0.94	0.66	0.66	0.64	0.49	0.24
8	0.54	0.35	0.33	0.66	0.60	0.47	0.66	0.60	0.66	0.70	0.47	0.28	0.66	0.56	0.49	0.66	0.48	0.25
9	0.66	0.99	0.34	0.94	1.05	0.66	0.94	0.93	0.66	1.03	1.24	0.53	0.94	1.07	0.66	0.94	0.96	0.47
10	0.86	0.85	0.52	1.06	0.94	0.94	0.94	1.05	0.66	0.98	1.15	0.55	1.05	0.95	0.66	0.91	0.90	0.48
11	0.97	0.52	0.47	0.94	0.66	0.66	1.05	0.66	0.67	1.19	0.44	0.56	1.03	0.66	0.45	0.96	0.46	0.36
12	0.70	0.52	0.47	0.94	0.66	0.67	0.94	0.65	0.66	0.81	0.30	0.62	0.94	0.66	0.66	0.85	0.33	0.47
13	0.74	0.50	0.33	0.66	0.47	0.42	0.66	0.66	0.66	0.88	0.83	0.28	0.53	0.67	0.47	0.80	0.72	0.26
14	0.97	0.52	0.50	1.06	0.66	0.47	1.06	0.66	0.66	0.87	0.28	0.20	1.05	0.66	0.45	0.86	0.29	0.17
15	0.66	0.52	0.52	0.94	0.94	1.06	0.66	1.05	1.05	0.81	0.70	0.73	0.66	0.66	1.05	0.73	0.63	0.63
16	0.52	0.52	0.52	0.66	0.94	0.66	0.66	0.94	0.66	0.62	0.44	0.44	0.66	0.66	0.66	0.49	0.45	0.42
Mean	0.72	0.54	0.42	0.87	0.69	0.61	0.80	0.76	0.67	0.83	0.56	0.44	0.85	0.68	0.62	0.78	0.51	0.39

ANT anterior, *SUP* superior, *POST* posterior

Results

Imaging findings

The cortical bone of a total of 16 mandibular condyles divided into anterior, superior and posterior portions was investigated (total number of sites=48). Imaging findings included cortical thinning (n=16), cortical erosions (n=6), cortical surface irregularities (n=24), subcortical bone cysts (n=3) and an anterior osteophyte (n=4).

Inter-observer agreements

Inter-observer agreements for performing all cortical bone thickness measurements were excellent (r=0.83–0.99, P< 0.01). Thus the mean of both observers' measurements was calculated and used for further statistical analyses.

Inter-observer agreements for the detection of cortical bone thinning, cortical bone erosions, cortical bone surface irregularities and subcortical bone cysts ranged from very good to excellent for all locations (i.e. anterior, superior and posterior; κ=0.67–0.85) and all MRI sequences (i.e. T1-2D-FSPGR, T2-FSE, T1-3D-FSPGR, PD-FS and T1-FSE: κ= 0.74–0.88). Inter-observer agreement for the detection of an anterior osteophyte was excellent for all MRI sequences (κ=1.0).

Objective analysis

All descriptive results for cortical bone thickness measurements are summarised in Table 2. Compared with the μCT-based measurements, statistically significant differences were found for all cortical bone thickness measurements performed upon the T2-FSE, the PD-FSE and the T1-2D-FSPGR sequences (i.e. anterior, superior and posterior portions) as well as the anterior and posterior cortical bone thickness measurements performed upon the T1-FSE (each P<0.05). No statistically significant differences were found for all T1-3D-FSPGR-based measurements (i.e. anterior [P=0.14], superior [P=0.60] and posterior [P=0.22]) and for the superior T1-FSE-based measurements (P=0.16) when compared with the μCT-based measurements.

Subjective analysis

Accuracy, sensitivity, specificity, and positive and negative predictive values for the depiction of cortical thinning, cortical erosions, cortical surface irregularities and subcortical bone cysts are illustrated in Table 3. When compared with the μCT-based evaluation, the T1-3D-FSPGR sequence was the most reliable in the assessment of cortical thinning, cortical erosions, cortical surface irregularities and subcortical bone cysts for both readers. The depiction of an anterior osteophyte was perfect upon all sequences for both readers. For imaging examples please refer to Figs. 2 and 3.

Discussion

It was the purpose of this study to determine the most suitable sagittal MRI sequence for the evaluation of the cortical bone of the mandibular condyles. Our results strongly support the T1-weighted 3D fast spoiled gradient recalled echo sequence (i.e. T1-3D-FSPGR) to be the best suited MRI sequence for this task. This sequence may be added to any MRI protocol of the TMJ increasing the total examination time by approximately 6 min.

We discovered significant differences among the evaluated MRI sequences regarding objective and subjective cortical bone assessments. These differences could be attributed

Table 3 Results from subjective analysis (mean of both readers)

	Cortical bone thinning					Cortical bone surface irregularities				
	T1-2D-FSPGR	T2 FSE	T1-3D-FSPGR	PD FSE	T1 FSE	T1-2D-FSPGR	T2 FSE	T1-3D-FSPGR	PD FSE	T1 FSE
Accuracy	0.73	0.69	0.79	0.65	0.73	0.51	0.54	0.88	0.58	0.56
Sensitivity	0.28	0.21	0.78	0.50	0.50	0.17	0.08	0.83	0.25	0.38
Specificity	0.91	0.88	0.79	0.71	0.82	0.94	0.96	0.92	0.92	0.75
PPV	0.57	0.42	0.61	0.41	0.54	0.80	0.67	0.91	0.75	0.60
NPV	0.76	0.73	0.90	0.77	0.80	0.46	0.52	0.85	0.55	0.55
	Cortical bone erosions					Subcortical bone cysts				
	T1-2D-FSPGR	T2 FSE	T1-3D-FSPGR	PD FSE	T1 FSE	T1-2D-FSPGR	T2 FSE	T1-3D-FSPGR	PD FSE	T1 FSE
Accuracy	0.90	0.92	0.88	0.69	0.79	0.94	0.94	1.00	0.94	0.94
Sensitivity	0.33	0.33	0.83	0.50	0.33	0.33	0.33	1.00	0.33	0.33
Specificity	0.98	0.99	0.88	0.71	0.86	0.98	0.98	1.00	0.98	0.98
PPV	0.67	0.67	0.50	0.20	0.25	0.50	0.50	1.00	0.50	0.50
NPV	0.91	0.93	0.97	0.91	0.90	0.96	0.96	1.00	0.96	0.96

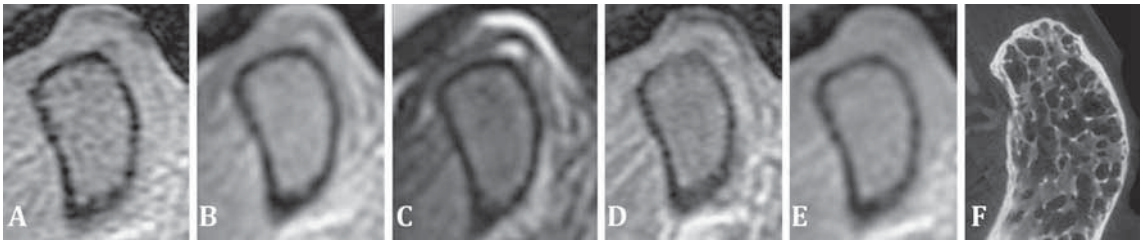

Fig. 2 **a** 2D fast spoiled gradient recalled echo (2D FSPGR), **b** intermediate-weighted proton density fast spin echo (PD-FSE), **c** T2-weighted fast spin echo (T2-FSE), **d** T1-weighted 3D fast spoiled gradient recalled echo (T1-3D-FSPGR) and **e** T1-weighted fast spin echo sequences (T1-FSE). The cortical surface irregularities of the superior portion confirmed by **f** micro CT are depicted by the T1-3D-FSPGR sequence only and seem to be absent on all other sequences

to previously described and well-known chemical shift and susceptibility artefacts occurring at the bordering regions between cortical bone and cartilage, fluid or soft-tissue structures of the TMJ [10–12, 15–19]. The resulting over- or underestimation, however, may lead to misinterpretation of the cortical bone surface and structure. Therefore, TMJ imaging protocols should be designed carefully to avoid such errors.

Over the last few years, the demand for cortical bone imaging using MRI has increased. As opposed to computed tomography (CT), which has been considered the imaging technique of choice for the depiction of osseous pathological features so far, MRI operates without applying ionising radiation to the patients. Continuous advances in technology (i.e. higher magnetic field strengths, more efficient software) and the ongoing effort of the musculoskeletal research community have elevated MRI to become the new imaging method of choice for the assessment of cortical bone, especially for serial follow-up studies in young patients. Various study groups have contributed to cortical bone imaging recently [20–22]. Louis et al. have demonstrated the power of high-resolution T1-weighted 3.0-T MRI in quantifying the cortical bone cross-sectional area at the level of the tibia in a comparison with quantitative CT [20]. Stehling et al. reported the delineation of the cortical bone of the mandibular condyle to be significantly better on images derived from a 3.0-T MRI system rather than a 1.5-T MRI system [22].

When performing MRI of the TMJ it is essential to evaluate the structure, thickness and shape of the cortical bone of the mandibular condyle. In patients with TMJ arthritis, especially in young patients and children suffering from juvenile idiopathic arthritis (JIA), the assessment of these cortical bone structures becomes even more important because cortical bone thinning, flattening of the mandibular condyle, the development of subchondral cysts and the presence of anterior osteophytes are regarded as biomarkers for MRI monitoring of the activity and possible progression of JIA [5, 7, 8].

Abramowicz et al. reported various pathological findings of the mandibular condyle such as erosions, articular surface flattening, subchondral sclerosis and osteophytes [4]. In particular the assessment of subchondral sclerosis may be challenged in this content because false-positive results may be acquired due to chemical shift artefacts. However, Abramowicz et al. evaluated the mandibular condyles upon T1-weighted and intermediate proton-density-weighted MR sequences. We were able to show significant differences in cortical bone thickness of the mandibular condyle between those two sequences, thus yielding a potential source of error for the assessment of subchondral sclerosis and cortical bone structure.

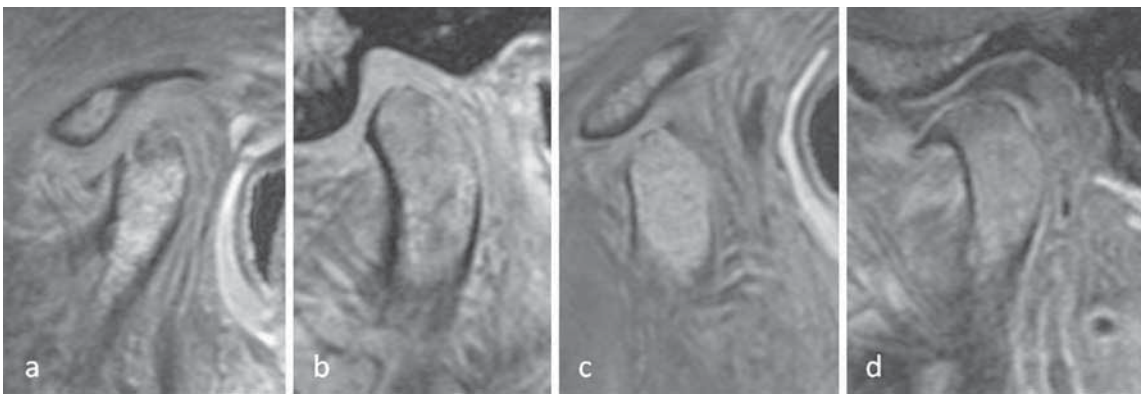

Fig. 3 Imaging example illustrating the ability of the T1-3D-FSPGR sequence to depict **a** subcortical bone cysts, **b** osseous erosions, **c** cortical bone surface irregularities and **d** the presence of an anterior osteophyte and cortical bone thinning of the superior portion

In a very recent publication on dynamic contrast-enhanced MRI of the TMJ, Tasali et al. described condylar sclerosis as one of their MRI findings [15]. However, no further details were provided on the definition of sclerosis and how it was assessed during image analysis. Because of the variable presentation of cortical bone on different sagittal MRI sequences, false-positive findings may become difficult to avoid.

Our study has some limitations. First, the number of evaluated specimens is low (n=16). However, for the chosen approach relying on cadaveric material this was the maximum number of specimens that could be obtained. Second, we limited our evaluation to the sagittal imaging plane. For the declared objective of our study, we considered the restriction appropriate as the sagittal imaging planes are the most important imaging planes in the MRI assessment of the TMJ.

In conclusion, our study showed that the T1-weighted 3D FSPGR sequence was the most suitable MRI method for the objective and subjective assessments of the cortical bone of the mandibular condyle.

Acknowledgements The authors would like to thank L. Völlmer, M. Studhalter, B. Werner and A. Jezler for their technical and logistical assistance.

References

1. Magnusson T, Egermark I, Carlsson GE (2000) A longitudinal epidemiologic study of signs and symptoms of temporomandibular disorders from 15 to 35 years of age. J Orofac Pain 14:310–319
2. Moen K, Hellem S, Geitung JT, Skartveit L (2010) A practical approach to interpretation of MRI of the temporomandibular joint. Acta Radiol 51:1021–1027
3. Cannizzaro E, Schroeder S, Muller LM, Kellenberger CJ, Saurenmann RK (2011) Temporomandibular joint involvement in children with juvenile idiopathic arthritis. J Rheumatol 38:510–515
4. Abramowicz S, Cheon JE, Kim S, Bacic J, Lee EY (2011) Magnetic resonance imaging of temporomandibular joints in children with arthritis. J Oral Maxillofac Surg 69:2321–2328
5. Müller L, Kellenberger CJ, Cannizzaro E et al (2009) Early diagnosis of temporomandibular joint involvement in juvenile idiopathic arthritis: a pilot study comparing clinical examination and ultrasound to magnetic resonance imaging. Rheumatology (Oxford) 48:680–685
6. Lewis EL, Dolwick MF, Abramowicz S, Reeder SL (2008) Contemporary imaging of the temporomandibular joint. Dent Clin North Am 52:875–890
7. Boyesen P, Haavardsholm EA, van der Heijde D et al (2011) Prediction of MRI erosive progression: a comparison of modern imaging modalities in early rheumatoid arthritis patients. Ann Rheum Dis 70:176–179
8. Lee EY, Sundel RP, Kim S, Zurakowski D, Kleinman PK (2008) MRI findings of juvenile psoriatic arthritis. Skeletal Radiol 37:987–996
9. McGibbon CA, Bencardino J, Yeh ED, Palmer WE (2003) Accuracy of cartilage and subchondral bone spatial thickness distribution from MRI. J Magn Reson Imaging 17:703–715
10. Reichert IL, Benjamin M, Gatehouse PD et al (2004) Magnetic resonance imaging of periosteum with ultrashort TE pulse sequences. J Magn Reson Imaging 19:99–107
11. Phan CM, Matsuura M, Bauer JS et al (2006) Trabecular bone structure of the calcaneus: comparison of MR imaging at 3.0 and 1.5 T with micro-CT as the standard of reference. Radiology 239:488–496
12. McGibbon CA, Dupuy DE, Palmer WE, Krebs DE (1998) Cartilage and subchondral bone thickness distribution with MR imaging. Acad Radiol 5:20–25
13. European Union (2002) Additional protocol to the convention on human rights and biomedicine, on transplantation of organs and tissues of human origin. ETS 186, Article 16–18
14. Swiss Academy of Medical Science (2008) Verwendung von Leichen und Leichenteilen in der medizinischen Forschung sowie Aus-, Weiter- und Fortbildung. Medical–Ethical Guidelines and Recommendations, pp 1–11
15. Tasali N, Cubuk R, Aricak M et al (2011) Temporomandibular joint (TMJ) pain revisited with dynamic contrast-enhanced magnetic resonance imaging (DCE-MRI). Eur J Radiol. doi:10.1016/j.ejrad.2011.01.044
16. McGibbon CA (2003) Inter-rater and intra-rater reliability of subchondral bone and cartilage thickness measurement from MRI. Magn Reson Imaging 21:707–714
17. McGibbon CA, Bencardino J, Palmer WE (2003) Subchondral bone and cartilage thickness from MRI: effects of chemical-shift artifact. MAGMA 16:1–9
18. Peh WC, Chan JH (2001) Artifacts in musculoskeletal magnetic resonance imaging: identification and correction. Skeletal Radiol 30:179–191
19. Zand KR, Reinhold C, Haider MA, Nakai A, Rohoman L, Maheshwari S (2007) Artifacts and pitfalls in MR imaging of the pelvis. J Magn Reson Imaging 26:480–497
20. Louis O, Cattrysse E, Scafoglieri A, Luypaert R, Clarys JP, de Mey J (2010) Accuracy of peripheral quantitative computed tomography and magnetic resonance imaging in assessing cortical bone cross-sectional area: a cadaver study. J Comput Assist Tomogr 34:469–472
21. Issever AS, Link TM, Newitt D, Munoz T, Majumdar S (2010) Interrelationships between 3-T-MRI-derived cortical and trabecular bone structure parameters and quantitative-computed-tomography-derived bone mineral density. Magn Reson Imaging 28:1299–1305
22. Stehling C, Vieth V, Bachmann R et al (2007) High-resolution magnetic resonance imaging of the temporomandibular joint: image quality at 1.5 and 3.0 Tesla in volunteers. Invest Radiol 42:428–434

ASSESSING THE LENGTH OF THE MANDIBULAR RAMUS AND THE CONDYLAR PROCESS: A COMPARISON OF OPG, CBCT, CT, MRI AND LATERAL CEPHALOMETRIC MEASUREMENTS

ASSESSING THE LENGTH OF THE MANDIBULAR RAMUS AND THE CONDYLAR PROCESS: A COMPARISON OF OPG, CBCT, CT, MRI AND LATERAL CEPHALOMETRIC MEASUREMENTS

G. Markic†, L. Müller†, R. Patcas, M. Roos, N. Lochbühler, T. Peltomäki, C. A. Karlo, O. Ullrich and C. J. Kellenberger

† These authors contributed equally to the accomplishment of the manuscript.

Corresponding author:
Dr. Goran Markic
Clinic for Orthodontics and Pediatric Dentistry, Center of Dental Medicine
University of Zurich, Plattenstrasse 11, 8032 Zurich, Switzerland
e-mail: goran.markic@zzm.uzh.ch tel.: + 41 44 634 33 79

Affiliation of authors:
Goran Markic, Clinic for Orthodontics and Pediatric Dentistry, Center of Dental Medicine, University of Zurich, Switzerland; e-mail: goran.markic@zzm.uzh.ch

Lukas Müller, Clinic for Orthodontics and Pediatric Dentistry, Center of Dental Medicine, University of Zurich, Switzerland; e-mail: lukas.mueller@zzm.uzh.ch

Raphael Patcas, Clinic for Orthodontics and Pediatric Dentistry, Center of Dental Medicine, University of Zurich, Switzerland email: raphael.patcas@zzm.uzh.ch

Malgorzata Roos, Division of Biostatistics, ISPM, University of Zurich, Switzerland; e-mail: mroos@ifspm.uzh.ch

Nina Lochbühler, Department of Diagnostic Imaging, University Children's Hospital Zurich, Zurich, Switzerland; e-mail: nina.lochbuehler@vr-web.de

Timo Peltomäki, Dental and Oral Diseases Outpatient Clinic, Oral and Maxillofacial Unit, Tampere University Hospital and Department of Otolaryngology, University of Tampere, Tampere, Finland; e-mail: timo.peltomaki@pshp.fi

Christoph A. Karlo, Institute of Diagnostic and Interventional Imaging, University Hospital Zurich, Zurich, Switzerland; e-mail: christoph.karlo@usz.ch

Oliver Ullrich, Institute of Anatomy, Faculty of Medicine, University of Zurich, Switzerland; e-mail: oliver.ullrich@anatom.uzh.ch

Christian J. Kellenberger, Department of Diagnostic Imaging, University Children's Hospital, Zurich, Switzerland; e-mail: christian.kellenberger@kispi.uzh.ch

SUMMARY

BACKGROUND/OBJECTIVES The aim of this study was to compare different imaging procedures (cone beam computed tomography (CBCT), computed tomography (CT), magnetic resonance imaging (MRI), orthopantomography (OPG) and lateral cephalometry (LC)) for assessment of mandibular height (RH) and condylar process (CP) length as they reflect mandibular growth.

MATERIALS/METHODS RH and CP were taken on 8 cadaver heads, each side separately, on CBCT, CT, MRI, OPG and LC. They were measured twice by two independent observers parallel to the posterior border of the mandibular ramus. Intraclass correlation coefficient (ICC) was used to assess inter- and intraobserver reliability. Coefficient of variation was used to investigate precision. Bland-Altman (BA) plots assessed agreement of procedures.

RESULTS All procedures except LC showed good intra- and interobserver reliability with excellent agreement (ICC >0.9). BA-Plot-Analysis for CP and RH showed similar ranges of agreement between MRI, CT and CBCT (maximum 5.5mm), but higher ranges for OPG and LC. MRI and OPG values were generally smaller.

CONCLUSIONS/IMPLICATIONS All 3D imaging procedures were almost equal for measuring of CP and RH. MRI is recommended since it avoids ionizing radiation and shows higher sensitivity in detection of inflammation. A two-year threshold for detecting growth in follow-up has to be taken into account for all 3D imaging methods. RH is recommended for follow-up of condylar growth, since reference values for annual increments are published. MRI measurements were generally smaller than those obtained by CT and CBCT. OPG and LC showed weak measuring performance in terms of accuracy and reliability for either RH or CP.

Introduction

The condylar cartilage is a major growth site of the mandible. Changes in lengths of mandibular ramus and condylar process either reflect mandibular growth (Buschang *et al.*, 1999, Riolo and Michael, 1974, Savara and Tracy, 1967, Tracy and Savara, 1966) or pathological processes in the temporomandibular joint (TMJ) (Pirttiniemi *et al.*, 2009).

Juvenile idiopathic arthritis (JIA) is the most common rheumatic disease in childhood (Gare, 1996), which can severely damage all involved joints and cause short- and long-term disabilities (Weiss and Ilowite, 2005). All synovial joints can be affected including the TMJ (Pedersen *et al.*, 2001, Pirttiniemi *et al.*, 2009, Ronning *et al.*, 1974, Still, 1897, Twilt *et al.*, 2004). The rate of TMJ involvement in patients with JIA varies from 17% to 87% depending on the examination method and the population being studied (Kuseler *et al.*, 1998, Mayne and Hatch, 1969, Ronning *et al.*, 1974).

TMJ arthritis leads both to masticatory dysfunction and mandibular growth disturbances (Bache, 1964, Kjellberg, 1995, Ronchezel *et al.*, 1995, Ronning *et al.*, 1994, Stabrun, 1991) resulting in craniofacial dysmorphology and dental malocclusion (Karhulahti *et al.*, 1993, Larheim and Haanaes, 1981, Ronning and Valiaho, 1981, Svensson *et al.*, 2001), including posterior rotated, retrognathic mandibles with overall small dimensions usually in combination with a dental angle class II/1 with increased overjet and anterior open bite (Bache, 1964, Barriga *et al.*, 1974, Jamsa and Ronning, 1985, Kreiborg *et al.*, 1990, Larheim and Haanaes, 1981). Unilateral TMJ arthritis, occurring with a rate of 40-50% (Pedersen *et al.*, 2001, Twilt *et al.*, 2004), can result in facial and dental asymmetries (Karhulahti *et al.*, 1990, Twilt *et al.*, 2004) increasing with longer disease duration (Karhulahti *et al.*, 1990, Kjellberg *et al.*, 1995, Stabrun *et al.*, 1988, Twilt *et al.*, 2004, Twilt *et al.*, 2003).

Condylar growth is an important indicator for therapeutic success. Not only inflammatory processes, but also some treatment strategies, such as intra-articular corticosteroid injections, were lately considered to reduce or stop condylar growth

(Stoustrup *et al.*, 2008). Condylar process and ramus height of JIA patients have been measured by different radiographic techniques (Kjellberg *et al.*, 1994, Kjellberg *et al.*, 1995, Stoustrup *et al.*, 2008, Stoustrup *et al.*, 2013, Twilt *et al.*, 2006), all exposing patients to ionising radiation. Computed tomography (CT) is considered the gold standard for bony measurements, but it also involves the highest radiation exposure, which should be avoided in growing individuals due to the increased risk of developing cancer (Boice *et al.*, 1991, Cardis *et al.*, 2005, Claus *et al.*, 2012, Einstein, 2012, Pearce *et al.*, 2012, Preston *et al.*, 1994).

Magnetic resonance imaging (MRI), on the other hand, doesn't expose patients to ionizing radiation and is considered the gold standard for early diagnosis of TMJ arthritis and deformation with high sensitivity compared to radiography (Kuseler *et al.*, 2005, Muller *et al.*, 2009, Pedersen *et al.*, 2008), making it an adequate mean for both initial assessment and follow-up of children with JIA.

The aim of this study was to compare the following imaging procedures for measuring the lengths of mandibular ramus and condylar process: Cone beam computed tomography (CBCT), CT, MRI, orthopantomography (OPG) and lateral cephalometry (LC). Our hypothesis was that MRI is an adequate method to replace radiographic procedures for ramus height and condylar process measurements.

Material and Methods

Material

Eight intact cadaveric human heads (5 women, 3 men; age range of 65-95 years) were acquired through a voluntary body donation program of the local anatomical institute, on the basis of an informed consent in accordance with state and federal regulations, the convention on human rights and medicine (Council of Europe, 2002) and the recommendation of the national academy of medical science. Within 4 days after decease the perfusion of the cadaveric heads was carried out with

a fixation liquid consisting of 2 parts of alcohol (70%), 1 part of glycerine and 2% almudor (containing 8.1% formaldehyde, 10% glyoxal and 3.7% glutaraldehyde).

Image data acquisition

For each cadaveric head digital CBCT, CT, MRI and OPG datasets were obtained and an analogue lateral cephalogram was taken. If necessary, the procedure was repeated until good quality was achieved.

The CT data were obtained on a commercially available 40 detector row CT system (Brilliance CT 40, Philips Healthcare, Eindhoven, the Netherlands) with the following scan parameters, which were identical for all specimens and correspond to usual clinical settings: tube voltage, 120 kV; tube current time product, 70 mAs; slice collimation, 20 x 0.625mm; pitch, 0.68; reconstruction slice thickness, 0.67 mm; reconstruction increment, 0.33 mm; window level setting, 2000/500 HU; voxel size, 0.39mm (x), 0.39mm (y) and 0.67mm (z); exposition time, 4.5 s.

The CBCT data were acquired using KaVo 3D eXam (KaVo Dental AG, Brugg, Switzerland) with the following scan parameters (tube current, 5mA; tube voltage, 120 KV; FOV, 100mm, landscape mode; reconstruction slice thickness, 0.4 mm; reconstruction increment, 0.4 mm; isotropic voxel size, 0.4mm (x,y,z); exposition time, 4 s), which are also routinely used and show a good balance between exposure to ionizing radiation, image quality and resolution for this size of field of view.

Every MRI of the TMJs was performed on a commercially available 1.5 Tesla scanner (Signa HDx, General Electric, Milwaukee, WI, USA) with a commercially available TMJ surface coil. Sagittal oblique, T1-weighted 3D fast spoiled gradient echo sequences were acquired separately for each side (i.e. left and right) parallel to the respective mandibular ramus with the following imaging parameters: flip angle, 20°; TR, 11.6 ms; TE, 4.1 ms; bandwidth, 15.63 kHz; NEX, 3; FOV, 10 cm^2; matrix, 256 x 192; slice thickness, 2 mm; spacing, 1 mm.

The OPG was produced using Cranex 3+ (SOREDEX, Tuusula, Finland) with the following settings: tube current, 6mA; tube voltage, 65 kV; exposition time, 20 s at 50 Hz; inherent filtration, 1.8mm AI; total filtration, 2.7mm AI.

The lateral cephalograms were taken on a custom-made X-Ray unit (COMET, 3175 Flamatt, Switzerland) with the following settings: tube current, 250 mA; tube voltage, 67 kV; tube current time product, 10mAs; exposition time, 0.04 s. The position of the head with the Frankfort plane parallel to the floor was fixed using ear rods and a nasal pointer. The focus-median plane distance was 200 cm, film-median plane distance was 15 cm (enlargement 7.5%).

Image data analysis

From the 3D datasets (CT, CBCT and MRI), projection images of the mandibular ramus and condyle were reconstructed with commercially available image processing software, using maximum-intensity projection for CT and CBCT, and minimum-intensity projection for MRI data. The orientation of the projection images was standardised to intersect the center of the condylar process, the coronoid process and the gonial angle (Figure 1). The slice thickness was defined as the smallest thickness, where the most cranial condylar point, the most caudal gonial point and the deepest point of the incisura mandibulae were included (Figure 1). The resulting projection images as well as the unchanged 2D image of the OPG were analysed on a high resolution diagnostic workstation (dx IDS5, Sectra PACS, Linköping, Sweden).

The analogue lateral cephalograms were hand-traced using a 0.3 mm lead on a 0.10 mm matte acetate tracing paper.

Tracing LCs as well as obtaining and measuring the projection images was each performed by two observers (C. K. and N. L. for MRI and CT; L. M. and G. M. for CBCT and LC) and repeated twice with an interval of at least 3 weeks. The observers were blinded for all other first and second tracings, images and measurements.

Measurements

For every image and every side three points (Co, Go and In) were defined and two linear measurements were performed parallel to the tangent at the posterior border of the Ramus (Figure 2):

- ***Ramus height (RH)*:** Measured between the most cranial point of the condyle (Co) and the intersection point with the lower border of the ramus mandibulae, the gonial point (Go). The intersection with the lower border of the ramus mandibulae was obtained using a line parallel to the tangent at the posterior border of the ramus and going through the most cranial point of the condyle (Co).
- ***Height of the condylar process (CP):*** Measured between the most cranial point of the condyle (Co) and the most caudal point of incisura mandibulae (In).

Calibration, construction of reference lines, landmark definition and distance measurements of all CBCT, CT, MRI and OPG images were performed digitally.

The same construction lines and landmarks were defined on LC tracings. Landmarks on LC were digitized using tablet digitizer NumonicsAccuGrid (Numonics, Landsdale, PA, USA) with a resolution of 1 mil. The distances were computed and corrected for enlargement using Excel 2010 (version 14.0.6112.5000, Redmond, USA).

Statistical Analysis

Standard statistical software packages SPSS version 20.0.0 (Chicago, Ill, USA), STATA version 10.1 (Texas, USA) and MedCalc version 12.2.1.0.-64bit (Mariakerke, Belgium) were used for statistical analysis.

Intra- and interobserver reliability were assessed using intraclass correlation coefficient (ICC) based on results of procedure “xtreg” in STATA for each imaging method separately.

The values used in the assessment of agreement were computed as follows: for each linear measurement the mean of the four values (double measurements of two

observers) was taken. This resulted in 16 values (left and right sides together) per linear measurement (RH and CP separately) with exception of the LC values. Because on a LC the left and right side could not be distinguished, the mean of left and right side values were taken resulting in only 8 values per measurement type. Measurements on the left and right side were considered to be independent. To assess the agreement between imaging methods for each measurement type Bland-Altman-Plots (BA-Plots) (Bland and Altman, 1986, Bland and Altman, 1999) with 95% limits of agreement extended by 95% confidence interval for mean difference (paired t-test) were computed. In addition, in order to facilitate interpretation, the range for the 95% limits of agreement (upper - lower) was provided.

To assess precision of measurements the coefficient of variation (CV) was computed for RH and CP separately. Computation of mean and SD was based on the four values of a linear measurement (double measurements of the two observers). CV was computed according to formula ($CV = \frac{SD}{\text{mean length}}$).

Descriptive statistics for CV with respect to RH and CP were computed separately. Shapiro-Wilk and Kolmogorov-Smirnov tests were used to check normality assumptions. Differences in mean CV between imaging methods were assessed using one-way ANOVA with Scheffé post-hoc after log-transformation assuring normal distribution. Differences between RH and CP were evaluated by two-sample t-test for each imaging method separately.

Results of statistical analysis with p-values smaller than 0.05 were considered to be statistically significant.

Results

Intra- and interobserver reliability (Table 1) showed excellent agreement (ICC >0.90) for all procedures with exception of LC. The highest ICC values were computed for OPG closely followed by CBCT, CT and MRI. ICC values for CP and interobserver ICC were generally smaller. LC values for CP (Intraobserver ICC: 0.79,

interobserver ICC: 0.59) and interobserver ICC for RH (0.82) were far below all other methods.

Agreement judged in terms of BA-Plot-Analysis (Table 2, Figure 3) showed similar ranges of agreement between MRI, CT and CBCT for CP and RH: MRI and CT RH (4.4mm) and CP (1.9mm), MRI and CBCT RH (4.4mm) and CP (5.5mm) and CT and CBCT RH (5.1mm) and CP (4.8mm). MRI and OPG measurements for RH and CP were significantly smaller than the measurements of all other imaging methods. OPG measurements were even significantly smaller than those obtained on MRI. Mean differences between MRI and CT measurements (MRI minus CT) were -1.4mm for RH and -1.2mm for CP. Mean differences between MRI and CBCT measurements (MRI minus CBCT) were -1.9mm for RH and -1.1mm for CP. OPG and LC showed least agreement with measurements based on 3D datasets and showed the widest limits of agreement.

Measurement precision judged in terms of CV for both measurements (RH and CP) showed highest precision with OPG followed in descending order by CBCT, CT, MRI and LC (Table 3, Figure 4). For RH only LC and for CP both LC and MRI were significantly less precise than the other imaging methods (Table 3). LC was significantly less precise than MRI for the CP measurements.

Discussion

The aim of the study was to determine if MRI is applicable to replace radiographic procedures for the assessment of mandibular growth. Our results show that measurements of the mandibular ramus and condylar process with MRI are comparable to CT and CBCT in terms of precision, intra- and interobserver reliability and agreement. For JIA patients with TMJ arthritis we suggest therefore to use MRI to quantitatively follow condylar growth by measuring ramus height and condylar process length, which are important indicators for long-term therapeutic success (Abramowicz *et al.*, 2011, Kuseler *et al.*, 1998, Savara and Tracy, 1967, Tracy and

Savara, 1966, Weiss *et al.*, 2008). Using only MRI for the follow-up of children with JIA would reduce costs and avoid the exposure to ionising radiation with potential harm to growing children (Claus *et al.*, 2012, Pearce *et al.*, 2012). Our results are in concordance with a recently published study that found equally and highly precise quantitative measurements on MRI, CT and CBCT (Gaudino *et al.*, 2011).

Measurements with MRI were generally smaller than with CT (RH: -1.4mm; CP: -1.2mm) and CBCT (RH: -1.9mm; CP: -1.1mm). This has to be taken into consideration when MRI measurements are compared to data and reference values based on other imaging procedures (Kjellberg *et al.*, 1994, Kjellberg *et al.*, 1995, Stoustrup *et al.*, 2008, Stoustrup *et al.*, 2013, Twilt *et al.*, 2006). Therefore these imaging methods (CT, CBCT and MRI) are interchangeable, but not directly comparable without correction for length differences. Due to the different mode of operation and data acquisition, MRI depicts different structures compared to 3-dimensional radiographic methods (CT and CBCT) (Gore *et al.*, 1981).

The CV quantifies precision as the fraction of the standard deviation relative to the mean length and is mathematically described as $CV = \frac{SD}{\text{mean length}}$. In contrast to RH, CP data show significantly elevated CV estimates proving inferior accuracy of the CP measurements with respect to the mean CP length (Figure 4). However, it has to be kept in mind that CV values below 5% show very good precision and therefore significant differences between RH and CP are below clinical relevance.

When looking at BA-plots, the range of agreement of all 3D imaging (CT, CBCT and MRI) methods was similar with a maximum range of agreement of 5.5mm. This corresponds to a probability of 95% (±1.96 SD) of agreement of measurements between two imaging methods to be within 5.5mm. Comparison with the anatomical truth would have been ideal. Since the construction and measurement protocol is difficult to simulate with a calliper on an anatomical specimen, obtaining comparable measurements would have been difficult and within certain limits of agreement, too. The range of agreement has also to be taken into consideration, when following growth longitudinally. In a growing individual an uncertainty of 5.5mm

corresponds to at least 2 years of growth, when assuming a mean condylar growth of 2mm to 3mm per year (Bjork, 1968, Buschang *et al.*, 1999). Therefore longitudinal follow-up of at least 2 years for all 3D imaging methods is necessary for conclusive information about condylar growth. In JIA cases MRI has two main advantages over radiologic procedures. First of all, it does not expose patients to ionizing radiation and secondly it shows high sensitivity for detection of inflammation (Kuseler *et al.*, 2005, Muller *et al.*, 2009, Pedersen *et al.*, 2008).

When measuring RH and CP bone remodelling has to be taken into consideration, which take place both at the gonial angle and the incisura mandibulae, affecting both RH and CP. RH as an outcome parameter might pretend condylar growth because of appositional processes at the gonial angle. JIA patients with TMJ arthritis often show a growth pattern with posterior rotation, which is associated with bony apposition at the gonial angle and antegonial notching (Bjork and Skieller, 1983, Jamsa and Ronning, 1985, Kreiborg *et al.*, 1990). Therefore, the differences in RH have to be interpreted with caution. Similarly, the measure of CP is influenced not only by condylar growth but also by physiological bony apposition at the incisura mandibulae (Bjork, 1963, Bjork and Skieller, 1983, Buschang *et al.*, 1999). A superimposition of 3D datasets relative to stable structures (Bjork, 1968, Bjork and Skieller, 1983, Buschang *et al.*, 1999) may be a possibility to assess not only the true amount of condylar growth, but also its direction. Nevertheless, annual increments for ramus height from three to sixteen years have been published for girls (Tracy and Savara, 1966) and boys (Savara and Tracy, 1967) and show clearly that grow is measurable using RH. Reference values for CP are, to the knowledge of the authors, not published in the literature.

Although the OPG provides best precision and reliability data, it shows poor agreement with the 3D procedures (CT, CBCT and MRI). The cause for this discrepancy is most likely the study protocol and demonstrates a limitation of our study. All 2D images and 3D datasets were generated only once and all further processing was based on these data. For 3D imaging and lateral cephalometric

images positioning of the specimen has very little effect. The OPG however is highly sensitive to positioning issues leading to magnification errors and disproportional enlargement (Habets *et al.*, 1987, McDavid *et al.*, 1981, Schulze *et al.*, 2000a, Schulze *et al.*, 2000b, Updegrave, 1971, Yeo *et al.*, 2002). Vertical measurements seem to be more accurate than horizontal and angular ones. Anyhow they are still prone to fail to represent anatomical truth (Van Elslande *et al.*, 2008). Positioning of the specimen in the OPG machine was adjusted until images of good quality were produced. Therefore constructions and landmark definitions were unambiguously leading to very high precision and reliability of the measurements. Although this is a weakness of this study, it shows that this part of the protocol can be carried out with very high precision and reproducibility. But when assessing agreement between OPG and 3D imaging measurements, the positioning issue with distortion became evident. Agreement was poor with the widest limits of agreement. Moreover, all measurements were significantly smaller and variation in magnification between devices is a known issue (Van Elslande *et al.*, 2008). The variation due to repeated positioning and picture recording could not be evaluated with our study protocol. Unfortunately, when the OPG data were evaluated, the specimens had already been dissected for further investigations and were therefore no longer usable for a repeated OPG study.

Lateral cephalogram measurements showed the worst results in precision, which were statistically and clinically significant. Intra- and interobserver reliability were far below all other imaging methods, especially for CP. Limits of agreement showed a very heterogeneous picture with partially very wide limits of agreement with 3D imaging methods. In contrast to the 3D imaging techniques, lateral cephalogram is a classical 2D radiograph, where the 3D structures are projected into a 2D plane. This makes it difficult and often almost impossible to distinguish either side and complicates landmark definitions due to overprojecting structures. This is especially true for the condylar point and the deepest point of the incisura mandibulae. The latter is determined by the edge of a narrowly tapered and thin

bone formation, which is rendered as a density gradient. This makes a clear distinction between bone and soft tissue very difficult. A similar situation is evident for the condylar point being superimposed by dense bony structures of the cranial base. The gonial point on the other hand has a clear edge between compact bone and soft tissue resulting in a clear step in density, but its position depends highly on the condylar point for its construction.

A limitation of our study is the small sample size. Since the voluntary body donation program of the local university has limited material and provides preparations for various teaching and research projects, not more than 8 unmitigated cadaveric heads could be provided for our study. However, although the power of the study may be reduced, the results provided are conclusive for the hypothesis tested.

Conclusions

- All 3D imaging procedures were almost equal for measuring of CP and RH with differences in agreement and precision below clinical relevance. MRI is recommended since it is not only an equal alternative for CT and CBCT, but also avoids ionizing radiation and shows higher sensitivity in detection of inflammation (Kuseler *et al.*, 2005, Muller *et al.*, 2009, Pedersen *et al.*, 2008), which is especially important for JIA patients.
- The maximum range of limits of agreement for all 3D imaging procedures for RH and CP corresponds to approximately the length difference of average condylar growth during two years (Bjork, 1963, Bjork, 1968, Buschang *et al.*, 1999). Therefore a two-year threshold for detecting growth in follow-up has to be taken into account for all 3D imaging methods.
- Since reference values for annual increments are published for RH (Savara and Tracy, 1967, Tracy and Savara, 1966), but not for CP, RH is recommended for follow-up of condylar growth.

- MRI measurements were generally smaller than those obtained by CT and CBCT, which makes them not directly comparable. This has to be taken into consideration when comparing MRI to data based on other imaging procedures.
- The susceptibility of OPG to head positioning leads to bad agreement with the 3D imaging procedures and the overall poor results of LC make it impossible to measure either RH or CP accurately and reliably enough.

References

Abramowicz S, Cheon J E, Kim S, Bacic J, Lee E Y 2011 *Magnetic resonance imaging of temporomandibular joints in children with arthritis.* Journal of Oral and Maxillofacial Surgery 69: 2321-2328

Bache C 1964 *Mandibular Growth and Dental Occlusion in Juvenile Rheumatoid Arthritis.* Acta rheumatologica Scandinavica 10: 142-153

Barriga B, Lewis T M, Law D B 1974 *An investigation of the dental occlusion in children with juvenile rheumatoid arthritis.* The Angle Orthodontist 44: 329-335

Bjork A 1963 *Variations in the growth pattern of the human mandible: longitudinal radiographic study by the implant method.* Journal of Dental Research 42(1)Pt 2: 400-411

Bjork A 1968 *The use of metallic implants in the study of facial growth in children: method and application.* American Journal of Physical Anthropology 29: 243-254

Bjork A, Skieller V 1983 *Normal and abnormal growth of the mandible. A synthesis of longitudinal cephalometric implant studies over a period of 25 years.* European Journal of Orthodontics 5: 1-46

Bland J M, Altman D G 1986 *Statistical methods for assessing agreement between two methods of clinical measurement.* The Lancet 1: 307-310

Bland J M, Altman D G 1999 *Measuring agreement in method comparison studies.* Statistical Methods in Medical Research 8: 135-160

Boice J D, Jr., Preston D, Davis F G, Monson R R 1991 *Frequent chest X-ray fluoroscopy and breast cancer incidence among tuberculosis patients in Massachusetts.* Radiation Research 125: 214-222

Buschang P H, Santos-Pinto A, Demirjian A 1999 *Incremental growth charts for condylar growth between 6 and 16 years of age.* European Journal of Orthodontics 21: 167-173

Cardis E, Vrijheid M, Blettner M, Gilbert E, Hakama M, Hill C, Howe G, Kaldor J, Muirhead C R, Schubauer-Berigan M, *et al.* 2005 *Risk of cancer after low doses of ionising radiation: retrospective cohort study in 15 countries.* Bmj 331: 77

Claus E B, Calvocoressi L, Bondy M L, Schildkraut J M, Wiemels J L, Wrensch M 2012 *Dental x-rays and risk of meningioma.* Cancer 118: 4530-4537

Council of Europe 2002 *Additional protocol to the Convention on human rights and biomedicine concerning transplantation of organs and tissues of human origin Strasbourg*, 24.1.2002 Council of Europe, Strasbourg

Einstein A J 2012 *Effects of radiation exposure from cardiac imaging: how good are the data? Journal of the American College of Cardiology* 59: 553-565

Gare B A 1996 *Epidemiology of rheumatic disease in children.* Current Opinion in Rheumatology 8: 449-454

Gaudino C, Cosgarea R, Heiland S, Csernus R, Beomonte Zobel B, Pham M, Kim T S, Bendszus M, Rohde S 2011 *MR-Imaging of teeth and periodontal apparatus: an experimental study comparing high-resolution MRI with MDCT and CBCT.* European Radiology 21: 2575-2583

Gore J C, Emery E W, Orr J S, Doyle F H 1981 *Medical nuclear magnetic resonance imaging: I. Physical principles.* Investigative Radiology 16: 269-274

Habets L L, Bezuur J N, van Ooij C P, Hansson T L 1987 *The orthopantomogram, an aid in diagnosis of temporomandibular joint problems.* I. The factor of vertical magnification. Journal of Oral Rehabilitation 14: 475-480

Jamsa T, Ronning O 1985 *The facial skeleton in children affected by rheumatoid arthritis--a roentgen-cephalometric study.* European Journal of Orthodontics 7: 48-56

Karhulahti T, Ronning O, Jamsa T 1990 *Mandibular condyle lesions, jaw movements, and occlusal status in 15-year-old children with juvenile rheumatoid arthritis.* Scandinavian Journal of Dental Research 98: 17-26

Karhulahti T, Ylijoki H, Ronning O 1993 *Mandibular condyle lesions related to age at onset and subtypes of juvenile rheumatoid arthritis in 15-year-old children.* Scandinavian Journal of Dental Research 101: 332-338

Kjellberg H 1995 *Juvenile chronic arthritis. Dentofacial morphology, growth, mandibular function and orthodontic treatment.* Swedish Dental Journal. Supplement 109: 1-56

Kjellberg H, Ekestubbe A, Kiliaridis S, Thilander B 1994 *Condylar height on panoramic radiographs. A methodologic study with a clinical application.* Acta Odontologica Scandinavica 52: 43-50

Kjellberg H, Fasth A, Kiliaridis S, Wenneberg B, Thilander B 1995 *Craniofacial structure in children with juvenile chronic arthritis (JCA) compared with healthy children with ideal or postnormal occlusion.* American Journal of Orthodontics and Dentofacial Orthopedics 107: 67-78

Kreiborg S, Bakke M, Kirkeby S, Michler L, Vedtofte P, Seidler B, Moller E 1990 *Facial growth and oral function in a case of juvenile rheumatoid arthritis during an 8-year period.* European Journal of Orthodontics 12: 119-134

Kuseler A, Pedersen T K, Gelineck J, Herlin T 2005 *A 2 year followup study of enhanced magnetic resonance imaging and clinical examination of the temporomandibular joint in children with juvenile idiopathic arthritis.* The Journal of Rheumatology 32: 162-169

Kuseler A, Pedersen T K, Herlin T, Gelineck J 1998 *Contrast enhanced magnetic resonance imaging as a method to diagnose early inflammatory changes in the temporomandibular joint in children with juvenile chronic arthritis.* The Journal of Rheumatology 25: 1406-1412

Larheim T A, Haanaes H R 1981 *Micrognathia, temporomandibular joint changes and dental occlusion in juvenile rheumatoid arthritis of adolescents and adults.* Scandinavian Journal of Dental Research 89: 329-338

Mayne J G, Hatch G S 1969 *Arthritis of the temporomandibular joint.* Journal of the American Dental Association 79: 125-130

McDavid W D, Tronje G, Welander U, Morris C R 1981 *Effects of errors in film speed and beam alignment on the image layer in rotational panoramic radiography.* Oral Surgery, Oral Medicine, Oral Pathology 52: 561-564

Muller L, Kellenberger C J, Cannizzaro E, Ettlin D, Schraner T, Bolt I B, Peltomaki T, Saurenmann R K 2009 *Early diagnosis of temporomandibular joint involvement in juvenile idiopathic arthritis: a pilot study comparing clinical examination and ultrasound to magnetic resonance imaging.* Rheumatology 48: 680-685

Pearce M S, Salotti J A, Little M P, McHugh K, Lee C, Kim K P, Howe N L, Ronckers C M, Rajaraman P, Sir Craft A W, *et al.* 2012 *Radiation exposure from CT scans in childhood and subsequent risk of leukaemia and brain tumours: a retrospective cohort study.* The Lancet 380: 499-505

Pedersen T K, Jensen J J, Melsen B, Herlin T 2001 *Resorption of the temporomandibular condylar bone according to subtypes of juvenile chronic arthritis.* The Journal of Rheumatology 28: 2109-2115

Pedersen T K, Kuseler A, Gelineck J, Herlin T 2008 *A prospective study of magnetic resonance and radiographic imaging in relation to symptoms and clinical findings of the temporomandibular joint in children with juvenile idiopathic arthritis.* The Journal of Rheumatology 35: 1668-1675

Pirttiniemi P, Peltomaki T, Muller L, Luder H U 2009 *Abnormal mandibular growth and the condylar cartilage.* European Journal of Orthodontics 31: 1-11

Preston D L, Kusumi S, Tomonaga M, Izumi S, Ron E, Kuramoto A, Kamada N, Dohy H, Matsuo T, Matsui T, *et al.* 1994 *Cancer incidence in atomic bomb survivors. Part III. Leukemia, lymphoma and multiple myeloma, 1950-1987.* Radiation Research 137: S68-97

Riolo M L, Michael L 1974 *Atlas of craniofacial growth cephalometric standards from the University School Growth Study, the University of Michigan University of Michigan.* Center for Human Growth and Development, Ann Arbor, Mich.

Ronchezel M V, Hilario M O, Goldenberg J, Lederman H M, Faltin K, Jr., de Azevedo M F, Naspitz C K 1995 *Temporomandibular joint and mandibular growth alterations in patients with juvenile rheumatoid arthritis.* The Journal of Rheumatology 22: 1956-1961

Ronning O, Barnes S A, Pearson M H, Pledger D M 1994 *Juvenile chronic arthritis: a cephalometric analysis of the facial skeleton.* European Journal of Orthodontics 16: 53-62

Ronning O, Valiaho M L 1981 *Progress of mandibular condyle lesions in juvenile rheumatoid arthritis. Proceedings of the Finnish Dental Society.* Suomen Hammaslaakariseuran toimituksia 77: 151-157

Ronning O, Valiaho M L, Laaksonen A L 1974 *The involvement of the temporomandibular joint in juvenile rheumatoid arthritis.* Scandinavian Journal of Rheumatology 3: 89-96

Savara B S, Tracy W E 1967 *Norms of size and annual increments for five anatomical measures of the mandible in boys from three to sixteen years of age.* Archives of Oral Biology 12: 469-486

Schulze R, Krummenauer F, Schalldach F, d'Hoedt B 2000a *Precision and accuracy of measurements in digital panoramic radiography.* Dentomaxillofacial Radiology 29: 52-56

Schulze R, Schalldach F, d'Hoedt B 2000b *Effect of positioning errors on magnification factors in the mandible in digital panorama imaging.* Mund-, Kiefer- und Gesichtschirurgie 4: 164-170

Stabrun A E 1991 *Impaired mandibular growth and micrognathic development in children with juvenile rheumatoid arthritis.* A longitudinal study of lateral cephalographs. European Journal of Orthodontics 13: 423-434

Stabrun A E, Larheim T A, Hoyeraal H M, Rosler M 1988 *Reduced mandibular dimensions and asymmetry in juvenile rheumatoid arthritis. Pathogenetic factors.* Arthritis & Rheumatism 31: 602-611

Still G F 1897 On a Form of Chronic Joint Disease in Children. Medico-Chirurgical Transactions 80: 47-60 49

Stoustrup P, Kristensen K D, Kuseler A, Gelineck J, Cattaneo P M, Pedersen T K, Herlin T 2008 *Reduced mandibular growth in experimental arthritis in the temporomandibular joint treated with intra-articular corticosteroid.* European Journal of Orthodontics 30: 111-119

Stoustrup P, Kuseler A, Kristensen K D, Herlin T, Pedersen T K 2013 *Orthopaedic splint treatment can reduce mandibular asymmetry caused by unilateral temporomandibular involvement in juvenile idiopathic arthritis.* European Journal of Orthodontics 35: 191-198

Svensson B, Larsson A, Adell R 2001 *The mandibular condyle in juvenile chronic arthritis patients with mandibular hypoplasia: a clinical and histological study.* International Journal of Oral and Maxillofacial Surgery 30: 300-305

Tracy W E, Savara B S 1966 *Norms of size and annual increments of five anatomical measures of the mandible in girls from 3 to 16 years of age.* Archives of Oral Biology 11: 587-598

Twilt M, Mobers S M, Arends L R, ten Cate R, van Suijlekom-Smit L 2004 *Temporomandibular involvement in juvenile idiopathic arthritis.* The Journal of Rheumatology 31: 1418-1422

Twilt M, Schulten A J, Nicolaas P, Dulger A, van Suijlekom-Smit L W 2006 *Facioskeletal changes in children with juvenile idiopathic arthritis.* Annals of the Rheumatic Diseases 65: 823-825

Twilt M, van der Giesen E, Mobers S M, ten Cate R, van Suijlekom-Smit L W 2003 *Abrupt condylar destruction of the mandibula in juvenile idiopathic arthritis.* Annals of the Rheumatic Diseases 62: 366-367

Updegrave W J 1971 *Visualizing the mandibular ramus in panoramic radiography.* Oral Surgery, Oral Medicine, Oral Pathology 31: 422-429

Van Elslande D C, Russett S J, Major P W, Flores-Mir C 2008 *Mandibular asymmetry diagnosis with panoramic imaging.* American Journal of Orthodontics and Dentofacial Orthopedics 134: 183-192

Weiss J E, Ilowite N T 2005 *Juvenile idiopathic arthritis.* Pediatric Clinics of North America 52: 413-442, vi

Weiss P F, Arabshahi B, Johnson A, Bilaniuk L T, Zarnow D, Cahill A M, Feudtner C, Cron R Q 2008 *High prevalence of temporomandibular joint arthritis at disease onset in children with juvenile idiopathic arthritis, as detected by magnetic resonance imaging but not by ultrasound.* Arthritis & Rheumatism 58: 1189-1196

Yeo D K, Freer T J, Brockhurst P J 2002 *Distortions in panoramic radiographs.* Australian Orthodontic Journal 18: 92-98

Figure Legends

Figure 1 Example of a 3D CT-dataset visualised using maximum-intensity projection and multiplanar reformatting with 3 orthogonal planes (a-c). The orientation of the slice c, used for the linear measurements, was standardized to intersect the center of the coronoid process (1), the condylar process (2) and the gonial angle (3). The thickness (4) of the slice (c) was defined as the smallest thickness, where the most cranial condylar point (5), the most caudal gonial point (6) and the deepest point of the incisura mandibulae (7) were included.

Figure 2 Constructions and both linear measurements (RH and CP) were performed parallel to the tangent at the posterior border of the ramus:
RH: measured between most cranial point of the condyle (Co) and intersection point with the lower border of the ramus (Go).
CP: measured between the most cranial point of the condyle (Co) and the most caudal point of incisura mandibulae (In).

Figure 3 Selected Bland-Altman-Plots with mean difference (black lines) extended by 95% CI (blue dash-dotted lines) and 95% limits of agreement (green dashed lines).

Figure 4 Boxplots of CV for both measurements (RH and CP) and all imaging methods.
* Significant differences according to two-sample t-test.

Figure 1

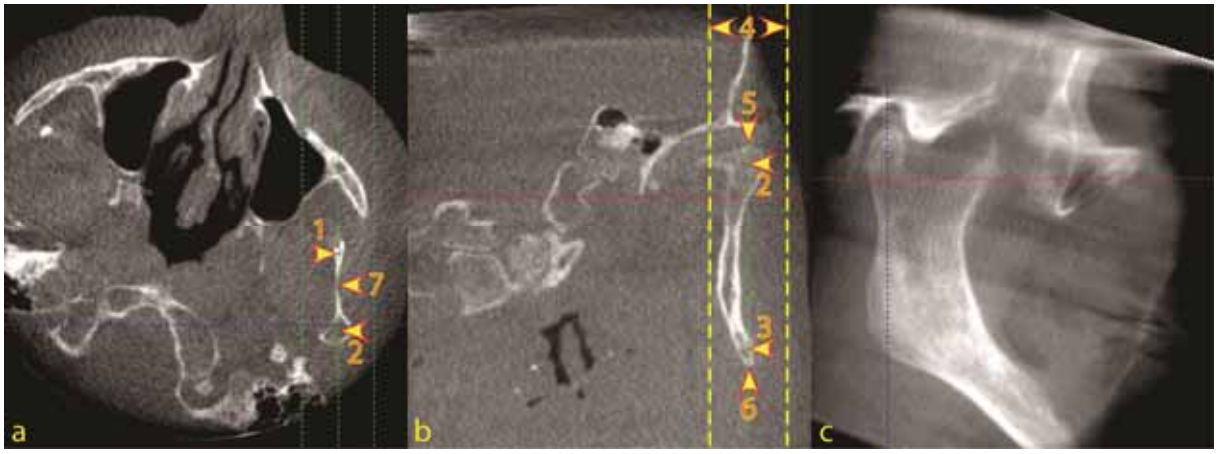

Figure 2

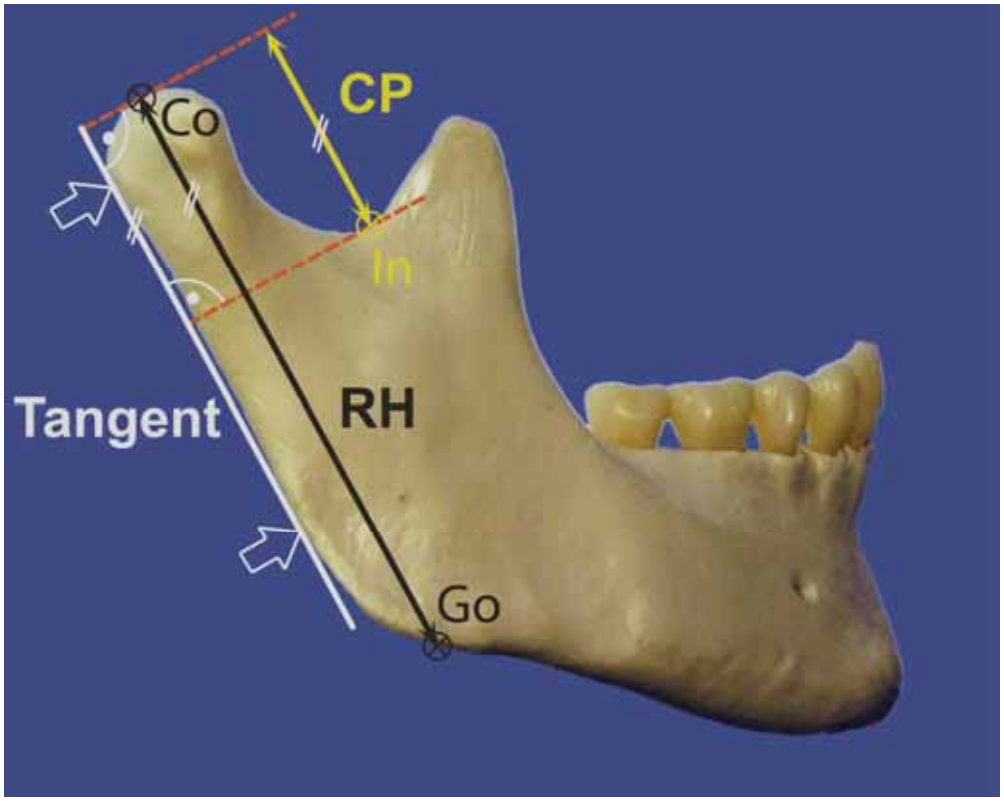

Figure 3

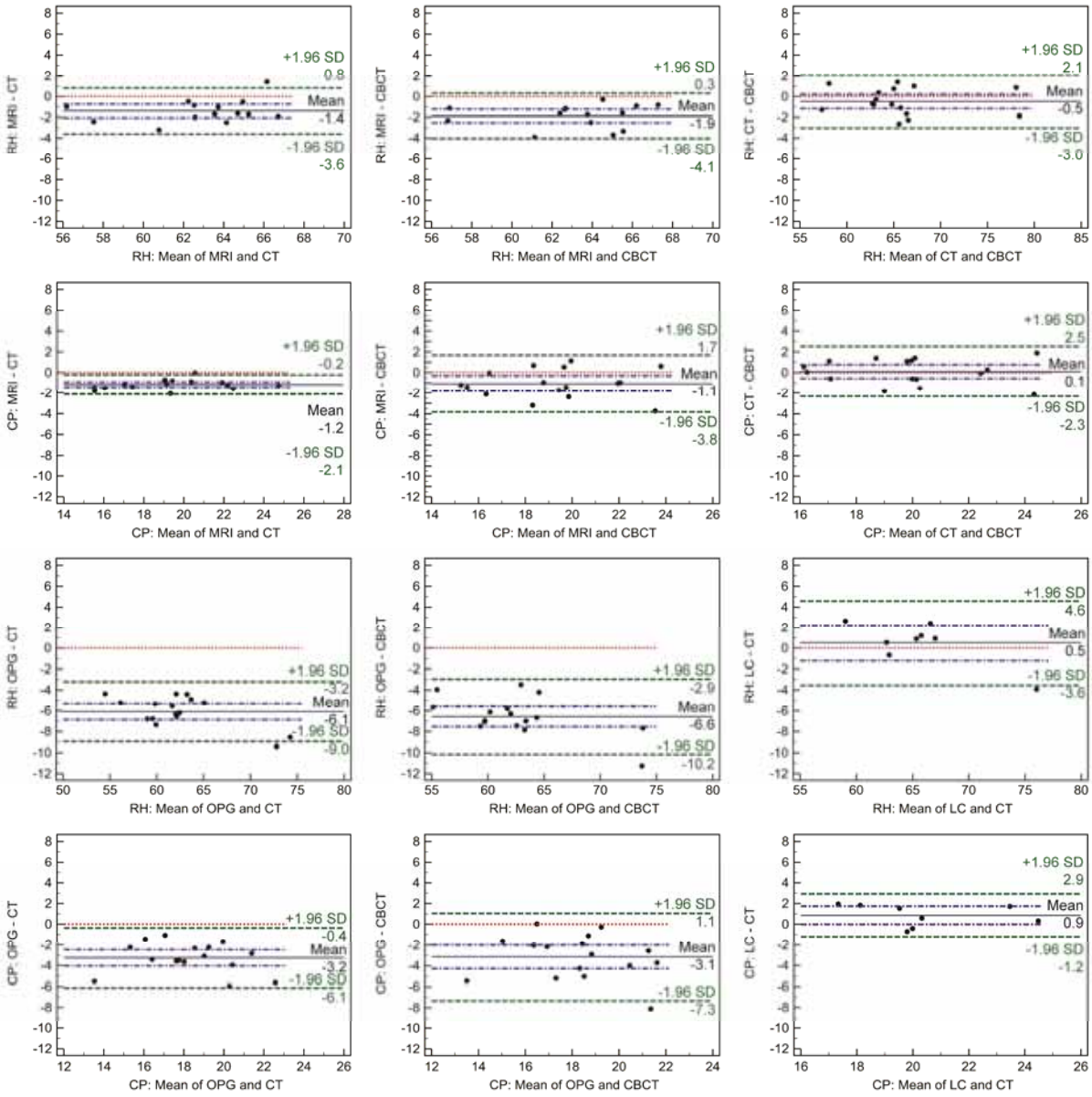

Figure 4

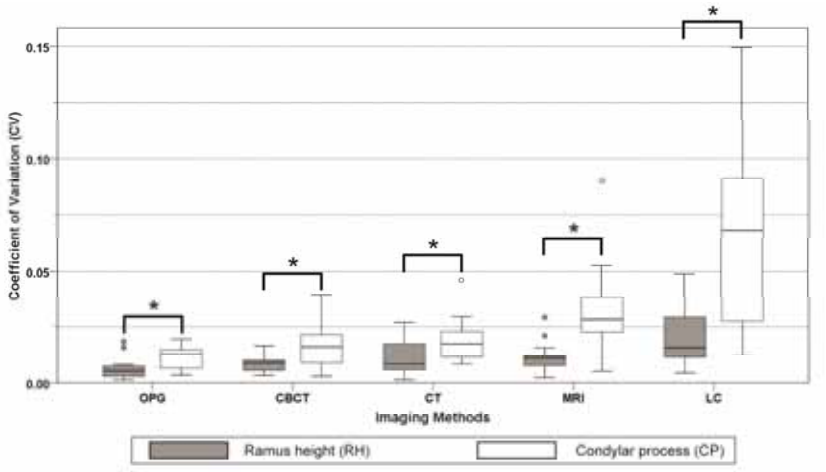

Tables

Table 1 *Intraclass correlation coefficient (ICC) showing intra- and interobserver reliability per measurement type and imaging procedure.*

	ICC	
	Intraobserver	*Interobserver*
Ramus height (RH)		
OPG	0.99	0.99
CBCT	0.99	0.99
CT	0.98	0.97
MRI	0.95	0.92
LC	0.93	0.82
Condylar process (CP)		
OPG	0.99	0.99
CBCT	0.98	0.98
CT	0.98	0.97
MRI	0.93	0.93
LC	0.79	0.59

Table 2 *Mean differences (upper value minus left value) [mm], range of 95% limits of agreement [mm] and 95% limits of agreement [mm] for CP (upper right) and RH (lower left).*

* Significant mean differences between methods according to paired t-test.

	Condylar Process (CP)					
		OPG	**CBCT**	**CT**	**MRI**	**LC**
Ramus height (RH)	**OPG**		3.1* (8.4: 7.3, -1.1)	3.2* (5.7: 6.1, 0.4)	2.1* (6.0: 5.1, -0.9)	4.1* (6.2: 7.2, -1.0)
	CBCT	-6.6* (7.3: -2.9, -10.2)		0.1 (4.8: 2.5, -2.3)	-1.1* (5.5: 1.7, -3.8)	1.0* (4.4: 3.2, -1.2)
	CT	-6.1* (5.8: -3.2, -9.0)	0.5 (5.1: 3.0, -2.1)		-1.2* (1.9: -0.2, -2.1)	0.9 (4.1: 2.9, -1.2)
	MRI	-4.3* (4.3: -2.1, -6.4)	1.9* (4.4: 4.1, -0.3)	1.4* (4.4: 3.6, -0.8)		2.0* (5.2: 4.6, -0.6)
	LC	-6.6* (4.4: -4.4, -8.8)	0.0 (8.0: 4.0, -4.0)	-0.5 (8.2: 3.6, -4.6)	-2.5* (4.9: -0.1, -5.0)	

Table 3 *Descriptive statistics (mean±SD, 95% CI) of the CV for both linear measurements (RH and CP) and all imaging methods. Distinct letters (a, b, c) indicate significant differences of imaging methods according to Scheffé post-hoc test. P-values from ANOVA (p < 0.001).*

	Mean ±SD	*95% CI*	
		lower	*upper*
CV of RH			
OPG	0.007[a] ±0.005	0.004	0.010
CBCT	0.009[a] ±0.004	0.007	0.011
CT	0.011[a,b] ±0.008	0.007	0.016
MRI	0.012[a,b] ±0.007	0.008	0.016
LC	0.021[b] ±0.014	0.014	0.028
CV of CP			
OPG	0.012[a] ±0.005	0.009	0.014
CBCT	0.017[a] ±0.011	0.011	0.023
CT	0.019[a,b] ±0.010	0.014	0.024
MRI	0.033[b,c] ±0.019	0.023	0.043
LC	0.065[c] ±0.039	0.044	0.086

Illusions of fusions: Assessing cervical vertebral fusion on lateral cephalograms, multidetector computed tomographs, and cone-beam computed tomographs

Raphael Patcas,[a] Dominika Tausch,[b] Nikolaos Pandis,[c] Mirjana Manestar,[d] Oliver Ullrich,[e] Christoph A. Karlo,[f] Timo Peltomäki,[g] and Christian J. Kellenberger[h]

Zurich and Bern, Switzerland, Corfu, Greece, and Tampere, Finland

Introduction: The aims of this study were to compare lateral cephalograms with other radiologic methods for diagnosing suspected fusions of the cervical spine and to validate the assessment of congenital fusions and osteoarthritic changes against the anatomic truth. **Methods:** Four cadaver heads were selected with fusion of vertebrae C2 and C3 seen on a lateral cephalogram. Multidetector computed tomography (MDCT) and cone-beam computed tomography (CBCT) were performed and assessed by 5 general radiologists and 5 oral radiologists, respectively. Vertebrae C2 and C3 were examined for osseous fusions, and the left and right facet joints were diagnosed for osteoarthritis. Subsequently, the C2 and C3 were macerated and appraised by a pathologist. Descriptive analysis was performed, and interrater agreements between and within the groups were computed. **Results:** All macerated specimens showed osteoarthritic findings of varying degrees, but no congenital bony fusion. All observers agreed that no fusion was found on MDCT or CBCT. They disagreed on the prevalence of osteoarthritic deformities (general radiologists/MDCT, 100%; oral radiologists/CBCT, 93.3%) and joint space assessment in the facet joints (kappa = 0.452). The agreement within the rater groups differed considerably (general radiologists/MDCT, kappa = 0.612; oral radiologists/CBCT, kappa = 0.240). **Conclusions:** Lateral cephalograms do not provide dependable data to assess the cervical spine for fusions and cause false-positive detections. Both MDCT interpreted by general radiologists and CBCT interpreted by oral radiologists are reliable methods to exclude potential fusions. Degenerative osteoarthritic changes are diagnosed more accurately and consistently by general radiologists evaluating MDCT. (Am J Orthod Dentofacial Orthop 2013;143:213-20)

[a]Senior lecturer, Clinic for Orthodontics and Pediatric Dentistry, Center of Dental Medicine, University of Zurich, Zurich, Switzerland.
[b]Research fellow, Clinic for Orthodontics and Pediatric Dentistry, Center of Dental Medicine, University of Zurich, Zurich, Switzerland.
[c]Private practice, Corfu, Greece; visiting assistant professor, Department of Orthodontics and Dentofacial Orthopedics, Dental School, Medical Faculty, University of Bern, Bern, Switzerland.
[d]Senior lecturer, Institute of Anatomy, Faculty of Medicine, University of Zurich, Zurich, Switzerland.
[e]Director and professor, Institute of Anatomy, Faculty of Medicine, University of Zurich, Zurich, Switzerland.
[f]Resident, Institute of Diagnostic and Interventional Radiology, University Hospital Zurich, Zurich, Switzerland.
[g]Head orthodontist, Dental and Oral Diseases Outpatient Clinic, Department of Ear and Oral Diseases, Tampere University Hospital, and Department of Otolaryngology, University of Tampere, Tampere, Finland.
[h]Head, Department of Diagnostic Imaging, University Children's Hospital Zurich, Zurich, Switzerland.
The authors report no commercial, proprietary, or financial interest in the products or companies described in this article.
Reprint requests to: Raphael Patcas, Clinic for Orthodontics and Pediatric Dentistry, Center of Dental Medicine, University of Zurich, Plattenstrasse 11, 8032 Zurich, Switzerland; e-mail, raphael.patcas@zzm.uzh.ch.
Submitted, revised and accepted, September 2012.
0889-5406/$36.00

http://dx.doi.org/10.1016/j.ajodo.2012.09.017

In recent years, orthodontists have expressed increasing interest in assessing the cervical spine on a lateral cephalogram. One clinical purpose is the determination of skeletal age based on the association between age-related morphologic changes of the upper cervical vertebrae and the somatic growth curve.[1,2] A further intent is the evaluation of the craniocervical angulation to characterize head posture, which has been linked to nasorespiratory function[3] and craniofacial morphology.[4] Moreover, the use of lateral cephalograms has also been recommended to study congenital anomalies of the cervical vertebrae, because cervical vertebral anomalies, particularly fusions, could be related to certain craniofacial syndromes and other dentoskeletal malformations.[5-16] Awareness that the spine is of clinical interest has led to the recommendation to use cephalometric radiographs to routinely screen the cervical vertebrae for anomalies and even to develop a tracing technique of this region.[17]

Fig 1. Congenital fusion of the right facet joint C2-C3. This specimen is from the collection of the Institute of Anatomy at the University of Zurich and is not part of the assessed specimens.

Fusions are most common between the facet joints of the second and third vertebrae (C2 and C3; Fig 1). Like all other cervical vertebral anomalies, osseous fusions are usually asymptomatic[18] and considered to be coincidental findings with no clinical relevance.[19] However, in a few patients, cervical vertebral anomalies cause compression of neurologic structures or biomechanical instability, leading to chronic pain.[18] Associations between cervical vertebral anomalies, notably fusion of C2 and C3, and congenital disorders or dentoskeletal malocclusions have been studied extensively. They include syndromic and nonsyndromic anomalies such as fetal alcohol syndrome[5] and cleft lip and palate.[6-9] In recent research examining cervical vertebral anomalies on lateral cephalograms, a high prevalence of cervical vertebral anomalies, particularly fusions of C2 and C3, was reported in orthodontic surgical patients with severe skeletal malocclusions. The described associations between cephalometric measurements and fusions include skeletal Class III and mandibular overjet[10] with 61.4% fusions, skeletal deepbite[11] with 41.5% fusions, skeletal open bite[12] with 42.1% fusions, and skeletal Class II and maxillary overjet[13,14] with 28% and 52.9% fusions, respectively. A similarly high prevalence of fusions has been documented in subjects with condylar hypoplasia[15] with 72.7% fusions (45% in C2 and C3) and in patients with obstructive sleep apnea[16] (46%).

These findings have been challenged by some who argued that it was difficult to reliably determine cervical vertebral anomalies on 1 lateral cephalogram.[20-22] Considerably lower prevalence numbers (<0.9%) have been reported in other studies with normal populations[6-8,20,21,23,24]; this could be because patients with severe malocclusions are significantly different from a normal population, but this dissonance in prevalence certainly raises the question as to whether lateral cephalograms are a reliable tool to assess cervical vertebral anomalies. Koletsis and Halazonetis[21] stated that no study investigating the reliability of cephalometric radiography in the cervical region has been published to date. To validate the assessment of the spine on lateral cephalograms, 3-dimensional radiological data[6,20,22,25-29] and direct observation (on autopsy material) have been suggested.[24,30] A cadaver study would allow for direct comparisons of different assessment methods and validate each diagnostic approach against the anatomic truth.

In addition, a cadaver study would serve another purpose: diagnostic thinking efficacy evaluates whether the information retrieved from radiologic images leads to a change in the clinician's diagnostic thinking.[31] This efficacy has been evaluated for cone-beam computed tomography (CBCT) in relation to impacted third molars, impacted canines, root resorption of adjacent teeth, and the temporomandibular joint, but it has not been appraised for the cervical spine.[32] Since the cervical spine is a region of interest for the orthodontist, it would be beneficial to assess the diagnostic efficacy of oral radiologists examining CBCT data and to compare it with that of general radiologists analyzing multidetector computed tomography (MDCT) data, and to verify the results against the anatomic findings.

The objectives of this cadaver study were therefore (1) to ascertain whether fusions of C2 and C3 suspected on lateral cephalograms would also be diagnosed by general radiologists on MDCT or oral radiologists on CBCT, and (2) to validate MDCT and CBCT assessments of congenital fusions and osteoarthritic changes against the anatomic truth.

MATERIAL AND METHODS

From a larger collection of perfused cadaver heads, 8 specimens were selected for which analog, postmortem lateral cephalograms were available (tube voltage, 67; tube current, 250 mA; exposure time, 0.04 second; tube current time product, 10 mAs; focus to coronal plane distance, 200 cm). The cadaver heads were supplied by the Institute of Anatomy at the University of Zurich in Switzerland in accordance with state and federal regulations (ie, voluntary body donation program on the basis of informed consent), the Convention on Human Rights and Medicine,[33] and the recommendation of the National Academy of Medical Science.[34] The perfusion was carried out within 4 days after death with a fixation liquid consisting of 2 parts alcohol (70%),

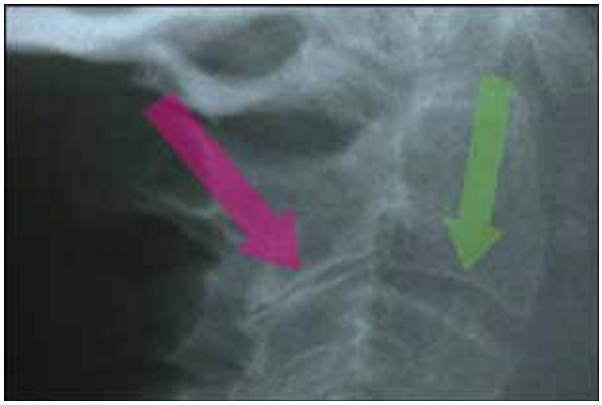

Fig 2. Lateral cephalogram of a specimen with continuous radiolucent areas between the articular facets of C2 and C3 (*purple arrow*) and the intervertebral disc space (*green arrow*). This specimen was excluded from the study.

1 part glycerine, and 2% almudor (containing 8.1% formaldehyde, 10% glyoxal, and 3.7% glutaraldehyde).

The lateral cephalograms were screened and assessed for potential fusions of cervical vertebrae by an author (D.B.) following the method prescribed in the literature: fusions were identified as an osseous continuity between C2 and C3 without complete separation at the articular facets or intervertebral disc space (see Fig 2 for an excluded specimen with a continuous radiolucent area).[7,20,21,35,36] Four specimens (3 female, 1 male; age range, 65-87 years; mean age, 78 years) fulfilled the inclusion criterion of a suspected cervical spine fusion at the level of C2 and C3 and were used for the study.

MDCT was performed on a 40-detector row computed tomography system (Brilliance CT 40; Philips Healthcare, Eindhoven, The Netherlands) with the following scan parameters kept identical for all specimens: tube voltage, 120 kV; tube current time product, 70 mAs; slice collimation, 20 × 0.625 mm; pitch, 0.68; reconstruction slice thickness, 0.67 mm; reconstruction increment, 0.33 mm; window level setting, 2000/500 Hounsfield units; voxel sizes, 0.39 mm (x-axis), 0.39 mm (y-axis), and 0.67 mm (z-axis). Sagittal and coronal reformatted images (slice thickness, 1 mm; increment, 0.5 mm) were viewed on a high-resolution diagnostic workstation (dx IDS5; Sectra PACS, Linköping, Sweden).

The CBCT scans were made on a scanner with an amorphous silicon flat panel (KaVo 3D exam; KaVo Dental, Bismarckring, Germany). The following scan parameters were kept identical during all CBCT examinations: tube voltage, 120 kV; tube current time product, 37.07 mAs; reconstruction thickness, 0.25 mm; reconstruction increment, 0.25 mm; voxel size, 0.25 mm (x-axis), 0.25 mm (y-axis), and 0.25 mm (z-axis). Digital imaging and communications in medicine (DICOM) files were reformatted in multiplanar reconstructions by using open-source postprocessing software (Workstation version 2.0 SP1; ClearCanvas, Toronto, Ontario, Canada).

Five general radiologists were asked to evaluate the MDCT data, and 5 dentists with special postgraduate training in oral radiology were asked to evaluate the CBCT data.

Three areas were assessed for a potential congenital fusion: facet joint (C2-C3) of the left and right articular processes and the intervertebral disc space between the 2 bodies, C2 and C3.

Additionally, the raters were requested to perform their radiological appraisals for the left and right facet joints in the following manner: (1) normal joint or (2) osteoarthritis (joint space entirely preserved, partially preserved, or not visible).

All radiologists assessed the images independently, in blinded fashion, and without knowledge of the anatomic findings.

After image acquisition, the cervical spines were isolated en bloc from the cadaver heads. Lipids were dissolved in a Supralan UF solution (Bauer Handels, Fehraltorf, Switzerland) with sodium chloride. Enzymatic maceration was performed with papain (Bauer Handels) at pH 6 to 7 in Supralan UF and a solution containing sodium chloride for up to 14 days.

The macerated spines were subsequently analyzed for fusions and osteoarthritis by a board-certified pathologist.

Statistical analysis

A standard statistical software package (version 11.4.1.0; MedCalc Software, Mariakerke, Belgium) was used for the descriptive data analysis. An unweighted Cohen kappa test was computed to evaluate the agreement between the CBCT and MDCT methods.[37] To determine interobserver agreement between the 5 CBCT radiologists and the 5 MDCT radiologists, a Fleiss kappa test[38] for multiple raters was calculated with StatTools.[39]

RESULTS

After the enzymatic maceration, the vertebral bodies C2 and C3 could be completely mobilized, proving the absence of congenital bony fusions in these vertebral segments (Figs 3-5). All facet joints showed degenerative osteoarthritic changes including osteophytes, peripheral eburnation, and gross irregularities of the subchondral joint surfaces of varying degrees. The facets of 2 specimens were more severely affected, exhibiting extensive osteophytes and ragged bony joint surfaces (Fig 5).

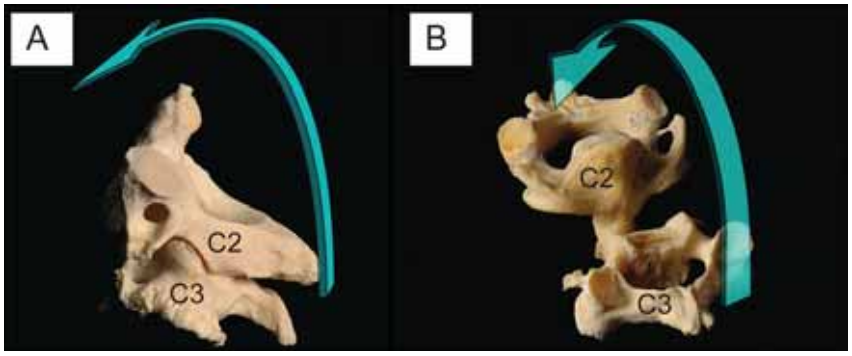

Fig 3. Explanatory illustration of how the specimens are depicted in Figures 4 and 5: **A,** C2 is rotated 180° to enable **B,** a direct view of all facets of the joints of the left and right articular processes and the intervertebral disc space.

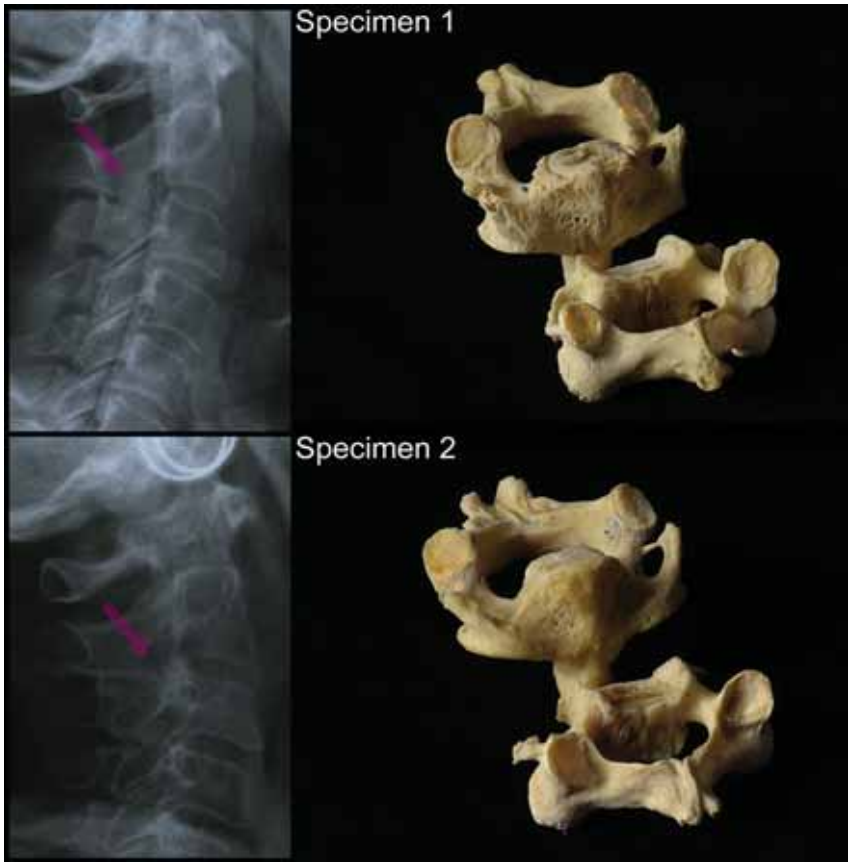

Fig 4. Specimens 1 (*top*) and 2 (*bottom*): the *left side* shows the lateral cephalogram of the intact cadaver head, and the *right side* shows the macerated vertebral bodies of C2 and C3.The *purple arrows* point to the suspected fusion.

All raters agreed that no congenital fusion was found by MDCT or CBCT, but there was disagreement concerning the prevalence of the osteoarthritic deformities. General radiologists assessing the MDCT recognized osteoarthritic changes in 100% (40/40) of the joint assessments, and oral radiologists evaluating the CBCT found osteoarthritic changes in 93.3% (38/40). Moreover, when evaluating the narrowing of the joint space in the affected osteoarthritic joints, the 2 rater groups differed substantially (Table I). The concordance

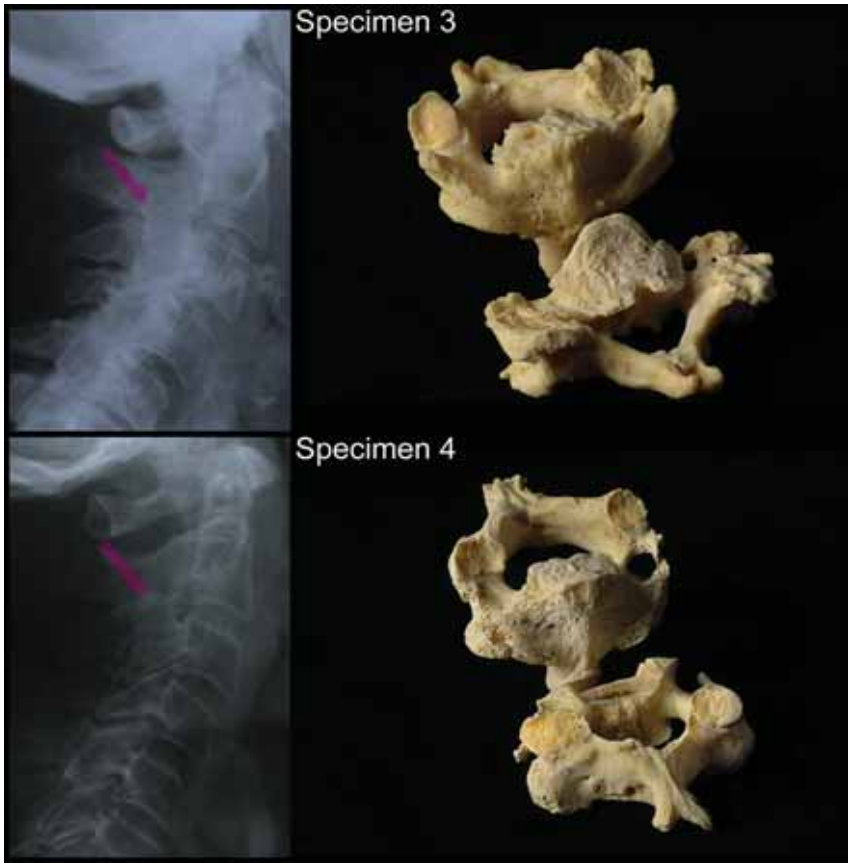

Fig 5. Specimens 3 (*top*) and 4 (*bottom*): the *left side* shows the lateral cephalogram of the intact cadaver head, and the *right side* shows the macerated vertebral bodies of C2 and C3. The *purple arrows* point to the suspected fusion.

Table I. Assessment of the osteoarthritic joints: evaluation of the joint space narrowing in joints affected with osteoarthritis

Osteoarthritic joint assessment	*General radiologists/ MDCT*	*Oral radiologists/ CBCT*
Osteoarthritic joint, joint space entirely preserved	80.0%	51.8%
Osteoarthritic joint, joint space partially preserved	20.0%	48.2%
Osteoarthritic joint, joint space not visible	0%	0%

between the 2 rater groups was rather modest (70%) with a kappa value of 0.452 (SE, 0.132; 95% confidence interval [CI], 0.193-0.711), indicating moderate agreement.[40]

In addition, there was a considerable difference regarding the agreement within each rater group when evaluating the narrowing of the joint space. The general radiologists assessing the MDCT data agreed more consistently with each other (kappa = 0.612) than did the oral radiologists assessing the CBCT data (kappa = 0.240; Table II). According to Landis and Koch,[40] the kappa value of 0.240 for the CBCT/oral radiologists corresponds to fair agreement, and the kappa value of 0.612 for the MDCT/general radiologists denotes substantial agreement.

Table II. Fleiss kappa for multiple raters: agreement (within each group) of the 5 general radiologists assessing MDCT and the 5 oral radiologists assessing CBCT

	Kappa	*SE*	*95% CI*
MDCT/general radiologists	0.612	0.0679	0.479-0.745
CBCT/oral radiologists	0.240	0.078	0.088-0.392

DISCUSSION

The evaluation of congenital vertebral fusions on lateral cephalograms has been studied extensively in the orthodontic literature, associating fusions with diverse anomalies and malocclusions. The use of lateral

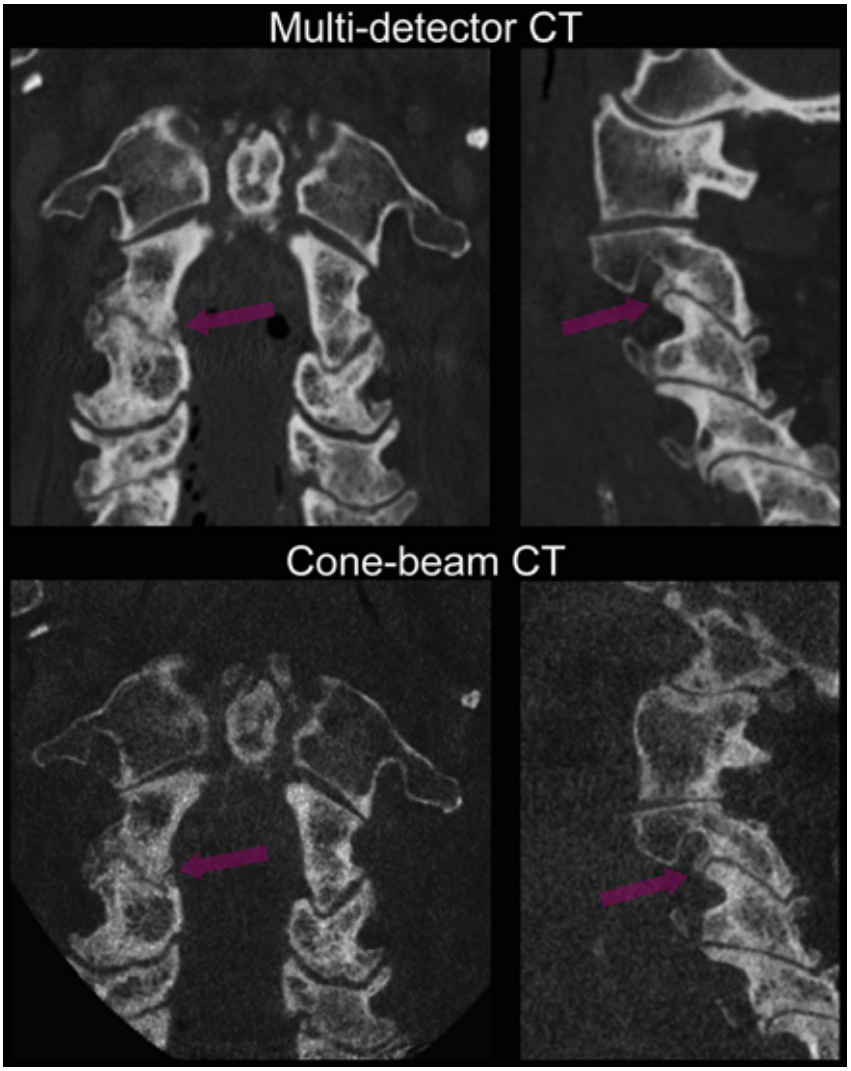

Fig 6. Coronal (*left*) and sagittal (*right*) reformatted MDCT images (*top*) and CBCT images (*bottom*) of specimen 3. The *purple arrows* point to the irregularly narrowed facet joints C2-C3 with subchondral sclerosis and spondylophytes, but no bony fusion. The images were rotated and cropped to facilitate a direct comparison. Note the close proximity to the edge of the volume in CBCT, seen on the coronal slide.

cephalograms, however, has been challenged by those who argue that 2-dimensional radiographs can yield deceptive impressions of "pseudo-fusions" in the C2-C3 facet joint because of their oblique orientation.[22] This study corroborates this concern by demonstrating that cephalograms do not provide reliable data to assess vertebral fusions in the cervical spine. All 4 specimens assessed positively for fusions on lateral cephalograms proved to be false positives. None had a fusion. Hence, the absence of a continuous radiolucent area between the articular processes (on cephalograms) as the sole radiologic criterion might not be a valid method to identify fusions on 1 lateral cephalogram.

All evaluated joints had osteoarthritic changes, some with gross irregularities and narrowed joint spaces. Based on our findings, a further reason for the erroneous assessment of fusions might be the misinterpretation of osteoarthritic changes as fusions. It is evident that a continuous radiolucent area might fade away because of irregularities, as shown in Figures 5 and 6 (see specimen 3).

The results demonstrate the limitations of lateral cephalograms as a diagnostic tool to assess the spine and raise doubts about the necessity of exposing the cervical vertebrae to radiation and, with it, the thyroid. Hence, the clinical recommendation to apply a neck

shield consistently on lateral cephalograms ought to be reinforced. Recent studies demonstrate that, if skeletal age estimation is needed, radiation exposure can be minimized by applying a neck shield and performing an additional hand-wrist radiograph.[41]

In this study, we also compared the different assessment outcomes between the general radiologists evaluating MDCT and the oral radiologists appraising CBCT of the cervical spine (Fig 6). The results demonstrate 2 important findings: (1) both rater groups performed equally well regarding the exclusion of possible fusions; and (2) concerning the appraisal of osteoarthritic deformities, the general radiologists assessing MDCT performed uncontestably better. They diagnosed osteoarthritic changes correctly in 100% of the cases and did so with considerable consistency in regard to their assessment of the joint spaces. Conversely, oral radiologists evaluating CBCT diagnosed only 93.3% of the osteoarthritic cases correctly and did so with more disagreement among themselves in their assessments of the joint spaces.

Two possible assumptions might explain why oral radiologists evaluating CBCT data do not perform as well as general radiologists with MDCT data. On one hand, oral radiologists are not used to assessing joints. The only joint in the maxillofacial region is the temporomandibular joint, which differs remarkably from other joints. Hence, it could be argued that general radiologists probably perform better because of their broader experience in assessment of articulo-osseous pathologies. On the other hand, there is an inherent problem with CBCT data. The image quality in the midplane is superior to more peripheral regions because the data acquired in a circular cone-beam scan are only sufficient for accurate image reconstructions in the middle of the volume. It is a well-known fact that image reconstruction at the periphery of the volume suffer from cone-beam artifacts.[42] Thus, the location of the cervical spine, because it is much off the center of the volume, could have caused the inferior results.

As with every cadaver study, our research had some limitations. One possible constraint is whether the maceration might have influenced the bone properties that would falsify the anatomic reference. Enzymatic maceration, in contrast to common maceration with aggressive solutions, is an established method for removal of soft tissues while maintaining the structural integrity of compact bone[43,44] and produces excellent results when applied to ethanol-fixed material.[45] Therefore, it seems safe to presume that the assessment of osseous anomalies in enzymatic macerated specimens is admissible.

The low number of specimens might also be considered a limitation, since it precludes the possibility of carrying out more comprehensive statistical testing. Engaging more radiologists to assess the sample would certainly generate sufficient data to account for statistical inferences in hypothesis testing and would additionally reduce the uncertainty (ie, the standard error) in the descriptive analysis. It has been shown that as the number of raters increases, the required number of subjects decreases. But the savings in sample size obtained by increasing the number of raters reportedly diminishes rapidly after the accrual of 5 raters.[46] Mindful of this constraint, we designed this study to produce no more than a descriptive analysis. Nonetheless, our results convey clear answers to the objectives of this study, making further statistical testing or more specimens unnecessary: lateral cephalograms can evidently cause false-positive findings of fusions, and the reported standard errors show that the descriptive values are accurate enough to draw clear conclusions about the MDCT and CBCT evaluations.

CONCLUSIONS

1. Because only a few specimens were evaluated, no general conclusions can be drawn about the prevalence. Yet, lateral cephalograms have been proven to cause false-positive detection of fusions. Lateral cephalograms are therefore a questionable means to assess cervical spine anomalies, and previous studies evaluating fusions in cervical spines, based on 1 lateral cephalogram, seem to be highly problematic.
2. Both MDCT data viewed by general radiologists and CBCT data screened by oral radiologists are reliable methods to exclude fusions.
3. General radiologists appraising MDCT data performed better in the assessment of osteoarthritic changes of the joints than did oral radiologists with CBCT data, but further studies with more specimens would be welcomed to confirm this finding.

We thank Philippe Halioua for the outstanding photographs and Sabrina Beutler and Axel Lang for macerating the specimens.

REFERENCES

1. Hassel B, Farman AG. Skeletal maturation evaluation using cervical vertebrae. Am J Orthod Dentofacial Orthop 1995;107:58-66.
2. Baccetti T, Franchi L, McNamara JA Jr. An improved version of the cervical vertebral maturation (CVM) method for the assessment of mandibular growth. Angle Orthod 2002;72:316-23.
3. Huggare JA, Laine-Alava MT. Nasorespiratory function and head posture. Am J Orthod Dentofacial Orthop 1997;112:507-11.
4. Solow B, Sandham A. Cranio-cervical posture: a factor in the development and function of the dentofacial structures. Eur J Orthod 2002;24:447-56.

5. Tredwell SJ, Smith DF, Macleod PJ, Wood BJ. Cervical spine anomalies in fetal alcohol syndrome. Spine (Phila Pa 1976) 1982;7: 331-4.
6. Rajion ZA, Townsend GC, Netherway DJ, Anderson PJ, Yusof A, Hughes T, et al. A three-dimensional computed tomographic analysis of the cervical spine in unoperated infants with cleft lip and palate. Cleft Palate Craniofac J 2006;43:513-8.
7. Sandham A. Cervical vertebral anomalies in cleft-lip and palate. Cleft Palate J 1986;23:206-14.
8. Ross RB, Lindsay WK. The cervical vertebrae as a factor in etiology of cleft palate. Cleft Palate J 1965;36:273-81.
9. Horswell BB. The incidence and relationship of cervical spine anomalies in patients with cleft lip and/or palate. J Oral Maxillofac Surg 1991;49:693-7.
10. Sonnesen L, Kjaer I. Cervical column morphology in patients with skeletal Class III malocclusion and mandibular overjet. Am J Orthod Dentofacial Orthop 2007;132:427.e7-12.
11. Sonnesen L, Kjaer I. Cervical vertebral body fusions in patients with skeletal deep bite. Eur J Orthod 2007;29:464-70.
12. Sonnesen L, Kjaer I. Cervical column morphology in patients with skeletal open bite. Orthod Craniofac Res 2008;11:17-23.
13. Sonnesen L, Kjaer I. Anomalies of the cervical vertebrae in patients with skeletal Class II malocclusion and horizontal maxillary overjet. Am J Orthod Dentofacial Orthop 2008;133:188.e15-20.
14. Arntsen T, Sonnesen L. Cervical vertebral column morphology related to craniofacial morphology and head posture in preorthodontic children with Class II malocclusion and horizontal maxillary overjet. Am J Orthod Dentofacial Orthop 2011;140:e1-7.
15. Sonnesen L, Pedersen CE, Kjaer I. Cervical column morphology related to head posture, cranial base angle, and condylar malformation. Eur J Orthod 2007;29:398-403.
16. Sonnesen L, Petri N, Kjaer I, Svanholt P. Cervical column morphology in adult patients with obstructive sleep apnoea. Eur J Orthod 2008;30:521-6.
17. Vastardis H, Evans CA. Evaluation of cervical spine abnormalities on cephalometric radiographs. Am J Orthod Dentofacial Orthop 1996;109:581-8.
18. Klimo P Jr, Rao G, Brockmeyer D. Congenital anomalies of the cervical spine. Neurosurg Clin N Am 2007;18:463-78.
19. Mcrae DL. The significance of abnormalities of the cervical spine. Am J Roentgenol Radium Ther Nucl Med 1960;84:3-25.
20. Bebnowski D, Hanggi MP, Markic G, Roos M, Peltomaki T. Cervical vertebrae anomalies in subjects with Class II malocclusion assessed by lateral cephalogram and cone beam computed tomography. Eur J Orthod 2012;34:226-31.
21. Koletsis DD, Halazonetis DJ. Cervical vertebrae anomalies in orthodontic patients: a growth-based superimpositional approach. Eur J Orthod 2010;32:36-42.
22. Massengill AD, Huynh SL, Harris JH Jr. C2-3 facet joint "pseudofusion": anatomic basis of a normal variant. Skeletal Radiol 1997; 26:27-30.
23. Tetradis S, Kantor ML. Prevalence of skeletal and dental anomalies and normal variants seen in cephalometric and other radiographs of orthodontic patients. Am J Orthod Dentofacial Orthop 1999; 116:572-7.
24. Brown MW, Templeton AW, Hodges FJ 3rd. The incidence of acquired and congenital fusions in the cervical spine. Am J Roentgenol Radium Ther Nucl Med 1964;92:1255-9.
25. Guille JT, Sherk HH. Congenital osseous anomalies of the upper and lower cervical spine in children. J Bone Joint Surg Am 2002; 84-A:277-88.
26. Hensinger RN. Congenital anomalies of the cervical spine. Clin Orthop Relat Res 1991;264:16-38.
27. McAfee PC, Bohlman HH, Han JS, Salvagno RT. Comparison of nuclear magnetic resonance imaging and computed tomography in the diagnosis of upper cervical spinal cord compression. Spine (Phila Pa 1976) 1986;11:295-304.
28. Carreon LY, Djurasovic M, Glassman SD, Sailer P. Diagnostic accuracy and reliability of fine-cut CT scans with reconstructions to determine the status of an instrumented posterolateral fusion with surgical exploration as reference standard. Spine (Phila Pa 1976) 2007;32:892-5.
29. Shi H, Scarfe WC, Farman AG. Three-dimensional reconstruction of individual cervical vertebrae from cone-beam computed-tomography images. Am J Orthod Dentofacial Orthop 2007;131: 426-32.
30. Templeton AW, Brown MW. The transverse processes of the cervical vertebral segment. A correlation of oblique roentgenograms with skeletonized material. Radiology 1964;82:912-5.
31. Fryback DG, Thornbury JR. The efficacy of diagnostic imaging. Med Decis Making 1991;11:88-94.
32. Halazonetis DJ. Cone-beam computed tomography is not the imaging technique of choice for comprehensive orthodontic assessment [Point/Counterpoint]. Am J Orthod Dentofacial Orthop 2012;141:402-11.
33. European Union. Additional protocol to the convention on human rights and biomedicine, on transplantation of organs and tissues of human origin. ETS 186, Art 16–18 2002. Strasbourg, France; January 24, 2002. Available at: http://conventions.coe.int/Treaty/en/Treaties/Html/186.htm. Accessed July 3, 2012.
34. Swiss Academy of Medical Science. Die verwendung von leichen und leichenteilen in der medizinischen forschung sowie aus-, weiter- und fortbildung. Schweiz Ärzteztg 2009;90:102-7.
35. Farman AG, Escobar V. Radiographic appearance of the cervical vertebrae in normal and abnormal development. Br J Oral Surg 1982;20:264-74.
36. Farman AG, Nortje CJ, Joubert JJ. Radiographic profile of the first cervical vertebra. J Anat 1979;128:595-600.
37. Cohen J. A coefficient of agreement for nominal scales. Educ Psychol Meas 1960;20:37-46.
38. Fleiss JL. Measuring nominal scale agreement among many raters. Psychol Bull 1971;76:378-82.
39. Chang A. StatTools. Available at: http://www.stattools.net/CohenKappa_Pgm.php. Accessed July 3, 2012.
40. Landis JR, Koch GG. The measurement of observer agreement for categorical data. Biometrics 1977;33:159-74.
41. Patcas R, Signorelli L, Peltomäki T, Schätzle M. Is the use of the cervical vertebrae maturation method justified to determine skeletal age? A comparison of radiation dose of two strategies for skeletal age estimation. Eur J Orthod 2012 Jul 30 [Epub ahead of print]. http://dx.doi.org/10.1093/ejo/cjs043.
42. Yu L, Vrieze TJ, Bruesewitz MR, Kofler JM, DeLone DR, Pallanch JF, et al. Dose and image quality evaluation of a dedicated cone-beam CT system for high-contrast neurologic applications. AJR Am J Roentgenol 2010;194:W193-201.
43. Sandstrom B. Enzymatic maceration of delicate bone and small skeletons. Acta Anat (Basel) 1969;74:487-8.
44. Yin L, Venkatesan S, Kalyanasundaram S, Qin QH. Influence of enzymatic maceration on the microstructure and microhardness of compact bone. Biomed Mater 2010;5:15006.
45. Bartels T, Meyer W. A quick and effective method for the maceration of vertebrates. Dtsch Tierarztl Wochenschr 1991;98: 407-9.
46. Altaye M, Donner A, Eliasziw M. A general goodness-of-fit approach for inference procedures concerning the kappa statistic. Stat Med 2001;20:2479-88.